VESTNIK

of Nosov Magnitogorsk State Technical University

№5 (45) 2013

The journal is the English edition of the Russian scientific research peer-reviewed journal «Vestnik of NMSTU» and is among the highest ranking Russian scientific journals. A wide spectrum of papers covering almost all aspects of recent theoretical and experimental achievements from mining and mineral processing, iron and steel and rolled manufacturing to downstream products processing for different Industries are published. Internet versions of the journal can be found in the Scientific Electronic Library collection in the Internet.

PUBLISHED SINCE MARCH, 2003

Registration certificate PI № FS11-1157 on April 18, 2007
Issued by the Federal Service for Supervision of Legislation in Mass of Communication and Protection of Cultural Heritage in the Urals Federal District.

Founder – State Educational Institution «Nosov Magnitogorsk State Technical University» (455000, Chelyabinsk Region, Magnitogorsk, Lenin prospect, 38)

16+ in according to the Federal Law 29.12.10. №436-FL

Editorship address:

455000, city Magnitogorsk, Lenin prospect 38
Phone number: (3519) 22-14-93. Fax: (3519)23-57-60
URL: http://www.vestnik.magtu.ru
E-mail: rio_mgtu@mail.ru; vestnik@magtu.ru

Prepared for publication by publishing center of NMSTU
Printed in the Printing NMSTU Area
Signed for press 2013.09.30.
Order 558. Circulation – 500 items. Free price.

CONTENTS

Kolokoltsev V.M., Petrochenko E.V.

STRUCTURE FEATURES AND PROPERTIES OF HIGH-ALLOY WHITE IRONS

Abstract. In this paper the regularities of structure formation, mechanical properties and wearability of chrome-vanadium white cast irons, depending on chemical composition, cooling conditions during solidification have been investigated.

The relation of wearability of chrome vanadium white cast irons with the morphology of carbide phase, types of binary and ternary eutectics, phase and chemical composition of metallic matrix of castings in abrasive wearing-out has been established.

The reasoning of the influence of structure formation features in chrome vanadium white cast irons on the mechanical and special features, forming during crystallization and the following effects of abrasive ambient are represented.

Cast iron classification according to metallic matrix structure, eutectic type and quantity, eutectic morphology, phase morphology, forming any eutectic, is suggested.

Keywords*:* structure, eutectic compositions, phase structure, phase composition, microhardness, wearability, straining martensitic transformation, classification according to white cast iron morphology.

White cast iron is widely used as a material for tools and machinery parts, which undergo intensive wear and oxidation. It was traditionally attributed to the class of fragile and low-strength materials and this fact significantly limited the area of its use. The progress in the field of white irons alloying, achieved in recent years, has significantly changed the ideas about their properties and possible applications.

Modern white cast irons are complex multicomponent alloys, different in structure and specific properties. They are a separate group of industrial cast irons, which composite structure is being formed during solidification. It is the group that determines the specific properties of white cast irons in the as-cast state.

Despite the literature readings abundance concerning the composition optimization of complex alloyed white irons of functional purpose, the effect of alloying elements on the crystallization processes and structure formation, mechanical and special (heat resistance, durability) properties of cast irons has not been considerably and systematically investigated. Especially, it concerns the formation conditions of various eutectic and carbide phase, containing some carbide-forming elements in iron composition.

In this paper the regularities of structure formation, mechanical and specific properties of chrome-vanadium white cast irons, depending on the chemical composition, cooling conditions during solidification have been investigated.

The selection of alloying structure and varying limits of alloying elements and carbon content largely determines the metallic matrix morphology, quantity, carbide phase type and eutectic, and, consequently, the alloy properties in whole and is settled by the following statements.

The most wear resistant, in accordance with Charpy principle, are cast irons requiring the complete inversion of phase location. It means the most solid structured constituents should lie in the form of isolated impurities, but the most viscous constituents should form a solid matrix, that provides not only high wear-resistant properties, but also strength, toughness, resistance to thermal cycling, etc.

Such phase arrangement inversion in the structure of austenitic-carbide eutectic can be achieved in high chrome cast iron alloying with more than 3% vanadium. Carbide is the branched phase but austenite or its transformation products are the matrix phase, being in general a cast composite.

Carbon is the main regulator of the carbide phase, which determines the properties of the present irons. Carbon addition of 3.2-3.6% provides the M_7C_3 carbides formation, which improves cast iron wear resistance. Carbon addition of less than 3.2% leads to the primary austenite quantity increasing. Carbon addition of more than 3.2% leads to the reducing of alloying elements content in the solid solution, and to the disruption of the cast structure uniformity at the expense of large branched carbides precipitation. Both negatively affect on cast iron properties.

Chromium can partially replace the iron atoms in the iron carbide $(Fe,Cr)_3C$ or it can form chromium carbides, in which the part of chromium atoms is substituted by iron: trigonal $(Cr,Fe)_7C_3$ and cubic $(Cr,Fe)_{23}C_6$. In α-iron chromium has unlimited solvency, in γ-iron chrome dissolves to 14% Cr. Chromium carbides have significantly higher hardness than chromium alloyed cementite, and it promotes cast iron durability and mechanical properties.

Cementite carbides in iron form a hard framing of ledeburite eutectic. Criteria of fragile destruction for such carbide hard framing are achieved earlier than for eutectic with carbides $(Cr,Fe)_7C_3$. Cast irons with carbides $(Cr,Fe)_7C_3$ (chromium content in the iron exceeds 11-14%) are of maximum wear resistance due to increased microhardness of these carbides and eutectic branched morphology. Carbide $(Cr,Fe)_{23}C_6$ microhardness is 2000 MPa below than carbide $(Cr,Fe)_7C_3$ microhardness. It is more crisp and intent to crushing through the process of coupling with abrasive particles that helps to reduce cast iron durability.

To form complex carbides $(Cr,Fe)_7C_3$, giving maximum cast iron durability, chromium levels range from 14,0-20,0% is required. When the chromium content is less than 14%, the formation of carbides $(Cr,Fe)_7C_3$ along with carbides $(Fe,Cr)_3C$ is possible reducing cast iron durability. When the chromium content is more than 20.0%, large and fragile carbides $(Cr,Fe)_{23}C_6$ appear in the iron structure, resulting in wear-resistant properties reducing.

Vanadium in the range of 3.0-9.0% forms special VC carbides with carbon of high microhardness (~ HV 3000). Moreover, two types of eutectic are formed in the iron struc-

ture: double austenitic-vanadium-carbide and triple austenitic-chrome-vanadium-carbide, which, being the composite strengtheners, greatly increase cast iron durability.

Investigations were carried out on Fe - C - Cr - V alloys, containing 2.6-3.2% C, 14,0-20,0% Cr, 3,0-9,0% V. The amount of silicon and manganese in the experiment alloys was at the permanent level: Si (0,4-0,6%); Mn (0,4-0,6%). The experimental alloys were melted in the induction furnace IST-006 with the basic lining. The cooling rate influence on the structure and wear resistance during crystallization was studied on the iron samples, poured into dry and wet sand and clayed molds (SCM) and casting mold [1, 2].

The chemical composition of the samples was determined by an emission spectrometer «Bird» and by a spectrometer OBLF QSG 750 GOST 18895-97.

The structure and phase composition of cast irons were examined with the help of metallographic and x-ray methods. X-ray imaging was carried out on a DRON-UM1 diffractometer (in the cobalt Kα radiation). The diffractometer was connected to a PC. Phase analysis was carried out with the help of XRAYAN program and PDF database.

Quantitative metallographic analysis, automated processing of microhardness measurement results were performed using a Thixomet PRO image analyzer. Microhardness measurement was carried out using a PMT-3 according to GOST 9450-76.

Micro X-ray spectrum studies of phase components in alloys were carried out using scanning electron microscopes «JEOL» JSM-6460 LV, «TESCAN VEGA II XMU», «Camscan» with micro X-ray spectrum analyzers.

Comparative tests of alloy and cast iron wear resistance in rubbing with semifixed abrasive particles were carried out according to GOST 23.208-79. Wear-out was performed by abrasive particles of various hardness (electrocorundum and periclase), allowing to define various mechanisms of wear-out. Testing corundum, whose hardness (20-22 hPa) is comparable with vanadium carbide hardness and exceeds chromium carbide hardness and martensite-austenite matrix, the main mechanism of surface destruction is microcutting. Periclase hardness (10-12 hPa) is lower than vanadium carbide hardness and close to chromium carbide and metallic matrix hardness, therefore coupling iron with periclase plastic ousting is the main wear-out mechanism.

Phase composition of chromium-vanadium irons in as-cast state presents α-phase (martensite), γ-phase (austenite), vanadium carbide (VC), chromium carbide (Fe, Cr, V)$_7C_3$. The combination of these phases provides two binary eutectics γ + VC, γ + (Fe, Cr, V) $_7C_3$ and triple eutectic γ + (Fe, Cr, V) $_7C_3$ + VC while crystallizing. The coexistence of carbides of different forms and types is determined by iron composition and its crystallizing conditions.

Carbide and metallic matrix composition is variable and depends on chemical composition of the alloy and cooling rate during solidification. Carbides (Fe, Cr, V)$_7C_3$ contain 26,0-48,0% iron, 41,0-52,0% chromium, 9,0-22,0% vanadium, vanadium carbide dissolves iron partially (up to 2,0-5,0%), chromium dissolves iron some more – (8,0-16,0%) [3].

The determination of vanadium carbide volume quantity was performed on unpickled sections. The determination of the chromium carbide amount and size, the volume quantity of eutectics and their dispersity was carried out on sections after pickling.

Depending on iron composition the following types of alloy structures are formed (structural classes) [4]:

1 – hypoeutectic, consisting of excessive austenite dendrites (or products of its decomposition) and triple eutectics γ + (Fe, Cr, V) $_7C_3$+ VC;

2 – structure, consisting of two eutectics γ + VC (spherulitic form) and γ + (Fe, Cr, V) $_7C_3$ + VC;

3 – structure, consisting of two eutectics γ + (Fe, Cr, V) $_7C_3$ and γ + (Fe, Cr, V) $_7C_3$ + VC;

4 – structure, consisting of pre-eutectic VC carbides and eutectic γ + (Fe, Cr, V) $_7C_3$ and γ + (Fe, Cr, V) $_7C_3$ + VC;

5 – structure, consisting of excessive VC carbides (or carbides (Fe, Cr, V) $_7C_3$) and eutectics γ + VC, γ + (Fe, Cr, V) $_7C_3$ + V (Fig. 1).

Eutectics γ + (Fe, Cr, V) $_7C_3$ and γ + (Fe, Cr, V) $_7C_3$ + VC are socket-shaped in cross section, and fan-shaped in longitudinal section.

Composition, structure and carbide phase properties depend on the ratio of chromium and vanadium in cast irons. When the content of carbon and alloying elements is excessive, massive branched dendrites of primary vanadium carbides are formed (see Fig. 1).

The chromium increasing in the alloy causes vanadium content reducing in the composition of carbides VC and (Fe, Cr, V) $_7C_3$. It manifests in microhardness decreasing of vanadium carbide from 22 to 18 GPa and complex chromium carbides from 16 to 10 GPa. The increasing of vanadium and carbon concentration in the alloy reduces iron content in carbides and increases chromium and vanadium content. As a result, carbide (Fe, Cr, V) $_7C_3$ microhardness rises up to 16-17 GPa.

The cooling rate increasing leads to the following change in carbides composition: reduces chromium content from 10 to 8% in VC carbide, increases iron content from 37 to 47% and reduces chromium content from 51 to 41% in complex carbide (Fe, Cr, V) $_7C_3$. As a result, the alloying level of metallic matrix increases.

Carbide phase volume in eutectics γ + (Fe, Cr, V) $_7C_3$ and γ + (Fe, Cr, V) $_7C_3$ + VC is 28-36%, in eutectic A + VC the amount of carbides is less – 10-15%. The difference in the eutectic structure determines their different properties.

Eutectic compositions are crystallized within the temperature range and have variable phase composition (Table 1), different density (by changing the amount of carbides in the eutectic, intercarbide distance) and carbide phase dispersion, depending on alloy chemical composition and cooling rate during solidification. Eutectic type and proportion in the structure of iron also depend on the alloy composition and cooling conditions, determining cast iron mechanical properties and wear resistance in wearing-out by different hardness abrasive.

Table 1

The influence of cooling conditions on the amount of martensite q**α**, austenite q**γ**, complex chromium carbides q1and vanadium q2, %

Dry SCM				Wet SCM				Chill mold			
$q_α$	$q_γ$	q_1	q_2	$q_α$	$q_γ$	q_1	q_2	$q_α$	$q_γ$	q_1	q_2
67,4	3,5	27,6	1,4	48,1	8,4	40,4	2,1	19,0	31,61	51,1	3,9

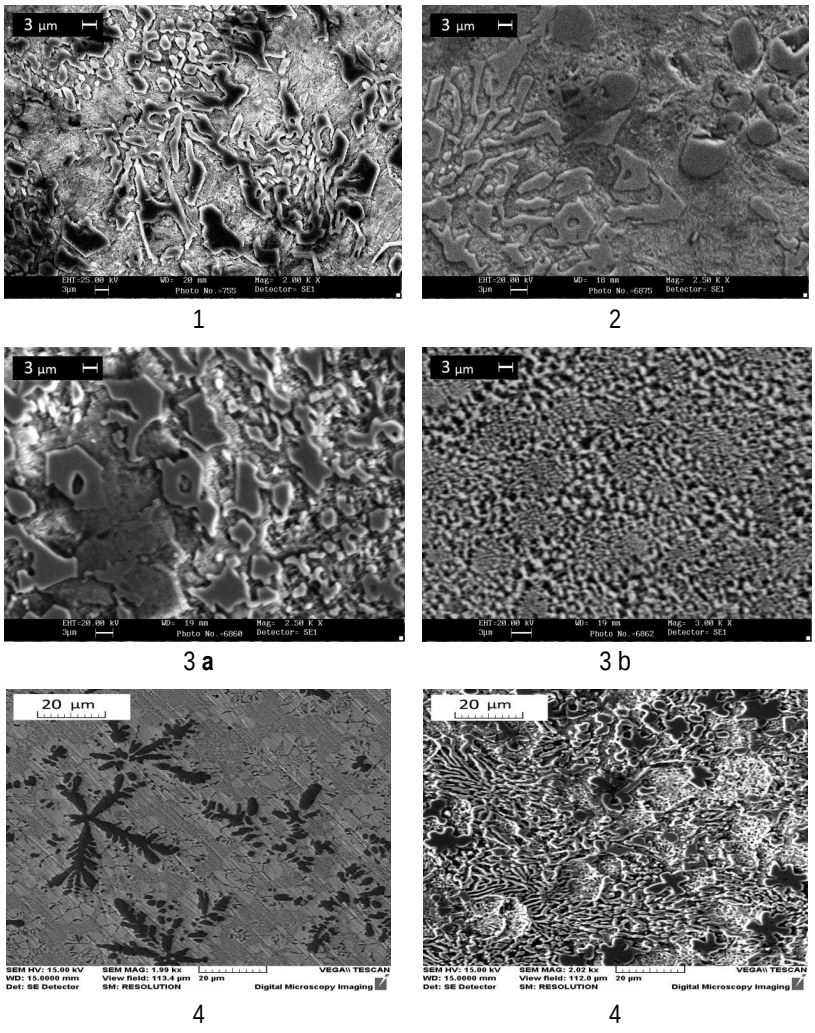

Fig. 1. Types of chrome-vanadium iron structures: 1 – A dendrites and eutectic **γ** + (Fe, Cr, V) $_7C_3$ + VC; 2 – eutectics **γ** + VC and **γ** + (Fe, Cr, V) $_7C_3$ + VC; 3 – eutectics **γ** + (Fe, Cr, V) $_7C_3$ and **γ** + (Fe, Cr, V) $_7C_3$ + VC (a - dry SCM; b - chill); 4 – excessive VC carbides and eutectics **γ** + VC (fibrous form), **γ** + (Fe, Cr, V) $_7C_3$ + VC; 5 – excessive VC carbides and eutectics **γ** + (Fe, Cr, V) $_7C_3$ and **γ** + (Fe, Cr, V) $_7C_3$ + VC

The features of formation of structure and properties of different structural types (classes) cast irons have been studied. There is one eutectic γ + (Fe, Cr, V) $_7C_3$ + V in cast iron structure of **the first structural class**. Complex (Fe, Cr, V) $_7C_3$ carbide is the predominant phase in the ternary eutectic.

3% vanadium content is sufficient concentration when it is not only in the solid solution and is a part of complex carbide (Cr, Fe) $_7C_3$, but forms separate VC carbides in the form close to spherical. The maximum size of carbides is 2, 5-6, 8 microns; the average size is 1.0-2.8 microns. Vanadium carbide is on chromium eutectic carbides.

With increasing chromium, carbon content and cooling rate, the volume fraction (from 58,8,0 to 27.6%) and primary austenite dendrites sizes (the average size from 13.7 to 28.0 mm) decline, the dispersion and the volume fraction of austenite--chromium carbide eutectic increase (Fig. 2a, b). Eutectic microhardness changes slightly 6.0-6.8 GPa. Hardness and wear resistance increase.

The cooling rate increasing causes martensite quantity reduction, but amount of austenite, at the same time, increases. This can be explained by matrix chemical composition changing: chromium content increases and iron content decreases, vanadium content changes slightly.

The increasing of chromium concentration in the alloy is accompanied by chromium content from 10% to 15% increasing in the metallic matrix of austenite--chromium carbide eutectic and reducing iron concentration from 87 to 80%. This causes temperature reducing at the martensite start M_s and results in martensite quantity reduction. Chromium content in chromium carbides increases from 40% to 50%, but vanadium content reduces. Matrix microhardness decreases from 7.1 to 4.4 GPa. Chromium carbide microhardness decreases from 15.1 to 13.9 MPa.

The metallic matrix consists of austenite and martensite, the ratio of these phases depends on the chemical composition of metallic matrix, which is defined by alloy composition and casting mould type. In chill casting chromium and vanadium content in the matrix increases, that causes the increasing of austenite proportion in the structure.

Different structural types are formed in cast irons of the following compositions, %: type 1 – 2,6 C; 14-20 Cr; 3 V and 3,2 C; 14 Cr; 3 V; type 2 – 2,6 C; 14 Cr; 9 V; 2,6 C; 14-20 Cr; 9 V; 3 type – 3,2 C; 20 Cr; 3 V; 4 type –3,2 C; 14 Cr; V 9 and 2.9 C, 17 Cr , 6 V; 5 type-3,2 C; 20 Cr; V 9.

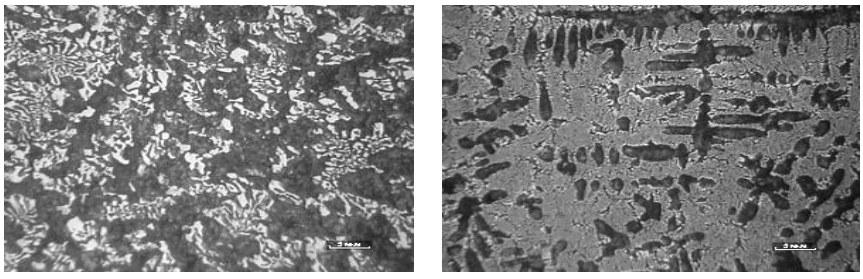

a b

Fig.2. Microstructure of the 1st type chrome-vanadium cast irons, poured into dry SCM (a) and chill mold (b), x500

The phase composition of cast iron samples, containing 3.2% C, 14% Cr, 3% V, depending on the cooling conditions is shown in Table 1.

Durability corundum is small and increases along with the growing of metallic matrix microhardness and the amount of cast irons carbide phase volume. Durability of chrome-vanadium cast irons containing periclase insignificantly depends on carbide phase volume and cast iron hardness, but depends on austenite quantity and its metastability towards straining martensitic transformation. Metastable austenite, being transformed into strain martensite during the wearing, strengthens the surface and improves durability (Table 2).

High chrome-vanadium cast iron durability under conditions of plastic push-off mechanism wear-out is due to surface layers hardening because of phase transformations and phase straining hardening.

Table 2

The influence of cooling conditions on the amount of transformed austenite $q_{\gamma p}$, H_a/H_b ratio and wear resistance in corundum K_c and periclase K_p

Mould type	$q_{\gamma p}$,%	H_a/H_b* corundum	H_a/H_b periclase	K_c	K_p
Dry SCM	0	1,3	1,1	4,2	17,6
Wet SCM	0	1,7	1,3	4,9	43,8
Chill mold	23,0-25,0	2,2	2,0	5,4	108,0

* H_b и H_a– microhardness of the metallic matrix before and after wear

The absence of straining martensitic transformation in cast irons, poured into dry and wet SCM, can be explained by a large amount of cooling martensite in the metallic matrix structure. Strain martensite formation during cast iron wear-out with corundum and periclase is relieved in the structure with metastable austenite predominance.

The features of the 2nd and 3d class structure formation. The structure of the 2nd class is formed in cast irons, containing 2.6% C; 14-20% Cr and 9% V; the structure of the 3d class is formed in cast iron composition,%: 3.2 C, 20 Cr; 3 V. Cast iron structure consists of two eutectics (refer to Fig. 1, 2 and 3). There is less amount of carbide phase in eutectic γ + VC than in eutectics γ + (Fe, Cr, V) $_7C_3$ and γ + (Fe, Cr, V) $_7C_3$+ VC.

With the help of X-ray mapping concentrated eutectic irregularities, determining their structure and properties, were revealed (Fig. 3).

With chromium content of 14% in the alloy the metallic matrix chemical composition in vanadium eutectic of irons of the 2nd structural class is,%: 5,79 V; 11,4 Cr and 82,0 Fe; ternary eutectic matrix composition is,%: 1,7 V; 13 9 and Cr 83,3 Fe.

The increasing of chromium content in the alloy up to 20,0% alters phase composition. Vanadium content reduces to 2.7% , but chromium content increases to 12.5% in metallic matrix of eutectic γ + VC. The amount of vanadium and chromium in eutectic matrix γ + (Fe, Cr, V) $_7C_3$ + VC increases up to 7.1 and 14.9%. That concerns not only with chromium quantity increasing in the alloy, but also with changes of volume fraction and vanadium and chromium carbide content. The difference in eutectic matrix compositions is shown in their properties: eutectic metallic matrix microhardness γ + (Fe, Cr, V) $_7C_3$ + VC is under 1200-2000 MPa. Thus, changing the quantitative ratio of eutectics with different properties it is possible to obtain various properties of the alloy in whole.

The volume fraction and size of binary eutectic vary depending on carbon and alloying elements content and cooling conditions. With increasing chromium content and the cooling rate the volume fraction of ternary eutectic, dispersion eutectic γ + (Fe, Cr, V) $_7C_3$ and γ + (Fe, Cr, V) $_7C_3$ + VC increase (see Fig. 1, 3a and 3b).

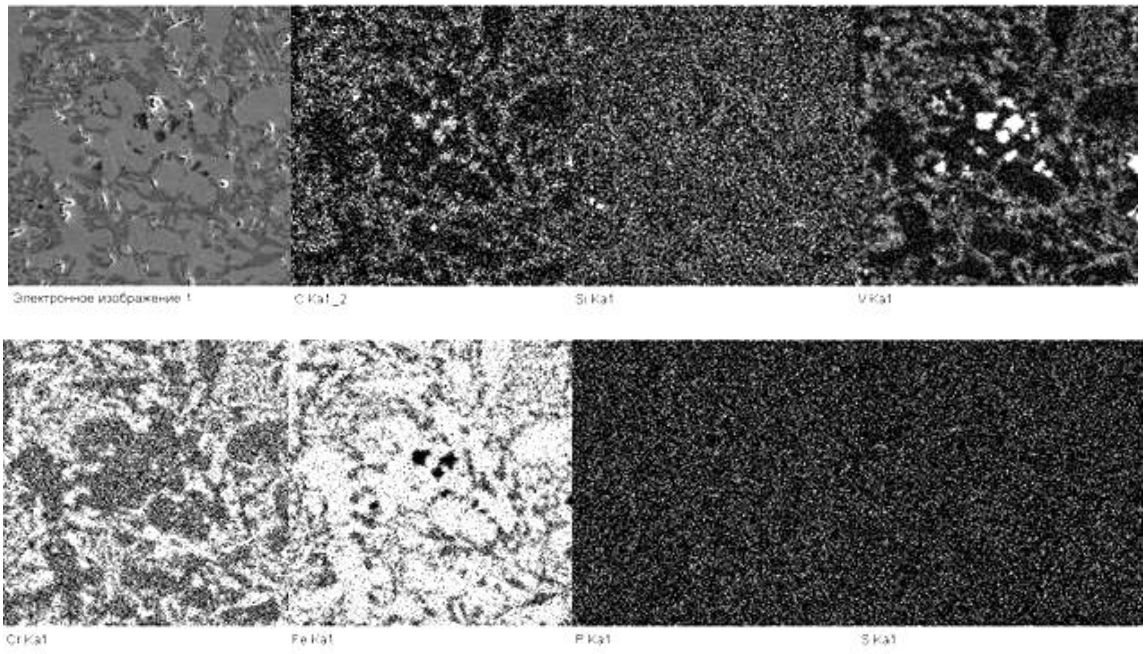

Fig. 3. Electron micrograph and element distribution in the structural constitutes of cast iron with eutectics γ + VC and γ + (Fe, Cr, V) $_7C_3$ + VC

In increasing cooling rate the density and dispersion of eutectic γ + VC increase (the number of vanadium carbides increases from 2705 up to 16410 1/mm^2, interparticle distance decreases from 62 to 21 microns and carbide size decreases from 6.5 to 2.8 microns).

Cooling martensite 72,2-90,0% prevails in cast iron structure of 2nd and 3^{d} classes, filled in dry and wet SCM.

Wear resistance of cast irons with corundum, poured into SCM is 4,5-10,1 units, with periclase it is 10,8-28,7 units. Wear resistance of cast irons of the 2nd and 3^{d} structural classes is higher than wear resistance of cast irons of the 1st type. Wear resistance of cast irons of the 2nd class is higher because of the presence of 7,5-9,1% vanadium carbides in the structure. Wear resistance of cast irons of the 3^{d} class is higher because of the presence 30,2-72,3% complex chromium carbides. In the cast irons of the 1st class volume ratio of vanadium carbides is 0,3-5,2%, 20,0-51,5% of chromium carbides.

In pouring into a mold the austenite proportion in iron-structure increases, straining martensitic transformation takes place with corundum and periclase wearing-out, resulting in significantly hardened surface (microhardness increases in 1.5-2.0 times). Wear resistance with corundum increases up to 9,1-13,0 units and in periclase up to 19,8-60,6 units.

There are dendrites of excessive vanadium carbides in the structure of irons of **the 4th and 5th structural classes**. The structure of irons of the 4th class consists of excessive VC carbides and eutectic γ + VC and γ + (Fe, Cr, V) $_7C_3$ + +VC; of 5th class of excessive VC carbides and eutectic γ+ + (Fe, Cr, V) $_7C_3$ and γ + (Fe, Cr, V) $_7C_3$ + VC (see Fig. 1, 4, 5). The structure of the 4th type is formed in cast irons with the following composition, %: 3,2 C; 14 Cr; V and 2.9 C 9, 17 Cr; 6 V; the structure of the 5th type is formed in cast irons with the following composition, %: 3,2 C; 20 Cr; V 9.

Using X-ray mapping the element distribution between iron structural components of the 4th and 5th structural classes was detected (Fig. 4, 5).

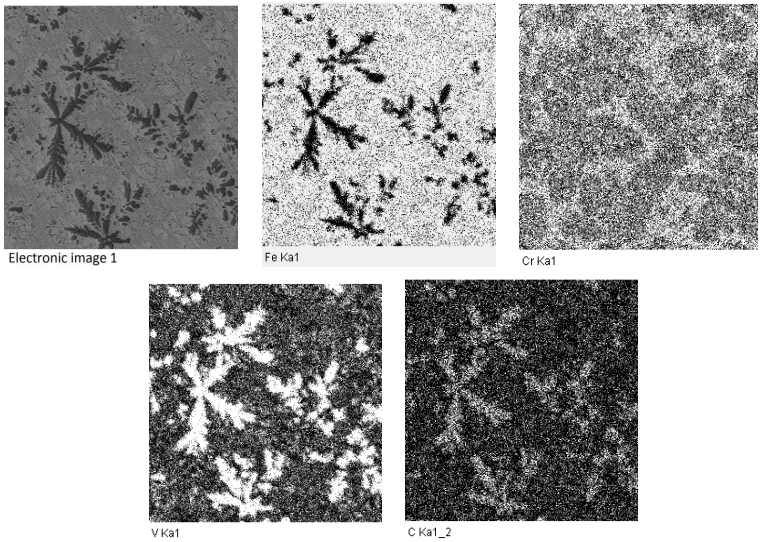

Fig. 4. Electron micrograph of iron of the 4th structural class and element distribution in structural components

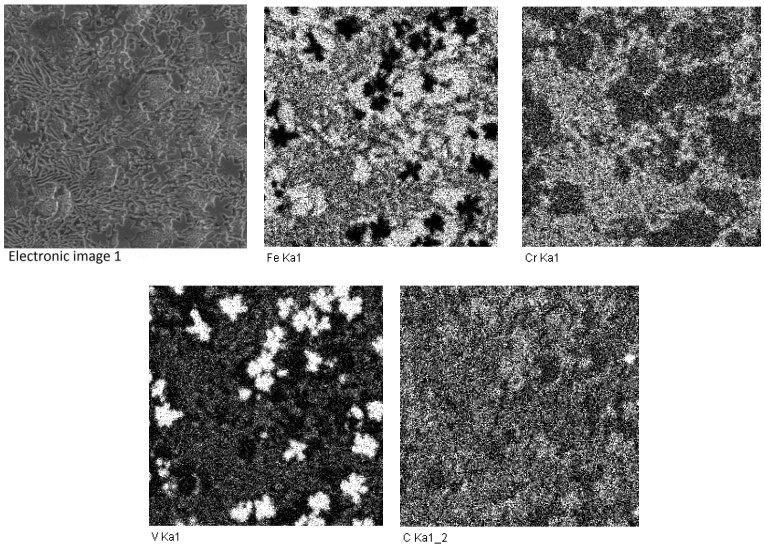

Fig. 5. Electron micrograph of cast iron of the 5th structural class and element distribution in structural components of cast iron with eutectics **γ** + VC and **γ** + (Fe, Cr, V) $_7C_3$ + VC

With cooling rate increasing volume fraction and sizes of vanadium carbides, binary eutectics decrease, the volume fraction of ternary eutectic increases. For example, in cast irons of the 4th class in casting into dry SCM volume fractions of structural components are as follows: 11.2% of vanadium carbides, 53.8% binary eutectic, 34.9% triple eutectic. In pouring into the mold the volumetric proportions of excessive VC carbides, eutectic γ + VC and γ + (Fe, Cr, V) $_7C_3$ + VC are 9,3; 38,5 and 51,7%, accordingly.

In the case of high cooling speed (chill casting) the nature of excessive phase changes in the alloy structure containing 2.9% C; 17% Cr; 6% V. Complex carbide (Fe, Cr, V) $_7C_3$ (Fig. 6b) becomes the excessive phase instead of vanadium carbide (Fig. 6a).

Wear resistance of cast irons of the 4th, 5th structural classes is 8,0-14,0 units with corundum, 33,0-99,0 units with periclase.

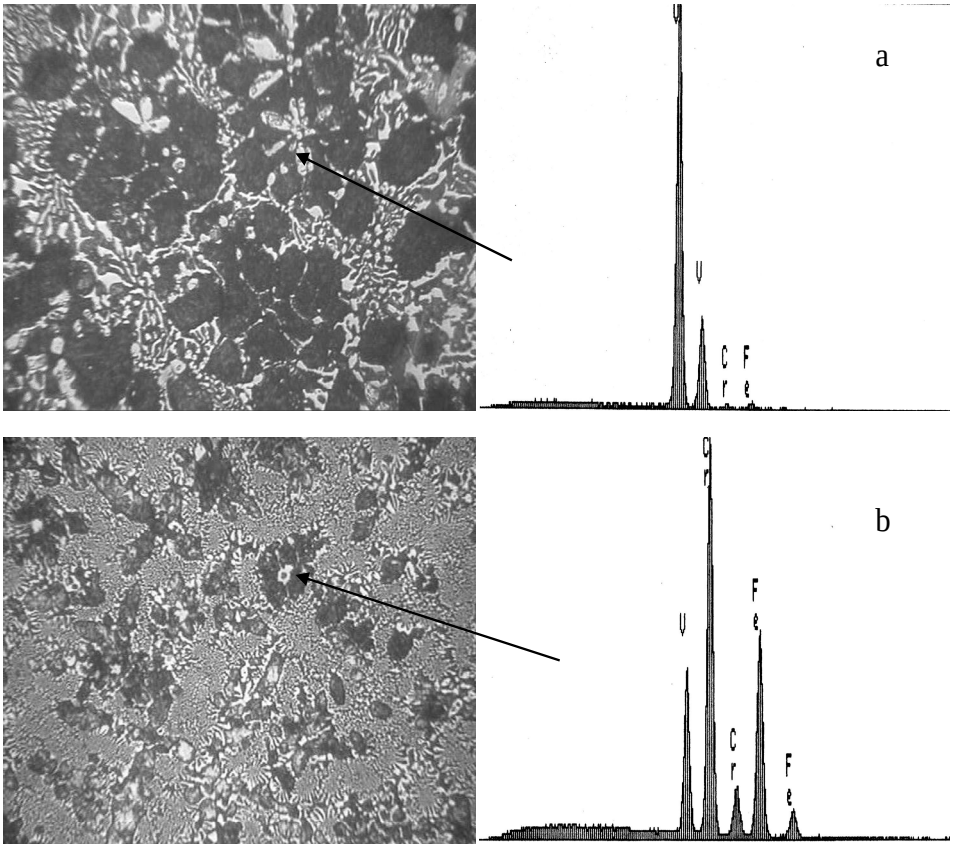

Fig. 6. Micrographs of irons of the 4th structural class and spectrograms of composition of excessive vanadium carbides (a) and chromium (b), x1000

As a result of analysis of the chemical composition and cooling condition effect on the types of chrome-vanadium iron structures in the studied concentrated intervals laws of morphology of excessive phases, eutectic composition and metallic matrix were established, which allowed to offer the classification according to the following criteria:

- ***according to the metallic matrix type:*** mainly martensitic and martensitic- austenite;

- ***according to the eutectic type:***

• with eutectic γ + carbides of M_7C_3 type;

• with eutectic γ + carbides of MC type, such as VC;

• with eutectic γ + M_7C_3 and MC, example (Fe, Cr)$_7C_3$ and VC, etc.;

– ***according to the number of eutectics and their constitutive phases:***

• cast irons with double and ternary eutectics (γ+MC and γ+MC+ M_3C; γ +MC and γ +MC+ M_7C_3, γ + M_7C_3 and γ +MC+ M_7C_3);

• cast irons with two double and ternary eutectics (γ +M_3C, γ + M_7C_3, γ+ M_7C_3 +MC) and others;

– ***according to the eutectic morphology:***

• spherulitic shape eutectic γ + VC;

• eutectics γ + (Fe, Cr,) $_7C_3$ and γ + (Fe, Cr, V) $_7C_3$+ +VC, having a socket shape in cross-sectional view, and a fan shape in longitudinal section;

– ***according to the phase morphology, forming eutectic:***

• branched (fibrous (γ + VC));

• compact (grained (γ + VC));

• rod (γ + Cr_7C_3).

References

1. Kolokoltsev V.M., Petrochenko E.V., Molochkov P.A. Complex effect on the structure of wear-resistant white cast irons in order to improve operational stability of castings *Vestnik Magnitogorskogo gosudarstvennogo tehnicheskogo universiteta im. G.I. Nosova*. [Vestnik of Nosov Magnitogorsk State Technical Univeersity]. 2004, no 4, pp. 23-29.
2. Kolokoltsev V.M., Petrochenko E.V., Molochkov P.A. Structure and wear resistance of chrome-vanadium cast irons. *Izvestiya vuzov. Chernaya metallurgia*. [Izvestiya VUZ. Ferrous metallurgy]. 2004, no 7, pp. 25-28.
3. Petrochenko E.V., Valishina T.S. The influence of the chemical composition, solidification conditions and heat treatment modes on microstructure features, mechanical properties and special properties of chrome vanadium white cast irons. *Izvestiya vuzov. Chernaya metallurgia*. [Izvestiya VUZ. Ferrous metallurgy]. 2009, no 2, pp. 39-42.
4. Petrochenko E.V. The relationship of the chemical composition, structure and properties of complex-alloyed white irons in the as-cast condition. *Izvestiya vuzov. Chernaya metallurgia* [Izvestiya VUZ. Ferrous metallurgy]. 2012, no 3, pp. 51-55.

Vdovin K.N., Gorlenko D.A., Zavalischin A.N.

STRUCTURE CHANGES OF CHROMIUM-NICKEL INDEFINITE CAST IRONS IN HEATING

Abstract. The paper studies the processes taking place in chromium-nickel indefinite cast iron heating. Intervals of these processes and their changes depending on the heating rate were defined.

Keywords: indefinite cast iron, abstraction, phase transformations, carbides, carbon, austenite.

Chromium – nickel cast irons are assigned to the class of alloy, wear resistant cast irons. Long run service ability without damage and with minimal wear is the main requirement for this group of irons [1].

There are considerable shrinkage and thermal stresses in the castings after solidification and cooling due to the production large mass and alloy cast iron low thermal conductivity, which are supplemented by phase strain hardening $\gamma \rightarrow \alpha$ transformation. Therefore, the product usage in the as-cast condition is not desirable, in view of possible product destruction. Long (for about six months) maturing in storehouses is one of the internal stress relieving methods. This is accompanied by a 30% stress relaxation. That is enough to increase service durability and preserve production hardness and, consequently, durability. It is not always economically effectually, because large areas are required. Tempering is the replacement of natural maturing, wherein the relaxation processes are much faster and required time varies from several hours to several days, depending on the product shape and massiveness. There is no common opinion concerning the tempering temperature. High temperature promotes more rapid processes and a 70% residual stress relieving, but wherein there is a significant decrease in hardness.

Ageing lower temperature results in only a 30 ... 50% stress relieving, wherein the hardness and wear resistance are less reduced, but the possibility of early cracking increases [2, 3]. Therefore, it is necessary to choose the optimal ratio between the structure, that determines product properties, and stresses by selecting the required tempering temperature.

Therefore, the aim of this work was to study the structure formation and its properties in cast iron during the heating after crystallization.

The studies were carried out on iron samples; iron chemical composition is shown in Table 1.

Table 1

White iron chemical composition, %

C	Si	Mn	S	P	Cr	Ni
3.05-3.20	0.7-1.0	0.75-0.95	0.015	0.045	1.5-1.85	4.0-4.6

Samples were selected from the castings after crystallization. The microstructure was studied with the help of a light microscope MEIJI 2700 at 50- to1000-fold magnification using an image analyzer Thixomet PRO. The processes, taking place during cast iron heating were determined with the help of a thermal analyzer NETZSCH STA 449 F3 Jupiter. The sample heating rate was from 5 to 30°C / min. The average microhardness of carbide and metal base stock was defined using a PMT-3 device, with 100 g load. To fix high-temperature structure, samples were cooled in water; thereby the secondary phase precipitation and austenite disintegration were mitigated.

Derivatograms exhibits some specific peaks, obtained in a 5°C / min heating rate, corresponding to the structural and phase transformations being accompanied by thermal effects (Fig. 1).

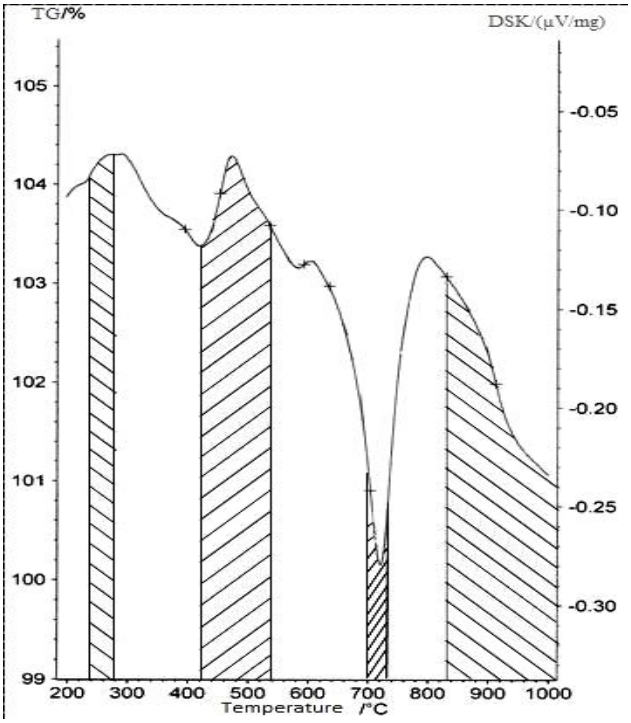

Fig. 1. Derivatogram, obtained in cast iron heating

The first reaction to the heating is observed when the temperature is in the range of 250-280°C, herewith with heating rate increasing, the range upper limit shifts to higher temperatures. The second peak at a 5°C / min heating rate occurs when the temperature is in the range of 420 ... 540°C.

With heating speed rising, reaction temperature range increases, along with the simultaneous temperature rising proportionally to the heating rate within the interval boundaries.

The third reaction to the heating is observed when the temperature is in the range of 700 ... 740°C and the temperature at the beginning and at the end does not significantly depend on the heating rate. The fourth reaction

takes place at temperatures above 830°C, and the starting temperature increases with the heating rate rising.

Exothermic peak at a temperature range of 260 to 280°C agrees with the secondary carbides releasing (Fig. 2a, b).

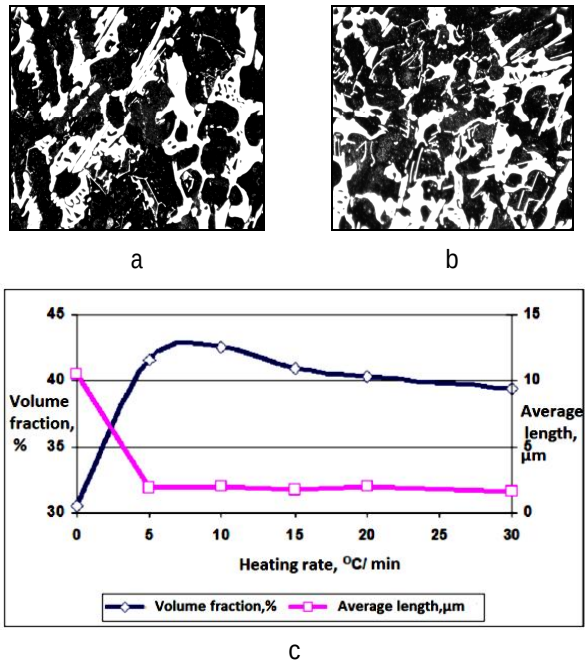

Fig. 2. The iron microstructure in as cast state (a), x200 after tempered at 300°C, 15 minutes ageing and quenched (b), x200 volume ratio and carbides average length dependence upon the heating rate (c)

The temperature reduction decreases the diffusion rate, making carbides precipitation difficult, and the abstraction process almost completely stops when the temperature is below 180°C. The most intense secondary carbides precipitation occurs at 10 ... 15°C / min heating rates (Fig. 2 c). The average microhardness of new extracted carbides increases from 810 to 1490 HV units.

Further heating speed rising produces a decrease in secondary carbides precipitation density, wherein the heating rate does not affect on the secondary carbides size. The average carbides microhardness decreases due to the «cast» carbides prevalence (Table 2).

Table 2

The base stock and carbides hardness and microhardness dependence on the heating rate

Heating rate, °C/ min	Hardness HRC	The average microhardness, HV	
		base stock	carbides
5	53,6	540…570	810…990
10	52,1	520…550	830…1440
15	54,5	490…550	980…1490
20	54,0	440…480	860…1100
30	53,6	440…490	830…1090

Temperature rising mitigates carbides precipitation and is replaced by a more active process of fine flaky graphite particles precipitation (Fig. 3a, b).

Endothermic reaction occurring in the temperature range of 350 to 550°C is in agreement with it (Fig. 1). The solid graphite mass is proportional to the ageing time and heat temperature.

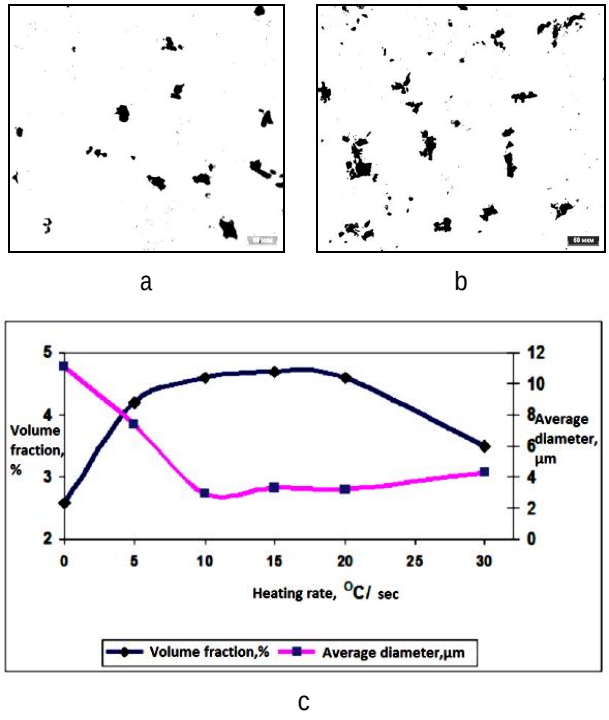

Fig. 3. The cast iron microstructure in as-cast condition (a) (not pickled.) X500; tempered at 550°C, 30 ageing and quenched (b), (not pickled.) x500; graphite nodules volume mass and average diameter dependence upon the heating rate (c)

The precipitation temperature range increasing results in the graphite quantity increasing with the heating rate rising to 15°C / min, and their average size is reduced, because of new impurities formation. With further heating rate increasing, the graphite quantity is reduced due to the precipitation time decreasing, and the average graphite size grows at the expense of the precipitation on the existing impurities (Fig. 3 c).

With ageing time increasing, temperature ranges of carbides and graphite precipitation collide and their simultaneous formation becomes possible. Therefore, it is possible to vary the required ratio of these phases by the heating rate and ageing time variation.

Endothermic reaction at the temperature of 720°C agrees with α-γ phase transformation, since other transformations and precipitations are mitigated by high heating rates. The subsequent high cooling rate stabilizes austenite and allows austenite and carbides, formed during crystallization, to be observed in the structure.

Consequently, in heating above 720°C, the cast iron structure is represented by austenite and carbides (Fig. 4), which begin to dissolve at the temperature of about 830°C, that is in agreement with endothermic reaction in the curve (see Fig. 1).

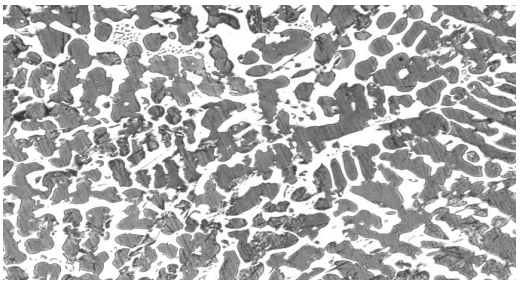

Fig.4. The cast microstructure after heating to 740°C, 10 minutes ageing and cooled in water, x100

With heating rate increasing, the temperature of carbides dissolving starting slightly rises and with the increasing of austenitizing temperature and ageing time, carbides volume fraction decreases from 30.5 to 16.0% (Fig. 5).

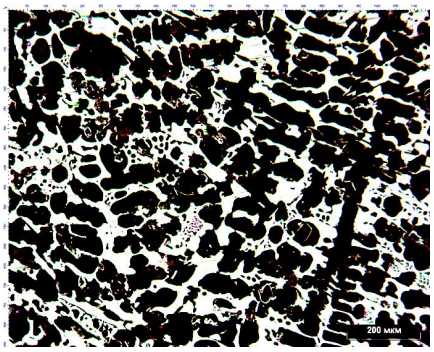

a

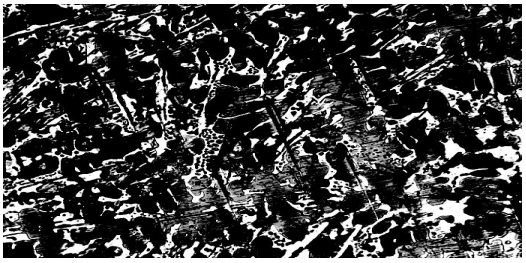

b

Fig. 5. Cast iron microstructure, x100: a – as-cast, b – after heating up to 1100 °C, 60 min ageing and cooling in water

Along with the carbides fraction reducing (Fig. 6 a) their microhardness decreases, resulting from elements redistribution between the eutectic carbides and the base stock (Fig. 6 b).

After 5 minutes ageing at the temperature of 900°C, the average microhardness falls from 1050 to 1000 HV units, at a 30 minutes ageing it reduces to 840 VH units, and it does not change at the further ageing. Ageing at the temperatures 1000 and 1100°C during one hour leads to the similar reduction of the average microhardness to 660 HV units.

Conclusions

1. Four thermal effects taking place during the process of indefinite chromium - nickel pig iron heating in the temperature range of 20 to 1100°C are observed in the derivatograms.

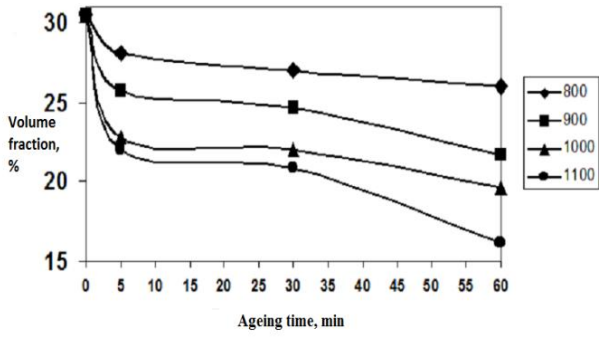

a

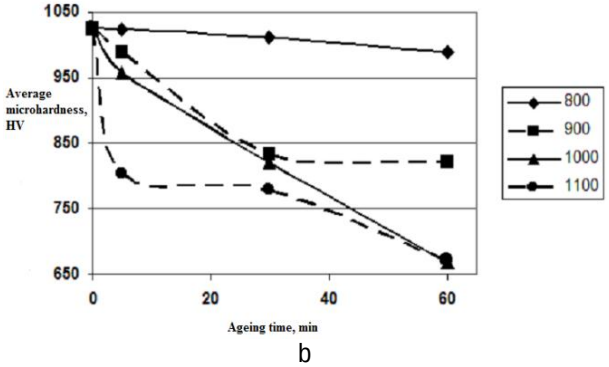

b

Fig.6. Volume fraction (a) and average microhardness (b) of carbides, depending on the temperature and ageing time

2. The first effect at the temperatures of 250 to 280°C matches to the secondary carbides precipitation. The graphite releasing takes place at the temperatures of 420 to 540°C. The third thermal effect is observed at the temperatures of 700 to 740°C and is connected with α-γ transformation. The latter effect occurs at the temperatures above 830°C and agrees with carbides dissolving.

3. With heating rate increasing, temperatures at the beginning and at the end of thermal effects shift. Temperature at the end of carbide precipitation shifts to the range of higher temperatures; temperature and range of graphite separation boundaries increase, the temperature of α-γ transformation is not significantly dependent on the heating rate, the temperature at the beginning of carbides dissolving increases proportionally to the heating rate.

4. In changing heating rate and temperature it is possible to control the phase relationship in indefinite chromium-nickel cast iron, which allows to adjust the tempering mode in order to obtain the required structures and properties.

References

1. Emelyushin A.N., Petrochenko E.V., Nefedjev S.P. Investigation of the structure and impact-abrasive wear resistance of coatings of Fe-C-Cr-Mn-Si system, additionally alloyed with nitrogen. *Svarochnoe proizvodstvo*. [Welding engineering]. 2011, no 10, pp.18-22.
2. Vdovin K.N., Gimaletdinov R.H., Kolokoltsev V.M. and others. *Prokatnye valki.* [Forming rolls]. Magnitogorsk, 2005, 543 p.
3. Vdovin K.N., Zaitseva A.A. Heat processing effect on roll-foundry iron, modified with boron. *Vestnik Magnitogorskogo gosudarstvennogo tehnicheskogo universiteta im. G.I. Nosova*. [Vestnik of Nosov Magnitogorsk State Technical Univeersity]. 2011, no 4, pp. 13-15.

Hamedon Z., Mori K.-I., Maeno T., YamashitaY.

HOT STAMPING OF TITANIUM ALLOY SHEET USING RESISTANCE HEATING

Abstract. A hot stamping process of a titanium alloy sheet using resistance heating was developed to improve the productivity. As the heating temperature increased, the bending load decreased and the titanium alloy sheet was successfully formed at elevated temperatures. As the heating temperature increased, the springback of the bent sheet decreased. Although needle-shaped martensite appeared at a heating temperature of 1050°C, the microstructure at a heating temperature of 880°C was similar to the as-received sheet. When the heating temperature increased to 880°C, the hardness increased to 370 HV20. It was found that the hot hat-shaped bending of the titanium alloy sheet using the resistance heating was effective in improving the productivity.

Keywords: Titanium alloy sheet, Ti-6Al-4V, hot stamping, resistance heating, springback.

1. Introduction

The usage of titanium alloy sheets for airplane parts increases due to the high strength at high temperatures, low density and high corrosion resistance, etc. Since the cold formability of the titanium alloy sheets is low, the sheets are generally formed at elevated temperatures. In coventional hot stamping using a furnace, the productivity is very low. The heating time of tools is about 2 h, and the heating time of the sheets in the furnace and the forming time are about several minutes, respectively.

Rapid resistance heating was effective in the hot stamping, only a time of 2 s to a heating time of 900°C. Resistance heating is generally employed for preheating of forging billets. Mori et al. have applied the resistance heating to the warm and hot stamping of ultra-high strength steel sheets [1], to the tailor die-quenching in hot stamping for producing ultra-high strength steel formed parts having a strength distribution [2], and to the spline forming of ultra-high strength steel gear drums [3], respectively. In addition, Mori et al. [4] have developed a punching process of ultra-high strength steel sheets using local resistance heating of a shearing zone. Although Ozturk et al. [5] applied the resistance heating to hot stamping of titanum alloy sheets, forming results were hardly shown.

In the present study, a hot bending process of a titanium alloy sheet using resistance heating was performed to increase the formability and to reduce the forming load. The springback and hardness of the hot bent sheet were also measured.

2. Procedure of hot stamping of titanium alloy sheet

2.1 Experimental procedure

An alpha-beta titanium alloy Ti-6Al-4V sheet (Al: 6.0%, V: 4.0%, Fe: 0.4%, O: 0.2%, C: 0.08%, N: 0.05%, H: 0.015%) having 1.2 mm in thickness was bent at elevated temperatures. The mechanical properties of the titanium sheet were measured in the uniaxial tensile test at different heating temperatures. A 50kN screw driven type universal testing instrument was used in the tensile test.

The variations of the tensile strength and elongation of the titanium alloy sheet with the heating temperature obtained by the tensile test are given in Fig. 1**.** As the heating temperature increases, the tensile strength decreases and the elongation increases, particularly above 560°C.

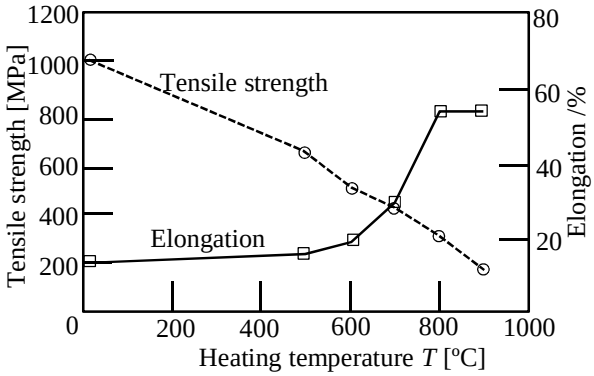

Fig. 1. Variations of tensile strength and elongation of titanium alloy sheet with heating temperature obtained by tensile test

The hot hat-shaped bending of the titanium alloy sheet using the resistance heating is shown in Fig. 2**.** The length and width of the sheet were 130 and 20 mm, respectively, and only the regions of 5 mm from both edges of the sheet were in contact with the electrodes, i.e. insufficient heating. During resistance heating, the sheet is not in contact with the die, punch and blankholders in order to prevent the heating of these tools.

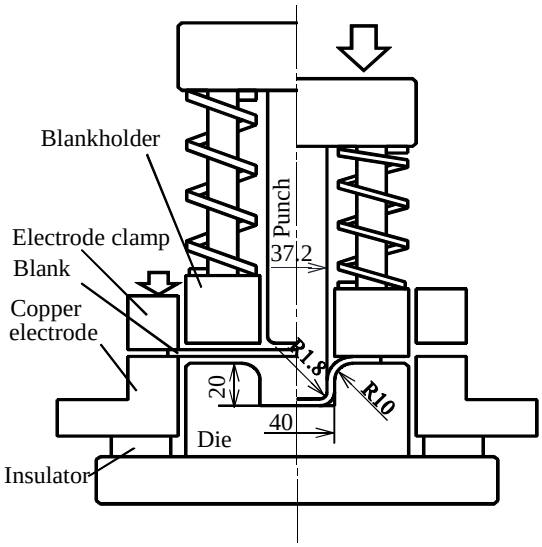

Fig. 2. Hot hat-shaped bending using resistance heating of titanium alloy sheet

A CNC servo press with a maximum load capacity of 800 kN is synchronised to a DC power supply with capacitors for the resistance heating, and the time interval between the end of heating and the beginning of the bending is only 0.2 s. The experimental conditions are given in Table.

Experimental conditions for hot bending

Sheet holder pressure [MPa]	0.6				
Electrode clamping pressure [MPa]	4				
Holding time at bottom dead centre t [s]	0, 3, 6				
Bending speed [mm/s]	150				
Current density [A/mm^2]	12.5				
Heating temperature T [ºC]	370	550	690	790	880
Heating time t_h [s]	2.8	4.9	6.1	7.3	8.0

2.2 Heating behaviour of sheet

The variation of the electrical resistivity of the titanium alloy sheet with the heating temperature is shown in Fig. 3. The variation of the electrical resistivity for the titanium alloy sheet is relatively small in comparison with the steel sheet. It is not easy to uniformly heat the sheet for the constant resistivity. The increase in resistance caused by the rise in temperature in local portions leads to the decrease in current, and thus the increase in temperature in these portions becomes small. The increase in resistivity has the function of uniform heating, and thus it is not easy to heat the titanium alloy sheet.

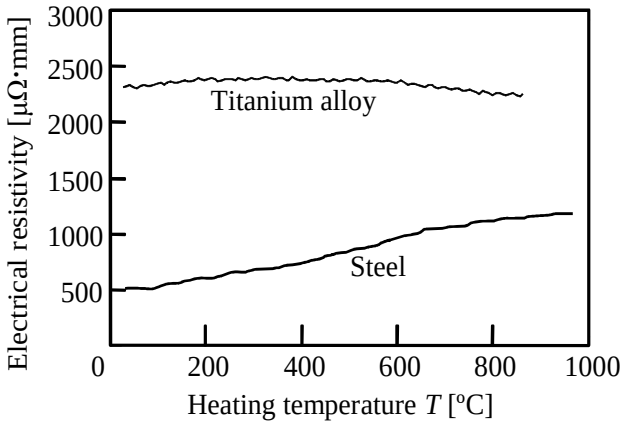

Fig. 3. Variations of electrical resistivity with heating temperature of titanium alloy and steel sheets

The distribution of heating temperature in the longitudinal direction of the titanium alloy sheet by the resistance heating is shown in Fig. 4. The heating temperature in the forming area is almost uniform, whereas both edges of the sheet are not sufficiently heated by the contact with the electrodes.

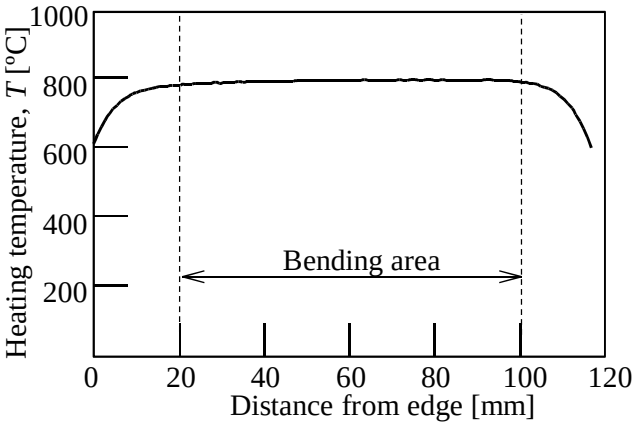

Fig. 4. Temperature distribution for resistance heating in longitudinal distance of titanium alloy sheet

3. Results of hot stamping of titanium alloy sheet using resistance heating

3.1 Stamped sheets

The hat-shaped bent sheet for resistance heating at T = 880°C is compared with that for furnace heating in Fig. 5. Although the springback and oxidation of the bent sheet for furnace heating are remarkably large, these are very small for resistance heating.

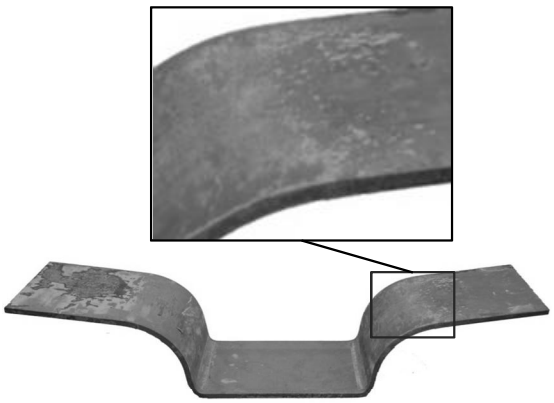

(a) Furnace heating, t_h = 240 s.

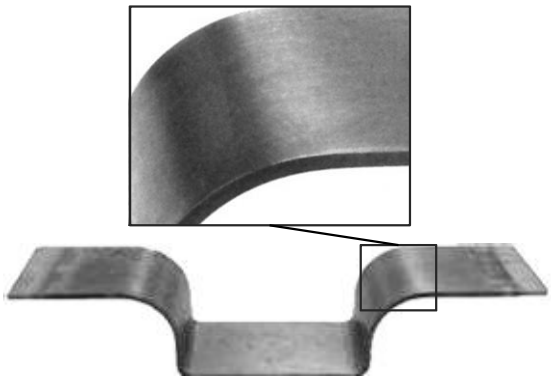

(b) Resistance heating, t_h = 8 s.

Fig. 5. Comparison between bent sheets for furnace heating and resistance heating for T = 880 ºC and t = 3 s

The non-destructive fluorescent penetrant test of the hat-shaped bent sheets was performed to check the occurrence of cracks. The reflective lighting of the bent titanium alloy sheet is shown in Fig. 6. Since the lighting was not observed for the bent sheets, no cracks occurred for the bent sheets.

(a) Example of reflective lighting for cracks

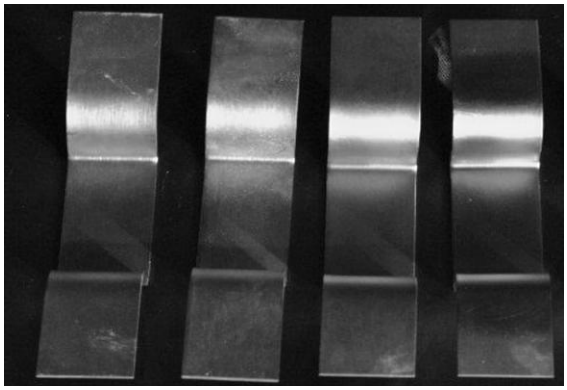

(b) T=560 ºC 690 ºC 790 ºC 880 ºC

Fig. 6. Bent sheets during non-destructive fluorescent penetrant test for t = 3 s

3.2 Bending load and springback

The relationship between the bending load and heating temperature is given in Fig. 7. Although the titanium sheet fractured at room temperature due to low ductility, the sheet was successfully formed at elevated temperatures above for T=370°C. As the heating temperature increases, the bending load decreases. The bending load for T=880°C is reduced from 6.5 kN at room temperature to 1.8 kN.

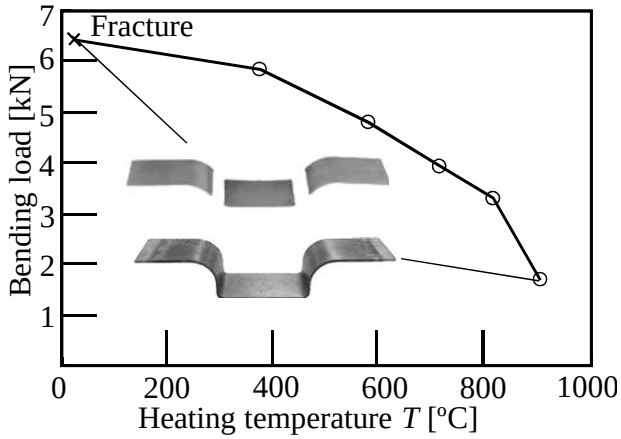

Fig. 7. Relationship between bending load and heating temperature for t=3 s

The relationships between the springback angle and heating temperature and between the corner radius and heating temperature in the hat-shaped bending for t = 3 s are illustrated in Fig. 8. As the heating temperature increases, the springback angle and the corner radius decrease. It is found that the hot bending is effective in preventing the springback of the titanium alloy sheet.

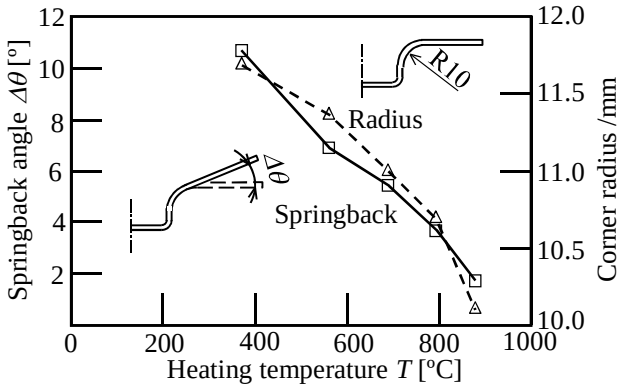

Fig. 8. Relationships between springback angle and heating temperature and between corner radius and heating temperature for t = 3 s

The relationships between the springback angle and holding time and the corner radius and holding time at the bottom dead centre for T=880°C are illustrated in Fig. 9. As the holding time increases, the springback angle and the corner radius decrease.

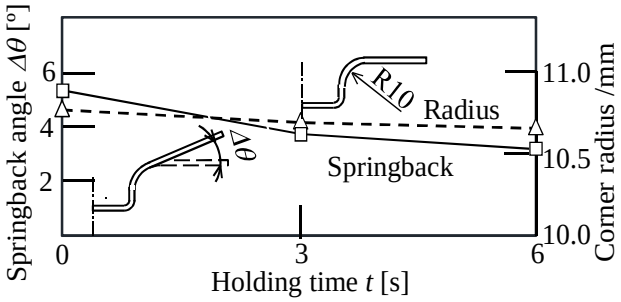

Fig. 9. Relationships between springback angle and holding time and between corner radius and holding time at bottom dead centre for T = 880°C

3.3 Microstructure and hardness of bent sheet

The microstructures of the bent sheet for the different heating temperatures are shown in Fig. 10. Although needle-shaped martensite having a low strength appears for T=1050°C, the microstructure for T=880°C is similar to that for the as-received sheet.

(a) As-received (b) T = 880 ºC (c) T = 1050 ºC

Fig. 10. Microstructures of bent sheet for different heating temperatures

The distributions of the Vickers hardness in the longitudinal direction for the different heating temperatures are shown in Fig. 11. The hardness at T=550 and 785°C is similar to that for the as-received sheet. When the heating temperature increases at 880°C, the hardness increases to 370 HV20. Therefore, the optimum heating temperature is T=880 ºC due the small springback, high hardness and no appearance of needle-shaped martensite.

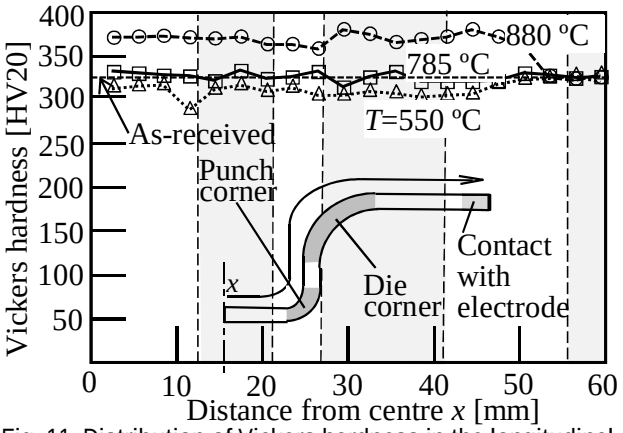

Fig. 11. Distribution of Vickers hardness in the longitudinal direction for different heating temperatures

4. Resistance heating of curved sheet

It is desirable in industry to bend curved sheets. For the curved sheets, the distribution of current density in the electrification direction becomes non-uniform as shown in Fig. 12(a), and thus the distribution of temperature becomes non-uniform. To obtain the uniform distribution of temperature, the electrodes are inclined as shown in Fig. 12(b).

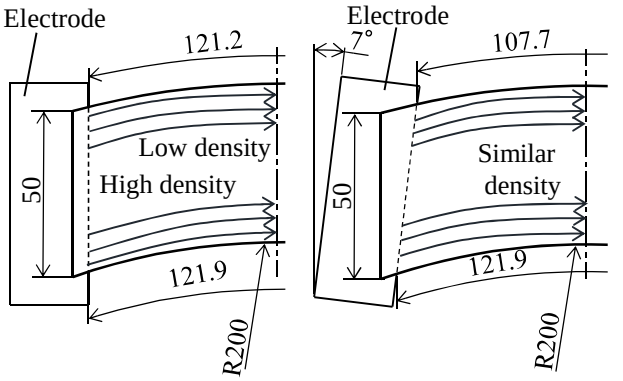

(a) Parallel electrodes (b) Inclined electrodes

Fig. 12. Distributions of current density in electrification direction of curved sheet for parallel and inclined electrodes

To calculate the distributions of heating temperature of the curved sheet for the parallel and inclined electrodes, the coupled thermal-electric analysis of the resistance heating was performed using the commercial FEM software ANSYS. In the calculation, the homogeneous contact between the sheet and the electrode was assumed. For the parallel electrodes, the distribution of temperature is not uniform as shown in Fig. 13(a), whereas the distribution of temperature in the bending area for the inclined electrodes is almost uniform, 825 ± 20°C as illustrated in Fig. 13(b).

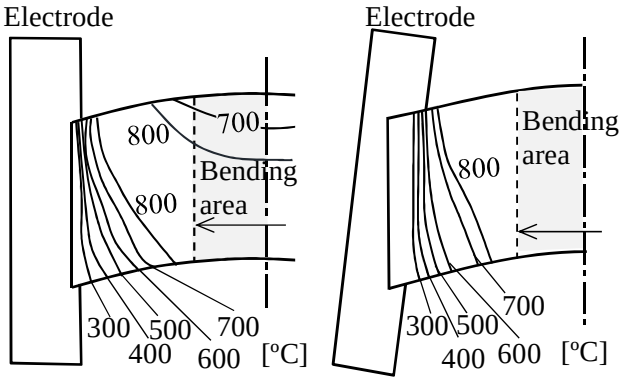

(a) Parallel electrodes (b) Inclined electrodes

Fig. 13. Distribution of temperature in curved sheet having thickness of 1.6 mm for current of 750 A.

5. Conclusions

The hot hat-shaped bending of the Ti-6Al-4V titanium sheet using resistance heating was carried out. The productivity of bending of the titanium alloy sheet was improved by the resistance heating, because the heating process of the dies was eliminated and the heating time of the sheet was reduced. Hot bending using resistance heating was also effective in preventing the springback and oxidation of the titanium alloy sheet. The sheet was successfully formed at the elevated temperatures above 370°C and the bending load at a heating temperature 880°C was reduce from 6.5 kN at room temperature to 1.8 kN. In heating of the curved titanium alloy sheet, the distribution of temperature became more uniform, 825°C±20°C for the inclined electrodes by 7°.

References

1. Mori K., Maki S., Tanaka Y. Warm and hot stamping of ultra-high tensile strength steel sheets using resistance heating, CIRP Annals – Manufacturing Technology, 54-1 (2005), 209-212.
2. Mori K., Okuda Y. Tailor die quenching in hot stamping for producing ultra-high strength steel formed parts having strength distribution, Annals of the CIRP–- Manufacturing Technology, 59-1 (2010), 291-294.
3. Mori K., Maeno T., Fukui Y. Spline forming of ultra-high strength gear drum using resistance heating of side wall of cup, CIRP Annals – Manufacturing Technology, 60-1, (2011), 299-302.
4. Mori K., Maeno T., Fuzisaka S. Punching of ultra-high strength steel sheets using local resistance heating of shearing zone, Journal of Materials Processing Technology, 212-2 (2012), 534-540.
5. Ozturk F., Ece R.E., Polat N., Koksal A. Assessment of electrical resistance heating for hot formability of Ti-6Al-4V alloy sheet, Key Engineering Materials, 473 (2011), 130-136.

Sztangret M., Pietrzyk M.

APPLICATIONS OF PLANE STRAIN COMPRESSION TESTS FOR IDENTIFICATION OF FLOW STRESS MODELS OF MATERIALS AND FOR PHYSICAL SIMULATION OF METAL FORMING PROCESSES

Abstract. Possibility of application of the plane strain compression test (PSC) to the determination of the flow stress was evaluated. It was shown that distributions of strains and stresses are very nonuniform, that makes interpretation of results difficult. Inverse analysis eliminates effects of inhomogeneities but in the case of the PSC it involves high computing costs. To improve the efficiency of the analysis PSC was simplified to 2D model. Application of the PSC test to physical simulations of multi pass rolling is discussed in the paper, as well.

Keywords: plane strain compression, flow stress, identification, physical simulation.

1. Introduction

The design of new industrial forming technologies is frequently based on numerical and physical simulations [1]. This approach allows to consider a variety of technological variants and to find the best solution in relatively short time and with low costs. In the case of metal forming processes the flow stress model used in simulation has an essential influence on the accuracy of simulations. Problem of selection and identification of the flow stress model has been discussed in numerous publications, see for example [2-4]. Flow stress models usually contain coefficients, which have to be determined on the basis of plastometric tests. Due to low costs the axisymmetric compression is the most commonly used plastometric test [4,5]. Plane strain compression (PSC) is the test, which have one important advantage: the state of strains in this test is similar to that occurring in flat rolling processes. On the other hand, due to very inhomogeneous strains, stresses and temperatures in this test interpretation of results of the plane strain compression is very difficult, what prevent its wide applications. Discussion of capabilities and limitations of the PSC test is the main objective of this paper.

2. Plane strain compression

2.1. General idea

Plane strain compression (PSC) is one of the plastometric tests, which is used for determination of the flow stress. In his test a cuboid sample is compressed between two flat dies, see Fig. 1a. This test permits large plastic deformation and the state of strains is similar to that, which occurs in the flat rolling process (Fig. 1b). The plane strain state is obtained due to two factors. The low width of the sample (b) – to width of the die (w) ratio prevents flow of the material in the width direction. It is similar to the flat rolling, where low length of contact (L) – to width of the strip (b) ratio fosters elongation and prevents spread. Influence of the so- called rigid ends is another factor, which constrains spread and involves plane strain state. Rigid ends are the parts of the sample beyond the area under the die. These parts are not compressed, therefore, they do not have tendency to spread. Moreover, when the samples are heated by resistance heating (eg. on Gleeble 3800) these parts are in lower temperature than the area under the dies and their resistance to deformation is higher. Due to all these discussed facts PSC is frequently used as physical simulation of the flat rolling process.

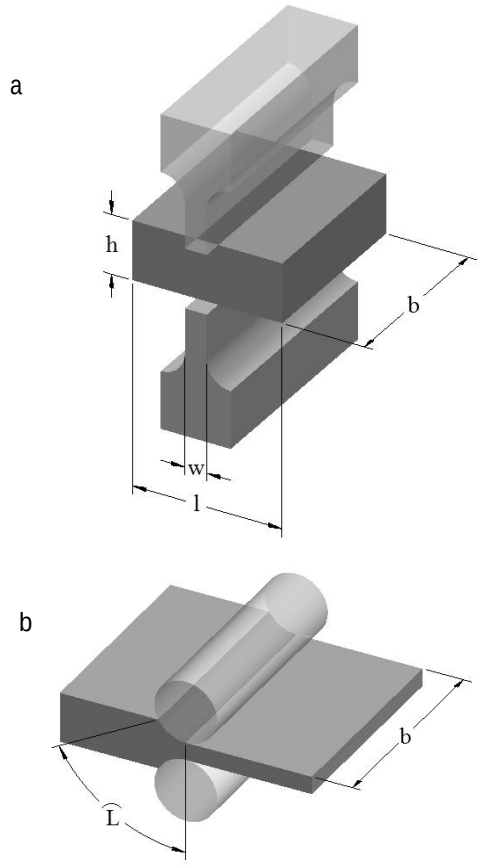

Fig. 1. Schematic illustration of the PCS test (a) and flat rolling process (b)

Plane state of strains, which is not reachable in other plastometric tests, has for years inspired the scientists to various applications of the PSC tests. Identification of the flow stress model is one of such applications and investigation of the microstructure evolution is another example. Among several research laboratories involved in investigations based on the PSC tests a team led by professor Sellars at the University of Sheffield should be mentioned. During 50-ies and 60-ies of the last century this test was commonly used there for investigation of materials and fundamental works on microstructure evolution [7] and on flow stress models [8] were a result of this research.

It should be emphasized, however, that various disturbances make interpretation of results of PSC tests very difficult. These tests are characterized by large inhomogeneity of deformation (Fig. 2a), which is caused by complex shape of the deformation zone (Fig. 1a) and by the effect of friction. Beyond this, heat generated due to plastic work and friction, as well as heat transfer to the tools and to the surrounding, cause strong inhomogeneity of the temperature in the sample (Fig. 2b).

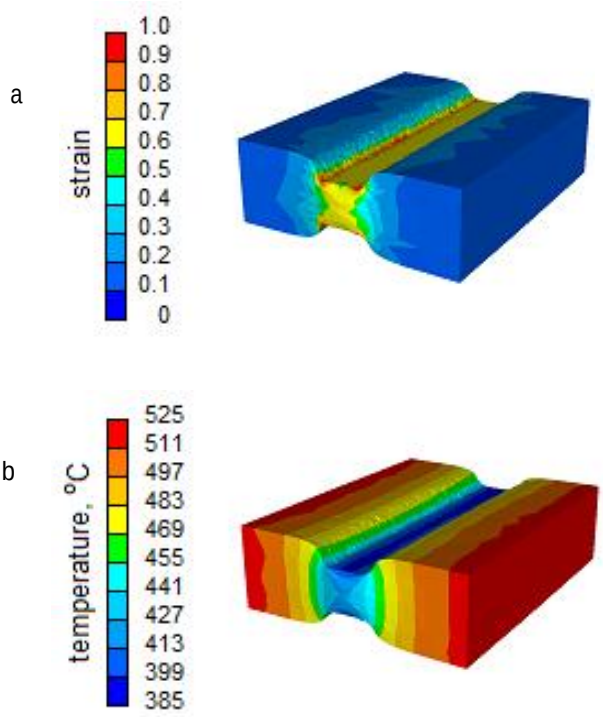

Fig. 2. Distribution of strains (a) and temperatures (b) in the PSC test

Further analysis of the PSC tests has shown that the flow stress determined from this test as ratio of the force (F) with respect to the contact surface (S) is sensitive to the parameters of the test. It is in contradiction with the theory of plasticity, which states that for isotropic material the flow stress is a property of this material independent of the type of the test, which was used for determination of this stress [9]. The flow stress calculated as the F/S ratio in the PSC for aluminium samples with various initial heights is shown in Fig. 3.

Plots in Fig. 3a represent an influence of the height of the sample on forces and calculated flow stresses. Careful analysis of these plots shows that at the beginning of deformation, when samples are higher, larger stresses are observed for higher samples. It is due to the effect of the rigid ends. When reduction of the height proceeds, the samples become lower and the effect of friction increases. In consequence, larger stresses are observed for lower samples.

Average force plotted in Fig. 3b is calculated as an integral of the force with respect to the strain and represents deformation work [10]. It is seen that minimum of this work exists for certain height of the sample. Left to this point an increase of the work is caused by the effect of the friction, which contributes more for lower samples. Right to this point an increase is caused by the effect of the rigid ends, which is larger when the ratio of the height of these ends with respect to the width of the sample increases.

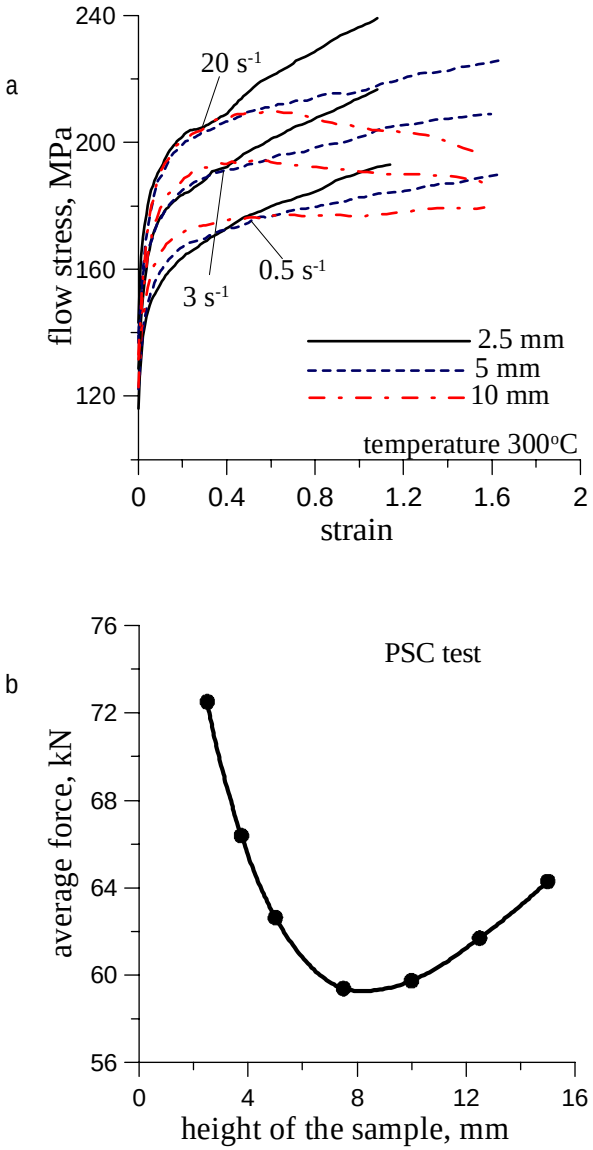

Fig. 3. Stress (F/S) as a function of strain (a) and integral of force with respect to strain (b) – various height of the sample

Character of the material flow in the PSC tests is sensitive to the height of the sample, as well [10]. For low samples (Fig. 4a) a side of this sample after deformation has the shape of the letter D. For high samples (Fig. 4b) the material flows easier under the die and, in consequence, side of this sample after deformation has the shape of the Letter B.

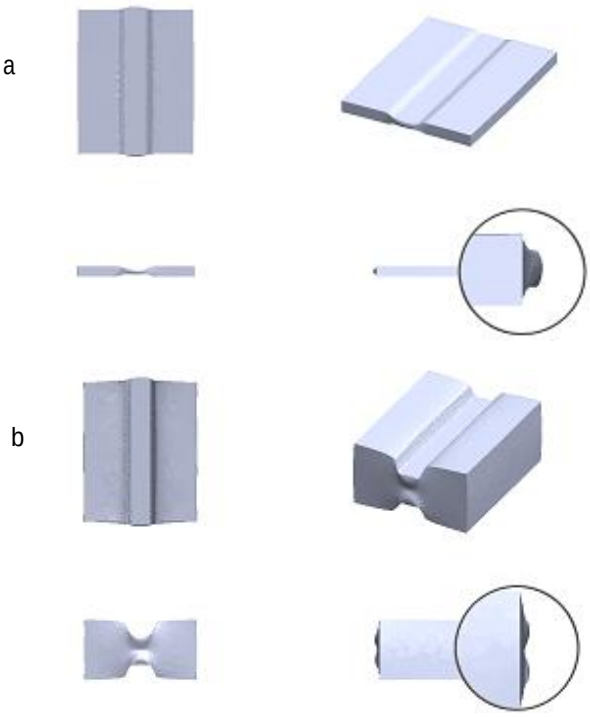

Fig. 4. View of the sample after PSC, initial height 2.5 mm (a) and 15 mm (b)

3.2. Sensitivity of the PSC results with respect to the parameters of the test

The scientists working with the PSC tests have realized inaccuracies and problems connected with interpretation of results of this test, which are caused by inhomogeneity of deformation and temperature. A lot of effort was made to development of methods of correction of the PSC test results [7,8,11-16]. In the present work finite element analysis of strains and stresses in the PSC test was performed and selected results are presented in Fig.5.

It is seen in Fig. 5 that the character of the distribution of strains and stresses changes drastically depending on the dimensions of the sample and the die. The idea of the shape coefficient $\Delta = w/h$, which was introduced in [17], was used in the present work to characterize the dimensions of the deformation zone. Values of this coefficient were 2, 1 and 0.5 respectively in Figs 5a, 5b and 5c. Decrease of the coefficient Δ leads to more uniform distribution of strains and stresses in the deformation zone. The effect of friction increases with Δ decreasing. Deformation cross characteristic for compression in flat dies, for example for free forging, is well seen for high coefficient Δ (Figs 5a and b). Plastic deformation does not penetrate through the whole thickness of the sample in this case. Performed analysis shows that deformation scheme in the PSC test is very sensitive to the dimensions of the sample and the die, which makes direct interpretation of results very difficult. Thus, inverse analysis was applied in the present work to solve this problem.

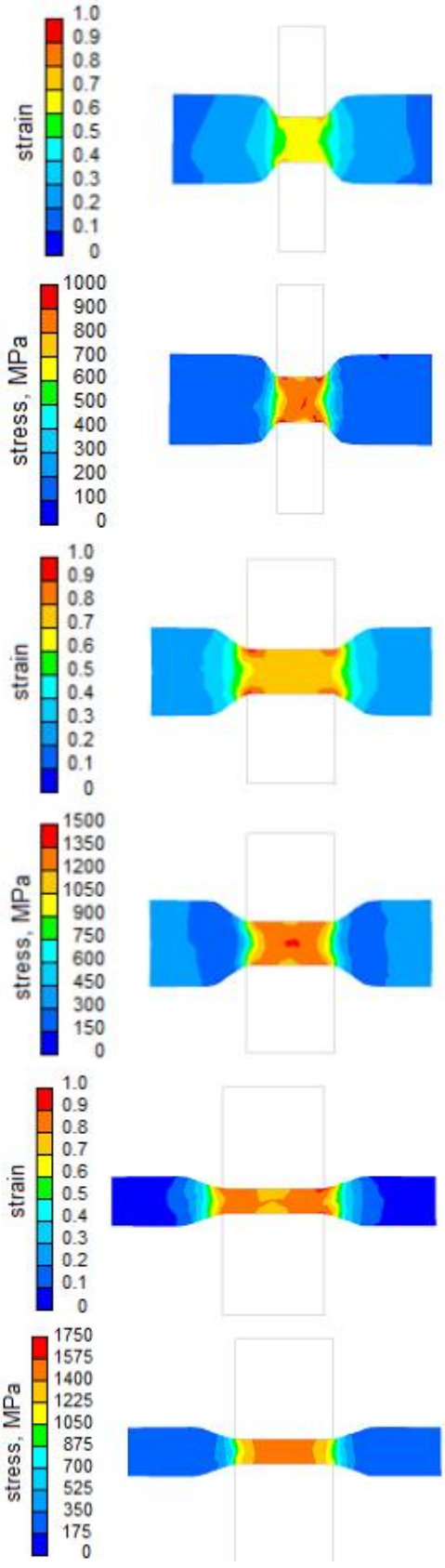

Fig. 5. Distribution of effective strains (left) and effective stress (right) in the PSC test, initial sample height – to - width of the anvil ratio equals 10/5 mm (a), 10/10 mm (b), 5/10 mm (c)

3. Inverse analysis

Inverse analysis was used to determine the real flow stress corrected against the effect of friction, rigid ends and deformation heating in the PSC tests. The algorithm descibed in [4] was applied. The flow stress values corresponding to the subsequent strains were determined using optimization techniques. The quadratic norm of the error between measured and calculated compression loads was used as the objective function, see details in [4].

Inverse procedure requires several simulations of the plane strain compression test. Due to high computing costs, 3D inverse analysis is practically impossible. As far as compression of axisymmetrical samples is simulated using 2D mesh, plane strain compression requires 3D mesh, which has to be very fine in the areas of contact with the edge of the die, see Fig. 8. In consequence, the costs of the PSC simulations are about hundred times higher comparing to the axisymmetrical ones.

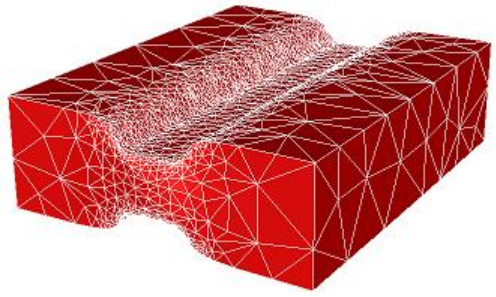

Fig. 8. Finite element mesh in the 3D simulation of the PSC test

These long computing times of the objective function in the PSC tests prevented wide applications of this test for the inverse analysis and evaluation of the flow stress of materials. Assessment of possibility of decreasing computing times necessary for the PSC test simulations and making the inverse analysis more effective is one of the objectives of the present work. To reach this goal, simulations were simplified to the 2D domain at the cross section of the sample. A correction proposed in [19] was used. This correction accounts for the slight increase of the contact surface due to spread under the die. This spread influences the current width of the sample, according to the formula:

$$b - b_0 = \left[1 + C - C\left(\frac{h}{h_0}\right)^{0,18}\right], \qquad C = \frac{\frac{b_f}{b_0} - 1}{1 - \left(\frac{h_f}{h_0}\right)^{0,18}}, \tag{1}$$

where b_0 is initial width, h_0 is initial height, b_f is final width, h_f is final height, b is current width, b is current height, C is coefficient.

This correction allowed to use 2D model in simulation of the PSC tests. Analysis of the effectiveness of the inverse solution has shown that even simplified 2D simulation for one PSC test, using FE mesh with 220 elements, requires about 5-10 min. Assuming that at least three temperatures and three strain rates are necessary to determine relation of the flow stress on these parameters, nine simulations of the test are needed for one evaluation of the objective function. In consequence, full inverse analysis would still require very long computing times. In order to make the analysis more efficient, the analysis was performed in two steps [4]. In the first step the stress-strain function was determined in a tabular form for each test separately. This function can be considered a property of material for isothermal, constant strain rate conditions. The functions introduced in the finite element program together with correction for variations of temperature and strain rate gives perfect agreement between measured and predicted forces. The correction is given by the following equation:

$$\sigma_p = \sigma_b \frac{\dot{\varepsilon}^m}{\dot{\varepsilon}_n^m} \exp\left[\frac{Q}{R}\left(\frac{1}{T} - \frac{1}{T_n}\right)\right], \tag{1}$$

where σ_p is flow stress, σ_b is isothermal constant strain rate value of the flow stress, determined from the inverse analysis, R is gas constant, Q is activation energy, $\dot{\varepsilon}_n$, T_n are nominal values of strain rate and temperature for a considered test, $\dot{\varepsilon}$, T is current local value of strain rate and temperature in the finite element node (or in the Gauss integration point).

The results given in a tabular form, which were obtained in the first step of the analysis, were approximated using equation, which describes flow stress as a function of strain, strain rate and temperature. The equation proposed in [18] was used:

$$\sigma = \sqrt{3}\left[a\varepsilon^n \exp\left(\frac{\beta}{T}\right)\exp\left(-q\varepsilon\right) + \left[1 - \exp\left(-q\varepsilon\right)\right] a_{sat} \exp\left(\frac{\beta_{sat}}{RT}\right)\right]\left(\sqrt{3}\dot{\varepsilon}\right)^m, \tag{2}$$

where ε is effective strain, $\dot{\varepsilon}$ is effective strain rate, T is temperature in K.

The coefficients in equation (2) obtained from the approximation were used as a starting point for the second stage of the inverse analysis. In this stage coefficients in equation (2) were optimization variables. The starting point was very close to the minimum and only few steps of the simplex method were needed to find this minimum. In consequence, a noticeable decrease of the computing costs was obtained

Inverse analysis was performed for the steel containing 0.075%C, 1.375%Mn, 0.25%Si, 0.3%Ni, 0.15%Cu, 0.15%Cr. The samples, which measured 20×25×35 mm, were compressed in the dies with the width of 16 mm at temperatures 800, 850, 900, 950, 1000, 1050 and 1100°C wand at strain rates 0.1, 1 and 10 s^{-1}. Three temperatures (800, 950, and 1100°C) were used in the identification phase and remaining four temperatures were used for the validation of the model. All tests were performed on the

Gleeble 3800 simulator in the Institute for Ferrous Metallurgy in Gliwice, Poland. Selected results of force measurements and flow stress determination are shown in Fig. 9.

Coefficients in equation (2) obtained from the second step of the inverse analysis are given in Table. The final value of the objective function in the inverse analysis is given in the last column of this Table. This value is a measure of the accuracy of the inverse solution.

Coefficients in equation (2) calculated using inverse analysis for the investigated steel

A	β	n	M	a_{sat}	β_{sat}	q	ϕ
8.363	3723.3	0.469	0.099	0.0642	7815.1	1.086	0.129

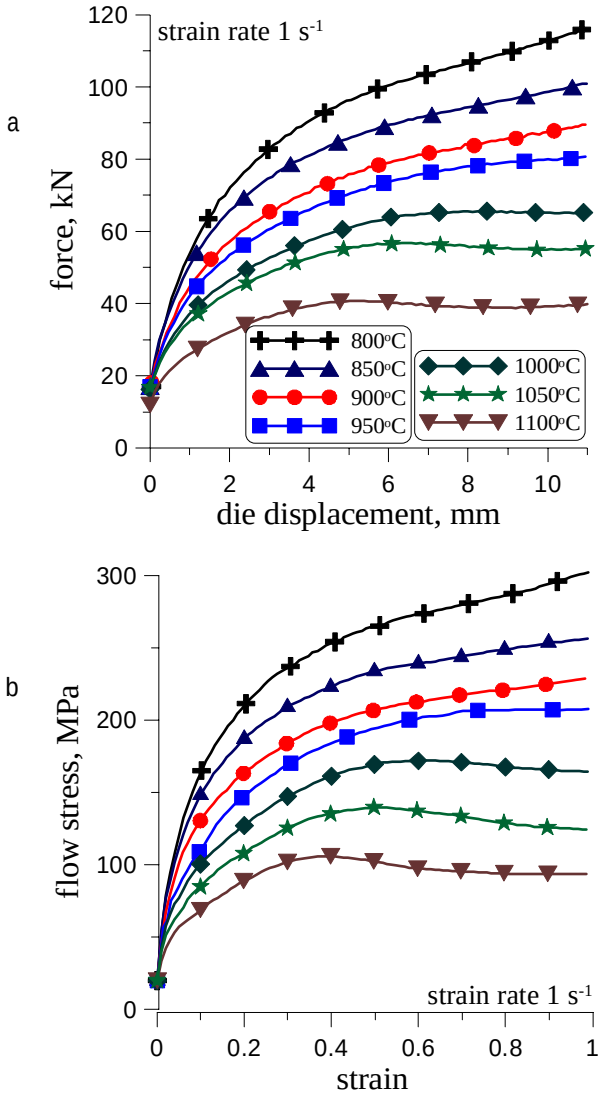

Fig. 9. Selected examples of recorded forces (a) and flow stress determined using inverse analysis of the PSC tests (b)

Comparison of measured forces and those calculated using FE program with equation (2), with coefficients in Table 1 as the flow stress model is shown in Fig. 10. Very good agreement was obtained in a wide range of temperatures and strain rate. It can be concluded that inverse analysis allows proper interpretation of results of the plane strain compression test and flow stress insensitive to the inhomogeneities in the test can be determined.

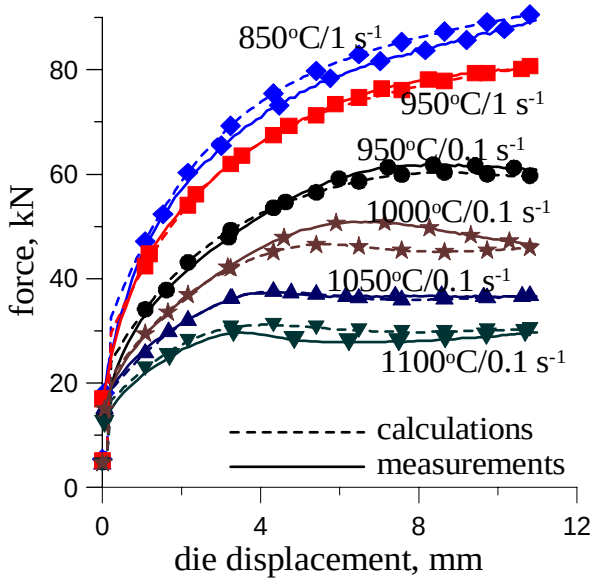

Fig. 10. Selected examples of comparison of forces measured and calculated using FE program with equation (2), with coefficients in Table 1 as the flow stress model

4. Physical simulation of hot rolling

Plane strain compression test has been for years used for physical simulation of rolling processes. Temperature and strain history can be easily reproduced in this test. Samples can be quenched after each deformation stage and microstructure can be investigated. However, problems with the interpretation of results of such physical simulation are similar to those discussed above for the single stage compression. Deformation and temperatures are inhomogeneous and, what is even more important, the shape coefficient Δ changes during the test (Δ = 0.667; 0.82; 1.17; 1.55 respectively for stages 1, 2, 3 and 4), what involves changes of the inhomogeneity of deformation. Thus, the general principle followed by the scientists was to investigate the material in the centre of the sample, assuming that strains and temperatures at that location are close to the nominal values in the test calculated as:

$$\varepsilon_h = -\frac{2}{\sqrt{3}} \ln\left(\frac{h_f}{h_i}\right), \qquad (3)$$

where h_i is initial height, h_f is final height.

It seams that FE simulation of the multi stage PSC test should help interpretation of the results.The 4 stage compression test performed on the Gleeble 3800 in the temperatures covering austenitic and ferritic range were investigated. The samples, which measured 15×20×35 mm,

were compressed in the dies with the width of 10 mm. Schematic illustration of the time-temperature-deformation history is given in Fig. 11. Subsequent deformations were carried out at temperatures T_1 = 1000°C, T_2 = 900°C, T_3 = 820°C and T_4 = 66680°C. Description of this test and results of measurements are given in [20].

Several samples were deformed in the experiment. The process was interrupted at various stages and samples were quenched to observe microstructure. All pictures of microstructure at the centre of the samples are shown in the publication [20]. Four of these pictures showing microstructures right after deformation are repeated in Fig. 12. In the present work FE simulations of the multi stage PSC test were performed, and distribution of strains were evaluated. Results of the 2D finite element simulations of the 4th experimental stage PSC test are shown in Fig. 13.

It is seen in Fig. 13 that different distributions of strains are observed for different stages of deformation. The largest inhomogeneity of deformation is observed in the 2nd stage. The most uniform deformation is in the last stage. It seams, however, that problem of strain level in the centre of the sample is even more serious. At this location the microstructure was analysed and it was referred to the nominal homogeneous strain in the compression. It is seen that local strains differ significantly from the homogeneous one (figure 14). It can be concluded that interpretation of the physical simulation based on the PSC tests should be combined with the FE simulations of these tests.

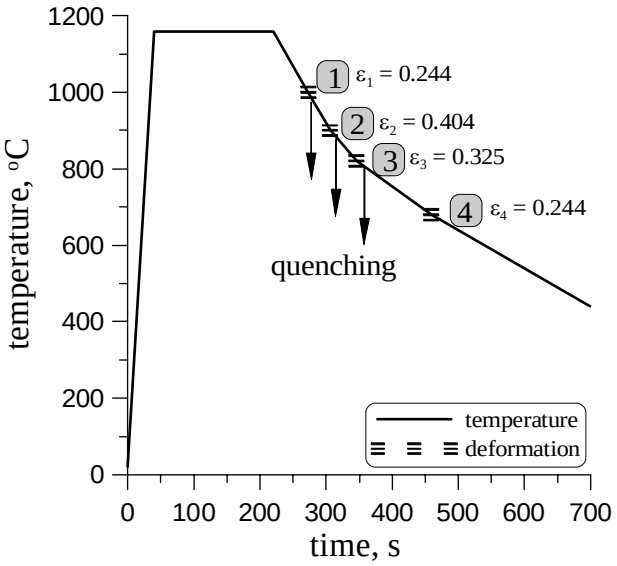

Fig. 11. Schematic illustration of the time-temperature-deformation history in the investigated multi-stage PSC test [20]

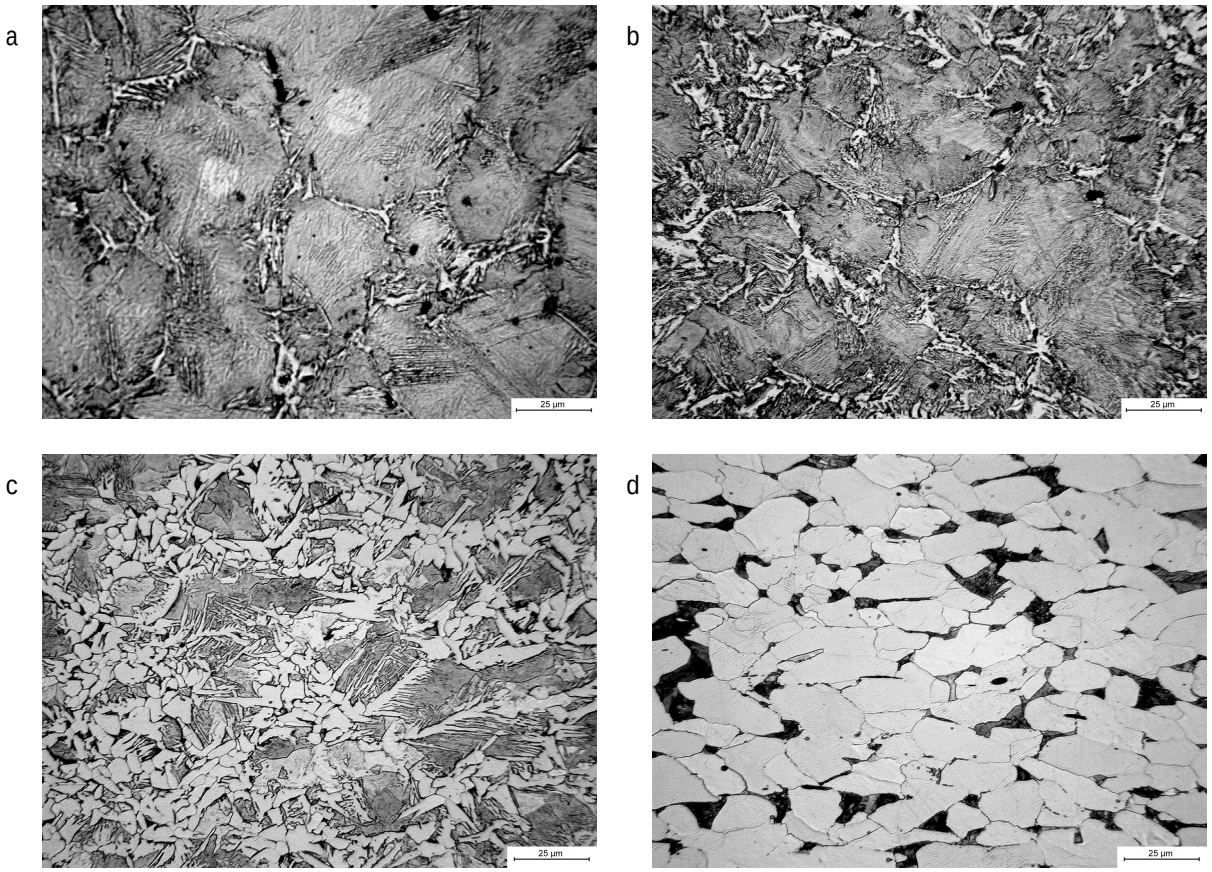

Fig. 12. Microstructure after deformation at 1000°C (a), 900°C (b), 820°C (c) and 680°C (d)

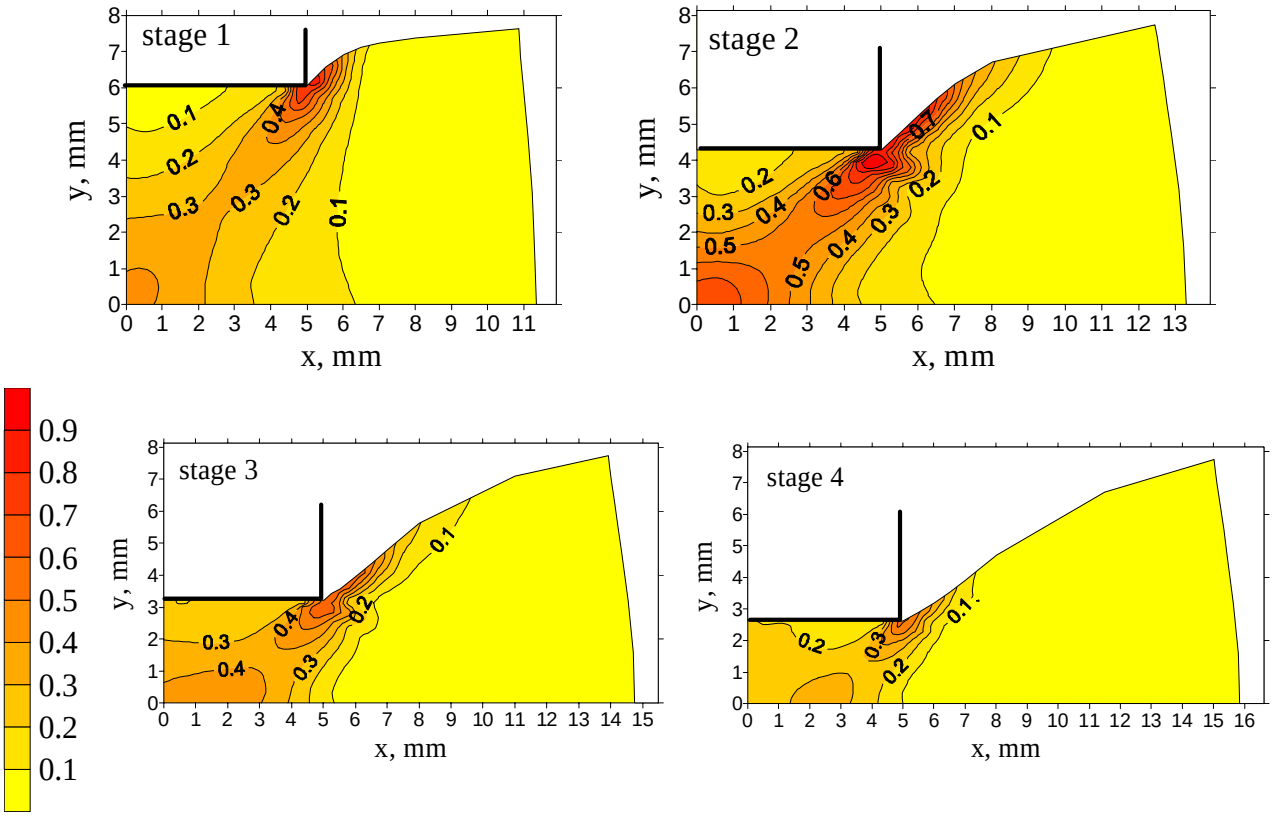

Fig. 13. Distribution of strains at subsequent stages of the multi-stage PSC test

Conclusions

- PSC test has several advantages, connected mainly with capability to reproduce state of strains, which is characteristic for rolling. It is shown in the paper how multi-stage compression allows to investigate microstructure evolution in multi pass rolling.
- Due to inhomogeneity of deformation and temperature interpretation of results of the PSC tests is difficult. It prevents wider application of this test.
- Finite element simulation combined with optimization methods allows realistic interpretation of results of the PSC test. The application of this solution is twofold. The first is inverse analysis and identification of the flow stress model. The second is interpretation of results of physical simulations of rolling processes.
- FE simulations of the PSC tests combined with optimization techniques require very long computing times. Low efficiency of this approach is its important drawback. Methods of improvement of this efficiency should be searched in the future. Application of the metamodel, which proved to be efficient for the axisymmetric tests [21], seems to be a promising solution and it will be an objective of the future research.

Acknowledgements

Financial assistance of the NCN, project N N508 629 740, is acknowledged.

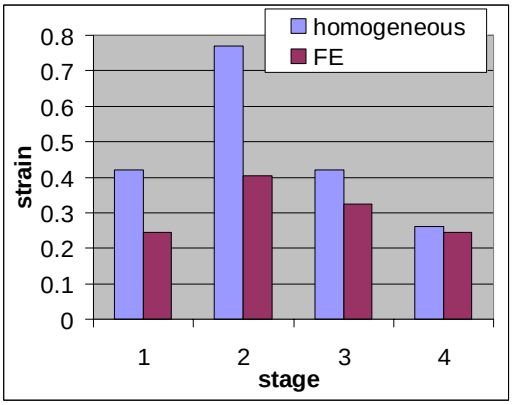

Fig. 14. Comparison of the homogeneous strains with strains in the centre of the sample calculated by the FE code and

References

1. Sztangret Ł., Milenin A., Sztangret M., Walczyk W., Pietrzyk M., Kusiak J., Computer aided design of the best TR forging technology for crank shafts, Computer Methods in Materials Science, 11, 2011, 237-242.
2. Grosman F., Application of the flow stress function in programmes for computer simulation of plastic working processes, J. Mat. Proc. Techn., 64, 1997, 169-180.
3. Bariani, P., Dal Negro, T., Bruschi, S., 2004, Testing and modelling of material response to deformation in bulk metal forming, Annals of the CIRP, 53: 573-594.
4. Szeliga D., Gawąd J., Pietrzyk M., Inverse analysis for identification of rheological and friction models in metal forming, Comp. Meth. Appl. Mech. Eng., 195, 2006, 6778-6798.
5. Hadasik E., Kuziak R., Kawalla R., Adamczyk M., Pietrzyk M., Rheological model for simulation of hot rolling of new generation steel strips for auto-

motive industry, Steel Research Int., 77, 2006, 927-933.
6. Kuc D., Pietrzyk M., Rheological model of the austenitic steel subjected to hot deformation, accounting for the microstructure evolution, Hutnik-Wiadomości Hutnicze, 76, 2009, 607-610.
7. Sellars C.M., Physical metallurgy of hot working, w: Hot working and forming processes, (ed.), Sellars C.M., Davies G.J., The Metals Soc., London, 1979, 3-15.
8. Davenport S.B., Silk N.J., Sparks C.N., Sellars C.M., Development of constitutive equations for the modelling of hot rolling, Mat. Sci. Techn., 16, 1999, 1-8.
9. Szeliga D., Matuszyk P., Kuziak R., Pietrzyk M., Identification of rheological parameters on the basis of various types of plastometric tests, J. Mat. Proc. Techn., 125-126, 2002, 150-154.
10. Sztangret M., Pietrzyk M., Próba ściskania próbek płaskich jako metoda symulacji fizycznej procesów przeróbki plastycznej oraz narzędzie do identyfikacji modeli reologicznych materiałów, Hutnik-Wiadomości Hutnicze, 79, 2012, (in press)
11. Kowalski B., Method of interpretation of results of plane strain compression tests for evaluation of rheological parameters of materials, Praca doktorska, AGH, Kraków, 2003.
12. Pietrzyk M., Lenard J.G., Dalton G.M., A study of the plane strain compression test, Ann. CIRP, 42, 1993, 331-334.
13. Pietrzyk M., Tibbals J.E., Application of the finite element technique to the interpretation of the plane strain compression test for aluminum, Mat. COMPLAS 4, ed., Owen D.R.J., Onate E., Hinton E., Pineridge Press, Barcelona, 1995, 889-900.
14. Silk N.J., Ban Der Winden M.R., Interpretation of hot plane strain compression testing of aluminum specimens, Mat. Sci. Techn., 15, 1999, 295-300.
15. Kowalski B., Sellars C.M., Pietrzyk M., Development of a computer code for the interpretation of results of hot plane strain compression tests, ISIJ Int., 40, 2000, 1230-1236.
16. Kowalski B., Lacey A.J., Sellars C.M., Correction of plane strain compression data for the effects of inhomogeneous deformation, Mat. Sci. Techn., 19, 2003, 1564-1570.
17. Backofen W.A., Deformation Processing, Addison-Wesley 1972.
18. Gavrus A., Massoni E., Chenot J.L., An inverse analysis using a finite element model for identification of rheological parameters, J. Mat. Proc. Techn., 60, 1996, 447-454.
19. Kowalski B., Wajda W., Pietrzyk M., Sellars C.M., Sensitivity of constitutive equations on strain and strain rate inhomogeneity determined for FE modeling of plane strain compression tests, Proc. 4th Conf. ESAFORM, ed., Habraken A.-M., Liege, 2001, 561-564.
20. Pietrzyk M., Kuziak R., Validation of a model of plastic deformation of C-Mn steels in the two-phase temperature region, Steel Research International, 80, 2009, 767-778.
21. Sztangret Ł., Szeliga D., Kusiak J., Pietrzyk M., Identyfikacja modelu materiału w prawie konstytutywnym w oparciu o rozwiązanie odwrotne z metamodelem, Mechanik, 84, 2011, 32-36 (in Polish).

Pesin A.M.

SCIENTIFIC SCHOOL OF ASYMMETRIC ROLLING IN MAGNITOGORSK

Abstract. The article presents some results of studies of Scientific School of Asymmetric Rolling in Magnitogorsk. This paper presents a classification and practical application of the asymmetric rolling processes. Further development of the asymmetric rolling process is their use as a severe plastic deformation method for ultra-fine structures of the metal.

Keywords: scientific School, classification, asymmetric rolling, shear deformation, severe plastic deformation, parts of large bodies of revolution, finite element method modeling.

Over 30 years Metal Forming Department at the Higher Professional Institution «Magnitogorsk State Technical University» has been developing the scientific direction of both current and new technologies of asymmetric plate rolling. This direction is headed by V. Salganik and dissertations for Ph. D degree on this theme were written by A. Pesin (scientific supervisor M. Polyakov), V. Rudakov, V. Lunev, I. Vier, G. Kunitsyn (scientific supervisor V. Salganik), K. Kuranov, D. Chikishev (scientific supervisor A. Pesin), M. Chernyakovsky (scientific supervisors V. Salganik, A. Pesin). A. Pesin, G. Kunitsyn (scientific advisor V. Salganik) and V. Salganik have written doctorate dissertations.

Since the foundation of Magnitogorsk scholar collaborations with V. Vydrin, L. Ageev (Chelyabinsk school), V. Potapkin, V. Fedorinov, A. Satonin (Kramatorsk school), S. Kotsar, V. Tretiakov, J. Mukhin (Lipetsk school), V. Polukhin, A. Pimenov, V. Skorokhodov, A. Traino, B. Kucheriaev have been established.

Nowadays several scientific projects have been carried out together with K. Dyja, A. Kawalek from Technical University in Czestochowa (Poland), K. Mori from Technical University in Toyohashi (Japan), V. Fedorinov, A. Satonin from State Engineering University in Donbass (Ukrain).

Metal Forming Department at the Higher Professional Institution «Nosov Magnitogorsk State Technical University» has solved the following challenging issues: 1) the processes of asymmetric rolling have been classified; 2) statics, geometry and kinetics of vertically asymmetric deformation site have been described; 3) special cases of vertically asymmetric rolling have been investigated; 4) a new integrated process of vertically asymmetric rolling and plastic bend of plate mill has been developed; 5) metal cross-section in horizontal asymmetric rolling has been investigated; 6) new technical schemes in horizontally and vertically asymmetric rolling have been found.

These days the research is focused on the following directions: 1) shape control of the front end of the strip in plate rolling; 2) ultrafine grain structure in asymmetric intensive plastic deformation.

1. The classification process of asymmetric rolling

Due to different criteria, there are various approaches to the cases, which take place in asymmetric rolling. The scientists from Magnitogorsk scholar have suggested the classification containing 3 hierarchal levels [1, 2]. The upper level regards the causes of asymmetry occurred deliberately or evoked by any disturbances. The next level considers asymmetry in space in relation to either horizontal or vertical plane or to both of them. Finally, the lower level includes factors that can define asymmetry (geometric, frictional, elastic, kinematic, etc.) Asymmetry of different kinds often occurs simultaneously.

These days the technical approaches to purposeful asymmetry in the vertical plane are widely spread and

promoted. The purposeful asymmetry is determined by the following main factors:

1) geometric asymmetry specified by roll geometry and inlet and outlet angles of the rolled stock; 2) kinematic asymmetry related to different velocity of roll periphery; 3) surface asymmetry concerned the quality and properties of the surface on working rolls and strip and its firm and rough surface; 4) physical and mechanical asymmetry caused by different physical and mechanical properties between Young's E-modulus and Poisson's ratio in the working rolls as well as mechanical and physical properties of rolled stock through thickness; 5) contact asymmetry developed due to substances that get into the deformation site between the surfaces of the working rolls and metal from outside; 6) temperature asymmetry provoked by nonuniform heating of metal and working rolls in rolling.

Asymmetry in the vertical plane alters kinematics in the deformation site i.e. changes in length of backward and forward creeps in the upper and lower rolls. Considering this fact, the following cases of asymmetric rolling are depicted:

1) a common case, when the deformation site has got 2 kinematic areas – backward and forward creep but their length in the upper and lower areas aren't equal (Fig. 2a);

2) a semi-extreme case when a roll has two areas – backward and forward creeps and the other – only one area: either backward or forward creep (Fig. 2b);

3) an extreme case when one roll has only a backward area and the other – a forward creep (Fig.2c).

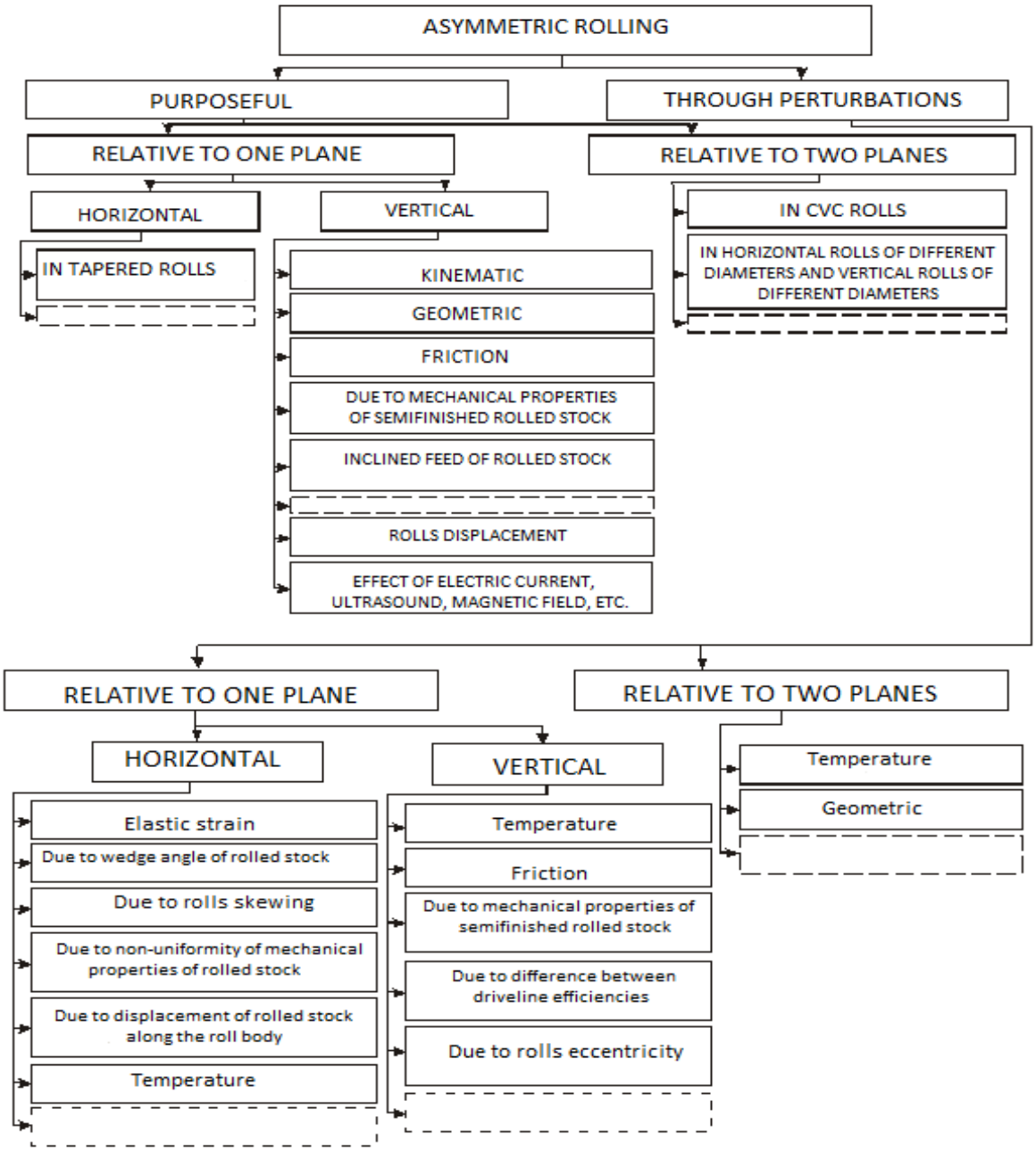

Fig.1. Classification of asymmetric rolling processes

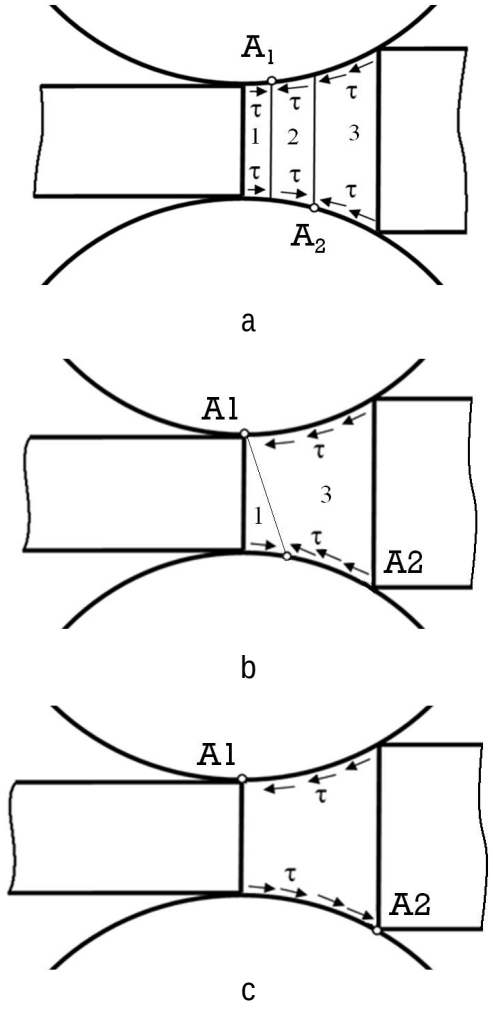

Fig. 2. Scheme of asymmetric deformation site:
a – common case, b – semi-extreme case,
c – extreme case

2. Statics, geometry and kinematics of vertically asymmetric deformation site

Mathematical description of asymmetric deformation site shows geometric ambiguity – while the radius of rolls and strip thickness in the inlet and outlet are well-known, the boundary points of the arc in the inlet and outlet cross-section are not depicted. Their rotation in the center of the rolls causes this situation. The asymmetric deformation site has got an area where friction goes to the opposite sides on the opposed areas of the arcs. It gives a rotation moment in the deformation site. As a result we get the above mentioned sectional rotation that is experimentally confirmed.

For a mathematical model of asymmetric rolling the balance of the whole deformation site that was influenced by contact loads and tensions of the outer parts of the strip were very favourable [1-3]. As a result, we received the following contact stresses through the length of the deformation site in common case (Fig. 3), where we observe all three kinematic areas, including forward, backward and mixed creeps. Both curves of contact stresses have two breaks in the cross-section corresponding to neutral one on each of the rolls. If one break on each curve is a point of neutral cross-section, the other break is a certain reaction on the opposite roll.

3. New integrated process of vertically asymmetric rolling and plastic bend of thick sheet

The mathematical models enable to calculate an extreme case when the whole deformation site is a mixed area, as well as a semi-extreme case when the deformation site has got two areas: either forward and mixed or backward and mixed. The mathematical models were confirmed experimentally by specialists in Czestochowa Technical University in Poland [4]. We got the mathematical model of integrated process of vertically asymmetric rolling and plastic bend for large rotary bodies (Fig. 4) [5-12].

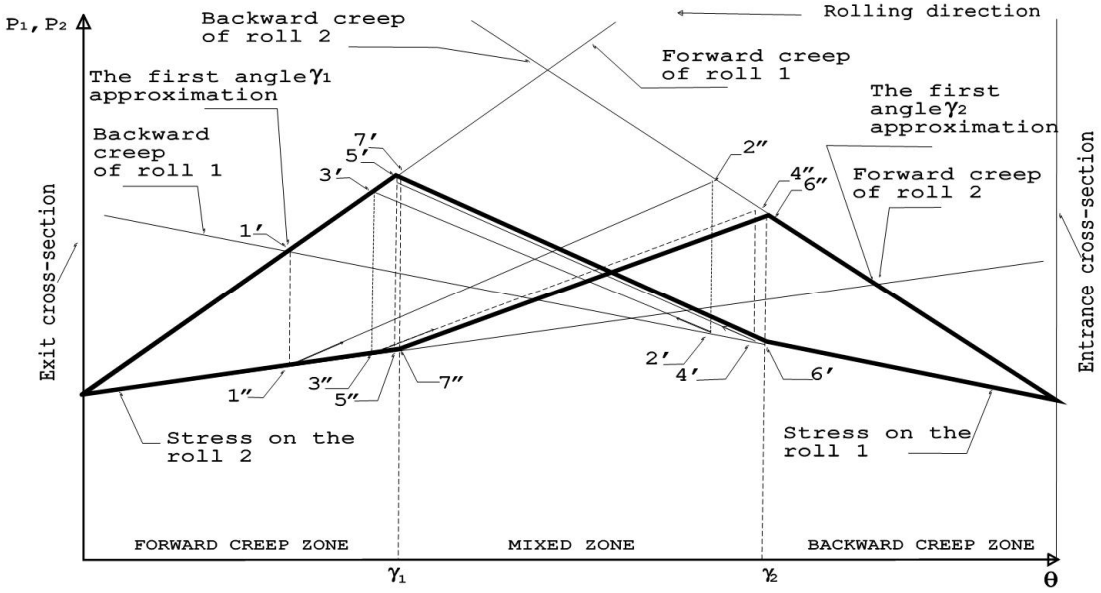

Fig.3. Search of normal contact stresses

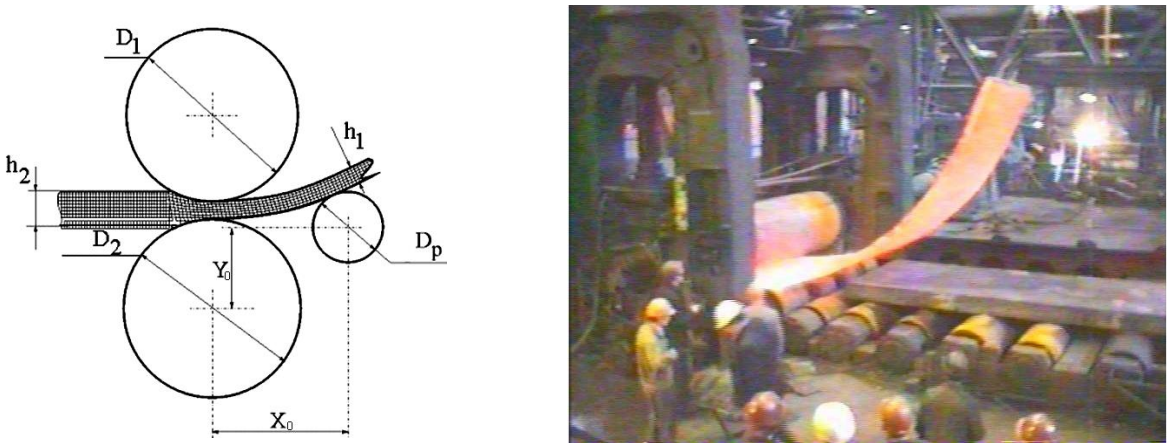

a b

Fig.4. Integrated process of asymmetric rolling and plastic bend: a – scheme, b – industrial experiment at Mill 4500at the OSJC «Magnitogorsk Iron and Steel Works»

The integrated process has three stages: vertically asymmetric rolling, when the front end of the sheet does not touch the detector roll; non-adjusted integrated process of vertically asymmetric rolling and plastic bend, when the front end of the sheet touches the detector roll; adjusted integrated process of vertically asymmetric rolling and plastic bend, when the front end of the sheet separates from the detector roll.

This technology gives us rotation items as a cylinder segment with 45°-60° angle made of stainless steel and following parameters: thickness – 40-220 mm, width – 4300 mm, length – 5000 mm, radius of curve – 1850-5000 mm.

The technology of large rotary bodies has been implemented at the OSJC «Magnitogorsk Iron and Steel Works». The cover units have been manufactured and installed for two converters in the oxygen-converter plant at the OSJC «Magnitogorsk Iron and Steel Works». The economical revenue of this technology is over $1 million.

This technology has a serious drawback such as a strong dynamic blow, when the front end of the sheet touches and shifts over the fixed detector roll. The upper roll has abrupt rolling process that can damage the equipment. It is caused by rigid fixing of the detector roll. To solve this problem new ways of this technology have been introduced: 1) roller aprons have been fixed to follow the detector roll; 2) the detector roll moves in the target track; 3) different speed of rolls have been used to increase accuracy of the curve .

The mathematical modeling shows the fact that new technical and technological changes makes a dangerous difference of moments decrease to 1.5-2.5 compared to the fixed detector roll. This work has been supported by the Grant of Analytical Target Program of the Russian Federation (grant №2.1.2/4390 Scientific development and enhancement of technical systems including new processes of metal items of large bodies of the fixed curve and by the grant «Participation in youth scientific contest» (UMNIK 2009) organized by the Fond of Small Business in scientific and technical sphere together with Federal Agency of Science and Innovations and Educational Agency.

4. The shape of the front end in plate rolling

These days Metal Forming Department at the Higher Educational Institution «Nosov Magnitogorsk State Technical University» studies asymmetric modes to decrease ski-effect in plate rolling at Mill 5000 at the OSJC «Magnitogorsk Iron and Steel Works» (Fig. 5).

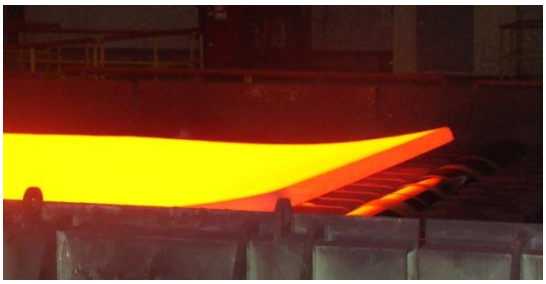

Fig.5. Ski-effect in plate rolling at Mill 5000 at the OSJC «Magnitogorsk Iron and Steel Works»

In plate rolling the rolls, which move at similar speed, bend vertically the front end of rolled stock. It is caused by geometrical, frictional and temperature asymmetry through the height of the deformation site. The rising vertical bend leads to the rolled stock stuck in the rolls of outlet table in the machine of preliminary melting. To decrease the vertical bend of the front end of the rolled stock in plate rolling it is necessary to apply kinematic asymmetry – difference in speed of the working rolls.

In plate rolling with different speed of the working rolls the bend can occur in the direction of the roll with higher speed or in the direction of the roll with lower speed. When the sheet decreases in thickness to 8-32 mm, the impact of different speed of the working rolls can be ambiguous. In the light draft the bend occurs in the direction of the roll with lower speed; in high draft the bend occurs in the direction of the roll with higher speed. Moreover, under certain circumstances, there is a neutral point when the vertical bend of the front end of the sheet does not occur in rolling with different speeds. Neutral point is a special point, which is not influenced by different speeds.

The scientists of the scholar developed a finite element mathematical model of stress and deformation metal state in the asymmetric deformation site with different temperature. The model was adjusted at Mill 5000 at the OSJC «Magnitogorsk Iron and Steel Works». New asymmetric modes of deformation have been elaborated due to the impact of the shape of the deformation site on the direction of bend of the front end of the sheet in rolling with different speeds.

5. Ultrafine grain structure in asymmetric intensive plastic deformation

Industrial technologies of flat long rolled stock produced of ultrafine grain materials can be based on the well - known process of metal forming such as rolling. However, classic symmetric rolling has a number of drawbacks: monotoneness and the lowest level of deformation so this process cannot be used for ultrafine grain structure.

One of the most efficient methods of intensive plastic deformation for flat long ultrafine grain metal materials as a strand and sheet is asymmetric rolling. It includes methods of intensive plastic deformation and has the following essential criteria to get an ultrafine grain structure: 1) high shearing deformation in each stage of treatment; 2) high level of accumulated shearing deformation e=2,0÷4,0; 3) non-monotoneness of deformation; 4) high tension in the deformation site to get flawless metal; 5) simultaneous impact on materials with high deformation of pressure and shift.

In the asymmetric site at the opposite arcs of the contact friction moves to the opposite sides that lead to the change of cross-sections and shearing deformations which are necessary for to get ultrafine grain structure. For instance, mathematical modeling shows the increase in shearing deformations throughout the cross-section of the strand as much 9 times compared to symmetric rolling (Fig. 6) [13]. The extreme cases of asymmetric rolling have better effect of fine crushing of metal.

On the one hand, asymmetry leads to decreasing in friction negative impact that leads to deformation pressure increasing. On the other hand, the site has considerable shearing deformation and strain rate rises (Fig. 7).

Special schemes of mechanical deformation to get an ultrafine grain structure can be applied: 1) asymmetric rolling, i.e. common case of asymmetry; 2) rolling-drawing, an extreme and non-extreme case of rolling; 3) deformation between the fixed element and driven roll that is also an extreme and non-extreme case of rolling. However, processes of asymmetric rolling belong to those methods of intensive plastic deformation where initial and final parameters do not coincide and it restricts it application.

The criterion of an ultrafine grain structure in asymmetric rolling: 1) scalar value $\Gamma = \sqrt{\frac{2}{3}}\sqrt{2\varepsilon_{yy}^2 + 6\varepsilon_{xy}^2}$ for flat deformation state which characterizes accumulated intensity of the shift deformation and that is defined by 2 tensor components: pressure deformation ε_{yy} and shift deformation ε_{xy}; 2) slope angle φ of vertical cross section. Target levels: $\Gamma \geq 2$; $\varphi \geq 45°$.

Asymmetric rolling can increase the intensity of shift deformation through the cross-section of the sheet (up to 3.5) and can be used to get an ultrafine grain structure for strands and sheets.

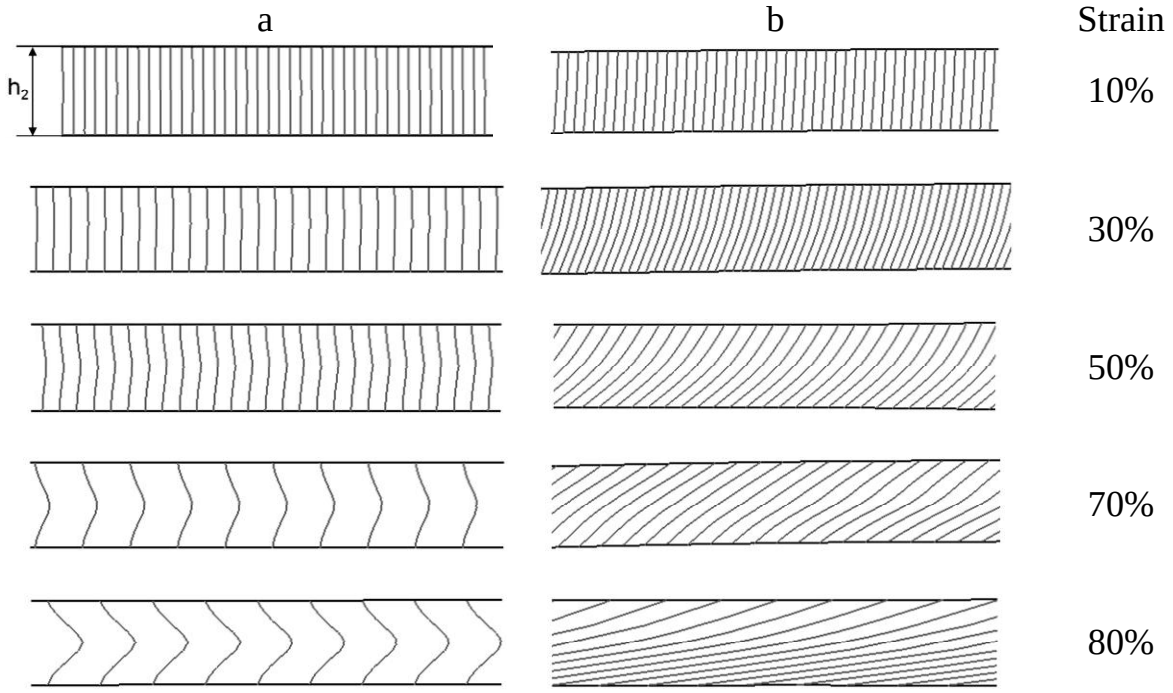

Fig.6. Distortion of vertical lines of asymmetric and symmetric rolling

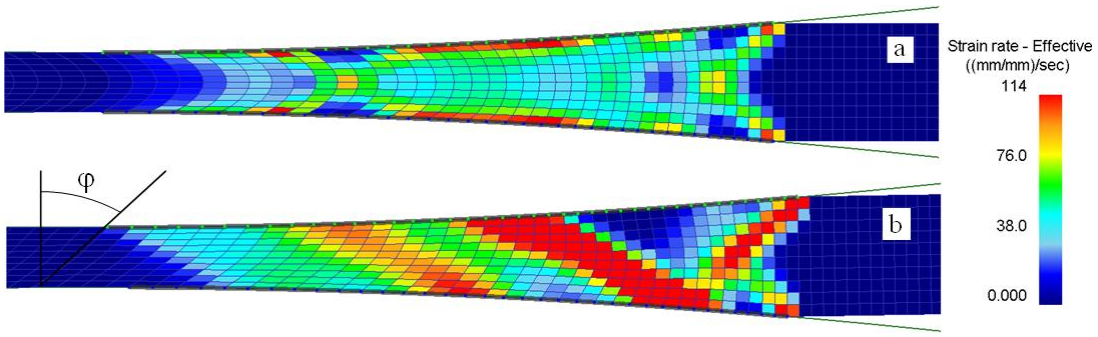

Fig.7. Field of strain rate in asymmetric and symmetric rolling

References

1. Pesin A.M. *Modelirovanie i razvitie processov asimmetrichnogo deformirovanija dlja povyshenija jeffektivnosti listovoj prokatki. Dokt. Diss*. [Modeling and development of the processes of asymmetric deformation to improve sheet rolling: thesis]. Magnitogorsk, 2003. 395 p.
2. Salganik V.M., Pesin A.M. *Asimmetrichnaja tonkolistovaja prokatka: razvitie teorii, tehnologii i novye reshenija* [Asymmetric rolling of thin sheet: the development of theory, technology and new solutions]. Moscow: MISIS, 1997. 192 p.
3. Pesin A.M. New technological solutions based on the modeling of asymmetric rolling. *Steel*, 2003, no. 2, pp. 66-68.
4. Dyja H., Pesin A.M., Salganik W.M., Kawalek A. Asymetriczne walcowanie blacli cienkicli: teoria, teclinologia i nowe rozwiazania: Seria Monografie nr 137. Wydawnictwo Politechniki Czestochowskiej. Czestochowa, 2008, 345 p.
5. Pesin A., Salganik V., Trahtengertz E., Drigun E. Development of the asymmetric rolling theory and technology / Proceedings of the 8-th International Conference on Metal Forming. Krakow / Poland / 3-7 September, 2000. Metal Forming 2000. Balkema / Potterdam / Brookfield / 2000. pp. 311-314.
6. Pesin A.M., Salganik V.M., E.M. Drigun, Chikishev D.N. *Ustrojstvo dlja asimmetrichnoj prokatki tolstolistovogo metalla*. [Device for asymmetrical rolling metal plate]. Patent RF, no. 38646, 2004.
7. Pesin A.M., Salganik V.M., E.M. Drigun, Chikishev D.N. *Ustrojstvo dlja asimmetrichnoj prokatki tolstolistovogo metalla.* [Device for asymmetrical rolling metal plate]. Patent RF, no. 2254943, 2005.
8. Pesin A., Salganik V., Sverdlik M., Pustovoytov D., Chikishev D. Theoretical Basis and Technology Development of the Combined Process of Asymmetric Rolling and Plastic Bending. *Proceedings of the 2011 International Conference on Mechanical Engineering and Technology UK ICMET* 2011, ASME Press, 2011, USA, pp. 95-98.
9. Pesin A.M., Salganik V.M., Chikishev D.N. Improvement of production technology of large parts of bodies of revolution on the basis of mathematical modeling. *Proizvodstvo prokata*. [Production of rolled]. 2007, no. 3, pp. 34-40.
10. Pesin A.M., Salganik V.M., Dyja H., Chikishev D.N., Pustovoitov D.O., Kawalek A. Asymmetric rolling: Theory and Technology. HUTNIK-WIADOMOSCI HUTNICZE. 2012, no 5, pp. 358-363.
11. Pesin A.M., Salganik V.M., Chikishev D.N., Drigun E.M. *Razvitie teorii i tehnologii poluchenija detalej krupnogabaritnyh tel vrashhenija: monografija.* [The development of the theory and technology of parts of large bodies of revolution: monograph]. Magnitogorsk: «NMSTU», 2010, 102 p.
12. Salganik V.M., Pesin A.M., Chikishev D.N., Lokotunina N.M., Pustovoitov D.O. *Prilozhenija teorii plastichnosti k razrabotke i analizu tehnologicheskih processov* [Applications of the theory of plasticity in the design and analysis process]. Magnitogorsk: «NMSTU», 2012, 251 p.
13. Pesin A.M., Pustovoytov D.O., Perehogih A.A., Sverdlik M.K. Simulation of shear strain in the extreme case of asymmetric sheet rolling. *Vestnik Magnitogorskogo gosudarstvennogo tehnicheskogo universiteta im. G.I. Nosova*. [Vestnik of Nosov Magnitogorsk State Technical University]. 2013. no 1, pp. 65-68.

Kawałek A., Dyja H.

ANALYSIS OF VARIATIONS IN ROLL SEPARATING FORCES AND ROLLING MOMENTS IN THE ASYMMETRICAL ROLLING PROCESS OF FLAT PRODUCTS

Abstract. The paper presents the results of investigation into the effect of roll peripheral speed asymmetry on the force and energy parameters of the process for the conditions of normalizing rolling of plates in the finishing rolling stand.

Keywords: numerical modelling; asymmetrical rolling; roll rotational speed asymmetry factor.

1. Introduction

An important problem that drives the upgrading of plate rolling mills are increasing demands on the geometrical dimensions of finished products. These demands force the manufacturers to implement roll gap control systems that helps to maintain stability and improve the geometrical parameters of rolled strip.

Works [1-4] have demonstrated that by using asymmetrical plate rolling process, improvement in the quality of plate geometry can be achieved. The idea behind the asymmetrical rolling technology consists in taking advantage of the positive effects of the asymmetrical deformation zone, which include primarily the reduction of the total roll separating force and the enhancement of the product service properties.

The asymmetrical rolling system relies chiefly on a direct action being exerted on the strip in the deformation zone, in which, owing to an asymmetry introduced to the working roll peripheral speed, longitudinal tensile stresses occur, whose effect is analogous to that of tension and back tension in continuous rolling mills. These stresses have the effect of reducing the magnitude of unit pressure in the roll gap and enhancing the equalization of the non-

uniform distribution of rolled strip thickness, at the cost of the elastic properties of the rolling stand itself. At the same time, the regulation of the distribution of thickness over the strip length, flatness and the cross-sectional strip shape occurs at a reduced total roll separating force [5-7].

Reducing the total roll separating force has a direct effect of decreasing the elastic deflection of the mill housing and rolls, and an indirect effect on the roll gap shape that determines the cross-sectional shape of rolled flat products.

2. Selection of the kinetic and initial parameters of the plate hot rolling process

The material used for tests was steel of the S355J2G3 grade. Working rolls of D = 1000 mm diameter and a constant lower working roll rotational speed equal to n = 50 rpm were assumed for the tests. The asymmetrical rolling process was run by varying the rotational speed of the upper roll, which was lower than that of the lower roll. The range of variation of the roll rotational speed factor, $a_v = v_l/v_u$ (where v_l, v_u – the rotational speed of the lower roll and the upper roll, respectively) was 1.01-1.15. A strip shape factor of h_0/D = 0.05-0.018 was assumed. The range of relative rolling reductions applied was ε = 0.08-0.50.

Moreover, the following input data were taken for simulation: tool temperature, 60°C; ambient temperature, 20°C; friction coefficient, 0.3; friction factor, 0.7; the contact thermal conductivity, α_{tool} = 3000 [W/Km^2]; and the heat transfer coefficient, $\alpha_{surface}$ = 100 [W/Km^2].

The temperature of the rolled strip was varied depending on the initial height h_0 within the temperature ranges for normalizing rolling:

h_0 = 50 mm, the rolling temperature T = 950°C,
h_0 = 27 mm, the rolling temperature T = 900°C,
h_0 = 18 mm, the rolling temperature T = 880°C.

The parameters describing the physical features of steel were adopted based on the material database enclosed to the Forge2008® program [8], and were as follows: thermal conductivity, 35.5 W/(m·K); specific heat, 778 J/(kg·K); steel density, 7 850 kg/m^3; emissivity, 0.88.

In order to implement asymmetrical rolling in the conditions of existing Rolling Mill it is necessary to consider conditions prevailing in that Rolling Mill and apply one of the newest, proven numerical methods for analysis.

On the date base given from industrial conditions said, then in the finishing mill of the Rolling Mill 3600 uneven loading of the driving motors is used. "Rough" wire rod (i.e. the strip obtained in the break-down stand) in the first two passes is deformed with relative rolling reductions as high as above 40%, whereas in the last passes the strip deformation is only at a level of a few percent. The rolling moments in the first roll passes exceed the nominal moment value. The driving motors are exposed to overheating. The use of driving motor power in the subsequent roll passes is lower from nominal, which allows the introduction of a difference in the rotational speeds of individual working rolls in the range of 4-9% in the intermediate roll passes and above 15% in the end roll passes.

Therefore, by introducing the asymmetric rolling system in the finishing mill of the Rolling Mill 3600 the achieving of favourable technical and economic effects (a reduction of thickness deviations over the band length and an improvement in the flatness of finished plate) should be fully ensured, despite the non-stationary temperature distribution in the deformed strip, which occurs under actual conditions [9].

3. Investigation results and their analysis

Figures 1-8 illustrate the effects of the working roll peripheral speed asymmetry factor, a_v, being variable in the range 1.01-1.15, and of the relative reduction ε =0.08-0.50, for the feedstock thickness range under investigation (h_0/D = 0.050-0.018), on the magnitude of unit pressures p_m [kN/mm]. As shown by data in Figs. 1, 4 and 5, for the feedstock of the greatest thickness, i.e. h_0=50 mm (h_0/D = 0.050), rolled asymmetrically with asymmetry factors from the range of a_v=1.01-1.15, no decrease in the unit pressure, p_m, was observed; just the opposite, even a slight increase in its magnitude occurred. This was caused by the non-uniform deformation over the strip height and by the different lengths of the contact arc, l_d, as a result of the large bending of the strip on exit from the deformation zone. The application of rolling reductions of ε>0.15 resulted in a reduction of unit pressure magnitudes from a few percent (for ε=0.20) up to approx. 8% for the larges values of the asymmetry factor, (Figs.1, 6-8).

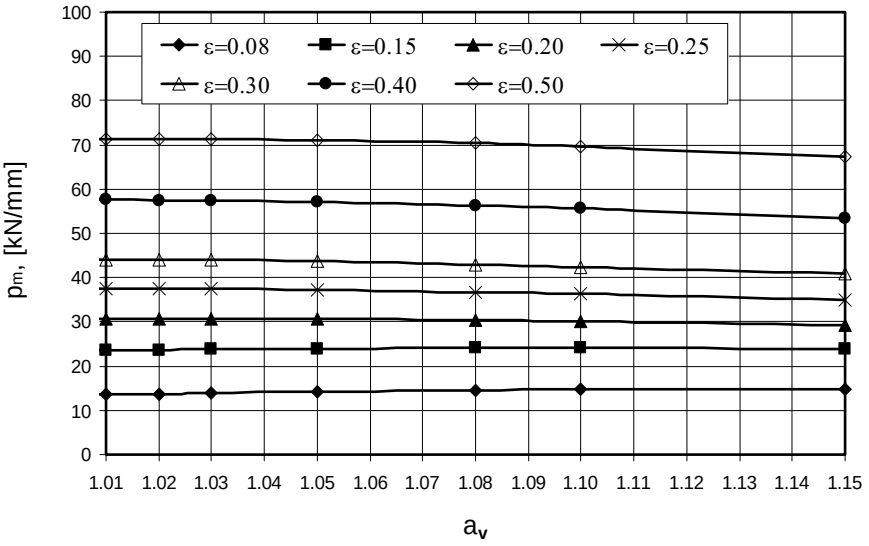

Fig. 1. Effect of the asymmetry factor a_v on the magnitude of the average roll separating force p_m for different relative rolling reduction values and a constant strip shape factor of h_0/D = 0.050

For the h_0=27 mm thick (h_0/D=0.027) feedstock rolled asymmetrically, using the least rolling reductions of ε=0.08-0.10, no decrease in the unit pressure magnitude was observed for the entire asymmetry factor range of a_v=1.01÷1.15 as a result of introducing asymmetric rolling; quite the opposite, a slight increase in the value of p_m occurred (Figs. 2 and 4). For rolling reductions ε>0.10, a drop in the unit pressure magnitudes by as much as approx. 11% was found for ε=0.15 and a_v=1.15 upon introducing asymmetric rolling (Figs. 2 and 5).

The application of asymmetric rolling for the h_0=18 mm thick (h_0/D=0.018) feedstock and asymmetry factors of a_v>1.01 resulted in a decrease in the average pressure magnitude by approx. 8% (for a_v=1.15) already for the lowest rolling reductions used, i.e. ε=0.08. After applying rolling reductions from the range of ε=0,15-0.30 with a_v=1.15, the pressure decrease was even greater, reaching nearly 22% (Figs. 3, 5 and 6). For rolling reductions of ε=0.40-0.50 and with small asymmetry factor values of a_v=1.01-1.03, no pressure force decrease was found, whereas for a_v>1.05 a pressure force reduction occurred, which was greater than 12% (for ε=0.40), Figs. 3, 7 and 8.

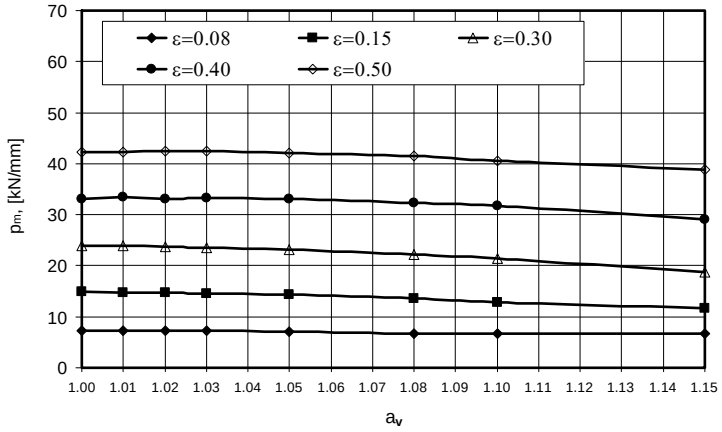

Fig. 2. Effect of the asymmetry factor a_v on the magnitude of the average roll separating force p_m for different relative rolling reduction values and a constant strip shape factor of h_0/D = 0.027

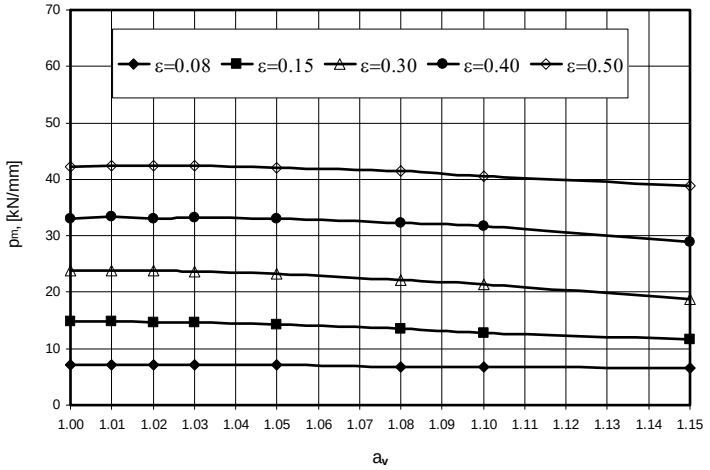

Fig. 3. Effect of the asymmetry factor a_v on the magnitude of the average roll separating force p_m for different relative rolling reduction values and a constant strip shape factor of h_0/D = 0.018

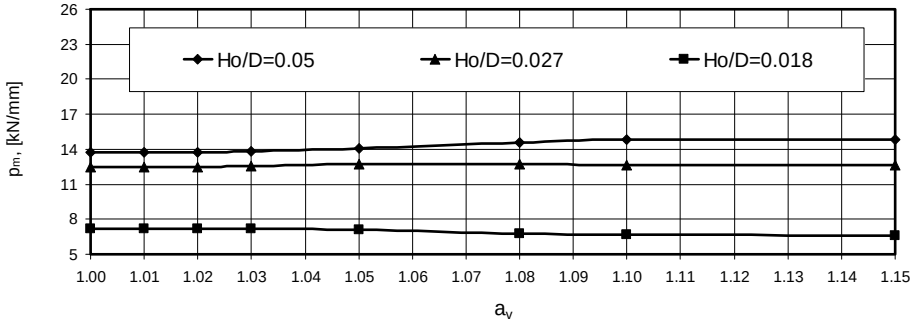

Fig. 4. Effect of the asymmetry factor a_v on the magnitude of the average roll separating force p_m for different shape factor of h_0/D and relative rolling reduction ε = 0.08

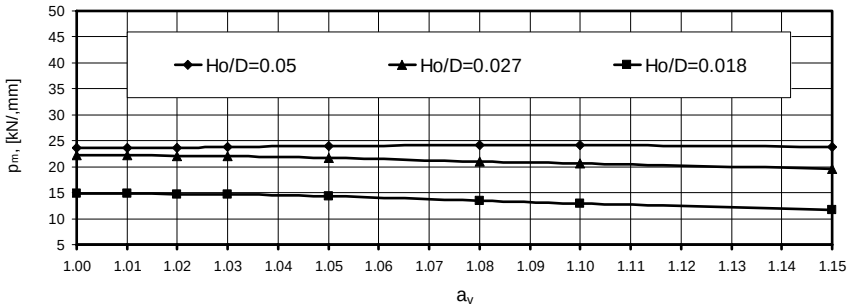

Fig. 5. Effect of the asymmetry factor a_v on the magnitude of the average roll separating force p_m for different shape factor of h_0/D and relative rolling reduction $\varepsilon = 0.15$

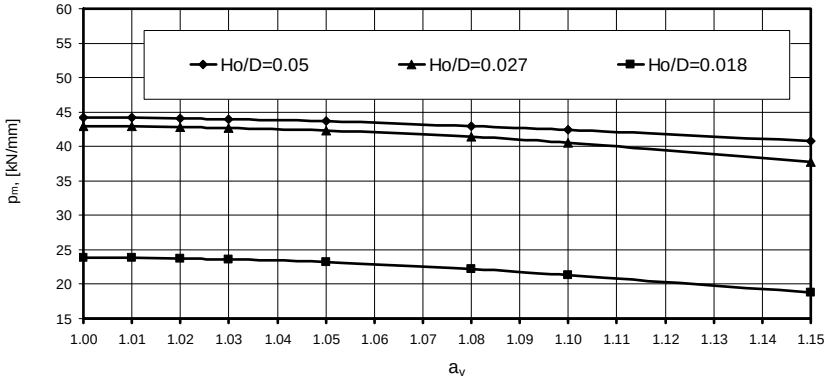

Fig. 6. Effect of the asymmetry factor a_v on the magnitude of the average roll separating force p_m for different shape factor of h_0/D and relative rolling reduction $\varepsilon = 0.30$

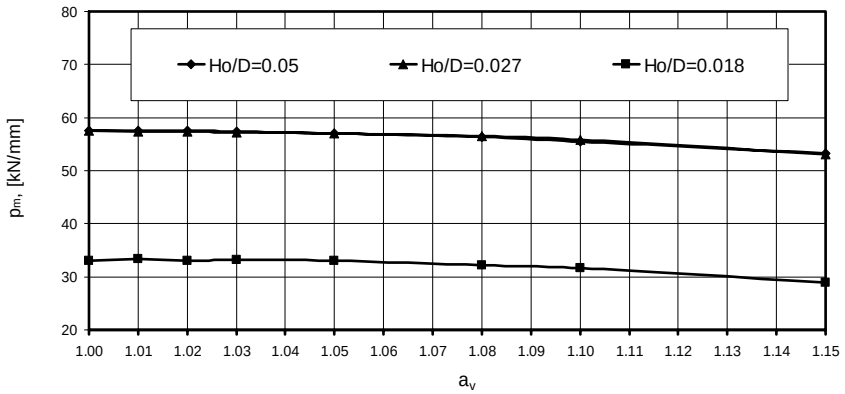

Fig. 7. Effect of the asymmetry factor a_v on the magnitude of the average roll separating force p_m for different shape factor of h_0/D and relative rolling reduction $\varepsilon = 0.40$

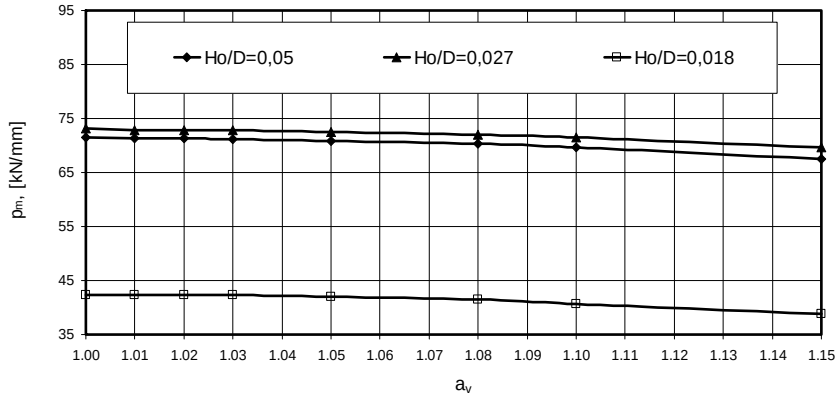

Fig. 8. Effect of the asymmetry factor a_v on the magnitude of the average roll separating force p_m for different shape factor of h_0/D and relative rolling reduction $\varepsilon = 0.50$

The data in figures 1-8 indicate that for the h_0/D strip shape factor values investigated in this work, the effect of the applied working roll peripheral speed asymmetry factor on the variation of the unit pressure magnitudes (as computed per unit width of rolled strip) is different and depends on the remaining process parameters, namely the feedstock thickness and the relative deformation used.

The effect of the asymmetric rolling process on the magnitudes and variations of rolling moments for particular working rolls and the total rolling moment is illustrated in Figs. 9-10.

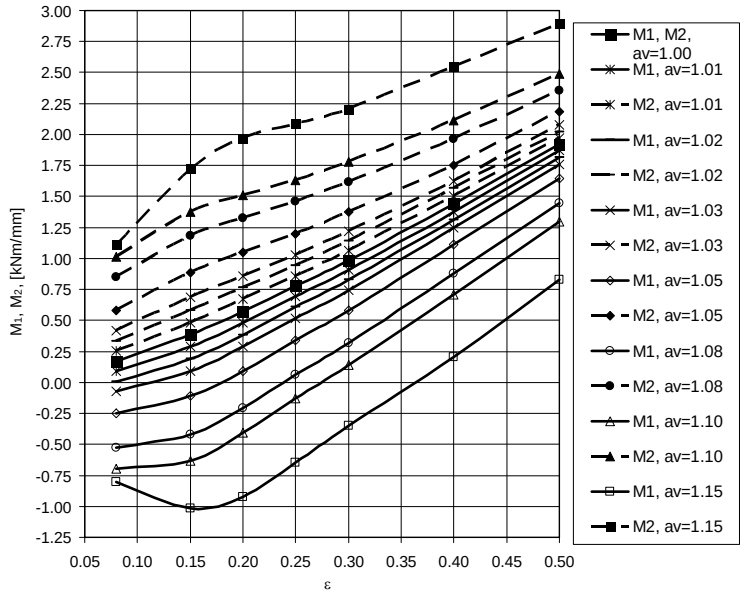

Fig. 9. Effect of the relative rolling reduction ε on the magnitude of rolling moments for a constant strip shape factor of h_0/D = 0.05

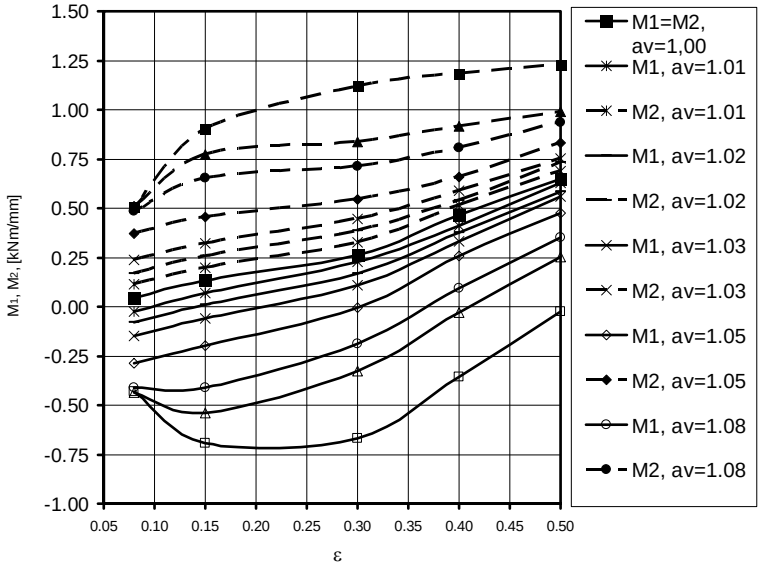

Fig. 10. Effect of the relative rolling reduction ε on the magnitude of rolling moments for a constant strip shape factor of h_0/D = 0.018

It can be found from the moment magnitude distributions shown in these figures that the moment on the roll with higher peripheral speed (the lower roll) is always positive. This roll is always a driving roll. The rolling moment on the roll with lower peripheral speed (the upper roll) may either be negative (then it becomes a driven roll), have a zero value, or be positive. The introduced asymmetry of roll peripheral velocities has a substantial influence on the value of the rolling moments M_1 and M_2. The greater feedstock thickness h_0, the greater moment is required for carrying out the rolling process. This is due to the greater absolute rolling reduction Δh in the case of rolling thicker strips, at the same magnitude of relative rolling reductions in particular passes. Depending on the magnitude of the asymmetry factor a_v, at the same magnitude of the relative rolling reduction ε, the magnitudes of M_1 and M_2 change. The presented results of the investigation of the effect of asymmetric rolling process parameters on the magnitudes of total roll separating forces (the average pressure per unit strip width) and the rolling moment distributions on particular working rolls were obtained on assuming a constant rotational (peripheral) speed of the lower roll and a reduced rotational (peripheral) speed of the upper roll. Such a method of asymmetric rolling cannot be used under the actual conditions of finishing mill operation, as the continual overloading of the main rolling mill motor driving the lower roll would result in its overheating (especially during summer months, at relatively high ambient temperature in the drives hall) and shutting it down.

Therefore, the rolling process asymmetry should be introduced alternately by applying a higher rotational speed of the lower and the upper rolls in successive passes, which will cause the rolls to be alternately driving and driven rolls, whereby their excessive overloading will be prevented.

4. Summary and conclusions

From the investigation carried out, the following conclusions have been drawn:

– by introducing the asymmetric plate rolling process through differentiating working roll peripheral speeds, depending on the asymmetry factor used, the magnitude of the total roll separating force can be reduced and, at the same time, a smaller elastic deflection of rolling stand elements can be achieved;

– thanks to the smaller elastic deflection of the working rolls, finished plate with smaller dimensional deviations across its width and length can be obtained;

– the asymmetry of the rolling process should be introduced alternately by applying

a higher rotational speed of the lower and the upper rolls in successive passes, which will cause the rolls to be alternately driving and driven rolls, whereby their excessive overloading will be prevented.

References

1. Dyja H., Sałganik A. M., Piesin A. M., Kawałek A. Asymetryczne walcowanie blach cienkich Teoria, technologia i nowe rozwiązania [M]. Wydawnictwo Politechniki Częstochowskiej, (Poland), 2008. 345.
2. Kawałek A., Dyja H., Knapiński M. Wpływ asymetrycznego walcowania na poprawę wskaźników techniczno-ekonomicznych procesu walcowania blach na gorąco [J]. Hutnik Wiadomości Hutnicze. 2008, 6: 266-270 (in Polish).
3. Markowski J., Dyja H., Knapiński M., Kawałek A. Theoretical analysis of the asymmetric rolling of sheets on leader and finishing stands [J]. Journal of Materials Processing Technology, 2003, 183-188.
4. Sinicyn V.G. Nesimmetrichnaja prokatka listov i lent [M]. Metallurgija, Moskva, 1984, 165 (in Russian).
5. Kawałek A. Analiza pól prędkości i prędkości odkształcenia w asymetrycznej kotlinie walcowniczej [J]. Hutnik Wiadomości Hutnicze. 2002, 12: 485-488, (in Polish).
6. Dyja H., Wilk K. Asymetryczne walcowanie blach i taśm [M]. Wydawnictwo WMiIM Politechniki Częstochowskiej, (Poland), 1998. 268.
7. Gorelik V.S., Nalcha G.I., Rudnev A.E., Klimenko I.V., Feofilaktov A.V. Uluchshenie sluzhebnykh svojstv tolstykh listov putem osvoenija tekhnologii asimmetrichnoj prokatki [J]. Stal', 11, 1991, 41-44 (in Russian).
8. Forge3® Reference Guide Release 6.2, Sophia-Antipolis, 2002.
9. Kawałek A. Asymetryczne walcowanie blach grubych w walcarce wykańczającej [J]. Hutnik Wiadomości Hutnicze, 2006, 6: 266-270, (in Polish).

Chukin M.V., Korchunov A.G., Gun G.S., Polyakova M.A., Koptseva N.V.

NANODIMENTIONAL STRUCTURAL PART FORMATION IN HIGH CARBON STEEL BY THERMAL AND DEFORMATION PROCESSING

Abstract. On the example of high carbon steel of grade 80, updated by boron, the ability of forming nanodimensional structural constituents has been proved. Special types of thermal and deformation processing are used. The thin- plate pearlite structure, obtained in this way, according to modern material science concept is considered to be a nanomaterial where interlamellar spacing in a ferrite-carbide mixture is a nanodimensional element. It is experimentally proved that interlamellar spacing decreasing takes place in steel, being investigated after heat treatment and further cold plastic deformation. The rate of interlamellar spacing, after heat treatment, and cold plastic deformation is 1,66, the rate of billet geometrical dimensions, before and after deformation, is 1,6. The results obtained are used to achieve desired properties of high-tensile reinforcing bars of 9,6 mm in diameter for the new generation of concrete sleepers.

Keywords: Nanodimensional structural constituents, high carbon steel, pearlite structure, interlamellar spacing, thermal processing, deformation processing

Achievement of high quality and field reliability of metallic constructions is possible on the basis of knowledge-intensive technologies of getting materials with a new unique property package. Nowadays such technologies are those, which allow obtaining ultrafine and nanostructures, which considerably affect metal and alloy mechanical properties during the production of hardware items of different purpose [1]. This investigation actuality is stipulated by searching of an effective complex of impacts on billet microstructure with major diameters (more than 10,0 mm) made from high carbon steel to get the highest strength and ductility.

The aim of this work is to study peculiarities of getting nanodimensional structural constituents in the billet from high carbon eutectoid steel of grade 80, updated by boron, after special types of thermal and deformation processing. The thin- plate pearlite structure, obtained in this way, according to modern material science concept is considered to be a nanomaterial with structural constituents of plate form. Interlamellar spacing in a ferrite-carbide mixture is a nanodimensional element of steel structure.

The subject matter of the chosen thermal processing lies in heating and isothermal holding in the field of minimal stability of overcooled austenite with further cooling in lead hot melt. The thermal processing task is formed, in major diameter billets, steel structure, providing the capability of the highest hardening during the following deformation effect with large total deformation degrees.

The history of steel structural constituent fine crushing is known to be determined mainly by accumulation of sharing deformation in processing. Considerable steel structure fine crushing is achieved by large degrees of plastic deformation close to 1. To provide such processing conditions, repetitive cold plastic deformation was used. The differential characteristic of offered deformation effect is that operation modes are appointed in such a way, that each deformation cycle initiates active dislocations sliding and it provides additional fragmentation of microstructure and the highest hardening of thermally processed steel.

The billet of diameter 16,0 mm from high carbon steel with carbon content of 0.8 % was used to carry out the experiments. Thermal processing was realized with the following parameters: reheat temperature range was 930°C to 970°C; isothermal holding temperature range was 4700°C to 550°C. Ageing time was chosen that way to provide finishing diffusional decay of overcooled austenite in the preset temperature. Cold plastic deformation was carried out with total deformation degree up to 60%. Herewith the billet diameter decreased from 16,0 mm to 10,0 mm. Scanning electron-microscope analysis of the bars was done on the electron microscope JEOL JSM-6490 LV with accelerating voltage 30 kW in modes of secondary and temporary reflected electrons in conditions of Nano Steel Research Studies Institute of Nosov Magnitogorsk State Technical University. Quality and quantity microanalysis was carried out on the metallographic mi-

croscope Meiji Techno using computer system of images analysis Thixomet Pro.

A steel structure in its initial state represents a ferrite-carbide mixture with interlamellar spacing from 0,22 μm to 0,28 μm (Fig. 1, a). Small sections of structurally free ferrite are presented in microstructure (Fig. 1, b).

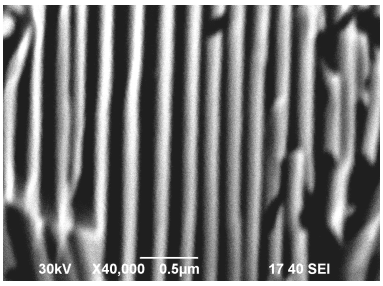

a

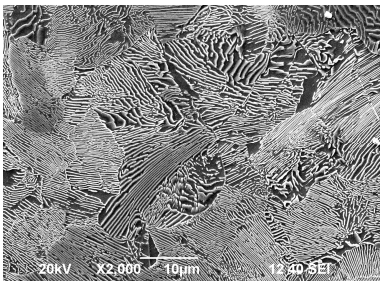

b

Fig. 1. Steel microstructure in its initial state

After thermal processing the microstructure consisted of a ferrite-carbide mixture and some quantity of structurally free ferrite as small islands on grain junction lines (Fig. 2, a) with interlamellar spacing of ferrite-carbide mixture from 0,12 μm to 0,16 μm (Fig. 2, b).

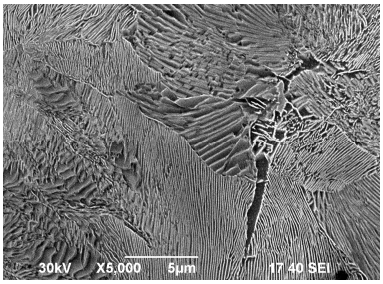

a

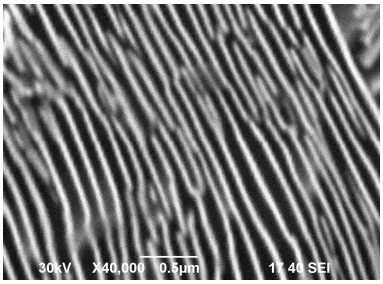

b

Fig. 2. Steel microstructure after thermal processing

Previous cold plastic deformation experiments showed that heat treated steel with interlamellar spacing in a ferrite-carbide mixture from 0,12 μm to 0,16 μm demonstrates the highest treatment and hardening capability [2]. Further decrease of interlamellar spacing in a ferrite-carbide mixture is observed in repetitive deformation processing for heat-treated steel with such structure parameters (Fig. 3).

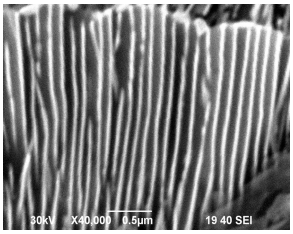

a

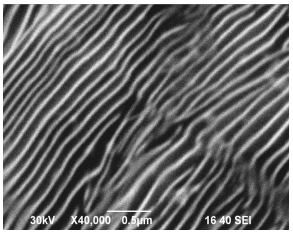

b

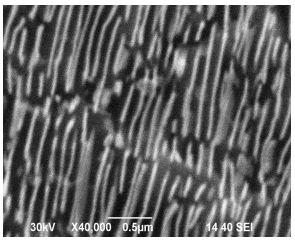

c

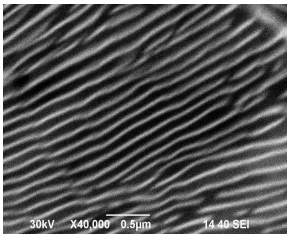

d

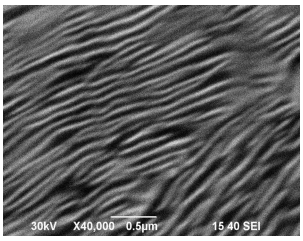

e

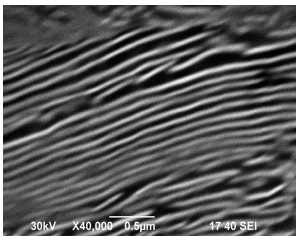

f

Fig. 3. Heat-treated steel microstructure at different total degree of cold plastic deformation:a – 21,8 %; b – 34,0 %; c – 43,3 %; d – 58,8 %; e – 56,3 %; f – 60,9 %

In Fig. 4 one can see interlamellar spacing value change in a ferrite-carbide mixture depending on total deformation degree.

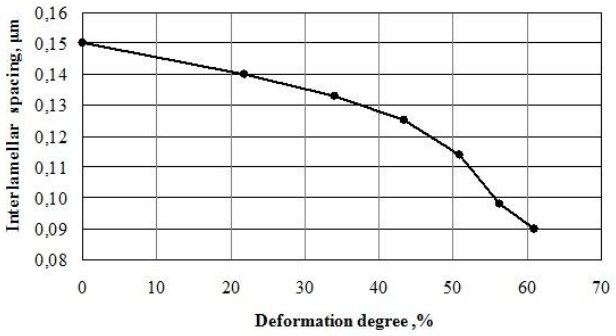

Fig. 4. Total deformation degree effect on interlamellar spacing value in a ferrite-carbide mixture

From the obtained data one can see that decrease of interlamellar spacing which is proportional to a diameter decrease of the billet, being processed, happens in the steel, being investigated, after heat treatment and further cold plastic deformation. The rate of interlamellar spacing after heat treatment and cold plastic deformation is 1,66, the rate of billet geometrical dimensions before and after deformation is 1,6. Thickness of cementite and ferrite plates in cold plastic deformation also decreases.

The results obtained are used in the established manufacturing for obtaining necessary properties for high-tensile reinforcing bars of 9,6 mm in diameter for concrete sleepers of new generation [3, 4]. Thermal and deformation processes combine, firstly, the special kind of thermal treatment of carbon steel, ensured the obtainment of nanostructured materials, possessed of high strength and ability to the subsequent deformation with high total deformation. For the purpose of producing nanostructured parts in the primary blank structure it intends to use the special kind of thermal treatment with mentioned above heating temperature and further isothermal holding. And secondly, highly productive constituent deformation process, activating free glide planes in every deformation cycle is used, which leads to additional fragmentation of material structure and provides maximal strengthening of the processed fittings. Deformation treatment modes set to activate new free glide planes in every deformation cycle which leads to additional dispersion of ultrafine grained stricture and fragmentation of ferrite solder pads in pearlite.

In Fig. 5 you can see the structure of quality indices of a high-tension reinforcement for armoring concrete sleepers.

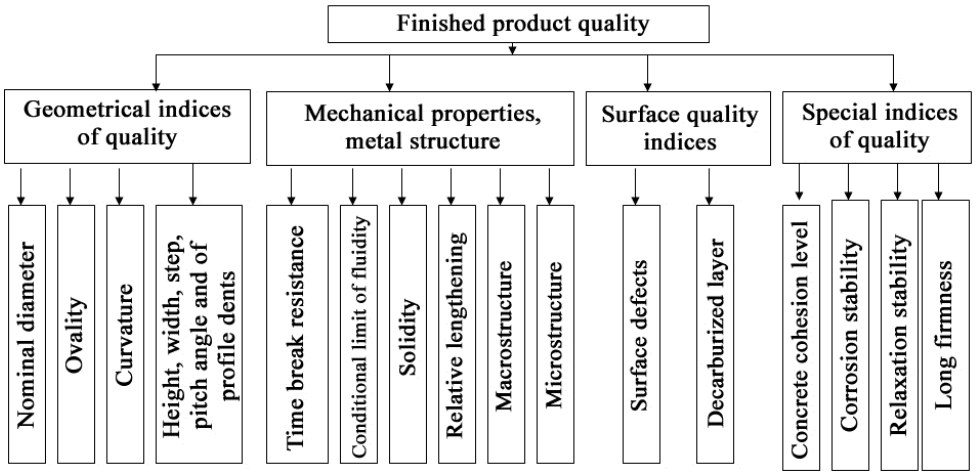

Fig. 5. Structure of quality indices of a high-tension reinforcement

Using such thermal and deformation processes in manufacturing of reinforcement for prestressed concrete constructions with enhanced apparent elastic limit and conventional yield strength enables to reach these values respectively not less than 80 and 90 % of sorting ultimate strength minimum. In these conditions reinforcement maintains sufficiently high ultimate elongation before rupture (not less than 4 %). Stress relaxation in reinforcement reduces sharply and do not exceeds 2 % at 1000 h under 20°C and accounts for 75% of tensile strength. Such complex of consumer attributes for end production diam. 9,6 mm is a conceptually new kind of product which cant be obtained by using tradition approaches to manufacture fittings for various applications.

Combination of mentioned treatment methods opens up high technological possibilities for enhancement of strength and special reinforcement properties keeping their high uniformity without steel alloying. The established high-technology production of high-tensile reinforcement with diameter of 9,6 mm for reinforcing of concrete sleepers for modern highways possesses the necessary characteristics of innovation technology. It's the first time of complex usage of modern science intensive thermal and deformation processes for influence on carbon steel structure with forming nanostructured state.

Post graduate students Gulin A., Dolgiy D., Constantinov D., Lysenin A. took part in the presented investigations.

The research corresponds to the realization of complex project for high-technology production development. This project is performed with participation of Russian higher education institute (contract 13.G25.31.0061), the program of the strategic development of the university 2012–2016 years (the competitive support of The Ministry of Education and Science of the Russian Federation the strategic development of SEI HPE) and Grant in the form of subsidy to support scientific researches (agreement № 14.B37.21.0068).

References

1. Chukin M., Koptseva N., Barushnikov M., Efimova Y., Nosov A., Noskov S., Kolomiets B. Innovative potential of new ware production technologies from nanostructured steels. *Vestnik Magnitogorskogo gosudarstvennogo tehnicheskogo universiteta im. G.I. Nosova.* [Vestnik of Nosov Magnitogorsk State Technical University]. 2009, no. 2, pp. 64-68.
2. Lebedev V., Chukin M., Gun G., Korchunov A., Polyakova M. Prospects of high-tensile in manufacturing of large diameter wire rod at «MMK-Metiz» – Magnitigorsk Hardware and Sizing Works / *CIS Iron and Steel Review*, 2011. pp. 18-21.
3. Chukin M., Gun G., Korchunov A., Polyakova M. Manufacturing prospects of high-tension reinforcement from high carbon steel. *Iron and Steel.* 2012. December. pp. 8-15.
4. Ushakov S., M.B. Chukin M., Gun G., Korchunov A., Polyakova M. High-tension reinforcement for armoring new age concrete sleepers. *The path and track facilities*. 2012. no. 11. P. 25-27.

Satonin A.V., Korenko M.G., Nastoyashchaya S.S., Perekhodchenko V.A.

THE DEVELOPMENT OF ENGINEERING METHODS FOR CALCULATING ENERGY-POWER PARAMETERS OF RELATIVELY THIN STRIPS HOT ROLLING PROCESS

Abstract. Based on the analytical solutions the engineering mathematical model of the relatively thin strips hot rolling process energy-power parameters has been and expanded.Criterion evaluation has confirmed a sufficient degree of accuracy of the engineering techniques obtained. It was done on the basis of the skidding lines fields' method which allows us to take into account two-dimensional character of plastic metal forming absolutely.

Keywords: power parameters, relatively thin strips, roll gap, engineering mathematical model.

Further development of ferrous and non- ferrous metallurgy is inextricably linked with the increasing automation of relatively thin sheet and strip hot rolling process. Alongside with the numeral solutions some engineering mathematical models of the technological scheme energy-power parameters are also of interest as the ones that are able to ensure the rational combination of complexity, performance, and the reliability of the results.

As for engineering methods for calculating the rolling of relatively thin sheets and strips one of the most frequently used technique is the A.I Tselikov's one, which is based on the analytical description of the external contact friction conditions expressed as the Amontons-Coulomb law. [1]. From the point of view of the conditions of the hot-rolling process realization it is more appropriate to use the Siebel's law as the one providing condition of non-exceeding tangential contact stresses τ_x shear resistance of the rolled metal K_x to the entire range of possible relative reduction. In this case it is necessary as well to take into account availability of an elastic recovery zone, as well as the influence of the stress deviator tangential components that may reach sufficiently large relative values.

The purpose of the work is to refine and expand the engineering power parameters of the mathematical model process of relatively thin strips hot rolling.

Engineering mathematical model of power parameters of relatively thin strips hot rolling process having been developed as similar to the methods of [1, 2] is based on the following basic assumptions adoption:

- rolled strips plastic changes are two-dimensional and temporally steady;
- deformation zone (Fig. 1a) includes the area of plastic forming with the length of $L_{nл}$ and area of the elastic recovery of the rolled strip with the length of L_{yn} ;the boundaries of plastic and elastic forming zones, and the cross section area of conjugation lag with the length of L_{om} and timing zone, with the length of L_{on}, are vertical, and parallel to the plane which is passing through the axis of the work rolls rotation;
- the current value of doubled $2K_x$ shear resistance and coefficient of friction of the plastic zone along the length of μ_x plastic forming is constant and equal to their average integral estimates $2K_c$ and μ_c ;
- forming surface work rolls in zone plastic metal forming approximated by chords, whereupon the current values of the angle α_x are constant (see Fig. 1);
- normal axial stress σ_x on height cross-section plastic forming zone not changed, and tangent components

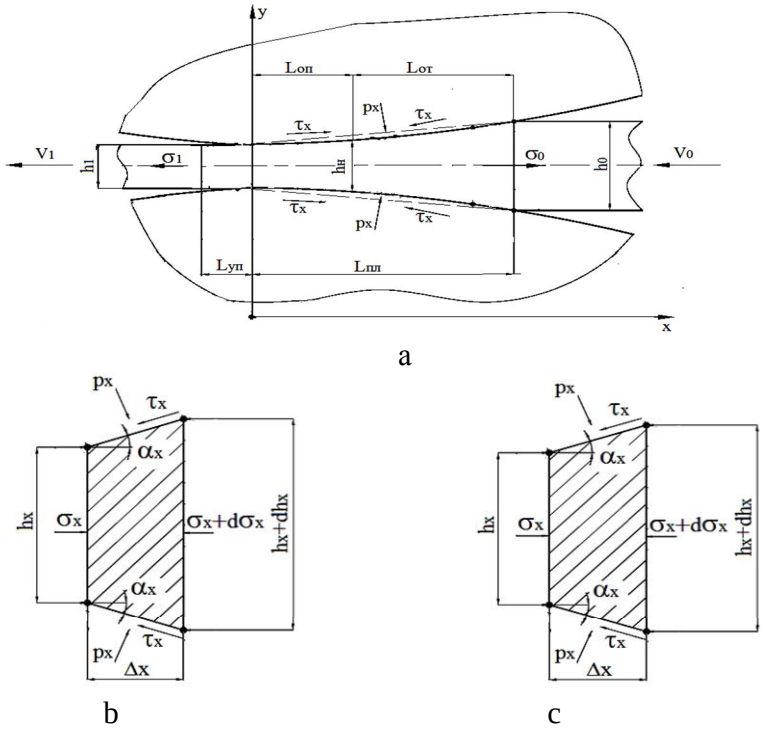

Fig. 1. Settlement schemes of the deformation integrated center (a), and also elementary volumes of metal in relation to engineering mathematical modeling of power parameters of relatively thin strips hot rolling process allocated in a lag zone (**б**) and in an advancing zone (**в**)

stress deviator τ_{xy} change in law close to linear and their average integral evaluation corresponds to the expression:

$$\tau_{xyc} = \tau_x / 2 = 2K_c\mu_c / 2. \quad (1)$$

Taking into account character of the accepted assumptions the equation of balance of metal elementary volume allocated in a zone of the lag (see fig. 1, a, b), looks like:

$$\sigma_x h_x - (\sigma_x + d\sigma_x)(h_x + dh_x) + 2p_{xот} tg\alpha dx - 2\tau_x dx = 0, \quad (2)$$

where p_x, σ_x, τ_x – are the current values of normal contact tension, normal axial and tangent contact tension, and compression tension is accepted as positive values of tension p_x and σ_x; α_x, h_x –are the current quantities of contact corners and thickness of the rolled strip corresponding to certain dependences of a kind (we take into account accepted assumptions):

$$\alpha_x = \alpha = arctg(0{,}5\Delta h / L_{пл}); \quad h_x = h_1 + \Delta h(x / L_{пл}). \quad (3)$$

Proceeding from the law of external contact friction used and neglecting infinitesimal of the second and more orders, the expression (2) is transformed into a kind:

$$-\sigma_x dh_x - d\sigma_x h_x + p_{xот} dh_x - 2K_c 2\mu_c dh_x / (2tq\alpha) = 0. \quad (4)$$

Following a full form of a plasticity condition record [1], the quantity of normal axial tension σ_x can be presented as:

$$\sigma_x = p_{xom} - \sqrt{4K_c^2 - 4\tau_{xy}^2} = p_{xom} - \sqrt{4K_c^2 - 4K_c^2\mu_c^2} = p_{xom} - 2K_c a_k, \quad (5)$$

where $a_k = \sqrt{1-\mu_c^2}$ – is the auxiliary variable providing a form record simplification.

After substitution of the condition (5) in the expression (2), we will receive:

$$2K_c a_k dh_x - dp_{xот} h_x - 2K_c \delta_\mu dh_x = 0, \quad (6)$$

Where $\delta_\mu = 2\mu_c L_{пл} / \Delta h$ – is the auxiliary quantity characterizing influence of geometrical parameters and conditions of external contact friction in the deformation center.

Having transformed the differential equation (6) to a kind:

$$2K_c(a_k - \delta_\mu)(dh_x / h_x) = dp_{xот}, \quad (7)$$

As a result of its integration we shall receive:

$$2K_c(a_k - \delta_\mu)\ln h_x = p_{xот} + C_{от}, \quad (8)$$

where $C_{от}$ – is the constant of integration defined for a lag zone which is preceded from known values of normal contact tension in section to the deformation center entrance $p_{xот|_{h_x=h_0}} = 2K_c a_k - \sigma_0$:

$$C_{от} = 2K_c(a_k - \delta_\mu)\ln h_0 - 2K_c a_k + \sigma_0, \quad (9)$$

where σ_0 – is tension quantity of a rolled strip back tension.

As a result of the substitution (9) in the condition (8) finally for normal contact tension p_{xom} in a lag zone is we have the following:

$$p_{xот} = 2K_c(\delta_\mu - a_k)\ln(h_0 / h_x) + 2K_c a_k - \sigma_0. \quad (10)$$

By analogy with (2) for an advancing zone (see Fig. 1 a, c) the differential equation of a condition of static balance of the allocated elementary volume looks like:

$$\sigma_x h_x - (\sigma_x + d\sigma_x)(h_x + dh_x) + 2p_{xоп} dx tq\alpha_x + 2\tau_x dx = 0, \quad (11)$$

and following that we will get the in accordance with above mentioned (3)-(8):

$$2K_c(a_k + \delta_\mu)\ln h_x = p_{xоп} + C_{оп}, \quad (12)$$

where $C_{оп}$ – is integrations permanent that is determined for the zone of passing, and based on the well-known quantities of normal pin tensions in a section on the plastic form destructing zone exit $p_{xоп|_{h_x=h_1}} = 2K_c a_k - \sigma_1$:

$$C_{оп} = 2K_c(a_k + \delta_\mu)\ln h_1 - 2K_c a_k + \sigma_1. \quad (13)$$

where σ_1 – is tension quantity of a rolled strip front tension.

Finally in relation to the tension quantities which are current on the length of advancing zone we have $p_{xоп}$:

$$p_{xоп} = 2K_c(\delta_\mu + a_k)\ln(h_x / h_1) + 2K_c a_k - \sigma_1. \quad (14)$$

On the principle that the value of normal pin tensions in a neutral section in thick $h_н$ (see Fig. 1 **а**) are equivalent both for the lag zone and for the one of advancing $p_{xот|_{h_x=h_н}} = p_{xоп|_{h_x=h_н}}$ in accordance with (10) and (14), it is possible to write down:

$$2K_c(\delta_\mu - a_k)\ln(h_0 / h_н) + 2K_c a_k - \sigma_0 = 2K_c(\delta_\mu + a_k)\ln(h_н / h_1) + 2K_c a_k - \sigma_1, \quad (15)$$

From where after some mathematical transformations the thickness of stripe in a neutral section $h_н$, and also extent of advancing zone $L_{оп}$ (see Fig. 1 **а**) can be defined as:

$$h_н = \sqrt{h_0 h_1}\exp\times$$
$$\times\left\{a_k \ln(h_1/h_0) + \sigma_1/2K_c - \sigma_0/2K_c)/(2\delta_\mu)\right\}; \quad (16)$$

$$L_{on} = (h_н - h_1)L_{пл}/\Delta h. \quad (17)$$

having integrated the distributions of normal pin tensions $p_{хот}$ (10) and $p_{хоп}$ (14) it is possible to define the quantity of the tense state coefficient n_σ as:

$$n_\sigma = (1/L_{пл})\left[\int_0^{L_{on}} p_{хоп}dx + \int_{L_{on}}^{L_{пл}} p_{хот}dx\right], \quad (18)$$

from where with an account of (10), (14):

$$n_\sigma = \frac{1}{L_{пл}}\left\{\int_0^{L_{on}}\left[(\delta_\mu + a_k)\ln\left(\frac{h_1 + \Delta hx/L_{пл}}{h_1}\right)\right]dx + \int_0^{L_{on}}\left(a_k - \frac{\sigma_1}{2K_c}\right)dx + \right.$$
$$\left. + \int_{L_{on}}^{L_{пл}}[(\delta_\mu - a_k)\ln(\frac{h_1 + \Delta hx/L_{пл}}{h_0})]dx + \int_{L_{on}}^{L}(a_k - \frac{\sigma_0}{2K_c})dx\right\} \quad (19)$$

As a result of integration (19) with the use of auxiliary variables $(h_1 + \Delta hx/L_{пл})/h_1 = U_1$, $(h_1 + \Delta hx/L_{пл})/h_0 = U_2$, we will get finally:

$$n_\sigma = (\delta_\mu + a_k)\left[\frac{h_н}{\Delta h}\ln\frac{h_н}{h_1} - \left(\frac{h_н - h_1}{\Delta h}\right)\right] + \left(a_k - \frac{\sigma_1}{2K_c}\right)\left(\frac{h_н - h_1}{\Delta h}\right) +$$
$$+\left(\delta_\mu - a_k\right)\left[\frac{h_0 - h_н}{\Delta h} - \frac{h_н}{\Delta h}\ln\frac{h_0}{h_н}\right] + \left(a_k - \frac{\sigma_0}{2K_c}\right)\left(\frac{h_0 - h_н}{\Delta h}\right), \quad (20)$$

and issued from that the quantity of average integrals on the length of plastic deformation zone of normal pin tensions p_c may correspond:

$$p_c = 2K_c n_\sigma. \quad (21)$$

Taking into account the well-known values $2K_c$, μ_c, $L_{пл}$, of radiuses R of working rollers and widths B of the rolled stripe the value of rolling total moment can be determined as:

$$M_\Sigma = 2\times 2K_c\mu_c RB(L_{пл} - 2L_{on}) =$$
$$= 2\times 2K_c\mu_c RBL_{пл}[1 - 2(h_н - h_1)/\Delta h]. \quad (22)$$

Criterion estimation of authenticity degree of the decisions received (10) and (14) was executed with the use of the fields of skidding lines method, allowing to take into account two-dimensional character of plastic metal deformation. Construction and subsequent analysis of the fields of descriptions in physical plane and plane of hodograph of speeds (Fig. 2) were produced numerically in accordance with methodologies of works [2, 3].

As an example of numeral realization results of solutions offered are presented on a Figure 3 the comparisons of calculation distributions of current $n_{\sigma x}$ values of the metal tense state coefficient which were received by analytical decisions using (10), (14) and on basis of the skidding lines fields method [2, 3].

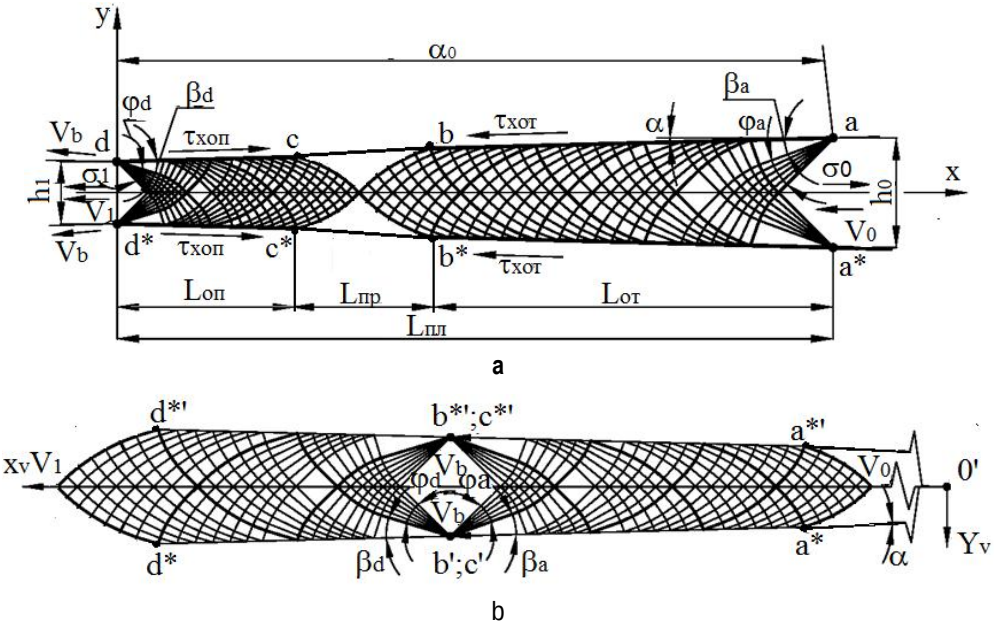

$$L_{пл}/h_{ср} = 10{,}0;\ \alpha = 1{,}5°;\ \mu_{om} = 0{,}4;\ \mu_{on} = 0{,}42;\ \sigma_1/2K_c = 0{,}0;\ \sigma_0/2K_c = 0{,}175$$

Fig. 2. The fields of descriptions in the physical plane of XOY(a) and planes of hodograph of speeds $X_V O'Y_V$ (b) as it applies to the process of the hot rolling of relatively thin stripes [2, 3].

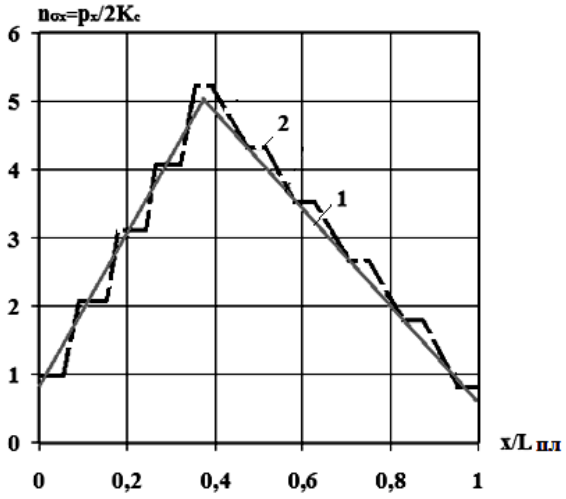

Fig. 3 Settlement data, received according to the considered technique (1) and on the basis of the skidding lines fields method of (2) distributions of the metal tension coefficient current values.

The analysis of these results confirmed the sufficient degree of reliability of the received engineering calculation procedure.

It should be noted that one of current trends of calculation engineering methods of power parameters development is the accounting of working rolls elastic flattening and existence of a strip elastic restoration zone not only at cold, but at hot rolling as well [1, 2, 4]. In relation to working rolls elastic flattening this approach can be realized by iterative determination of plastic forming zone extent $L_{плс}$ and the subsequent determination of the elastic deformed working rolls radius $R_д$:

$$L_{плс} = \sqrt{R\Delta h + x_L^2} + x_L; \quad R_д = L_{плс}^2 / \Delta h, \qquad (23)$$

where $x_L = 8Rp_c(1-\omega_в^2)/(\pi E_в)$ is the auxiliary variable used for simplification of a form of record [1]; $\omega_в$, $E_в$ is Poisson's coefficient and a model of working rolls material elasticity.

The accounting of existence of a rolled strip elastic restoration zone in sections at the working rolls exit (see. Fig. 1, a) can be carried out on the basis of algorithmic sequence of a kind:

$$p_{x1} = 2K_{x1} - \sigma_1; \quad \delta h_1 = p_{x1}(1-\omega_п^2)/E_п; \quad L_{уп} = \sqrt{R_д \delta h_1}, \qquad (24)$$

where $p_{x1}, 2K_{x1}, \delta h_1$ is the normal contact tension, doubled value of resistance to rolled metal shift and the quantity of a strip elastic deformation in section at the plastic forming exit zone; $\omega_п, E_п$ is Poisson's coefficient and elasticity model of the rolled strip material, which take into consideration its temperature.

Proceeding from dependences structure (20), (21), (23) and (24) force value at hot rolling of relatively thin strips is defined as (and we take into account working rolls elastic flattening and existence of a elastic restoration zone):

$$P = (p_c L_{плс} + p_{x1} L_{уп}/2)B, \qquad (25)$$

Thus, owing to existence of functional interrelations $p_c = F(L_{плс})$ and $L_{плс} = F(p_c)$ direct determination of P force can be carried out iteratively using standard approaches [1, 2] at which in the calculations first cycle working rolls are accepted to be absolutely rigid, normal contact tension p_c, the value of a plastic forming zone extent $L_{плс}$, are defined and after taking it into account calculation p_c is repeated and so on. As convergence criteria assessment of the decision iterative procedure relative degree of discrepancy of extents $L_{плс}$ in this and in previous calculation cycles was used.

Conclusions

On the basis of analytical decisions the engineering mathematical model of hot rolling process power parameters of relatively thin strips is specified and expanded. This model is distinguished by the correct accounting of external contact friction conditions and also of tangents components of a tension deviator influence indicators, as well as accounting of rolled metal elastic restoration zone existence. The criterion sufficient degree of authenticity of the decision is confirmed by the results of comparison with the analogical quantitative estimations, which we got on the basis of method of the skidding lines fields that allow taking into account two-dimensional character of plastic form destruction throughout metal at the relatively thin stripes hot rolling.

References

1. Celikov A.I., Nikitin G.S., Rokotyan S.E. *Teoriya prodol'noj prokatki.* [The theory of longitudinal rolling]. Moscow : Metallurgiya, 1980, 320 p.
2. Fedorinov V.A., Satonin A.V., Gribkov E.P. *Matematicheskoe modelirovanie napryazhenij, deformacij i osnovnyx pokazatelej kachestva pri prokatke otnositel'no shirokix listov i polos : monografiya.* [Mathematical modeling of stresses, strains, and the main indicators of the quality of the rolling sheets and relatively broad bands: monoraph]. Kramatorsk : DGMA, 2010, 243 p.
3. Potapkin V.F. *Metod polej linij skol'zheniya v teorii prokatki shirokix polos : monografiya.* [The method of slip-line field theory rolling in broad bands: Monograph]. Kramatorsk : DGMA, 2005, 316 p.
4. Kozhevnikova I.A. Garber E.A. *Proizvodstvo prokata. Razvitie teorii tonkolistovoj prokatki dlya povysheniya e'ffektivnosti raboty shirokopolosnyx stanov.* [Production of rolled products. The development of the theory of sheet rolling to improve the efficiency of broadband mills]. Moscow : Teplotexnik, 2010, vol. 1, kn. 2, 251 p.

Borovik P.V.

3D MODEL OF CUTTING BY ROLLING CUT TYPE SHEARS

Abstract. 3D model of rolling cut process by shears on the base of finite element method is developed and dependence of maximum cutting force on the knife curve radius is detected. Suggestions directed to increase of productivity of shears are recommended.

Keywords: shears, rolling cut, curved knife, cutting force.

Separation operations are widely used in rolling production and establish quality and cost price of metal products. One of such separation operations is thick sheet cutting using the rolling cut type shears [1, 2].

Rolling cut is used for longitudinal and sectional cutting of sheets. With this type of cutting one can almost avoid deformation of cutting edge at circulated shear movement [1, 2].

As experience shows, at rolling cut a dependence of cutting force on the starting point of the cutter going into metal has got apparent peak (Fig. 1,b) that can be explained by less value of cutting angle. Because of various model shears difference between maximum and fixed cutting force can be about 30…60%. This fact helps in increasing shears metal content.

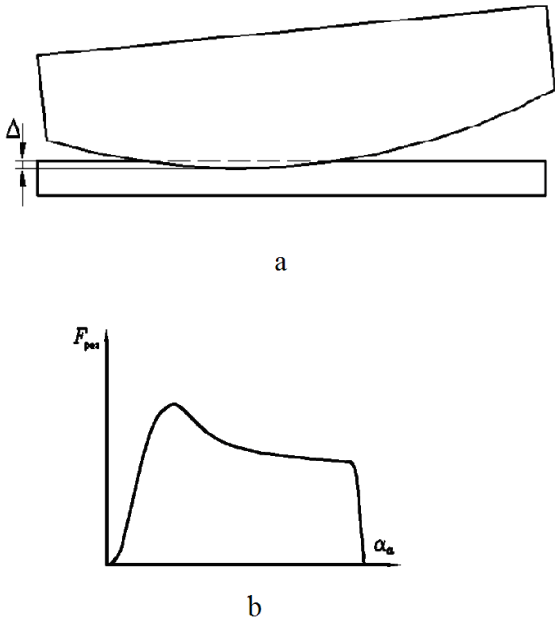

Fig. 1. Scheme for rolling cut (a) and specific dependence of cutting force (b)

There are technical decisions known [3, 4] that tend to reducing the peak loads during rolling cut which is made by changing the shears design. But such approach has low technical efficiency during manufacturing.

In present days due to advanced computational tools and progress in theoretical researches simulation techniques for different pressure treatment technological processes aiming to their thoroughly studying and improvement are widely used.

Therefore, to give full image of rolling cut process it is necessary to use modern theoretical approaches and methods among which finite element method (FEM) has got a special role [5, 6].

The purpose of this work is to develop 3D model of rolling cut process on the base of finite element method and detect factors affecting the cutting force value.

To get to the purpose set theoretical researches have been made using ABAQUS software. 3D model has been developed for this describing cutting process of sheets with curved knife on the shears with rolling cut in Lagrange formula using ALE (Arbitrary Lagrangian Eulerian) mesh adaptation and including gravity.

A model (Fig. 2) is for extremely hard analytical rigid body – a holder, a Table, upper curved and lower stationary knife, as well as deformable beam as a model of sheet being cut.

And as an analog to real design of rolling cut type shears a motion is transmitted to upper curved knife along the specific trajectory and to the Table in vertical direction while the lower knife and a holder are fixed.

Deformable beam is a mesh of isoparametric an 8-node linear brick elements with reduced integration scheme and hourglass control, having the features of entire deformable material. Mesh configuration is irregular getting compacting in the shearing zone (Fig. 3).

Friction between contact surfaces models Coulomb's friction law. Herewith, constant of friction is fixed and characterizes the relation between contact pressure and equivalent shear stress.

Material fracture was simulated using a method of elimination of elements from the calculations after the ductility resources were over in accordance with ductility curve [6].

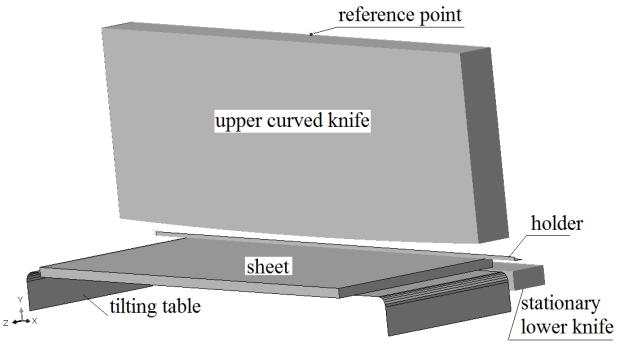

Fig. 2. General view of cutting process simulation for sheets using curved knife on rolling cut type shears

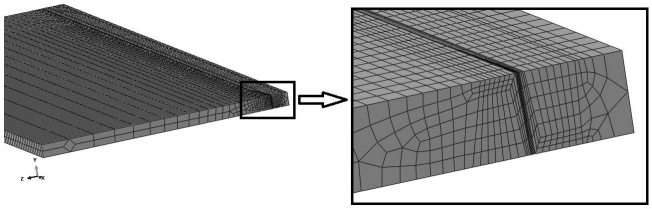

Fig. 3. Initial mesh configuration

For simulating in cutting processing they used steel grade St2ps. Sheet depth is 50 mm, width – 2500 mm.

On the first study stage through famous methods [1,2,7] calculations of kinematic operation parameters of shears have been made. Two-crank shears from NMBW (Novokramatorsk Machine - Building Works) has been taken as a model. Fig. 4 shows the calculated trajectory for reference point which afterwards has been put into a model for simulating the upper knife motion.

In the studied model of rolling cut type shears a radius of curved knife in the initial point is 47m, and a clearance between knives in the initial point is 148 mm. Fig. 5 shows the simulation results.

As you can see from the results presented the maximum cutting force is ≈1,6 times more than steady cutting. So, further researches have been directed to reveal the possibilities of reducing such gap.

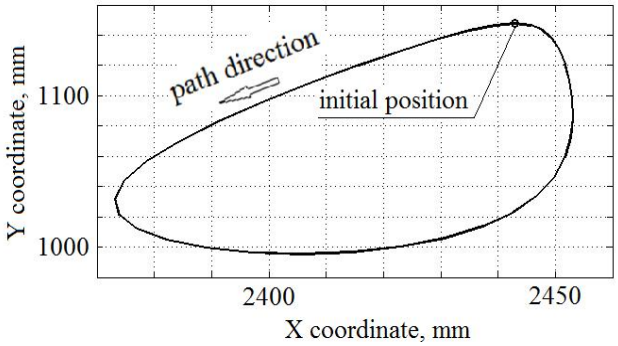

Fig. 4. Path the reference point of upper knife

In this way they changed the radius of knife curve at constant clearance between the knives and kinematics of system movement. The results revealed that increasing the knife radius promotes reducing the force in the starting cutting moment and its simultaneous raise at the end of cutting (Fig. 6, **a**). Basing on the results achieved the dependence of maximum cutting force on the knife curve radius was obtained (Fig. 6, b).

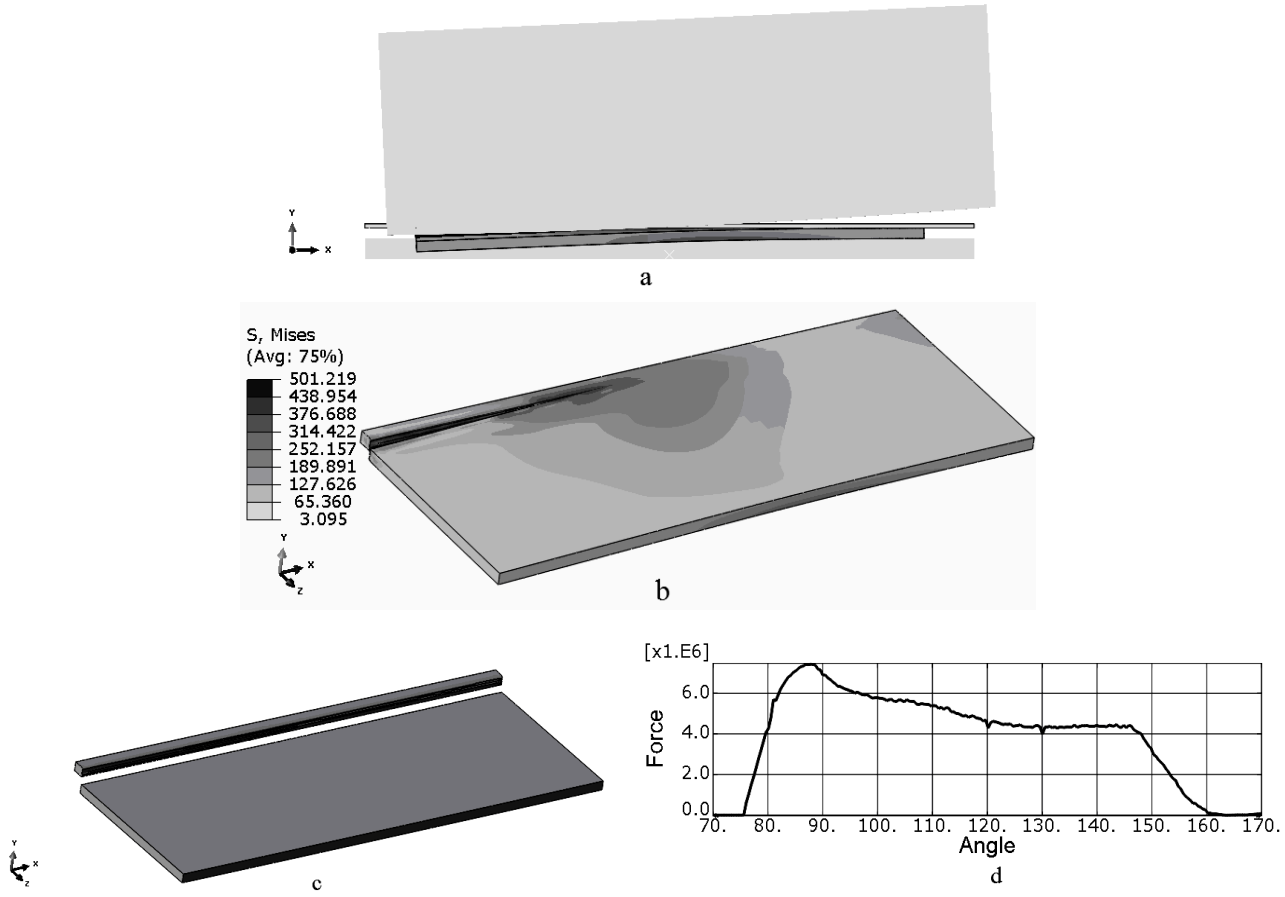

Fig. 5. Simulation results: a – knife position in moving of cams to 99°;
b – stress-strained state of sheet in the same position; c – configuration after full separation of the sheet;
d –cutting force $\left(N \times mm\right)$ dependence on rotation angle of cams

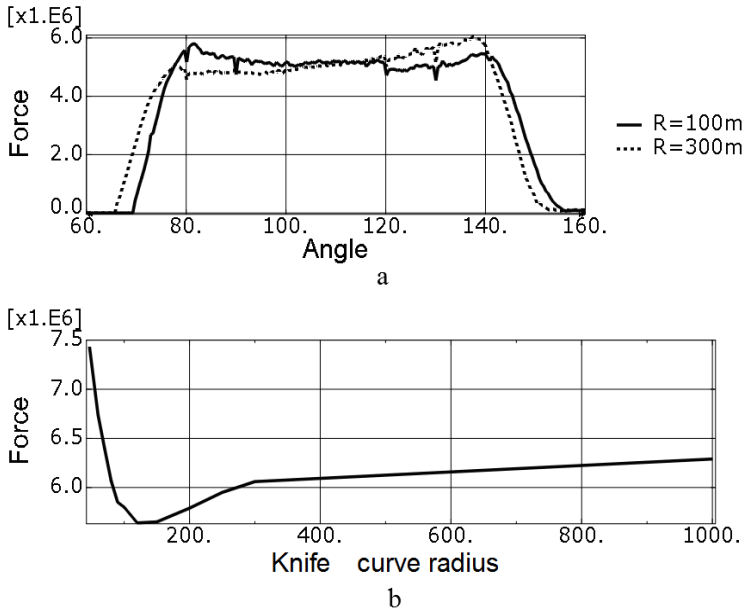

Fig. 6. Effect of knife curve radius to cutting force: **a** – specific dependences of cutting force in increasing knife curve radius; b – dependence of maximum cutting force on knife curve radius

According to the results of the work one can summarize:

– technological opportunities of rolling cut type shears are not always used in full volume due to large (about 60%) divergence between maximum cutting force and its steady value;

– increasing the knife curve radius to certain value provides more even distribution of force during cutting process and then its visible growth on knife coming out of cut;

– applied to the given shears design at cutting the sheets with maximum depth 50 mm knife curve radius 80…200 meters allows to obtain more stable force distribution during the cutting process;

– in given conditions maximum cutting force relatively to curve radius of 47 m reduces for 25…30 %, that indicates to real opportunity to increase the range of cut sheets.

The results of the work can be used for practical application and during research and development of cutting process for rolling cut type shears.

References

1. Korolev A.A. *Konstrukcija i raschet mashin i mehanizmov prokatnyh stanov*. [Design and calculation of rolling mill machinery]. Moscow : Metallurgija, 1985. 376 p.
2. Ivanchenko F.K., Grebenik V.M., Shirjaev V.I. *Rozrahunok mashin i mehanizmiv prokatnih cehiv*. [Machinery calculating for rolling mills]. Kiev: Vishha shk., 1995. 455 p.
3. Adamovich R.A., Rudel'son L.M., Rogoza A.M., Pal'min A.D. *Nozh dlja listovyh nozhnic s katjashhimsja rezom*. [Knife with rolling cutter for sheet shears]. A.s. USSR, no. 810403, 1981.
4. Adamovich R.A., Rudel'son L.M., Rogoza A.M., Pal'min A.D. *Nozh dlja nozhnic s katjashhimsja rezom.* [Knife shears with rolling cutter]. A.s. USSR, no. 902989, 1982.
5. Liu G.R., Quek S.S. The Finite Element Method: A Practical Course, 2003, 348 p.
6. Borovik P.V., Usatjuk D.A. *Novye podhody k matematicheskomu modelirovaniju tehnologicheskih processov obrabotki davleniem*. [New approaches to the mathematical modeling of pressure treatment processing]. Alchevsk : DonGTU, 2011. 299 p.
7. Notchenko V.D, Bojdenko A.N., Emchenko E.A., Cherkasov N.D., Zozulja E.S., Poslushnjak A.V. Chislennoe matematicheskoe modelirovanie processa rezanija listovogo metalloprokata na nozhnicah s dugoobraznym nozhom. [Numerical mathematic process simulation of sheet metal cutting with shears with embowed knife]. *Udoskonalennja procesiv i obladnannja obrobki tiskom v mashinobuduvanni i metalurgii : temat. zb. nauk. pr*. [Pressure treatment processing and machinery improving in machine building and metallurgy: Col.of Scient. Papers]. Kramators'k, 2001. pp. 454-457.

Gribkov E.P., Danilyuk V.A.

MATHEMATICAL MODELLING OF SRTESS-STRAIN BEHAVOIR IN ROLLING OF THE COMPOSITIONS INCLUDING POWDER MATERIALS

Abstract. The developed mathematical model of rolling of two-layer powder materials allows to determine the rational technological parameters of process excluding deformation of a substrate and raising an exit of suitable by production of inserts of sliding bearings. It is established that the less thickness of a metal substrate, the more subjects is deformed, and respectively, powder is less deformed. In increasing the layers ratio the force and the rolling moment growing and the increasing of final relative density of powder composition are observed.

Keywords: mathematical model, rolling, powder materials, substrate, relative density, deformation center.

One of the perspective directions in the field of composite hardware production is rolling of compositions with using the powder materials, allowing to receive wide assortment of production with simultaneous ensuring specific operational properties and simultaneous economy of extremely scarce and expensive materials. The most widespread ways of rolling of such type production is rolling of compositions powder-powder and powder-monometal.

The mathematical model of rolling single-layer powder materials [1] was taken as a principle of numerical mathematical model of rolling of two-layer powder materials. The settlement scheme of the integrated deformation center used in this case is submitted in figures 1 and 2.

Splitting of a consolidation zone into a final set of elementary volumes and definition of geometrical characteristics, and also tensions σ_x, τ_x and p_x in a final and differential form (Fig. 2) was carried out by analogy to a technique stated in work [1].

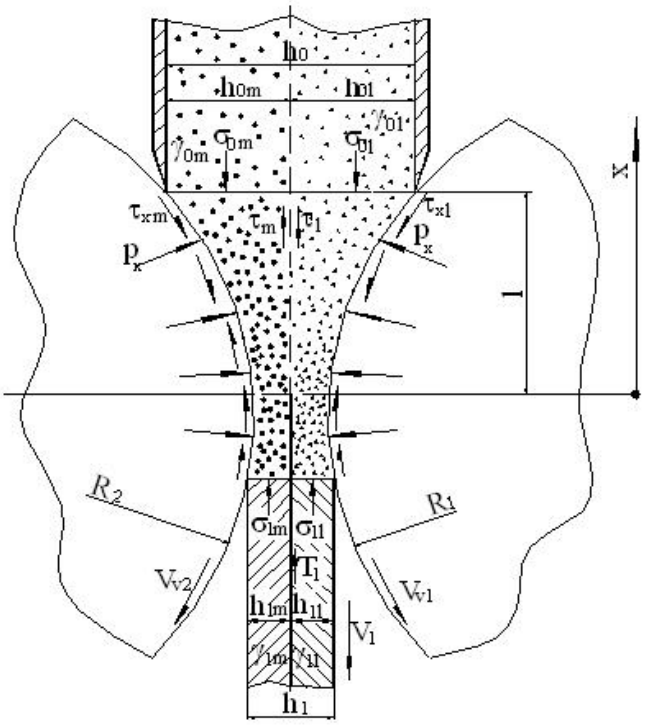

Fig. 1. The settlement scheme of the integrated deformation center in realization of rolling of composition powder (m) – powder (l)

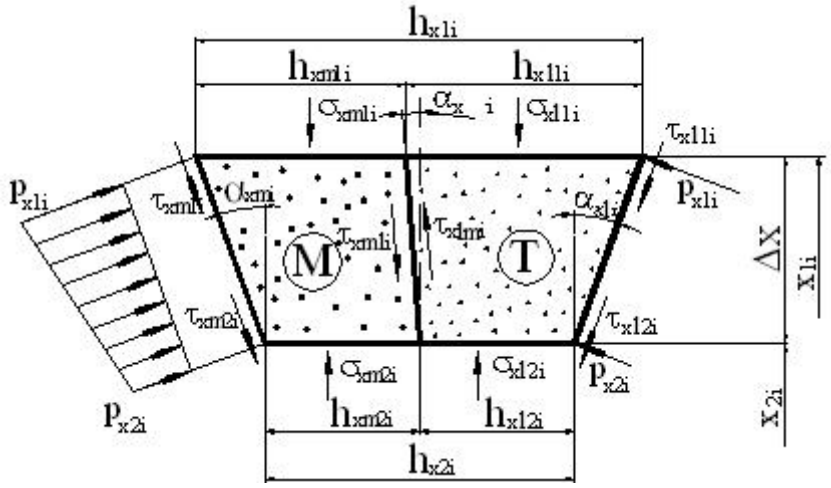

Fig. 2. The settlement scheme of allocated i-th of elementary volume of the deformation center in realization of rolling of composition powder (m) – powder (l)

At the same time it should be noted that friction existence between layers alters a condition of static balance of the allocated elementary volume of the deformation center, having the following appearance:

for less plastic component:

$$\sum F_{xil} = \sigma_{x2il} h_{x2il} - \sigma_{x1il} h_{x1il} - 0.5\Delta x(p_{x1il} f_{x21i} + p_{x2il} f_{x22i}) \mp 0.5(p_{x1il} + p_{x2il})\Delta x f_{ci} + 0.25(p_{x1il} + p_{x2il}) \times (h_{x1i} - h_{x2i}) \pm 0.5(p_{x1il} + p_{x2il}) \times (h_{x1il} - h_{x2il} - (h_{x1i} - h_{x2i})/2) = 0; \quad (1)$$

for more plastic component:

$$\sum F_{xim} = \sigma_{x2im} h_{x2im} - \sigma_{x1im} h_{x1im} - 0.5\Delta x \times (p_{x1im} f_{x11i} + p_{x2im} f_{x12i}) - 0.5(p_{x1im} + p_{x2im}) \times \Delta x f_{ci} + 0.25(p_{x1im} + p_{x2im})(h_{x1i} - h_{x2i}) = 0, \quad (2)$$

where $h_{x1il(m)}$, $h_{x2il(m)}$ are the current thickness less (more) strong components at the entrance and at the exit from the allocated elementary volume, respectively; h_{x1i}, h_{x2i} are the current thickness of all compositions at the entrance and at the exit from the allocated elementary volume, respectively; Δx is the extent of the allocated elementary volume of the deformation center; $f_{x11(2)i}$, $f_{x21(2)i}$ are the current values

of friction coefficients at the entrance and at the exit from the allocated elementary volume, respectively; f_{ci} is the current value of friction coefficient between composition layers; $p_{x1il(m)}$, $p_{x2il(m)}$ are the current values of normal contact tension at the entrance and at the exit from the allocated elementary volume, respectively; $\sigma_{x1il(m)}$, $\sigma_{x2il(m)}$ are the current values of normal tension at the entrance and at the exit from the allocated elementary volume, respectively.

Substituting in the equation of static balance a condition of plasticity for loose environments [2]:

$$\sigma_x = \frac{1-2\alpha_x}{1+4\alpha_x} p_x - \sqrt{p_x^2\left[\left(\frac{1-2\alpha_x}{1+4\alpha_x}\right)^2 - 1\right] + \frac{4}{3}\frac{1+\alpha_x}{1+4\alpha_x}\beta_x\sigma_{sx}^2}, \quad (3)$$

it is possible to determine normal contact tension:

$$p_{x2}^2\left(t_1^2 - t_3\right) + 2p_{x2}t_1t_2 + t_2^2 - t_4 = 0, \quad (4)$$

for less plastic component:

$$t_1 = \frac{1-2\alpha_{x2l}}{1+4\alpha_{x2l}} h_{x2l} + \frac{1}{2}\left(\Delta h_{xl} - f_{x22}\Delta x + f_c\Delta x\right);$$

$$t_2 = 0.5p_{x1}\left(\Delta h_{xl} - \Delta x f_{x21} + f_c\Delta x\right) - \sigma_{x1l}h_{x1l};$$

$$t_3 = h_{x2l}^2\left[\left(\frac{1-2\alpha_{x2l}}{1+4\alpha_{x2l}}\right)^2 - 1\right];\ t_4 = \frac{4}{3}h_{x2l}^2\frac{1+\alpha_{x2l}}{1+4\alpha_{x2l}}\beta_{x2l}\sigma_{x2sl}^2,$$

for more plastic component:

$$t_1 = \frac{1-2\alpha_{x2m}}{1+4\alpha_{x2m}} h_{x2m} + \frac{1}{2}\left(\Delta h_{xm} - f_{x12}\Delta x - f_c\Delta x\right);$$

$$t_2 = 0.5p_{x1}\left(\Delta h_{xm} - \Delta x f_{x11} - f_c\Delta x\right) - \sigma_{x1m}h_{x1m};$$

$$t_3 = h_{x2m}^2\left[\left((1-2\alpha_{x2m})/(1+4\alpha_{x2m})\right)^2 - 1\right];$$

$$t_4 = \frac{4}{3}h_{x2m}^2\left[(1+\alpha_{x2m})/(1+4\alpha_{x2m})\right]\beta_{x2m}\sigma_{x2sm}^2.$$

where α_x, β_x are the coefficients characterizing mechanical properties of powder materials of various structure depending on value of relative density; σ_{sx} is a limit of fluidity of a firm phase of powder composition.

As entry conditions, that is geometrical characteristics for the first elementary volume, accepted the following:

$$h_{x2m} = h_{x1m}h_{x2}/h_{x1};\quad h_{x2l} = h_{x2} - h_{x2l};$$
$$h_{x1m}\big|_{i=1} = h_{x0m};\quad h_{x1l}\big|_{i=1} = h_{x0l}. \quad (5)$$

Final thickness of the first layer h_{x2m} determined from a condition of equality of normal contact tension between layers:

$$h_{x2im} = h_{x2im} + A_s\ \ sign\left\{p_{x2im} - p_{x2il}\right\}, \quad (6)$$

where A_s is a step of change of the layer thickness, which size to dependences on extent of approach to initial result was accepted by a variable; sign{p_{x2im}-p_{x2il}} is a gradient assessment of the direction of the increment.

As a whole, the considered analytical decisions along with iterative procedure of extent deformation center determination, the accounting of elastic flattening of working rolls surface, procedure of numerical integration of the main indicators of process made full algorithm on numerical one-dimensional mathematical modeling stress-strain behavior when rolling two-layer powder materials. As an example of result of numerical realization of the received mathematical model in figure 3 settlement distributions of local and integrated characteristics of process are presented.

Integrated characteristics of process, namely, settlement distributions of force P and the moment M of rolling, indicators of final relative density γ_{2m}, γ_{2l} and the relation of final thickness of layers h_{2m}/h_{2l} of dependence on the size of relative reduction ε are submitted in figure 1a. Local characteristics, that are distributions of the current thickness h_{x2m}, h_{x2l} and relative density of each composition γ_{x2l}, γ_{x2m}, are submitted in figure 1b. From the analysis of the presented settlement distributions it is visible that with increase in relative reduction the intensive growth of the moment and rolling force, and also final relative density takes place.

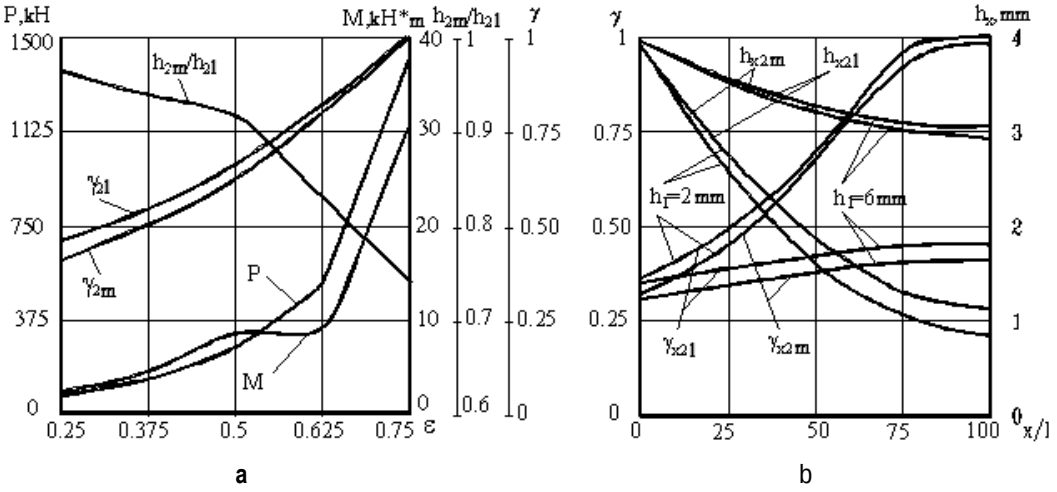

Fig. 3. Settlement distributions integrated (a) and local (b) characteristics of rolling of two-layer powder preparation depending on reduction: m – Cu; l – Fe

Besides, results from numerical realization established that increasing in coefficient of external friction of more intensive deformation are observed from a firm component, growth of normal contact tensions, force and the total moment of rolling.

In increasing the ratio of thickness of soft component to thickness firm to h_{1m}/h_{1l}=1.75 some decreasing in the total moment and increasing in force of rolling are observed. However, in case of further increasing in this ratio there is a boomerang effect. Change of the relation of thickness does not practically influence on the final relative density.

Comparison of the received settlement distributions with experimental [3] showed that the error of determination of final relative density was made by about 8%, rolling forces – about 5%, the rolling moment – about 10%. It confirms sufficient degree of reliability of the received mathematical model and legitimacy of its use for design of the mechanical equipment of specialized camps and calculation of technological modes of rolling powder compositions.

The other perspective direction in the field of production of composite hardware is rolling of powder materials on a metal substrate. Features of this process at half-devout rolling are a bend of the rolled leaf towards a steel substrate and the existence of cross cracks in a layer of the rolled powder material. These defects are caused mainly by deformation of a metal substrate, which leads to different longitudinal deformations of layers of composition, and respectively to above-mentioned defects. One of ways of this problem solution is the choice of such mode of reduction at which powder would be only deformed, that can be possible with using of mathematical model, which would predict substrate deformation.

Considered earlier mathematical model of rolling of composition powder- powder was put in the basis of considered numerical one-dimensional mathematical model of rolling of two-layer composition powder-monometal. The problem definition and character of assumptions were similar to the previous case.

Full calculation stress-strain behavior for separately allocated elementary volume is also reduced to definition of normal σ_{x1}, σ_{x2} and normal contact tensions p_x on the basis of the directed search of thickness h_{x1}, h_{x2} by criterion of section balance at the exit from elementary volume in the vertical plane:

$$p_{x2m} = p_{x2l} = p_{x2}, \tag{7}$$

where «l» and «m» are indexes determine accessory by a tear of monometal and a tear of a powder material, respectively.

Having substituted in the equation (1) condition of plasticity for continuous environments:

$$\sigma_x = p_x - 2K_x, \tag{8}$$

where $2K_x$ is a coefficient of the doubled resistance of deformation of shift which can be determined by [4]:

$$2K_x = 1.155\left(a_0 + a_1\varepsilon_x + a_2\varepsilon_x^2 + a_3\varepsilon_x^3\right); \tag{9}$$

a_0, a_1, a_2, a_3 are the coefficients of regression characterizing intensity of deformation hardening of metal.

The normal contact tension operating at the exit from elementary volume of the deformation center:

$$p_{x2l} = \left[2K_{x2l}h_{x2l} + \sigma_{xl1}h_{x1l} + \frac{1}{2}p_{x1l}f_{x1}\Delta x + \right.$$
$$\left. + \frac{1}{2}p_{x1l}f_c\Delta x - \frac{1}{2}p_{x1l}\left(h_{x1l} - h_{x2l}\right)\right] / \tag{10}$$
$$\left[h_{x2l} - \frac{1}{2}f_{x2}\Delta x - \frac{1}{2}f_c\Delta x + \frac{1}{2}\left(h_{x1l} - h_{x2l}\right)\right].$$

The further solution of the task (definition of entry conditions, conditions transition to the following section, iterative procedure by definition of the current geometrical characteristics of composition components) is similar to the previous case, the case of rolling of powder-powder composition.

As an example of numerical realization of the developed mathematical model of rolling of powder-monometal composition in figure 4, settlement distributions of local characteristics of rolling of powder bronze-graphite (79% Cu; 15% Sn; 4% Pb; 2% C) under following conditions: radius of rolls – R=125 mm; substrate material – steel DC 01; initial thickness of a powder layer – 5 mm; the initial relative density of a powder material – γ_0=0.27; final thickness of all composition – 4 mm; strip width – 100 mm; initial thickness of a substrate – 4 mm are presented.

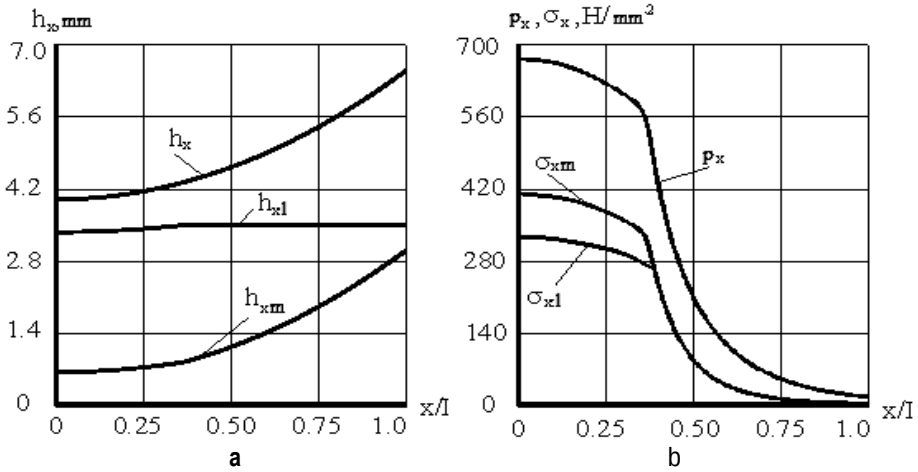

Fig. 4. Settlement distributions of local characteristics of rolling of composition the powder M1 – steel DC 01

From the analysis of the presented settlement distributions it is possible to draw a conclusion that deformation of a metal substrate begins near the neutral line of rolling. As well as at the time of the beginning of its deformation intensity of growth of normal contact tensions p_x sharply decreases, and is observed and with intensity of growth of normal tensions σ_x, the difference in the size of normal tension of a powder material and a metal substrate is also visible.

In figure 5 settlement distributions of integrated characteristics of process depending on a ratio of powder layers and steel are presented. That is at a fixed thickness of powder – h_{po1}=4 mm and the variable thickness of a metal substrate is h_{pl1}=1.2…12 mm. Apparently from the presented settlement distributions than less thickness of a metal substrate of subjects it is more deformed, and powder respectively is less deformed. Also in increasing of a ratio of layers growth of force and the rolling moment, increasing in final relative density of powder composition is observed.

The developed mathematical model allows to determine the rational technological parameters of process excluding deformation of a substrate and raising at the exit of suitable by production of bearings sliding inserts.

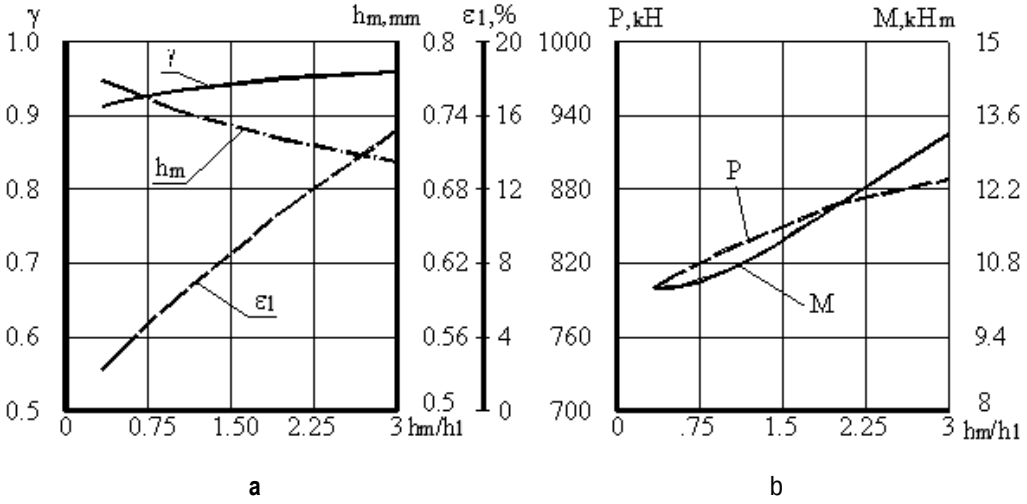

Fig. 5. Settlement distributions of integrated characteristics of rolling of composition powder-steel

References

1. Levkin A.N., Gribkov E.P., Vorobyev Yu.A. Mathematical modeling stress-strain behavior and geometrical characteristics at realization of rolling of bimetallic powder compositions. Kramatorsk, 2000. pp. 360-363.
2. Volkogon G.M., Dmitriev A.M., Dobryakov E.P. etc. Progressive technological processes of stamping of details of powders and equipment. Moscow : Mechanical engineering. 1991, 320 p.
3. Tselikov A.I., Nikitin G.S., Rokotyan S.E. Theory of longitudinal rolling. Moscow : Metallurgy, 1980, 320 p.
4. Potapkin V.F. Levkin A.N., Satonin A.V., Romanov S.M., Vorobyev Yu.A., Gribkov E.P. Stressed state and kinematics in the rolling of powder materials on a metal substrate. Powder Metallurgy and Metal Ceramics, 2000, vol. 39, no. 1-2, pp. 11–17. ISSN 0032-4795.

Tulupov O.N., Moller A.B., Kinzin D.I., Levandovskiy S.A., Ruchinskaya N.A., Nalivaiko A.V., Rychkov S.S., Ishmetyev E.N.

STRUCTURAL-MATRIX MODELS FOR LONG PRODUCT ROLLING PROCESSES: MODELING PRODUCTION TRACEABILITY AND FORMING CONSUMER PROPERTIES OF PRODUCTS

Abstract. The development of rolling production processes towards flexible manufacturing schemes in tightening quality factors makes the search of methods of effective influence on the process, labor management and personnel competence relevant.

To resolve the problems it is expedient to utilise structural matrix of mathematical models based on matrix presentation of long product rolling processes, and on a body of structural matrixes. In order to create mathematical apparatus we proposed to assign a sophisticated structure matrix consisting of units (cells) to each process operation and operation result. These results are identified with a rolling phase, while the process operation – with transformation of the product.

Structural matrix description of a process phase includes blocks that contain data of rolling process factors and parameters. To describe the dynamics of rolling process was presented the relationships between separate process states in a matrix form, e.g. as matrices of technological transformations.

Keywords: long products, rolling processes, structural-matrix models, computer simulation, consumer properties.

Introduction

The main merit of structural-matrix approach is the ability to link various models comprehensively in developing systems to analyze and control long product rolling processes.

Methodological integration of Ishikawa's diagram and structural matrix approach provides science-based solutions of the following problems using databases and IT:

- integrated accounting of the factors that influence the forming, and the forming influence on the process;
- adaptability (various complexity levels of shape rolling process description, on various production sites with no need to change the description structure);
- embedding individual models into an integrated system that links the rolling parameters;
- models compliance with up-to-date requirements for automation systems;
- application of simulators to train technical, technological and management personnel of long product mills and to improve their professional skills.

Examples and results of this approach:

- roll pass designs (for bars, wires, and structural shapes), and operation efficiency of rolls considering wear prediction have been improved;
- the amount of non-conforming products has been cut, the equipment workloads has been reduced, and the strength grades of structural shapes have been increased;
- new decisions to form the mechanical properties have been made;
- an effective system of corrective and preventive actions for long product mills has been created;
- testing, evaluation and flexible training programs on the basis of the above have been developed.

Structural matrix approach and models based on it with reengineering of long product rolling processes allows to solve main issues of traceability of consumer properties. The solutions could be rational for modern challenges of long product rolling technology and quality.

The development of rolling production processes towards flexible manufacturing schemes, while tightening quality factors, makes the search for methods of effective influence on the process, labor management and personnel competence relevant. It also includes the flow control of metal products at the enterprise.

Account should be taken of widespread development and application of automated process control systems and schemes, which require relatively simple, versatile, fast, easily expandable and reliable models meeting the requirements of object-oriented mathematical software. The structure of such models should conform to the principles of decomposition and hierarchical ordering of preserving the unity of mathematical apparatus. Often, embedded systems are highly specialized and do not always agree with each other, poorly adapted to the changing technological conditions of production process, and they forbid rapid analysis of alternative technological schemes. There is also a lack of unity in math approaches: the description of cross-sectional area [1] and the methodology of quality management of various long products [2, 3]. That hinders the monitoring of product quality factors.

Therefore, the relevant scientific and technical challenge: develop and improve comprehensive, integrated and adaptive long products quality control methods on a unified mathematical basis and unified data representation principles about quality factors.

The adaptive control problem and product traceability should be considered in two aspects:

- adaptability of models and systems to various technological schemes and changing conditions of production;
- adaptability to specific management, engineering and technical problems.

The proposed modelling approach is based on a few concepts which are listed below.

Methods

First, to resolve process tasks of both the analysis and the control of rolling process patterns for rolled sections of various shapes, a proper mathematical body should be created. Moreover, it should comply with unified concepts of data processing, storage and presentation. In order to create this mathematical body, it is proposed to assign a complex matrix, consisting of blocks (cells), tied to each technological process and to each result of this process. The results are identified with a rolling process phase, while the process itself is identified with technological transformation of the product.

Structural matrix description of a single process phase [A] includes blocks, containing monotype data of rolling process factors and parameters.

To describe rolling process in its dynamics, the relationships between single process states should be represented in the matrix form, i.e. as matrices of technological transformations $[И]_i = 1…n$. Then 'i' process phase is described by the following matrix equation:

$$[A]_{i-1} \times [C]_i \rightarrow [A]_i \qquad (1.1)$$

Whereas the rolling process itself is described by the following system containing *n* number of matrix equations:

$$\begin{cases} [A]_0 \times [C]_1 \rightarrow [A]_1 \\ \cdot \\ \cdot \\ [A]_{i-1} \times [C]_i \rightarrow [A]_i \\ \cdot \\ \cdot \\ [A]_{n-1} \times [C]_n \rightarrow [A]_n \end{cases}, \qquad (1.2)$$

where $[A]_o$, $[A]_n$ are matrices, which describe initial and final technological states respectively; $[И]_1$, $[И]_n$ arematrices, which describe the first and the last process operations respectively;

Such form of process presentation is convenient for data processing and computer simulation. Matrices of technological states transformation description $[И]_i$, as well as matrices of technological states $[A]_i$, are complex

structural matrices consisting of certain finite number of blocks (cells).

Second, structure and contents of the internal blocks are determined by the model purpose and by the type of the problem to be resolved. In general, the following internal blocks are: the block of shape description [Ф], the block of properties description [С] (i.e. block of mechanical properties description), the block of process parameters description [П]. These blocks can be block matrices themselves consisting of individual cells.

Data on the shape of rolled section is contained in the shape description block $[Ф]_i$. For this purpose any complex cross-section is subdivided into finite number of simple elements *k*, which can be described according to the concept of vector description of simple cross-sections. To render the description coherent and non-ambiguous, a matrix of centres [Ц] is introduced. This matrix contains data on the location of centres of simple elements with respect to the common centre of the description. To determine the connection between local and common centres of the description, two values are introduced: distance between the centres, and angle between the vertical line and their connection line. The number of significant vectors $[Ф]_i$. will depend on the complexity of the cross-section, and the *k* can be used as an indicator of shape complexity.

Mechanical properties of the feed are contained in the block of properties description [С]. Each matrix $[C]_i$ consists of a set of vectors: $C_i = 1…p$, determining the location of isometric lines of mechanical properties. The choice of *p* (a number of subdivisions of cross-section plane into isotropic areas of mechanical properties) is determined by specific conditions of each description task, by the required accuracy of consideration of mechanical properties distribution across the cross-section. Besides, the value p_i depends on complexity of properties transformation process and can be regarded as an indicator of process sophistication. If average values are sufficient to determine mechanical properties, it is suggested that a block of properties description should be regarded as a degenerated matrix, while values of mechanical properties should be regarded as σ_τ, δ for these particular conditions.

Block of parameters description [П] can comprise sub-blocks: [Т] is a matrix of temperature conditions; [М] is a matrix of speeds, [ε] is a matrix of boundary conditions; [Ин] is a matrix of tool conditions (wear, etc.); [Д] is a matrix of tool characteristics. Individual matrixes of process parameters represent a set of finite number of elementary blocks. Data presentation is equal to the one of shape description block, i.e. values of a specific parameter are determined at intersection points of basic radius-vectors with cross-section outline and as such are stored into memory of this parameter to be utilized for data loading into matrix [Д], [Ин], [ε], [V].

When it is necessary to know parameter value in any point of cross-section in order to resolve a problem (e.g. temperature field), then data presentation concept in such blocks (e.g., [Т]) is identical to the description block [С].

Third, matrices of technological transformation have block structures and block sizes equivalent to those matrices of technological states. Blocks of matrix $[И]_i$ can contain vector-type data (a set of figures ordered according to a certain principle, e.g. matrix of shape deformation – $[ИФ]_i$), analytical or empirical dependencies (i.e. models). In any case irrespective of method of data presentation, all cells are included in general matrix model.

Structural matrix of the 'i'-th process transformation $[И]_i$ includes the blocks $[ИФ]_i$, $[ИС]_i$, $[ИП]_i$, change of section shape, properties and process parameters respectively: $[ИФ]_i = [Ф]_i / [Ф]_{i-1}$; $[ИС]_i = [С]_i / [С]_{i-1}$; $[ИП]_i = [П]_i / [П]_{i-1}$, where $i = 1…m$.

According to this approach, deformation is described by means of deformation blocks, representing ratio between the matrices «before» and «after» deformation. Deformation block is a diagonal matrix. Its rank is defined by the size of shape description block. The advantage of such interpretation of deformation is essentially in the possibility to computer process the roll pass designs.

Fourth, relations between process parameters at each rolling process phase are logged into the technological transformation matrix (1.3) as lateral components (blocks) of this matrix. These blocks may contain both numerical factors obtained empirically (e.g. relation of tonnage of rolled stock per groove to matrix components that describe roll wear), as well as the entire mathematical models that establish a relation between single parameters (e.g. relation of deformation temperature to speed, relation of steel's tensile strength to spread).

$$\begin{bmatrix} [C'_1] \\ [C'_2] \\ \vdots \\ [C'_m] \end{bmatrix} = \begin{bmatrix} [И_1] & З_{12} & \cdots & З_{1m} \\ З_{21} & [И_2] & \cdots & З_{2m} \\ \vdots & \vdots & \ddots & \vdots \\ З_{m1} & З_{m2} & \cdots & [И_m] \end{bmatrix} \begin{bmatrix} [C_1] \\ [C_2] \\ \vdots \\ [C_m] \end{bmatrix} \quad (1.3)$$

where:

$[C_m]$ is a matrix that describes initial state of one of the entity's properties;

$[C'_m]$ is a matrix that describes final state of one of the entity's properties;

$[И_m]$ is a matrix of state transformation;

З denotes relations between various variation matrices (e.g. «deformation-temperature» relations).

Therefore, this feature presents an important advantage of structural matrix models, since it allows to comprise and implement the possibilities of other efficient models within the frames of common integrated approach.

Thus, the suggested approach to modelling metal forming processes, and, in particular to modelling shape rolling processes for wire rods, bars, and structural shapes, ensures the following advantages:

- integrated accounting of the factors which have direct impact on the deformation process, and the impact of shape deformation itself on the rolling process aspects;
- versatility (unified method of data interpretation, suitable for computer processing);
- adaptability to metal forming processes (the ability to describe processes of various complexity, on various production sites, with no need to change the description structure);
- adaptability to the tasks of rolling patterns analysis and control to be solved [4, 5, 6];

- embedding individual models into an integrated system that links the rolling parameters;
- accordance with the modern approaches to creation of computer-aided systems of process engineering and control.

Results

Methodological integration of Ishikawa scheme and structural matrix approach using databases and IT provides science-based and effective solutions of the assigned problems.

The developed complex of mathematical models and descriptions of its practical implementation are listed hereinafter.

To control the quality of rolled stock we improved «the uneven deformation ratio» – *UDR* (the criterion that helps evaluate and compare alternative roll pass designs). As a result, the amount of non-conforming products reduced along with lower equipment loads and higher strength grade of structural shapes.

Instrument was found to form mechanical properties of rebar by defining the boundaries of the magnetic phase sensor values variation and to obtain the required mechanical properties of wire rod using commercial quality steel (C 0.06-0.12%, Mn 0.25-0.50%, Si 0.15-0.30%, S ≤ 0.050%, P ≤ 0.040%, Cr ≤ 0.30%, Ni ≤ 0.30%, Cu ≤ 0.30%) instead of expensive alloyed steel (C 0.20-0.29%, Mn 1.2-1.6%, Si 0.6-0.9%, S ≤ 0.045%, P ≤ 0.040%, Cr ≤ 0.30%, Ni ≤ 0.30%, Cu ≤ 0.30%).

Previously developed matrix evaluation criteria for simple shape gauges transformed into the universal criteria for evaluating structural shapes. Besides, we developed adaptive matrix model of complex productibility, precision, and stability analysis of forming and energy consumption during rolling.

The matrix method of describing the forming process and the principle of least resistance lead to new formulae that calculates power parameters and deformation during section rolling.

A new way was introduced to describe the geometric parameters of axial segregation during billet deformation – a supplement to the bar rolling process modelling using matrix approach and to effectively implement computer modelling of segregation.

«LEAN-production» plays an important role in the quality management strategy. As a part of mathematical apparatus we proposed individual wear index U_{in}, and used it to figure out the schedule of ring rolls and profile changes depending on roll material and diameter (decreased unnecessary supplies, process steps, and changes of expensive ring rolls). Systematization of acquired knowledge eases the development and effective use of section mills, equipped with three-roll RSB stands. Accumulated and generalized experience of using carbide ring rolls could be applied on modern wire-rod mills, equipped with expensive durable rolls in their high-speed finishing blocks.

To assess effectiveness of any process, we need measurements to ensure the process to be streamlined and maintained. The extent of regulatory compliance and performance results are usually determined through a comparison of the results to assessment criteria. Using the criteria approach to quality management, based on the development of structural matrices, we developed new indicators of profile conformity, characterized by a deviation of profile distribution (DPD), expressed as a single number – the integral profile deviation (IPD), index of profile match (IPM) of the logical type reflecting compliance deviation allowable range. These indicators and a new tool for maintaining quality – model cards – are used to develop a method for determining the corrective and preventive actions. Experience in creating tables of preventive actions revealed stands affecting the set up of the mill to the greatest degree and to propose criteria that defines their priority. The fewer stands involved in the set up lead to fewer changes of the roll gaps, decreasing overall value of priority coefficient C_{pr}.

The ability to solve local problems and skills of system analysis by a group of experts – that is the functionality of our instruments to manage the quality rolling system (*UDR*, U_{in}, DPD, IPD, IPM, C_{pr}). Mathematical apparatus created includes new rolling quality indexes and technological personnel competence assessment and it has the potential to produce a synergetic effect to improve product quality at the long product mill.

The use of such models corresponds with the trends of modern management and takes into account a range of factors: reengineering processes (a), adoption of IT (b), product quality control during teaching or retraining the employees (c) and during production process within the framework of traceability and forming consumer properties of products [7, 8].

The further development of the matrix approach and mathematical models, which were listed above, is the methodology of the information model formation [9], which will become the basis for an automated tracking system of metal products. We propose to use the following scheme of information flow that describes the process of passing of semi-finished products through long product mill (see figure).

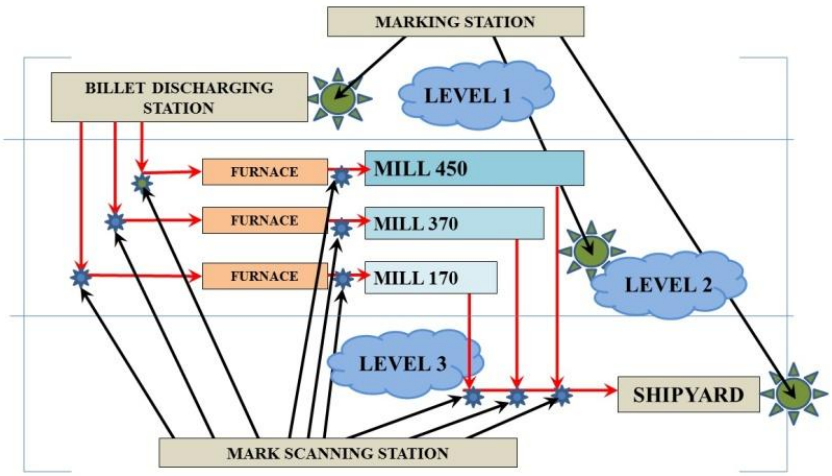

Information flow scheme at the shape rolling shop of OJSC «MMK»

Inheritance of technological and organizational measures of previously passed metallurgical conversions as well as follow-up ones takes part in ensuring the required level of consumer properties that will let us predict, monitor and improve the quality of long products.

Created adaptive complex comprises: an information flow scheme (a); new quality indexes of the rolling process (b); methodology to assess and improve the technological competence of personnel (c); methodology of quality control during design, implementation, long products production and improving.

The considered solution of the information model organization correlates well with object-oriented database creation process used in modern automatic process control systems as well as on all CAM systems on all automation levels up to the MES systems and enterprise management systems.

Immutability of the essence of applied mathematical apparatus and the basic principles of its construction to solve technical and technological problems and challenges of quality management makes it possible to adapt and use the developed approach in overlapping technical areas.

References

1. Tulupov O.N. *Structure-matrix models for improving the efficiency of rolling grades:* Monograph. Magnitogorsk: Nosov Magnitogorsk State Technical University, 2002. 224 p.
2. Tulupov O.N., Ruchinskaya N.A., Moller A.B., Limarev A.S., Lutsenko A.N.Quality management of long products by using rational preventive actions in mill setting *Vestnik Magnitogorskogo gosudarstvennogo tehnicheskogo universiteta im. G.I. Nosova.* [Vestnik of Nosov Magnitogorsk State Technical University]. 2007, no 4, pp. 73-80.
3. Lewandowski S.A. Effectiveness enhancement of section mills by the quality management model improving: PhD Dissertation. Magnitogorsk, 2006.
4. Alekseev A.M., Loginov V.G., Zaitsev A.A., Tulupov O.N., Moller A.B., Rashnikov S.F., Morozov A.A. *A method of rod rolling*. Patent RUS no. 2148443, 1998.
5. Tulupov O.N., Moller A.B., Kinzin D.I., Lewandowskiy S.A., Limarev A.S., Zavyalov K.A., Richkov S.S., Loginova I.V., Unruh C. J., Nowitskiy R.V. Resistance increasing of the 370 mill roller by cooling system improving. Research report (*«Magnitogorsk Iron and Steel Works»*).
6. Kinzin D.I., Kalugina O.B. Evaluation of values impact of the distortion structure on widening in rolled section *Vestnik Magnitogorskogo gosudarstvennogo tehnicheskogo universiteta im. G.I. Nosova.* [Vestnik of Nosov Magnitogorsk State Technical University]. 2011, no 4, pp. 21-23.
7. Nalivayko A.V., Steblov A.B., Tulupov O.N., Rychkov S.S. Issledovaniye urovnya mekhanicheskikh svoystv armatury klassa A500S s tsel'yu otsenki vliyaniya osobennostey tekhnologii na pokazateli kachestva. *Vestnik Magnitogorskogo gosudarstvennogo tehnicheskogo universiteta im. G.I. Nosova.* [Vestnik of Nosov Magnitogorsk State Technical University]. 2010, no. 2, pp. 69-73.
8. Moller A.B., Tulupov O.N., Kinzin D.I., Levandovskiy S.A., Limarev A.S., Zav'yalov K.A., Nazarov D.V., Novitskiy R.V., Rychkov S .S., Loginova I.V. Razrabotka i opytno-promyshlennoye oprobovaniye ekspluatatsii bandazhirovannykh valkov v predchistovoy gruppe kletey stana 170 STS OAO «MMK» [Designing and experiment industrial testing of tire rolls running at millstand 170 of «MMK»]. Research report (*«Magnitogorsk Iron and Steel Works»*).
9. Ruchinskaya N.A., Zaytsev O.YU., Tulupov O.N., Lutsenko A.N. Printsipy sozdaniya informatsionnykh modeley upravleniya kachestvom sortovogo prokata. [The principles of creating long products quality management information models]. *Proizvodstvo prokata.* [Rolling processes]. 2007, no. 8, pp. 33-41.

Logunova O.S., Matsko I.I., Posochov I.A.

INTEGRATED SYSTEM STRUCTURE OF INTELLIGENT MANAGEMENT SUPPORT OF MULTISTAGE METALLURGICAL PROCESSES

Abstract. The necessity to invent a universal technology for creating the intelligent management support of multistage processes, which is able to interface process variables between local loops at each stage of production is determined. The integrated system structure of intelligent management support of multistage metallurgical processes and production stage models are suggested. The improved method of billet macrostructure assessment and block designing technology of intelligent management support of continuous casting billet production are described.

Keywords: control systems, intelligent support, multistage metallurgical processes, continuous cast billet, billet macrostructure assessment.

The actuality of the study

Modern Industries require new systems for multistage process management. These requirements are due to the new priority trends in accordance with Russian state policy. One of these trends is the development of information and telecommunication technologies, which are integrated in automated control systems (ACS) of large industrial enterprise production. The use of new ACS modules for multistage manufacturing processes facilitates unit performance increasing and provides reduced quantity of low-quality products.

From the management point of view, multistage technology of steel products is a complicated process. Such technologies require the system allowing to monitor output product quality in on-line and providing intelligent decision support of process control.

In developing and implementing new modules, which enlarge already existing ACS, the necessity to use graphic information obtained during quality estimation procedure of finished products and semi-finished products emerges.

The effectiveness of using graphic information and decision-making in ACS production is illustrated by theory and practice.

Methods of image obtaining, processing and segmentation can be found in foreign and Russian scientific pub-

lications. Mathematical theory development in improving and graphical information segmentation was defined in scientific papers [1-3]. An overview on the topic of decision-making on basis of tree-type structure was presented by Quinlan J.R., Janikow C.Z., Hastie T., Tibshirani R., Friedman J., Berestneva O.G. and others. The practical application of fuzzy set theory and fuzzy logic refers to Zadeh L.A., Esposito F., Malebra D., Semeraro G., J.J. Dyulichevoy and others.

However, despite the studies carried out and large number of publications in the field of automated control systems (ACS) in steel production [4-7], the following issues are of current interest:

– the lack of automated systems permitting to ensure technological processes control, based on output product quality information;

– the lack of techniques of graphic information collection and processing about the quality of steel products using low-contrast images with irregular shaped elements;

– the lack of application packages for intelligent decision support in automated control systems (ACS) of multistage production, based on adaptable fuzzy trees with dynamic structure, taking into account the values of attributive quality characteristics of products.

In the current circumstances, there is a need to develop a universal technology of creating the intelligent support system of multistage process management, which is able to interface process variables between local loops at each stage of production.

The structure of research object

Fig. 1 illustrates the diagram of a manufacturing process with *N* stages. The following notations are displayed in Fig. 1: {Zi} is a task vector for technological parameters values of the i-th process; {Ri} is a decision vector of parameters values changing of the i-th process; {Mi} is a vector of estimation (indicators) of product or semi-product quality, resulting in redistribution at the N selected stages, Z is a value of final parameters for product assigned position.

A typical example of a multistage manufacturing process is the production of continuous cast billet, with three main stages: steel melting in alternating-current (AC) electric arc furnace (EAF), steel processing in a ladle furnace unit (LFU) and continuous steel casting in billet continuous casting machines (BCCM).

An illustrative diagram of a multistage production for the chosen technology, where N = 3, is represented in Fig. 2. All input and output parameters, shown in Fig. 2, become of specific physical and technologic significance (see Table).

Values, which are transmitted between production stages and determine the operation mode choice of the next step unit, are highlighted in Table. The presence of binding parameters permits to organize the integrated management of all production stages.

The list of major task vectors for continuous cast billet production stages

Vector set	Vector coordinates	Physical or technological significance of coordinates
$\{Z_1\}$	d	charge materials ratio (crowbar / pig iron), %
	$\{c_i\}$	percentage of chemical elements in steel at EAF exit,%
	t_1	arc time under the current, min
	I_1	current strength, MA
	U_1	current voltage, MV
	$\{l_i\}$	elements proportion of non-metallic charge, %
	$\{v_{i1}\}$	flow-rate of solid oxidizer additives kg
	$\{g_{i1}\}$	flow-rate of gas oxygen, m³ / h
	$\{f_{i1}\}$	discharge intensity of ferroalloys, kg / t
	T_1	metal temperature at EAF exit, °C
$\{Z_2\}$	T_1	metal temperature at EAF exit, °C
	$\{c_i\}$	percentage of chemical elements in steel at EAF exit, %
	t_2	arc time under the current, min
	I_2	current strength, MA
	U_2	current voltage, MV
	$\{g_{i2}\}$	argon gas flow rate m³ / h
	$\{f_{i2}\}$	discharge intensity of ferroalloys, kg / t
	T_2	metal temperature in steel teeming ladle at LFU exit, °C
$\{Z_3\}$	T_2	metal temperature in steel teeming ladle at LFU exit, °C
	T_3	metal temperature in tundish ladle at BCCM exit, °C
	$\{c_{ie}\}$	percentage of chemical elements in steel teeming ladle at EAF exit, %
	v	billet drawing rate, m / min
	$\{F_{ij}\}$	water flow rate for secondary cooling zones BCCM, m³ / h
	$\{D_{ij}\}$	air flow rate for secondary cooling zones BCCM, m³ / h
	w	crystallizer oscillation frequency
	F	water flow rate on crystallizer m³ / h
	$\{\boldsymbol{M}_{i3}\}$	task aimed to billet macrostructure evaluation, grade
$\{Z\}$	$\{\boldsymbol{M}_{i3}\}$	task aimed to billet macrostructure evaluation, grade
	$\{c_{in}\}$	percentage of chemical elements in tundish ladle BCCM, (last test), %
	$\{l_i\}$	Information about template selection for quality evaluation
$\{M_i\}$	$\{O_i\}$	actual results of quality evaluation, grade
	$\{l_i\}$	Information about template selection for quality evaluation

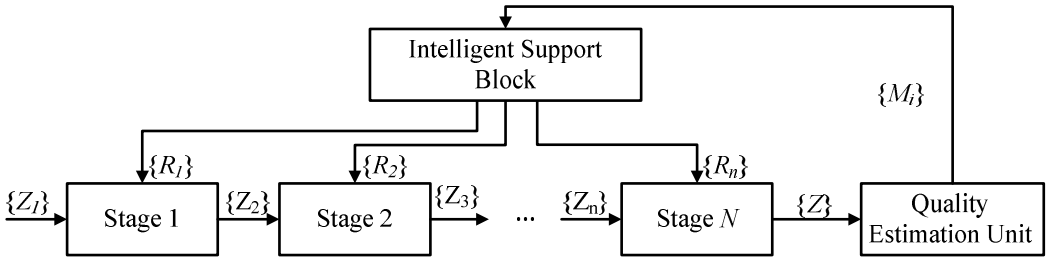

Fig. 1. Diagram of multistage production with integrated system of intelligent management support

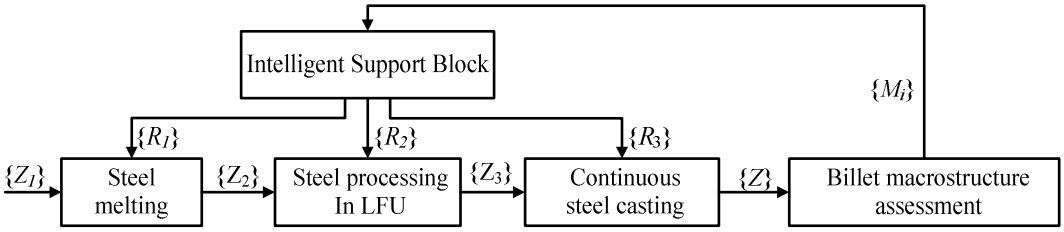

Fig. 2. Diagram of multi-stage continuous cast billet production

The structural model of the i-th production stage

The block of each stage (Fig. 1) has a complex structure, which comprises: mathematical process models, visualization module of expected result, current process monitoring module, decision-making block, systems of local loops of process variable control (technologic unit or its field). The structural diagram of each stage can be unitized according to the diagram shown in Fig. 3.

The following notations are introduced in Fig. 3: $\{R_{iм}\}$ is a decision vector leading to the i-th process parameter points changing, as a result of modelling; $\{ \Delta Z_i \}$ is a correction vector for the task point of process control; $\{ Z_{ient} \}$ is a task vector for the system of local loops of control object; $\{ Z_{iex} \}$ is a vector of technologic parameter values transmitting to the control object; $\{ Z_{i+1}\}$ is a vector of technologic parameters, obtained after the i-th stage production ending and transmitting to the stage i +1 as a task.

Decision-making blocks, which can be implemented using different technologies, both in automated and automatic modes are represented in Fig. 1 and Fig. 3. Currently, decision-making technologies based on the classification with the help of neural networks, fuzzy logic and tree-like structures are the most widespread [4, 8, 9]. A combination of many tree-like structures and fuzzy membership functions about the received quality indicator level is one of the options, taking into account the information fuzziness and taxonomic criterion of product quality. Taking into account plenty quality indicators and production process dynamism, an adaptive forest of dynamic structure fuzzy trees is formed. Each tree adaptability permits to retrain the decision tree in changing the technologic process running and response to the situations, unspecified in the decision tree. Dynamism allows to change the relevance level of process control variables after a set of tree adaptations towards providing shorter decision branches, reducing the parameters, requiring correction.

View module (Fig. 3) is designed to exhibit results of modelling, and its construction is a separate scientific problem in the field of information processing. The module is optional and it is not included in many process control systems because of implementation complexity in mapping results in real time.

The block «System of local loops» also has a complex structure and can combine M subsystems, which are responsible for process variable selection and stabilization. The peculiarity of the suggested solution is the integrated result examination in changing values of many process parameters not only at the selected i-th stage but also between stages. Therefore, vector representation of input and output parameters is shown between the diagram blocks, shown in Fig. 1 and Fig. 3.

Fig. 4 illustrates the example of structural scheme of continuous steel casting stage applicable for arc-furnace steelmaking plant of OJSC «Magnitogorsk Iron and Steel Works».

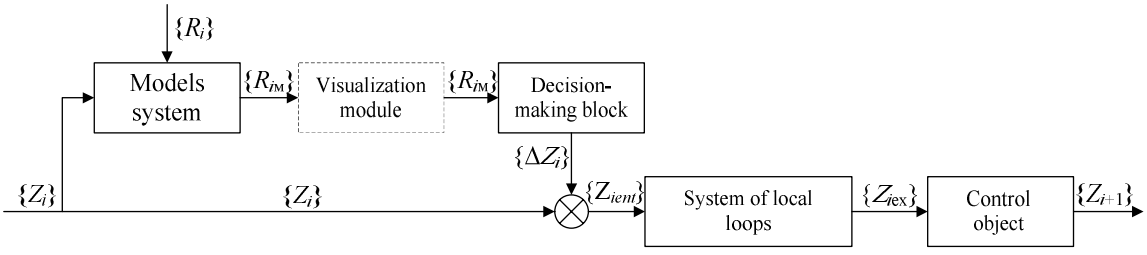

Fig. 3. Structural diagram of the i-th production stage

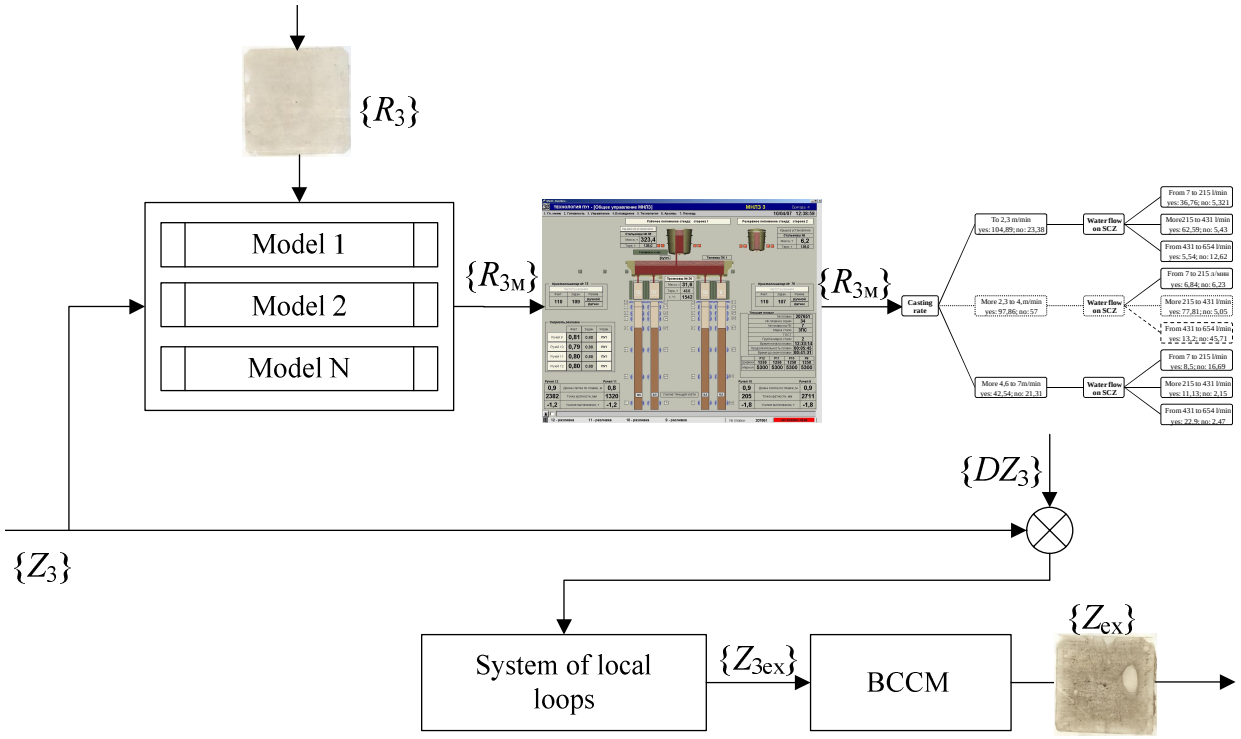

Fig. 4. Structural scheme of continuous steel casting stage

As shown in Fig. 4, a signal of suggested billet quality $\{R_3\}$ is received from the intelligent support block. Binding components of vector $\{Z_3\}$ enter the modeling block of continuous casting of steel. A system of sub-models is represented in this block, including the model of identification of heat transfer coefficient from the billet surface, the model of the billet thermal state, the model of billet damage forming, the model of billet quality forecasting, etc. The simulation data $\{R_{3m}\}$ enter consistently the rendering module, implemented on the SCADA platform, and the decision-making block. The use of adaptive fuzzy trees with dynamic structure is one of the ways of decision-making block building aimed to adjust the values of process variables. Melting mass; metal temperature after EAF discharging; metal temperature in pony ladle; oxidation of metal; steel casting rate; the content of basic chemical elements in steel are defined as the linguistic variables for the decision making tree of the possible damage origin.

A method of billet macrostructure evaluation

Speaking about steel product quality, firstly macro- and microstructures values are noticed, and these values are foundational for such mechanical properties as strength, formability, wearability. Discontinuity flaw geometric dimensions, obstacles quantity, density from metal distribution in given volume are the characteristics of metal macro- and microstructures. The determination of the degree of discontinuities flaw extension is generally defined by the appropriate field and state standards such as OST 4.14.73 or OST 14-1-235-91. The process of expert knowledge base formation, in order to assess metallurgic product quality, is the most time-consuming. Hitherto, information acquisition and processing are carried out by traditional methods, based on product visual inspection results. With modern computing facilities it becomes possible to develop automated system of metal macro- and microstructure assessment. However, the development of a decisive rule base for decision-making is possible only on the basis of «practical» expert knowledge. Such knowledge processing leads to the input of membership function of fuzzy sets and rules of their use. Intelligent support system of billet continuous cast production at arc-furnace plant of the OJSC Magnitogorsk Iron and Steel Works (MMK) was built based on technology, developed by the authors [9]. Points of the internal macro-damage extension have been selected as product quality indicators. Macro-damage rating is carried out on crosscut templates and sulphuric marks. The following types of damage such as axial looseness, dotty obstacle and cracks, perpendicular to the billet edges were examined. Length, width, strength and ratio of total damage area to template size are the characteristics of damages. According to the OST 14-1-235-91 membership functions for evaluating each type of damage were classified in tabulating.

Algorithm S4.5 and algorithm of decision-making fault reducing in fuzzy tree using were selected as the basis of classification algorithm. In order to construct a fuzzy tree forest, which allows to take into account predicable quality classification criteria from the tabulation, linguistic variables to describe damage parameters such as width, length, relative length, relative width, area, maximum area, relative area, length-width ratio, width-length ratio, strength and section attachment have been introduced. Tree type structure building results in order to assess the axial looseness of continuous casting billet are shown in Fig. 5. Full forest of fuzzy trees contains from 800 to 2,000 leaves. Branches for damage, which has an average size, are allocated in Fig. 5 and its part is located in

section 3. If 10% of damage is in section 3, then template attachment to target class (qualitative template) is 0.334 that corresponds to 2.5 points according to the OST.

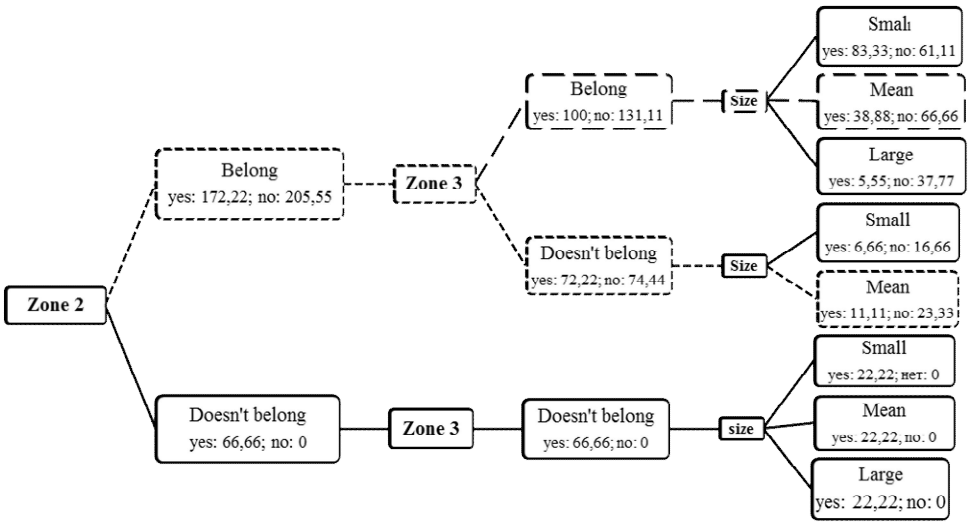

Fig. 5. A segment of the classification tree of internal macro damages of continuous casting billet

Building block method of intelligent management support of continuous cast billet production

In creating the integrated system of intelligent management support of multi-stage processes it is necessary to establish cause-and-effect relationships between product quality indexes and process variable values, which need to be built at the stage of expert knowledge formalization.

One of the ways to formalize expert knowledge is adaptive fuzzy tree with dynamic structure (Fig. 6).

Melting mass; metal temperature after EAF discharging; metal temperature after secondary treatment; metal temperature in pony ladle; oxidation of metal; steel casting rate; the content of the basic chemical elements in steel are defined as the linguistic variables for the decision making tree of the possible damage origin.

Taking into account that the built tree leaves are presented in Fig. 6, the decision uses only two branches marked with a dotted line. The solution pertains to the upper branch per 0.14 and to the lower branch per 0.86. It can be defined for this solution that the resulting billet has 0,357 grade of membership to a class of usual quality billets, and that corresponds to 2.5 points according to the OST.

The billet is qualitative if the point is less than 2. Consequently, it is necessary to modify existing solutions. According to the developed algorithm, the control parameter change is performed. It means to reduce fuel cooler flow from 444 to 438

l / min, in this case billet quality assessment is reduced to 2 points, and that is sufficient for its ordinary quality classification.

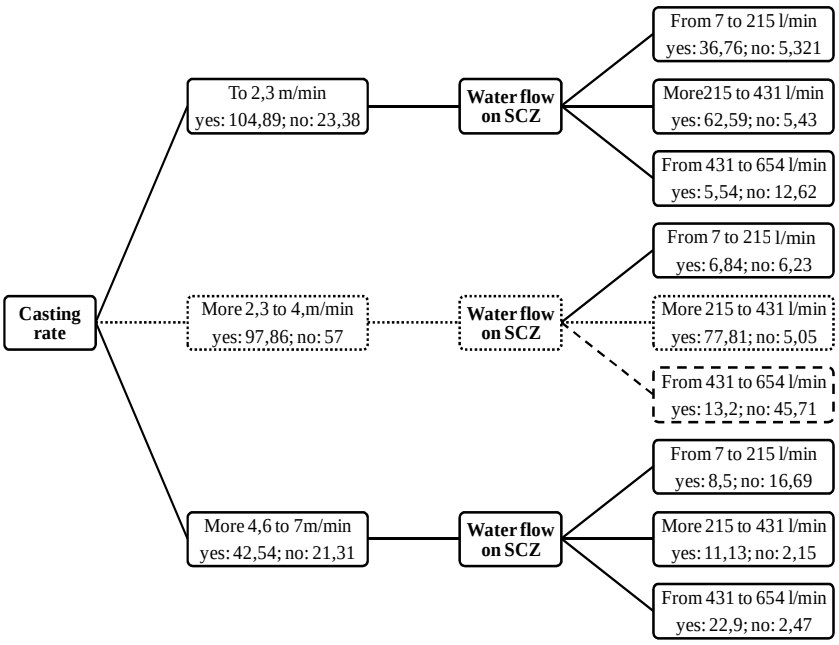

Fig. 6. Moving path fraction in decision-making based of fuzzy tree structure in order to forecast continuous casting billet quality

Conclusion

Thus, granting modern decision-making methods it is possible to develop existing production control systems for their intellectualization. The use of an integrated system of intelligent management support of multistage metallurgical processes permits to carry out multiple factor analysis. Herewith, both well-known deterministic and statistical modelling process methods and unitized way of decision making, based on «practical» expert knowledge, are used in this analysis.

References

1. Shapiro. L., Stockman G. *Computer Vision*. Moscow: BI-NOM. Knowledge laborator, 2006, 752 p.
2. Gonzales R.C. and Woods R.E. *Tsyfrovaya obrabotka izobrazheniy* [Digital Image Processing], Tekhnosfera, Moscow, Russia, 2005, 1072 p.
3. Pratt W.K. *Digital Image Processing*. New York: Wiley, 1978. Translated under the title Tsifrovaya obrabotka izobrazhenii, Moscow: Mir, 1982, 312 p.
4. Ryabchikov M.Y., Parsunkin B.N., Andreev S.M., Logunova O.S., Ryabchikova E.S., Golovko N.A., Polko P.G. Achieving maximum perfor-

mance optimized ore grinding process in utilizing fuzzy extreme control principles. *Vestnik Magnitogorskogo gosudarstvennogo tehnicheskogo universiteta im. G.I. Nosova.* [Vestnik of Nosov Magnitogorsk State Technical University]. 2011. no. 2, pp. 5-9.
5. Tutarova V.D., Logunova O.S. Analysis of the surface temperature of continuosly cast ingot beyond the zones of air cooling. *Steel in Translation*. 1998. no. 8. pp. 21-23.
6. Logunova O.S., Matsko I.I., Safonov D.S. Modelling of the thermal state of the infinitely extended body with the dynamically changing boundary conditions of the third kind. *Bulletin of the South Ural State University. Series: Mathematical modeling and programming*. 2012, no. 27, pp. 74-85.
7. Logunova O.S. Internal-defect formation and the thermal state of continuous-cast billet. *Steel in Translation*. 2008, vol. 38, no. 10, pp. 849-852.
8. Golovko N.A., Logunova O.S., Parsunkin B.N., Andreev S.M. Adaptive system of automatic control of stochastic nonlinear processes. *Scientific Review*, 2013, no. 1, pp. 166-170.
9. Matsko I.I., Logunova O.S., Pavlov V.V., Мацко О.С. Adaptive fuzzy decision tree with dynamic structure for automatic process control system of continuous-cast billet production. *IOSR Journal of Engineering.* 2012, vol. 2, no. 8, pp. 53-55.

Shatokhin I.M., Bigeev V.A., Shaymardanov K.R., Manashev I.R.

INVESTIGATION OF COMBUSTION IN TITANIUM-FERROSILICON SYSTEM

Abstract. Results of self-sustaining combustion process in the titanium-ferrosilicon system investigations are presented. These data were used for experimental-industrial technology developing of production ferro silico titanium with high titanium content for steel alloying.

Keywords: titanium, titanium containing steel, ferrotitanium, ferrosilicotitanium, titanium ferrosilicide, self-propagating high-temperature synthesis, combustion rate, combustion temperature.

At present, titanium is actively used for alloying of wide assortment of steel thanks to its specific properties. Titanium is used for modern HSLA-steels, pipe-steels, stainless steels and others. Mainly, the mechanism of its influence on steel quality is associated with formation of titanium carbides, nitrides and carbonitrides in steel.

Ferrotitanium is usually used for steel alloying. Depending on the method of production, ferrotitanium can be with high (~70% Ti) and low (≤40% Ti) titanium content. High-grade ferrotitanium is usually obtained by melting titanium-containing waste in induction furnaces. Low-grade ferrotitanium is produced by recovery from ilmenite in special melting aggregates. Ilmenite concentrate, iron ore, aluminum powder, ferrosilicon and lime are used as raw materials. Sometimes, when high-purity steel grades are produced, vacuum-melted ferrotitanium is used. Standard ferrotitanium contains considerable amount of impurities (such as non-ferrous metals, nitrogen, oxygen, hydrogen, carbon, sulfur, phosphorus), which come to alloy from raw materials and atmosphere during production. Moreover, assimilation degree of titanium from ferrotitanium remains low.

That is why, full or partial replacement of ferrotitanium by alternative titanium containing alloys is actual. This problem can be solved by creating of complex master-alloys, which contain titanium as basic element and high-level elements, such as Si, Al, Ca, etc. It is supposed, that these elements will protect titanium against oxidation, because they are strong deoxidizers. In this way, titanium assimilation will be higher.

Thus, to be most effective, new alloy should meet the following requirements:

- high titanium content;
- low impurities content;
- the presence of elements with high affinity to oxygen.

This alloy will give high and stable titanium assimilation, will allow to produce steels with narrow titanium limits and will reduce impurities content in metal. The most economical alternative to ferrotitanium can be ferro silico titanium.

Usually ferro silico titanium is obtained by melting titanium, metallic silicon and low-carbon steel in induction furnace or by recovery from ilmenite ore.

But it is impossible to produce ferro silico titanium with high titanium content (more than 30% Ti) by furnace methods, because of high melting point of titanium silicides and strong liquation during crystallization. Moreover, alloy, obtained by furnace methods, has higher concentration of nitrogen, oxygen and hydrogen, penetrating into the melt from the atmosphere. So, it is important to use fundamentally different method of titanium ferrosilicide obtaining that enables high product recovery with low impurities content with the lowest electricity costs. Such method is self-propagating high-temperature synthesis (SHS). When SHS is applied, no traditional furnaces are used. The process is carried out in special SHS-reactors at the atmosphere of inert gas or vacuum. At the combustion synthesis, as well as at the traditional metallothermic process, energy source is the heat of chemical reactions. But unlike metallothermy, SHS is slagless.

The Ti-Si system has 5 silicides: TiSi, $TiSi_2$, Ti_5Si_3, Ti_3Si_4 и Ti_3Si. Ti_5Si_3 has the highest melting point. Physical and chemical properties of titanium silicides are presented in Table 1. The formation of titanium silicides occurs with great heat release, so that adiabatic combustion temperature is high. Regularities of interaction of titanium and silicon are studied in detail in works [3, 4]. It was shown, that combustion in powder compound of titanium and silicon can be implemented in a wide range of parameters changing such as the components ratio, powders dispersion, etc. It can be expected, that heat release during chemical interaction in ternary system Ti-Si-Fe will be enough to carry out the process in self-propagating mode.

Table 1

Physical and chemical properties of titanium silicides [5]

Characteristics	Ti_5Si_3	TiSi	$TiSi_2$	Ti_3Si_4	Ti_3Si
Heat formation, kJ/mol	581,2	132,8	136,6	–	–
Crystallization temperature, °K	2120	1760	1540	1920	1170
Density, g/cm^3	4,3	4,03	4,21	–	–
Adiabatic combustion temperature, °K	2500	2000	1800	–	–

It is known, that high exothermicity of raw materials interaction is the essential condition for all SHS-reactions. To determine the possibility of self-propagating process, calculation of adiabatic temperature in ternary system Ti-Si-Fe with iron content of 0 to 90% was carried out using thermodynamic data and methodology, represented at [5, 6]. During calculation it was assumed, that iron did not take part in the reaction and titanium silicide Ti_5Si_3 and α-iron are combustion products:

$$5Ti + 3Si + xFe \rightarrow Ti_5Si_3 + xFe \quad (1)$$

Combustion temperature was calculated using the following formula:

$$(1-\mu)\cdot\Delta H_{Ti_5Si_3}^{T_{ad}} + \mu\cdot\Delta H_{Fe}^{T_{ad}} = \\ = (1-\mu)\cdot(Q - \nu_{Ti_5Si_3}\cdot L_{Ti_5Si_3}), \quad (2)$$

where $L_{Ti_5Si_3}$, $\nu_{Ti_5Si_3}$ are the heat and the degree of Ti_5Si_3 fusion respectively; $\Delta H_{Ti_5Si_3}^{T_{ad}}$ and $\Delta H_{Fe}^{T_{ad}}$ are enthalpy change of titanium silicide formation and iron when temperature increases from T_o to T_{ad}; μ is the amount of iron in the combustion products.

The results of calculation are presented in Fig. 1. It is relationship curve between adiabatic temperature of combustion of (5Ti + 3Si)-Fe-compound and concentration of iron in it.

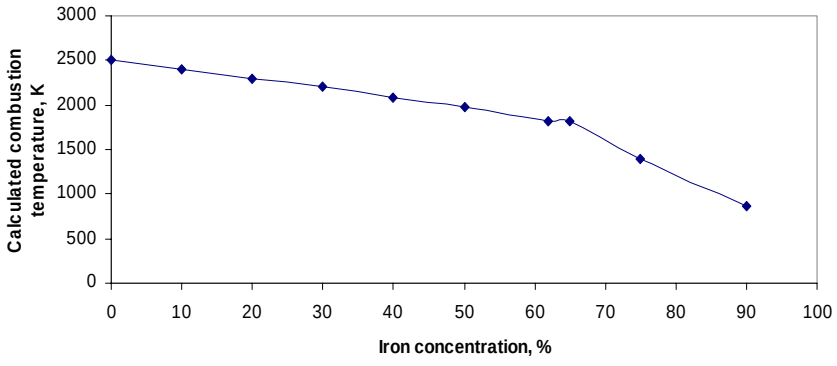

Fig. 1. Influence of iron concentration on adiabatic temperature of combustionof (5Ti + 3Si)-Fe-compound

The results show, that adiabatic temperature remains enough high despite heat effect reduction, when iron is added to (5Ti + 3Si)-compound (more than 2000°K when iron concentration is changed between 0 and 50%). Therefore, we can expect, that process can be carried out in self-propagating mode in wide range of Ti, Si, Fe concentration.

To carry out the researches, a laboratory SHS-reactor with 20 liters volume was constructed. This plant allows to carry out researches of SHS-processes in a wide range of pressure: from 0,01 to 10 MPa. Ti-Si-Fe-system is qualified as SHS-gas-free system, that is, all raw materials and products are in condensed state. There is no relationship between combustion parameters and pressure and this is the distinction of these systems. The relationships between combustion rate, combustion temperature, raw components ratio and particle size of titanium powder in titanium-ferrosilicon system were investigated using a laboratory SHS-reactor (Fig. 2).

Porous titanium powder TPP-4 TU 1791-449-05785388-99 produced by JSC «VSMPO-AVISMA Corporation» and ferrosilicon powder FeSi75 GOST 1415-93 produced by JCS «Chelyabinsk Electrometallurgical Integrated Plant» are used as raw materials. The temperature was measured by thermocouple method using tungsten-rhenium thermocouples TR-5/TR-20, an analogue transducer RL-16AIF and a signal multiplier RL-4DA200. The combustion rate was measured by a video camera.

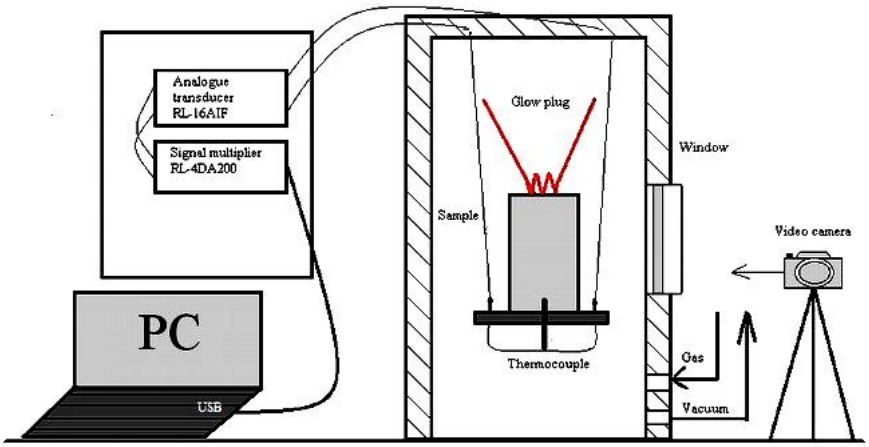

Fig. 2. Laboratory SHS reactor scheme

Combustion rate and temperature are basic parameters of a SHS-method. These parameters determine process productivity and safety, as well as equipment requirements. It is known, that modes and possibility of SHS depend on many factors. Most important factors, except high exothermicity, are raw components ratio and powder particle size.

In general, combustion synthesis in Ti-Si-Fe-system can be implemented using different schemes: Ti + Si + Fe; Ti + FeSi + Fe; Ti + FeSi; FeTi + Si + +Fe; FeTi + Si and others. In this work

processing in titanium-ferrosilicon system is investigated.

Combustion synthesis in this system was carried out in a wide range of raw components ratio (Fig. 3 and 4). As a result of combustion product with 60-75% Ti and 18-27% Si is formed. Fig. 3 shows the relationship between combustion temperature and titanium/ferrosilicon ration in the mixture.

As we can see, combustion temperature depends weakly on components ratio and remains almost constant in a wide range of raw components ratio (1720 ± 50°K). We think it happens because the changing of raw components ratio in studied ranges affects only on the proportion of the liquid phase in products, but the temperature of forming melted products, that is close to measured temperature, remains constant.

Fig. 4 shows the relationship between combustion rate and component ratio of (5Ti + 3Si)-Fe-compound

We can see from the figure, that combustion rate reduces both when titanium concentration increases and when it reduces. Maximum combustion rate was obtained on the compound with 72% Ti.

Fig. 5 shows the relationship between combustion temperature and titanium powder particle size when component ratio provides formation of Ti_5Si_3.

The figure shows that temperature remains at the same level (1720 ± 50°K) and changes weakly when titanium powder particle size is varied.

The next figure presents the relationship between combustion rate and titanium powder particle size (Fig. 6). This figure demonstrates, that combustion rate changes weakly (2 mm/s ± 0.25 mm/s) when titanium powder particle size is varied. Fig. 5 and 6 demonstrate that combustion in this system can be carried out in wide range of titanium powder particle size and combustion temperature with almost constant rate.

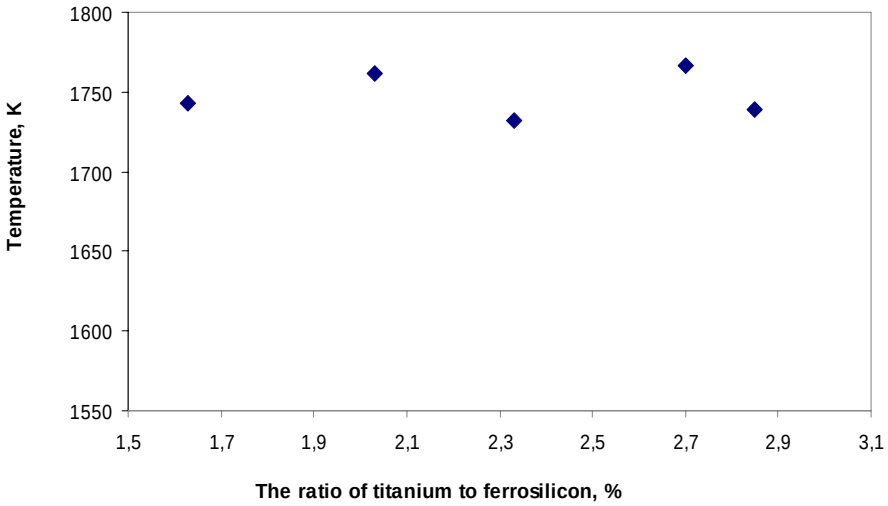

Fig. 3. Relationship between combustion temperature and components ratio

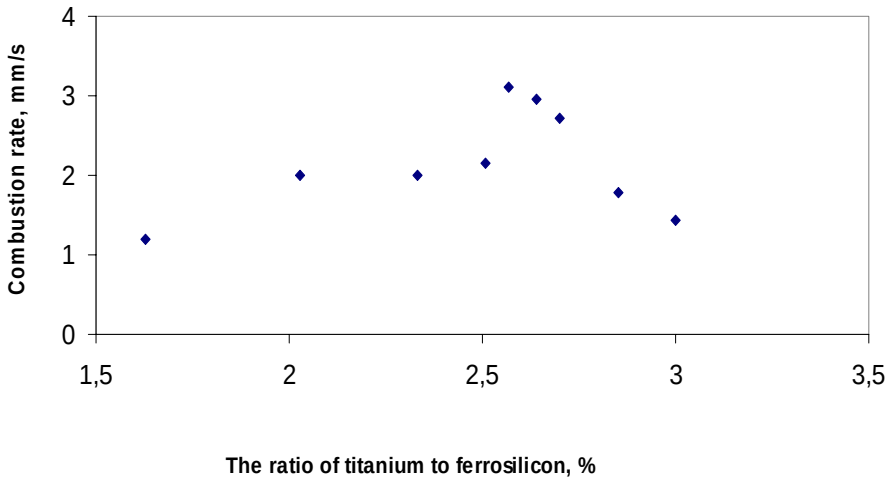

Fig. 4. Relationship between combustion rate and components ratio

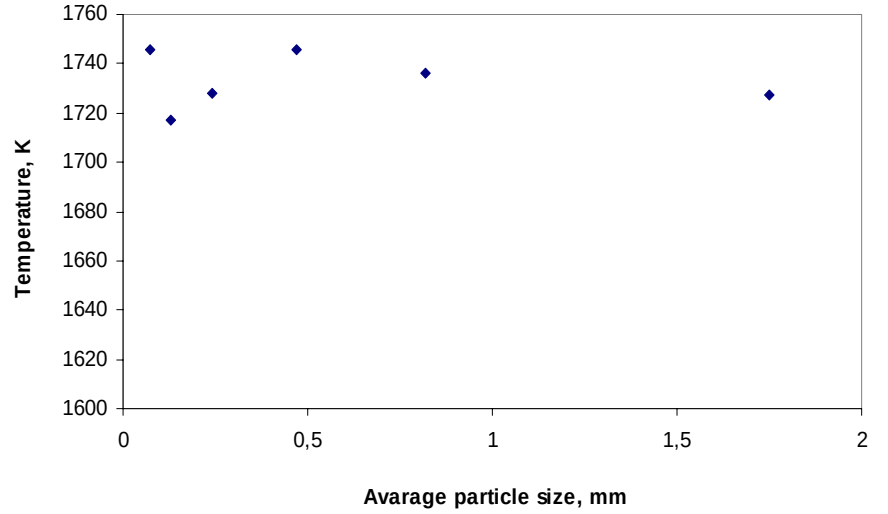

Fig. 5. Relationship between combustion temperature compound and titanium powder particle size in titanium-ferrosilicon compound

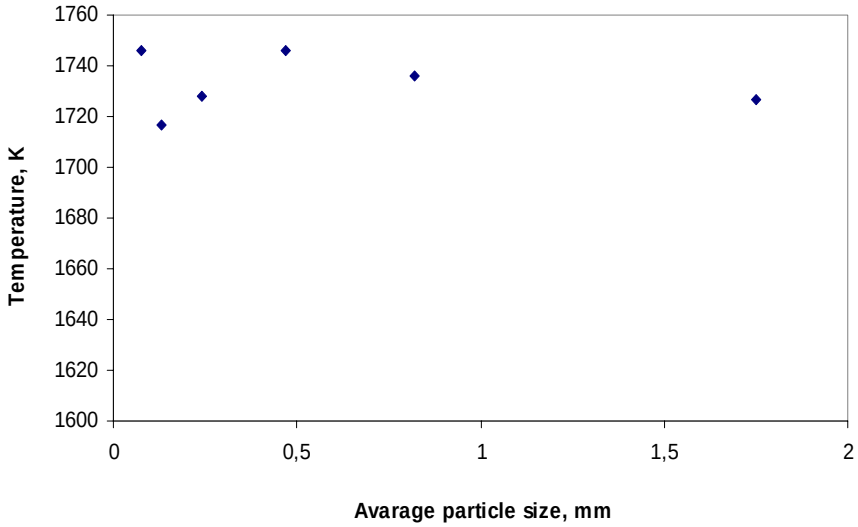

Fig. 6. Relationship between combustion rate and titanium powder particle size in titanium-ferrosilicon system

Thus, these investigations have shown that SHS-technology can be applied to obtain ferro silico titanium with high titanium content. It is possible to obtain alloys with various titanium content and various densities by varying of initial mixture and particle size of initial powders. Moreover, lack of waste and electricity consumption will bring low cost and provide high competitiveness of products. At the same time, producing of new alloy in inert gas atmosphere will increase the purity of end product.

Investigations results were used for developing the experimental-industrial technology of ferro silico titanium production by SHS-method. Specifications for optimal SHS-ferro silico titanium composition are developed (Table 2).

Table 2

Chemical composition of SHS-ferro silico titanium

Grade	Ti	Si	C	S	P	O	N	H
			max					
FST 70	61-74	18-27	0,15	0,005	0,009	0,1	0,05	0,005

Conclusions

The process of obtaining ferro silico titanium with high titanium content (to 75%) by self-propagating high-temperature synthesis was investigated. The relationships between combustion rate, combustion temperature and initial components ratio, titanium powder particle size were obtained. As it turned out, temperature depends weakly on initial components ratio and titanium powder particle size and remains at the same level (about 1720 ± 50°K). Combustion rate is also weakly depends on titanium powder particle size, but we can see, that combustion rate reduces when titanium content both increases and reduces. Maximum combustion rate was obtained on the compound with 72% titanium. Based on these data, experimental-industrial technology of obtaining ferro silico titanium by SHS-method was developed.

References

1. Lyakishev N.P., Pliner, U.L., Lappo S.I. *Legiruyuschie splavy i stali s titanom.* [Alloys and alloying steel with titanium]. M.: Metallurgiya, 1985, 230 p.
2. Gasik M.I. *Teoriya i tekhnologiya proizvodstva ferrosplavov.* [Theory and technology of production of ferroalloys]. Moscow: Metallurgiya, 1988, 340 p.
3. Sarkisyan A.R. and other. Some laws of combustion of mixtures of transition metals with silicon and silicide synthesis. *Fizika goreniya i vzryva.* [Physics of combustion and explosion]. 1977, no. 3, pp. 34-40.
4. Azatyan T.S. Some laws of combustion of titanium with silicon. *Fizika goreniya i vzryva.* [Physics of combustion and explosion]. 1978, no. 1, pp. 44-49.
5. Novikov N.P., Borovinskaya I.P., Merzhanov A.G. Thermodynamic analysis of self-propagating high-temperature synthesis reactions. *Protsessy goreniya vkhimicheskoy tekhnologii i metallurgii.* [Combustion Processes in Chemical Technology and Metallurgy: Proceedings]. Ed. A.G. Merzhanov. Chernogolovka, 1975, pp. 174-188.
6. Bukreev A.E., Manashev I.R., Nikiforov B.A., Bigeev V.A. New nitrogen-containing chrome nitride based alloys, obtained by SHS. *Vestnik Magnitogorskogo gosudarstvennogo tehnicheskogo universiteta im. G.I. Nosova.* [Vestnik of Nosov Magnitogorsk State Technical University]. 2008, no. 1, pp 49-51.

Parsunkin B.N., Andreev S.M., Akhmetov T.U., Mukhina E.Y.

OPTIMAL ENERGY-EFFICIENT COMBUSTION PROCESS CONTROL IN HEATING FURNACES OF ROLLING MILLS

Abstract. Considering continuous energy price rising, energy- efficient combustion process control is of current interest because circa 15% of the consumed firing is expended in rolling production for metal heating.

Effective solution of this problem is possible by using the automated systems of optimal control, based on optimizing control algorithms of search type. Such management systems have the ability to provide search and to maintain the maximum value of the optimized parameters under uncertainty and the lack of accurate quantitative model of the processing.

Keywords: temperature, air volume control, objective variable, extremal control, combustion control.

In iron and steel industry circa 15% of the consumed firing is expended in rolling production in metal heating. Therefore, energy-efficient combustion process control is of current interest, especially considering continuous energy price rising.

Optimal energy-efficient combustion process control is a difficult task in continuous furnaces of modern high-performance hot rolling mills, when their operating rate varies from 100 up to 1000 t / h, and the initial temperature of continuous cast billets, feeding to heating, ranges

from 0 to 600°C. Effective solution of this problem is possible by using optimal control automated systems, based on the principles of search optimizing algorithms. Such extreme control systems possess a unique ability to provide effective control under uncertainty and absence of accurate quantitative model of the optimizing processing.

In automatic combustion process controlling, under plant conditions, method of volumetric flow rate of firing and air is frequently used. This method provides target value stabilization of air flow rate – $\alpha_A^з$ in accordance with the following condition:

$$\alpha_A^з = \frac{V_A(\tau)}{V_F(\tau) \cdot L_O} = const,$$

where $V_F(\tau)$ is the current air flow, m^3 / h; $V_F(\tau)$ is the current firing rate, m^3 / h; τ is the current time, s; L_O is a coefficient, defining required air quantity for complete combustion of one unit measure of used fuel.

The combustion process investigation showed that there is individual dependency of value α_A on the gas flow, when the best energy firing conditions are provided for each type of combustion units (burners) and for each zone of heating furnace.

For example, rational values α_A dependency on gas flow for top zones №1, 3, 5 of a modern high-performance 10-zone continuous furnace № 1at Mill 2000 OJSC «MMK» with walking beams, with roof top and side lower natural gas firing, designed for continuous cast billet heating with 250 mm thickness and from 5000 to 12000 mm length is shown in Fig. 1 [1].

Overstated air flow under low gas flow rates is determined by the necessity to maintain the required kinetic energy of the gas-air jet in order to provide the flow «sticking» to the flat furnace roof surface. Under high gas flow rate, less air flow is required in comparison with theoretically calculated one, since oxygen in intensive mixing enters gas jet from the workspace by means of inleakage, where the oxygen content is 5-8%.

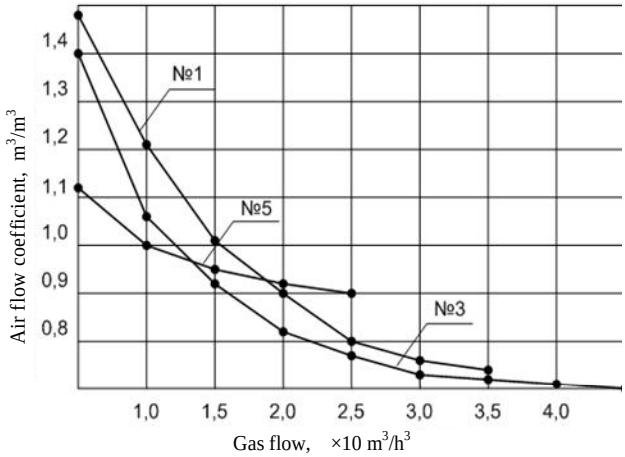

Fig. 1. Dependencies of rational values of air flow rate α_A on the gas flow for the upper zones **№**1, 3, 5 of continuous furnace **№** 1 at the Mill 2000 OJSC «MMK»

Target value $\alpha_A^з$ maintaining on required rational value involves constant operator intervention into combustion process control mode in each gas flow changing. It is physically impossible under non-steady furnace operation behavior. Therefore, overstated $\alpha_A(\tau)$ is set for all flow-rates in zones. This reduces the efficiency of fuel combustion process control and increases discharge intensity.

Energy-saving automated system is effectually used to implement the optimal fuel combustion process control. This system should independently (without operator intervention) define and maintain that sort of α_A value, which enables firing to cause maximum thermal effect, with furnace characteristics and external influences changing accidentally.

The obligative and necessary functioning condition of this optimal fuel combustion process control system is unimodal (one-extreme without derivative breaking) type of optimization process steady-state characteristic [1].

The experimental dependencies of top zones workspace temperatures of continuous furnace №1 at the Mill 2000 OJSC «MMK» on value α_A in each zone are presented in Fig. 2.

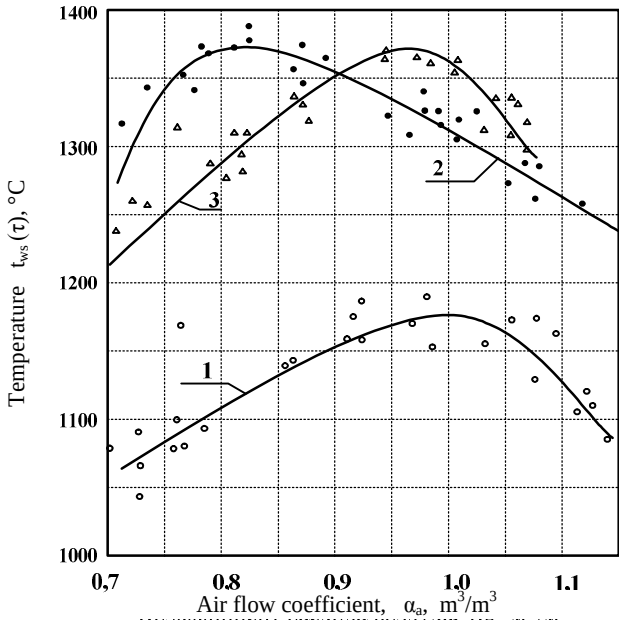

Fig.2. Dependency of workspace temperature in the top welding zones according to zone thermal couple readings upon air flow rate: 1) zone **№**3, V_{TC} = 1020m3 / h, and 2) zone **№**3, V_{TC} = 2600m3 / h, and 3) zone **№**5, V_{TC} = 1100m3 / h

Dependencies analysis obtained proves the ability and expediency to use optimal fuel combustion process control system in each top zone of fired continuous furnaces.

Long-term practice of automatic optimization systems (AOS) using under real operation conditions showed that such systems should be two loop circuit [1,7].

The first loop is stabilizing, providing volumetric gas and air flow proportion, realizes fast but rough firing and air flow ratio. This allows the control system to response

quickly to deep technological indignation, when changing firing rate and temperature.

The second loop is optimizing, begot on extreme control principles, allows to carry out, within a dedicated work area for this circuit, more sensitive optimal condition adjustment of combustion process, but more slowly.

Block diagram of two-loop automatic control system of optimum combustion process is shown in Fig. 3.

The stabilizing loop, implementing standard PI or PID controller theory, includes firing rate FS and air rate AS sensors with rate transmitters V_F and V_A. Functional generator composes the required air flow rate $V_{\text{A}}^3(\tau)$ in accordance with the expected rational air flow $V_F^3(\tau) = F\left[V_{\text{F}}(\tau)\right]$ (see Fig. 1). The value $F\left[V_{\text{F}}(\tau)\right]$ is compared in comparison element CE with the current air flow rate value $V_A(\tau)$. The signal $\Delta V_A(\tau)$ is generated at comparison element output.

$$\Delta V_A(\tau) = F\left[V_F(\tau)\right] - V_A(\tau),$$

where $F\left[V_{\text{F}}(\tau)\right] = V_F(\tau) \cdot L_O \cdot \alpha_{\text{A}}^3(\tau)$ is required current «target» air flow into a zone.

Signal $\Delta V_A(\tau)$ is fed to the input of switch control unit SCU.

At the same time, signal $\Delta V_{\text{A}}^3(\tau)$, which is formed by a setting device SD and defines target work area of optimizing loop, is fed to the SCU input.

The switch control unit switches over the control of the air flow actuating unit AU in accordance with the following condition:

$$\sigma(\tau) = \begin{vmatrix} \sigma_1(\tau), if\ \Delta V_{\text{A}}(\tau) > \Delta V_{\text{A}}^3(\tau) \\ \sigma_2(\tau), if\ \Delta V_{\text{A}}(\tau) \le \Delta V_{\text{A}}^3(\tau), \end{vmatrix}$$

where $\sigma_1(\tau)$, $\sigma_2(\tau)$ are the switching functions, defining the current travel direction of the actuating unit (AU), that changes the air flow accordingly to stabilizing or optimizing loops in accordance with the following expression:

$$V_{\text{A}}(\tau) = \text{V}_{\text{AI}} + \sigma_i(\tau) \cdot \text{K}_{\text{AU}} \cdot \tau, \quad i = 1,2,$$

where V_{AI} is the initial value of the air flow; $\sigma_i(\tau) \in (+1, -1)$ is the current direction of the air flow rate changing; K_{AU} is constant speed of the actuating unit (AU), according to technical characteristics.

Optimizing loop involves a heating area temperature detector TE, a rate converter RC and an optimizer, begot on the extreme control principle, providing the detection and maintenance of optimal combustion conditions within a set zone $\Delta V_{\text{A}}^3(\tau)$ in accordance with the extreme type dependency t°C=φ($\alpha_A(\tau)$), (see Fig. 2).

Under normal operating conditions, type of steady-state extreme characteristics and extremum location in the field «control action – optimizing variable» have not been defined. Therefore, the using of continuous extreme control system with the remembering of optimized parameter speed extremum and with actuating unit stop at the moment of maximum speed changing is the most acceptable.

Dynamics of a searching process in such automatic management optimization system (AMOS) of combustion process is determined by the equations set and logical conditions [5,6]:

$$\overline{Y}\left[X(\tau)\right] = a_0 + a_1 X(\tau) + a_2 X^2(\tau) + \ldots + a_n X^n(\tau)$$
$$T_o dZ(\tau)/d\tau + Z_1(\tau) = Y\left[X(\tau)\right];$$
$$T_\phi dZ(\tau)/d\tau + Z(\tau) = Z_1(\tau).$$

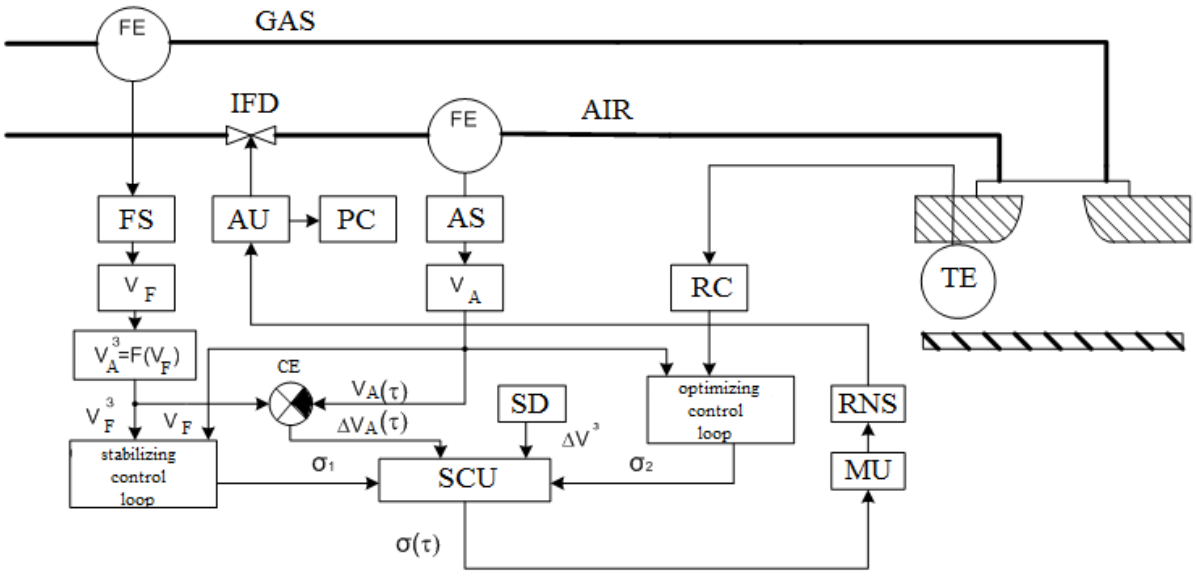

Fig. 3. Block diagram of two-loop system of combustion process control optimization in the workspace of industrial furnaces

In the case of $\frac{dZ(\tau)}{d\tau} \geq 0$

$$U(\tau) = \begin{cases} +1, \text{ if } \dot{Z}(\tau) - \dot{Z}(\tau)_{\max} + \Delta\left(\dot{Z}(\tau)\right)_H > 0; \\ 0, \text{ if } \dot{Z}(\tau) - \dot{Z}(\tau)_{\max} + \Delta\left(\dot{Z}(\tau)\right)_H \leq 0. \end{cases}$$

In the case of $\frac{dZ(\tau)}{d\tau} = \dot{Z}(\tau) < 0$

$$U(\tau) = -1, \text{ if } \dot{Z}(\tau) + \Delta\left(\dot{Z}(\tau)\right)_H < 0.$$

If $U(\tau) = +1$, then $\sigma_2(\tau+1) = \sigma_2(\tau)$.

If $U(\tau) = 0$, then $\sigma_2(\tau+1) = 0$.

If $U(\tau) = -1$, then $\sigma_2(\tau+1) = -\sigma_2(\tau)$,

where $(\tau-1)$, τ, $(\tau+1)$ denote the past, current, posterior time intervals respectively; $X(\tau) = V_A(\tau)$ is the current value of the control parameter; $Z(\tau)$, $\dot{Z}(\tau)$ are current values of optimizing parameter and its change rate over time respectively; $\overline{Y}[X(\tau)]$ is the set optimizing parameter point in accordance with the steady-state characteristic of the optimized process; $T_0 = T_{obj} + T_L$ is the equivalent object time coefficient, characterizing optimizing process persistence – T_{obj} and lagging – T_L; T_F is the smoothing filter time coefficient, used for high frequency information signal interference rejection $\dot{Z}(\tau)$; $\dot{Z}(\tau-1)_{\max}$ is the maximum rate changing value of the optimized parameter, achieved in the by-past time period; $\Delta\left(\dot{Z}(\tau)\right)_{DZ}$ is the optimizing loop dead zone.

The value $\dot{Z}(\tau-1)_{\max}$ is formed by a memory unit in accordance with the following condition:

if $\dot{Z}(\tau) \geq \dot{Z}(\tau-1)_{\max}$, then $\dot{Z}(\tau-1)_{\max} = \dot{Z}(\tau)$;

if $\dot{Z}(\tau) < \dot{Z}(\tau-1)_{\max}$, then $\dot{Z}(\tau-1)_{\max} = \dot{Z}(\tau-1)_{\max}$.

The study was made of the automatic optimization system efficiency on the laboratory setup [1,4], under conditions close to real.

The trajectories of changing $Z(\tau)$, $\dot{Z}(\tau)$ and $X(\tau)$ parameters over time, during search operation mode of automatic management optimization system AMOS of combustion process, in using this extremum search method, are presented in Fig. 4.

The following time intervals are identified in Fig. 4: 0-1 elapsed time of stabilizing loop, 1-2 elapsed time of optimizing loop; 2-3 conditioning period before the next search cycle; 3-4 elapsed time of optimizing loop after AU forced reverse; 4-5 conditioning period before the next cycle of search, etc.

The time interval τ_C – conditioning before verificatory forced reverse is required for the accumulation of information about optimizing process current state.

Engineering implementation of two-loop AMOS of combustion process on the basis of domestic CJSC Mekhanoremontny Komplex (Mechanical Repair Shop) is examined in detail in [2].

The property of this extremum search method is the absence of AMOS operation periodic mode and considerably high accuracy in the extremum error less than 5%.

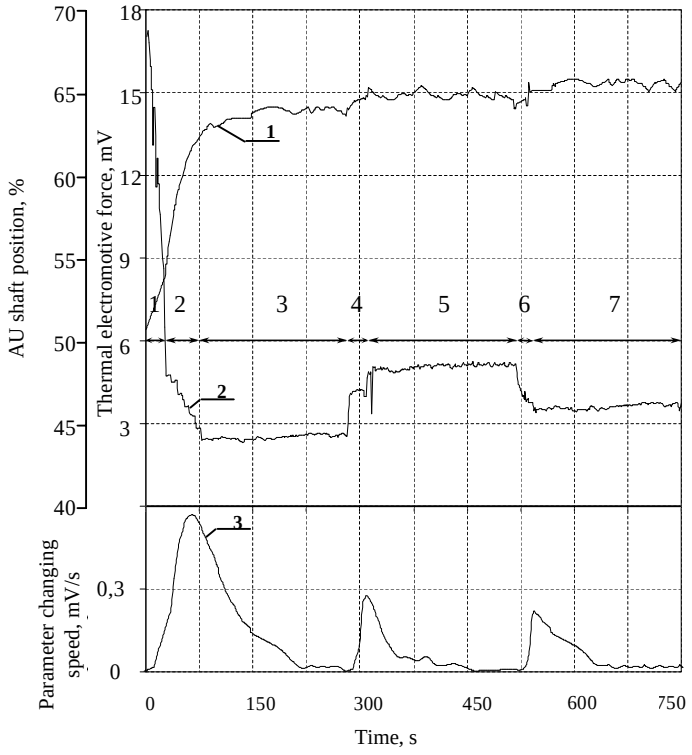

Fig. 4. Change over time $Z(\tau)$, $\dot{Z}(\tau)$, $X(\tau)$ in introducing AMOS of combustion process in the furnace workspace: 1 – relative changing of temperature detector; 2 – air flow changing, 3 – temperature changing rate

The utilization of the introduced software-programmable optimization technology of control energy-intensive process of combustion in industrial furnaces workspace enables 1.5-2.5% reduction of firing discharge intensity. That becomes possible due to more effective and operational control of air flow under heating furnaces nonsteady behavior.

Moreover, combustion process stabilization will lead to the stabilization of thermal state of heating billets and will permit to improve calculation accuracy of the strip thermal state during rolling [8]. Such firing combustion control systems are applicable for almost all thermal energy consuming units, operating in nonsteady mode, in which gaseous firing is used as the source of heat [9].

References

1. Parsunkin B.N., Andreev S.M., Akhmetov U.B. *Optimization of processing control in metallurgy.* Magnitogorsk: Nosov Magnitogorsk State Technical University, 2006. 198 p.
2. Kazakevitch V.V., Rodov A.B. *The automatic optimization systems*. Moscow: Energy, 1977, 288 p.
3. Parsunkin B.N., Andreev S.M. Processing control optimization of fuel combustion in heating furnaces workspace. *Steel.* 2000, no. 5, pp. 48-52.
4. Parsunkin B.N., Andreev S.M., Obukhova T.G. Study of optimum energy efficient fuel combustion process in metallurgical furnaces workspace. *Vestnik Magnitogorskogo gosudarstvennogo tehnicheskogo universiteta im. G.I. Nosova.* [Vestnik of Nosov Magnitogorsk State Technical University]. 2005, no. 4, pp. 28-36.
5. Parsunkin B.N., Bushmanova M.V., Andreev S.M. *Calculations of automatic systems of processing optimization in metallurgy: Textbooks*. Magnitogorsk: Nosov Magnitogorsk State Technical University, 2003, 267 p.
6. Sayrov A.M. Optimization of thermal management in heating furnace workspace. *Automated technologies and production: Collection of Scientific Papers.* Ed. Parsunkin B.N. Magnitogorsk: Nosov Magnitogorsk State Technical University, 2013. no. 5, pp. 296-301.
7. Parsunkin B.N., Andreev S.M. Ways to improve the efficiency and noise immunity of processing control automatic optimization. *Automated technologies and production: Collection of Scientific Papers.* Ed. Parsunkin B.N. Magnitogorsk: Nosov Magnitogorsk State Technical University, 2013. no. 5, pp. 277-290.
8. Rumyantsev M.I., Shubin I.G., Nosenko O.U. Model designing to calculate the temperature of low-alloy steels in hot rolling. *Vestnik Magnitogorskogo gosudarstvennogo tehnicheskogo universiteta im. G.I. Nosova.* [Vestnik of Nosov Magnitogorsk State Technical University]. 2007, no. 1, pp. 54-57.
9. Zadonskaya T.A., Shvetsova E.S., Koptsev V.V. Firing of high-speed streams of natural gas. *Vestnik Magnitogorskogo gosudarstvennogo tehnicheskogo universiteta im. G.I. Nosova.* [Vestnik of Nosov Magnitogorsk State Technical University]. 2009, no. 3, pp. 67-68.

Antsupov A.V., Antsupov A.V. (jun), Antsupov V.P.

DESIGNED ASSESSMENT OF MACHINE ELEMENT RELIABILITY DUE TO EFFICIENCY CRITERIA

Abstract. The universal method of reliability assessment of mechanical system loaded elements at the design stage as a sequence of steps within the procedure of constructing physical and probabilistic models of parametric failure formation based on various criteria is suggested. The methodology of forecasting durability of parts by kinetic strength is represented and an example of its implementation is shown.

Keywords: methodology, forecasting, reliability, dependability, durability, failure, damage susceptibility, gamma-percent life.

The main problem of the reliability theory is behavior prediction of mechanical system parts and components in supposed conditions of external loading, when it becomes possible to evaluate their reliability and durability in early stage design. In this case, the assessment of system element behavior and their parameters changing over time in future running is carried out on the dynamic, physical and probabilistic models [1].

A single, universal methodological approach to probability forecasting of trouble-free operation and resource characteristics of loaded elements of mechanical systems according to various criteria of their performance was stated in this paper, on basis of mathematical formalization of reliability theory basic concepts of engineering objects (GOST 27.002-89), and general concept of their gradual failure formation [2-4].

To describe theoretically the objective formation of technical product failures during their damageability (degradation) under external affecting, the suggested approach is stated as a series of rules of their parameter reliability dynamic models designing.

This approach is presented in a probabilistic form, and is a combination of the following steps.

I. Selection of object state basic parameter.

Parameter X_t (a random variable) is selected for the testing product type, according to the standard (GOST 20911-89) definition of «object state». Variable changing over time simulates the parameter behavior (state changing) during the entire operation period under certain external affecting conditions.

II. The equation formulation of object state.

Random function (dependency) elaboration or choosing, that describes parameter X_t increasing (+) or decreasing (-) changing over time, and models the product state changes in aging (degradation) during the operation can be written as the following:

$$X_t = X_0 \pm \int_0^t \dot{X}_t \cdot dt \,, \qquad \text{(I)}$$

where X_0 is X_t parameter distribution at time $T = t_0$ characterizing the initial object state; $\dot{X}_t = dX_t / dt$ denotes random variable current distribution of object damageability rate at time $T = t$;

If a random variable of object damageability rate does not change over time – $\dot{X}_t = \dot{X} = const$, then the conditions (I) can be written as follows:

$$X_t = X_0 \pm \dot{X} \cdot t \qquad \text{(I.a)}$$

Equations (I) simulate object damageability over time.

III. The formulation of object efficiency condition.

In accordance with the standard definition of «object performance capability», according to GOST 27.002-89, the condition of its performance is mathematically formulated in the form of one possible inequality:

$$X_t = X_0 + \int_0^t \dot{X}_t \cdot dt < x_L \text{ or}$$
$$X_t = X_0 - \int_0^t \dot{X}_t \cdot dt > x_L, \qquad \text{(II)}$$

where x_L is a limit value of X_t parameter, established in

technological standards (TS) or assigned under the operating experience of such objects.

If the random variables in the condition (I) are normally distributed, and $\dot{X}_t = \dot{X} = const$, then performance capability conditions (II) can be written as the following:

$$X_t = X_0 + \dot{X} \cdot t < x_L \text{ and } X_t = X_0 - \dot{X} \cdot t > x_L . \quad \text{(II.a)}$$

Centring and normalizing values X_t and x_L, inequalities (II.a) can be written, using proper quantiles, as the following:

$$U_t < u_{L(t)} \text{ or } U_t > u_{L(t)} . \quad \text{(II.b)}$$

Expanding the current value of parameter standard normal distribution quantile (SND), conditions (II.b) can be written as following:

$$\frac{X_t - \left(\overline{x}_0 + \overline{\dot{x}} \cdot t\right)}{\sqrt{\sigma_{x0}^2 + \sigma_{\dot{x}}^2 \cdot t^2}} < u_{L(t)} \text{ or}$$
$$\frac{X_t - \left(\overline{x}_0 - \overline{\dot{x}} \cdot t\right)}{\sqrt{\sigma_{x0}^2 + \sigma_{\dot{x}}^2 \cdot t^2}} > u_{L(t)} . \quad \text{(II.в)}$$

where $u_{L(t)} = \dfrac{x_L - \left(\overline{x}_0 \pm \overline{\dot{x}} \cdot t\right)}{\sqrt{\sigma_{x0}^2 + \sigma_{\dot{x}}^2 \cdot t^2}}$ denotes the current limit value of SND quantile of a random variable $X_t = x_L$; $\overline{x}_0 = (x_{0\max} + x_{0\min})/2$; $\sigma_{x0} = (x_{0\max} - x_{0\min})/6$ are numerical characteristics (mean and standard) of a random parameter $X_t = X_0$ of object state at the initial instant of time $T=t_0$; $x_{0\max}$, $x_{0\min}$ are maximum and minimum values of object X_0 parameter, defined as the initial conditions; $\overline{\dot{x}}$ и $\sigma_{\dot{x}}$ are numerical characteristics of a random parameter $\dot{X}$.

Equations (II) reflect the range of all possible operable object states.

IV. Elaboration of equations for object reliability assessment.

Using the basic concepts "distribution function" of the probability theory makes possible to formulate the dependencies for estimation of object failure-free operation probability - condition efficiency probability (II) for any fixed instant of future operation:

$$P(t) = P(X_t < x_L) = P((X_0 + \int_0^t \dot{X}_t \cdot dt) < x_L) = F(x_L) \text{ or}$$
$$P(t) = P(X_t > x_L) =$$
$$= 1 - P((X_0 - \int_0^t \dot{X}_t \cdot dt) < x_L) = 1 - F(x_L) . \quad \text{(III)}$$

If the normal distribution of $\dot{X}_t$ parameter is constant over time ($\dot{X}_t = \dot{X} = const$), the main indicator of reliability is denoted using SND function $F(u_{L(t)}) = F_t(x_L)$ or the Laplace function $\Phi(u_{L(t)})$:

$$P(t) = P(X_t < x_L) = F(u_{L(t)}) =$$
$$= \Phi(u_{L(t)}) = \Phi\left(\frac{x_L - \left(\overline{x}_0 + \overline{\dot{x}} \cdot t\right)}{\sqrt{\sigma_{x0}^2 + \sigma_{\dot{x}}^2 \cdot t^2}}\right) \text{ or}$$
$$P(t) = P(X_t > x_L) = 1 - F(u_{L(t)}) =$$
$$= 1 - \Phi(u_{L(t)}) = 1 - \Phi\left(\frac{x_L - \left(\overline{x}_0 - \overline{\dot{x}} \cdot t\right)}{\sqrt{\sigma_{x0}^2 + \sigma_{\dot{x}}^2 \cdot t^2}}\right). \quad \text{(III.a)}$$

Equations (III.a) define the object reliability law in the integral (or differential $f(t) = -dP(t)/dt$) form, the law of object gradual failure formation in solving the direct task of the reliability theory. According to [2], it is asymmetric and does not obey the normal distribution.

V. The formulation of the object transition equation to the limit state (the state of parametric failure).

According to GOST 27.002-89 standard definitions of «object performance capability» and «parametric failure», the conditions of product transition into the parametric failure state in the form of limit value achieved by X_t parameter are formulated as following:

$$X_t = X_0 \pm \int_0^t \dot{X}_t \cdot dt = x_L , \quad \text{(IV)}$$

If the normal distribution of $\dot{X}_t$ parameter is constant over time ($\dot{X}_t = \dot{X} = const$), the models (IV) can be expressed as

$$\frac{X_t - \left(\overline{x}_0 + \overline{\dot{x}} \cdot t\right)}{\sqrt{\sigma_{x0}^2 + \sigma_{\dot{x}}^2 \cdot t^2}} = u_{L(t)} \text{ or}$$
$$\frac{X_t - \left(\overline{x}_0 - \overline{\dot{x}} \cdot t\right)}{\sqrt{\sigma_{x0}^2 + \sigma_{\dot{x}}^2 \cdot t^2}} = u_{L(t)} . \quad \text{(IV.a)}$$

Equations (IV) reflect the range of all possible object limit states.

VI. Elaboration of equations for object durability assessment (service life characteristics).

In accordance with GOST 27.002-89 gamma-percent resource t_γ definition, the dependences are derived for its assessment by equation (IV) solution concerning $t = t_\gamma$ for assigned accepted value of failure-free operation probability $[P(t)] = \gamma$ and the relevant distribution quantile $[u_{L(\gamma)}]$ value owing to the known law of X_t random variable. In general, this dependence can be represented by any function:

$$t_\gamma = f(\bar{x}_0, \sigma_{x0}, \bar{\dot{x}}, \sigma_{\dot{x}}, [u_{L(\gamma)}]). \quad (V)$$

If the normal distribution of $\dot{X}_t$ parameter is constant in time ($\dot{X}_t = \dot{X} = const$), gamma-percent resource is determined by equation (IV.a) solution concerning $t = t_\gamma$ during $X_t = x_L$ and $u_{L(t)} = [u_{L(\gamma)}]$ substitution in the form of:

$$t_\gamma = \frac{(\pm\bar{\dot{x}})\cdot\Delta\bar{x}_L - \sqrt{(\Delta\bar{x}_L\cdot\bar{\dot{x}})^2 - ([u_{L(\gamma)}]^2\cdot\sigma_{\dot{x}}^2 - \bar{\dot{x}}^2)\cdot([u_{L(\gamma)}]^2\cdot\sigma_{x0}^2 - \Delta\bar{x}_L^2)}}{\bar{\dot{x}}^2 - [u_{L(\gamma)}]^2\cdot\sigma_{\dot{x}}^2}, \quad (V.a)$$

where the value $[u_{L(\gamma)}]$ is determined by assigned accepted value of failure-free operation probability $[P(t)] = \gamma$, and the value $\Delta\bar{x}_L = x_L - \bar{x}_0$ is the assessment of mathematical expectation of ΔX_t limit change of X_t parameter;

VII. Elaboration of kinetic equation of object damageability.

On basis of any theory, concept or experimental researches, a kinetic equation is stacked up to estimate object damageability rate $\dot{X}_t$, depending on its geometrical and microgeometrical d_i, Δ_t characteristics, σ_i material properties, power and kinematic parameters F, external impact V, time t and other factors.

In general, it can be represented in the form of any random function:

$$\dot{X}_t = f(d_i, \Delta_t, F, V, \sigma_i, t, ...). \quad (VI)$$

The represented methodological approach (I)–(VI) can be formulated in the form of a separate methodology of reliability assessment (prediction) of certain groups of technical objects, using one of the possible criteria such as performance conditions (II) [1-4]:

– static or kinetic strength;
– durability;
– hardness;
– bearing value;
– heat resistance and others.

When selected X_t parameter, the status of a particular product (parts, unit) and known data about:

– law of its distribution;

– boundary conditions, describing the object loading diagram, its properties, and the initial state in supposed operating conditions;

– its damageability equation (VI) for $\dot{X}_t$ assessment, designated sequence of steps produces a sequence of operations (probabilistic technique) of quantity estimation of failure-free measure $P(t) = P(X_t < x_L)$ or $P(t) = P(X_t > x_L)$ and durability t_γ of the investigated object either in its designing, or in running.

In particular, in publications [5-11], this approach is implemented as a reliability parametric prediction strategy of a large object group – «stationary» triboconjugation, by their component wear resistance criterion.

Beneath, on basis of suggested approach a reliability prediction strategy of different object group - machine and unit loaded elements, according to kinetic strength criterion, is formulated.

Currently, the problem of the strength of solid bodies under load is considered from the point of kinetic approach [12-13]. From this point of view, the destruction process is represented as evolutive process of material structural damage accumulation in time.

In reaching material structure defect by current solidity in any local volume - its damageability, a limit value, microcrack occurrence takes place, which extends through the most loaded material volumes and leads to its division into parts (destruction).

The degree of local volume structure damage of part material at any fixed time point t is estimated quantitatively by density value of potential defect energy $u_e(t) = u_{et}$, which is determined by the external loading conditions and material properties [13].

Taking into account the aforementioned, the methodology steps of loaded part reliability and durability prediction may be formulated according to (I) - (VI), in a sequence of the following operations.

At the first stage as part state $\dot{X}_t$ parameter, in which internal stresses σ emerge, affected by external loading at temperature T, we take the potential energy density of defects u_{et}, which characterizes the actual degree of structure damage of material part local volumes [13]. Herewith, according to the central limit theorem of probability theory, we consider normal the distribution of a random variable $X_t = u_{et}$ at any time t, as a parameter, depending upon a set of independent random factors [1]. Furthermore, to simplify mathematical expressions we will operate with its mean value $\bar{u}_{et}$.

At the second stage, we will formulate the equation of loaded element states:

$$\bar{u}_{et} = \bar{u}_{e0} + \int_0^t \bar{\dot{u}}_{et}\cdot dt. \quad (1)$$

where $\bar{u}_{e0}$ is the average density of material component part potential energy in the initial state (at $t = 0$), which, according to [13], can be defined as a function of hardness average value HV according to Vickers:

$$\bar{u}_{e0} = \frac{(0{,}071\cdot HV)^{2{,}4}}{6\cdot G(T)\cdot(6{,}47\cdot10^{-6}\cdot HV + 0{,}12\cdot10^{-2})^2}; \quad (1.a)$$

where $\bar{\dot{u}}_{et} = d\bar{u}_{et}/dt$ denotes damageability average velocity (damage accumulation) of element material structure at time t.

At the third stage, we will state the condition of loaded component part performance efficiency:

$$\bar{u}_{et} = \bar{u}_{e0} + \int_0^t \dot{\bar{u}}_{et} \cdot dt < u_{e*}, \qquad (2)$$

where $u_{e*} = u_* - u_T$ denotes the critical density of structure defects energy of material local volumes of loaded component part [13]; u_* is the critical density of material internal energy (critical energy intensity), which is equal to its melting enthalpy in solid ΔH_S or liquid ΔH_L state; $u_T = \int_0^T \rho \cdot c dT$ denotes the thermal component of the material internal energy density of loaded component part at a given temperature T; ρ, c are density and heat capacity of the component part material.

At the fourth stage we will write the expression for loaded element reliability evaluation at time t, using as an indicator the reliability safety factor (safety margin), calculated according to the average value $\bar{u}_{et}$ of state parameter [1]:

$$n_t = u_{e*} / \bar{u}_{et} = u_{e*} / \left(\bar{u}_{e0} + \int_0^t \dot{\bar{u}}_{et} \cdot dt \right). \qquad (3)$$

At the fifth stage we will formulate the equation of loaded component part transition to the marginal state (parametric failure state):

$$\bar{u}_{et} = \bar{u}_{e0} + \int_0^t \dot{\bar{u}}_{et} \cdot dt = u_{e*}, \qquad (4)$$

At the sixth stage, using the expression (5), we formulate the equation, its solution for $t = \bar{t}_L$, will define the average limit resource to element failure (damage):

$$\int_0^{t_{np}} \dot{\bar{u}}_{et} \cdot dt = u_{e*} - \bar{u}_{e0}. \qquad (5)$$

At the seventh stage as a damageability kinetic equation for the evaluation of average velocity $\dot{\bar{u}}_{et}$ of element damageability, which is in the loaded state, which is included in the equation (1)–(5) of its failure forming general diagram, one can use V.V. Fedorov dependency, he stacked up in the publication [13] using long-time strength thermodynamic criterion.

In general, this equation is the following:

$$\dot{\bar{u}}_{et} = f(\sigma, T, u_{et}, t, ...). \qquad (6)$$

In carrying out engineering calculations we use one of the simplified versions of this dependency to determine the time constant value $\dot{\bar{u}}_{et} = \dot{\bar{u}}_e$:

$$\dot{\bar{u}}_e = M_R^2 \cdot k_\sigma^2 \cdot \sigma^2 \cdot A_0 / (6 \cdot G \cdot \nu), \qquad (6.a)$$

where $M_R^2 = \left((1+r)^2 + (1-r)^2\right)/4$ is a equivalency coefficient of non-stationary tension state (non-stationary tension state with a coefficient of skewness $r = \sigma_{\min}/\sigma_{\max}$ transition to the equivalent steady state with voltage $\sigma = \sigma_a$); $\sigma_{\min}$, $\sigma_{\max}$, σ_a are minimum, maximum and peak cycle stresses; $k_\sigma = 1/\left(6{,}47 \cdot 10^{-6} \cdot HV + 0{,}12 \cdot 10^{-6}\right)$ denotes an overstress coefficient of interatomic bonds; G and ν are modulus of rigidity and coefficient of internal energy distribution irregularity over the loaded component part, the value of which is selected referring to [13];

Coefficient A_0 of stress tensor ball portion influence on interatomic bond damage activation energy, is expressed according to [13]:

$$A_0 = \frac{\nu \cdot U(\sigma, T)}{h \cdot N_0} \exp\left[-\frac{U(\sigma, T)}{R \cdot T} \right], \qquad (6.b)$$

where h is the Planck constant; N_0 is the Avogadro number; R is the universal gas constant; $U(\sigma, T)$ is activation energy of interatomic bond damage process at the given voltage σ and temperature T:

$$U(\sigma_a, T) = U_0 - \Delta U(T) - \\ -\left(M_R^2 \cdot k_\sigma^2 / (18 \cdot \nu \cdot K)\right) \cdot \sigma^2; \qquad (6.c)$$

where U_0 is free energy of process activation at $T = 0$ and $\sigma = 0$; $\Delta U(T) = \frac{3}{2} \cdot \alpha_0 \cdot K^{-1} \cdot T$ is activation energy quantity, determined by the temperature; $K = E/(3 \cdot (1 - 2 \cdot \mu))$ is all-round material compression index; α_0, μ, E are linear thermal expansion coefficient; the Poisson's ratio and material elastic modulus.

Complex equations (6.a-c) denote a mathematical model of machine element and construction stationary damageability process, in which internal static or dynamic tensions σ emerge, affected by external loading and constant temperature T.

For a loaded element stationary damageability process (with constant rate $\dot{\bar{u}}_{et} = \dot{\bar{u}}_e$, defining by models (6.a-c)), the safety margin average value at any time t is determined by the simplified expression (3):

$$n_t = u_{e*} / \bar{u}_{et} = u_{e*} / (\bar{u}_{e0} + \dot{\bar{u}}_e \cdot t). \qquad (3.a)$$

and the ultimate resource is determined by the simplified expression solution (5) – $\dot{\bar{u}}_e \cdot t_L = (u_{e*} - \bar{u}_{e0})/$ respectively to $t = \bar{t}_L$ as:

$$t_L = (u_{e*} - \bar{u}_{e0}) / \dot{\bar{u}}_e. \qquad (5.a)$$

The complex of equations (3.a), (5.a)–(6.a-c) denotes a physical probabilistic model of the formation process of

gradual failures of machine elements, in which internal static or dynamic tensions σ emerge, affected by external loading and constant temperature T.

The sequence of mathematical operations, based on this model in order to estimate the expected average resource $\bar{t}_L$, defines their durability forecasting method and is the academic analogue of S.N. Zhurkov famous experimental equation [12, 13].

The example of the suggested method implementation is shown in figure. A graphical interpretation of the equation solution (5.a), taking into account (6.a-c) for a spindle from 25 steel grade with mechanical properties $\sigma_T = 230\,MPa$, $\sigma_B = 420\,MPa$ and $HV = 2020\,MPa$, exposed to static uniaxial tension at different temperatures, is represented. In particular, at $\sigma = 142,9\,MPa$ and temperature $T = 40°C$ its forecast limit time – average limited endurance under these conditions, comprises $t_L \approx 3,7 \cdot 10^6\,s \approx 1,43\,mo$ (see marked point ordinate in figure).

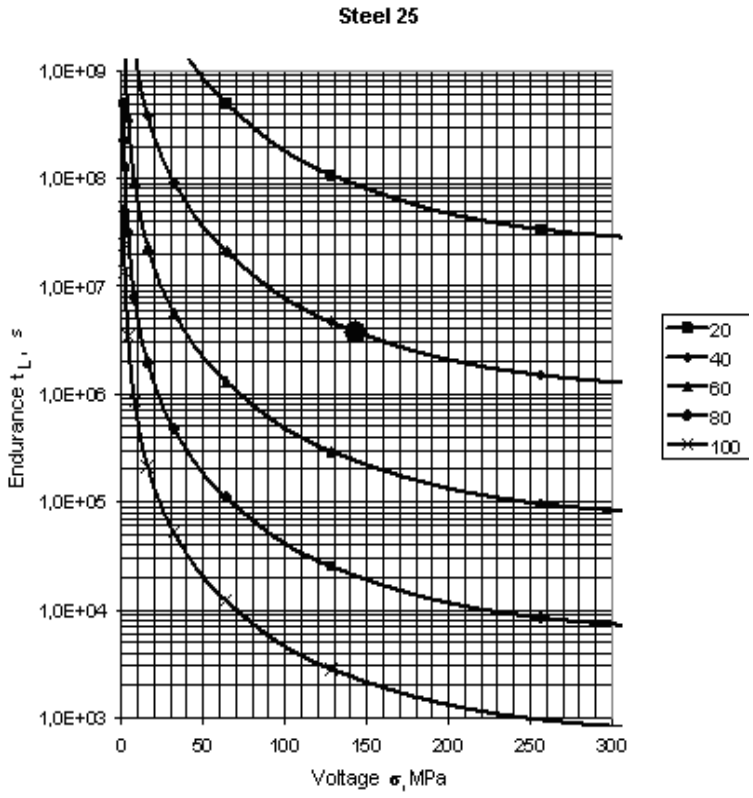

Nomograph for loaded element durability estimation

The suggested approach, in our opinion, allows to forecast different loaded parts durability, taking into account the expected values of maximum tension σ, temperature T and physical and mechanical material properties, as well as to analyze the possible ways of their life improving at the design and operational stage.

For example, as can be seen from the nomograph, spindle durability can be greatly prolonged by its temperature reduction, physical and mechanical properties changing, as well as other parameters, included in the equations (5.a)–(6.a c).

References

1. Pronikov A.S. *Parametricheskaya nadezhnost' mashyn*. [Machine parametric safety]. Moscow: The Bauman University Publishing House 2002, pp. 560.
2. Antsupov A.V., Antsupov A.V. (Jr.), Antsupov V.P. et al. Ocenka dolgovechnosti nagruzhennyh detalej po kineticheskomu kriteriju prochnosti. [Evaluation of durability stressed parts on the kinetic strength criterion]. *Materialy 70-j nauchno-tehnicheskoj konferencii: Sb. dokl.* [Proceedings of the 70th Scientific Conference: Sat Reports]. Nosov Magnitogorsk State Technical University, 2012, vol. 1, pp. 137-141.
3. Antsupov A.V., Antsupov A.V. (Jr.), Antsupov V.P. et al. Metodologija analiticheskoj ocenki nadezhnosti tehnicheskih ob'ektov [Analytical methodology for evaluating the reliability of technical objects]. *Materialy 70-j nauchno-tehnicheskoj konferencii: Sb. dokl.* [Proceedings of the 70th Scientific Conference: Sat Reports]. Nosov Magnitogorsk State Technical University, 2012, vol. 1, pp. 141-144.
4. Antsupov A.V., Antsupov A.V. (Jr.), Antsupov V.P. and others. The methodology of probabilistic assessment of machine elements according to different criteria. *Mehanicheskoe oborudovanie metallurgicheskih zavodov: Mezhregion. sb. nauch. tr.* [Mechanical equipment of metallurgical plants: Interregional Collection of Scientific Papers]. Ed. Korchunov A.G. Magnitogorsk, 2012, pp. 29-37.
5. Antsupov A.V., Antsupov A.V. (Jr.), Slobodyanskii M.G. et al. Reliability prediction and other friction units based on the thermodynamic analysis of the process of friction. *Vestnik Magnitogorskogo gosudarstvennogo tehnicheskogo universiteta im. G.I. Nosova.* [Vestnik of Nosov Magnitogorsk State Technical University]. 2010, no. 3, pp. 54-60.
6. Antsupov A.V., Antsupov V.P., Antsupov A.V. et al. Prediction reliability friction units by the criterion of wear on the stage of their projection-transformation. *Trenie i smazka v mashinah i mehanizmah.* [Friction and lubrication in machinery]. 2010, no. 11, pp. 38-45.
7. Antsupov A.V., Antsupov A.V. (Jr.), Gubin A.S. et al. Triboconjugation reliability predicting. *Materialy 68-j nauchno-tehnicheskoj konferencii: Sb. dokl.* [Proceedings of the 68th Scientific Conference]. Magnitogorsk, 2010, vol. 1, pp. 262-264.
8. Antsupov A.V. The scientific and methodological basis of forecasting reliability triboconjugation parametric design stage. *Sovremennye metody konstruirovanija i tehnologii metallurgicheskogo mashinostroenija: Mezhdunarodnyj sb. nauch. tr.* [Modern construction methods and technologies metallurgical engineering: International Collection of Scientific Papers]. Ed. N.N. Ogarkov. Magnitogorsk: Pabl. Nosov Magnitogorsk State Technical University, 2011, pp. 36-39.
9. Antsupov A.V., Antsupov A.V. (Jr.), Gubin A.S. et al. The methodology of probabilistic forecasting reliability and service life of tribological. *Izvestija Samarskogo nauchnogo centra RAN.* [Proceedings of the Samara Scientific Center of Russian Academy of Sciences]. 2011, vol. 13, no. 4 (3), pp. 947-950.
10. Antsupov A.V., Chukin M.V., Antsupov A.V. (Jr.), Antsupov V.P. The scientific and methodological basis of forecasting reliability triboconjugation at the design stage. *Vestnik Magnitogorskogo gosudarstvennogo tehnicheskogo universiteta im. G.I. Nosova.* [Vestnik of Nosov Magnitogorsk State Technical University]. 2011, no. 4, pp. 56-61.
11. Antsupov A.V., Antsupov A.V. (Jr.), Antsupov V.P. Methodology for predicting the reliability of tribological. *Trenie i smazka v mashinah i mehanizmah*. [Friction and lubrication in machinery], 2012, no. 2. pp. 3-9.
12. Regel V.R., Slutsker A.I., Tomaszewski E.E. *Kineticheskaja priroda prochnosti tverdyh tel.* [The kinetic nature of the strength of solids]. Moscow, 1974, 560 p.
13. Fedorov V.V. *Kinetika povrezhdaemosti i razrushenija tverdyh tel.* [Kinetics of solid damageability and break-down]. Tashkent: Publ. «Fan» UzSSR, 1985, 165 p.

Gun G.S., Rubin G. Sh., Chukin M.V., Gun I.G., Mezin I.U., Korchunov A.G.

METALLURGY QUALIMETRY THEORY DESIGN AND DEVELOPMENT

Abstract. The theory of complex quantitative quality assessment (qualimetry) of metalware products and production technologies, based on the same design principle of metalware properties structurization and systematic approach to product quality and technological process assessment has been developed.

The functionally-aimed analysis as the methodological basis of metalware products quality and technologies research has been suggested.

Keywords: qualimetry, metalware production, effectiveness, reinforced bars for concrete sleepers.

Qualimetry is a scientific theory of the quantitative quality determination, firstly represented by G.G. Azgaldov [1], who stated the main principles of general, special and objective qualimetry, being successfully developed in various fields of science, technology and, as well as in the assessment of social phenomena, system and state conditions.

For 35 years the authors have been developing the theory of complex quality assessment – metallurgy qualimetry [2-24]. During these years a significant number of researches in the field of assessment, prediction and control of metalware product quality and their production processes have been performed (Fig. 1).

A number of problems (see the Table) of the general theory of qualimetry have not been solved till the present, and many research object appendixes are lack of correct operational methods and algorithms of products and technologies quality assessment.

There are the most significant problem-solving procedures carried out by the authors (Fig. 2):

- qualimetry categorical apparatus has been developed on the basis of the following concepts: the function of the evaluation object, the consumer phase of the object, interaction;
- structuring principles of object quality using functional approach have been developed;
- new determination methods of the impact level of separate structural units and quality hierarchy on group and complex assessments have been developed;
- methods of quality assessment convolution in group assessment, taking into account the synergistic system effect have been developed;
- indicators and methods of technological processing complex assessment have been introduced;
- methods of operational analysis of technological processing quality have been developed.

The above mentioned solutions allowed to develop and implement a strategy of complex quality assessment of hardware and its production technologies, based on:

– a single constructive principle of metalware properties structurization;

– a systematic approach to product quality and technological process assessment;

– estimation of direct processing parameters, not only the goods quality.

The functional objective analysis strategy [14, 18] to control metalware production was developed. It is based on:

– the determination of definition «function» on the basis of physical interaction;

– the determination of life cycle, which is called a consumer phase, concerning the product assessment period;

– the allocation of three stages of a consumer phase, such as transport, mounting and operational.

The basis of the functional-specific analysis comprises the following:

– a systematic approach to the integrated quality assessment;

– a process approach to the process effectiveness evaluation;

– process control methods in order to obtain the desired quality of hardware; improve the efficiency of the process.

Qualimetry main issues

Position	Issue
The tree type structure of properties	The lack of structuring principle
Convolution of estimations, taking into account weightiness properties	The lack of an effective method for weightiness determining
Convolution with the help of medium and triangular shape formulas	The lack of formulas for the dominant properties convolution taking into account weightiness
	The system properties interaction isn't taken into account
Quality is the totality of features with a focus on satisfying the definite needs	The period of any object life cycle, where evaluation takes place, is not defined

Thus, it was possible to develop general, specific, and objective qualimetry applied to hardware production (Fig. 2).

The academic staff of Nosov Magnitogorsk State Technical University together with industrial engineers managed to solve a number of current challenges for quality assessment, new technologies development and production management at Russian enterprises such as: OJSC «MMK-Metiz Works», «Avtonormal» Belebeevsk Plant, Beloretsk Metallurgical Plant, and Cherepovets Steel Rolling Mill.

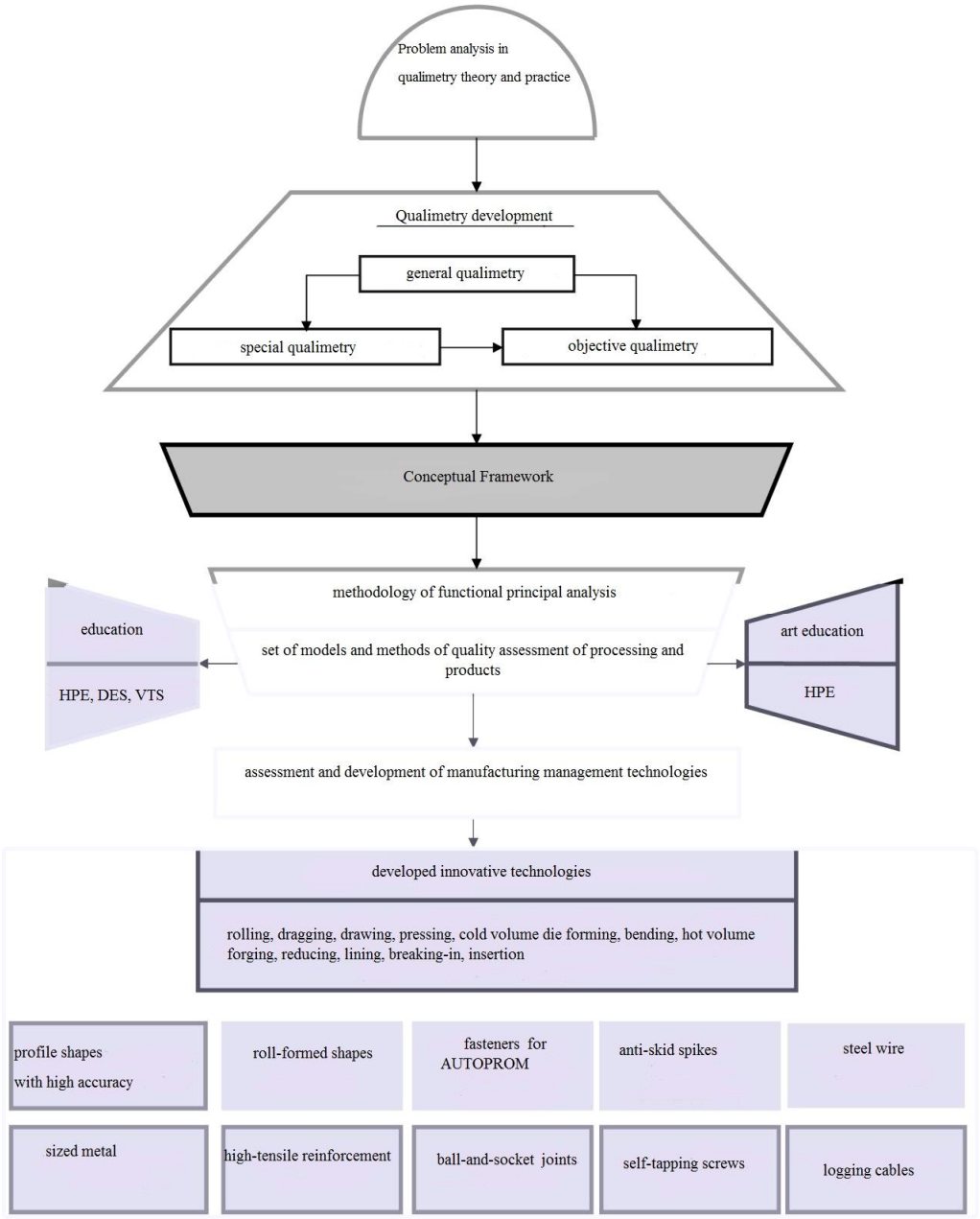

Fig. 1. Diagram of NMSTU researches in hardware production qualimetry

We developed methods of assessment calculation, technology selection, the first of which were tested on steel profiles of high accuracy and calibrated metal at Cherepovets Steel Rolling Mill and OJSC «MMK METIZ».

Serious cycles of researches and implements were carried out on the basis of quality control by the expert team of «BelZAN» and «Belmag» CJSC NPO which allowed to introduce new types of fasteners and ball joints and to improve the efficiency of their manufacturing processes.

Along with modern methods of quality assessment and management, in «MMK METIZ» production, the following high-tech technologies are used:

– a special kind of carbon steel heat treatment, that provides to obtain material ultra fine grained and nanostructures, having high strength and ability to be influenced by straining with large total strains;

– high-performance multiple straining cold plastic processing using cone shaped surface tools, activating available glide planes within each straining cycle, which leads to additional fragmentation of material structure and provides a maximum hardening of treating reinforcement.

– a special kind of thermal straining processing, consisting in the simultaneous effect of plastic deformation in covering die-rolled section on the rebar surface and thermal effect under strong tension, providing a high set of special properties of nanostructured reinforcement: coupling with concrete, relaxation resistance, cyclic strength and corrosion resistance.

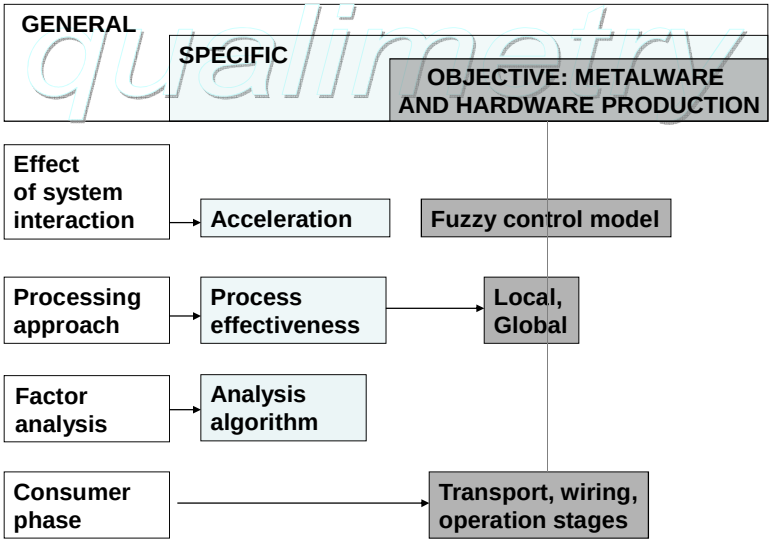

Fig. 2. Structural and logic diagram of research

For the first time, in Russia, commercialization of project innovative scientific and practical results allows to establish knowledge-intensive rebar production for reinforcement concrete sleepers of new generation, on basis of carbon steels thermal straining nanostructuring, that provides to achieve nanostructured state of processing material and improve finished product operating performance.

Due to the success of the university research team it became possible to found a unique Doctoral Council in Quality Management in metallurgy at NMSTU (the sole Council in Russia). A number of specialties in the field of certification and production quality management were opened; the branch of the Academy of Quality Problems of Russian Federation was organized in Magnitogorsk.

References

1. Azgaldov G.G., Raykhman E.P. *O kvalimetrii.* [About the quality control]. M.:Standarty [Moscow : Publishing house «Standards»]. 1972. 172 p.
2. Rubin G.Sh., Gun G.S. *Logicheskie zakony otsenki kachestva produktsii.* [Logical rules of product quality rating]. Magnitogorsk, 1981. 23 p. Deposited by VINITI 19.09.1981, №4105-81 B.
3. Gun G.S. *Upravlenie kachestvom vysokotochnykh profiley*. [Quality management of high-precision profiles]. M.: Metallurgiya [Moscow: Publishing house «Metallurgy»].1984, 152 p.
4. Gun G.S., Chukin M.V. *Optimizatsiya protsessov tekhnologicheskogo i ekspluatatsionnogo deformirovaniya izdeliy s pokrytiyami* [Processes optimisation of technological and exploitation deformation of coated products]. Magnitogirsk : Nosov Magnitogorsk State Technical University, 2006. 323 p.
5. Zakirov D.M., Rubin G.Sh., Mezin I.Yu. et al. *Kvalimetricheskaya otsenka proizvodstva avtomobilnogo krepezha : monografiya.* °[Quality control estimation of automobile hardware production : monography]. Magnitogirsk : Nosov Magnitogorsk State Technical University, 2007, 158 p.
6. Zakirov D.M., Rubin G.Sh., Mezin I.Yu. *Upravlenie kachestvom pri proizvodstve shipov protivoskolzheniya : monografiya.* [Quality control during the production of anti-sliding pins: monography]. Magnitogirsk : Nosov Magnitogorsk State Technical University, 2008, 114 p.
7. Gun I.G., Rubin G.Sh., Salnikov V.V. *Kompleksnaya otsenka effektivnosti protsessov proizvodstva sharovykh paltsev*. [Complex efficiency evaluation of production processes of ball pins]. Magnitogirsk : Nosov Magnitogorsk State Technical University, 2008. 133 p.
8. Rubin G.Sh., Gun I.G., Kireev I.N. et al. *Metodika vybora ratsionalnoy tekhnologicheskoy skhemy proizvodstva profiley kalibrovannogo metalla* [Methodology for the selection of a rational production scheme of calibrated metal profiles. *News of HIGH SCHOOLS. Ferrous Metallurgy*. 1980, no. 11, pp 40-42.
9. Rubin G.Sh., Gun G.S., Pudov E.A. and others. *Vybor effektivnoy tekhnologii polucheniya profiley povyshennoy tochnosti dlya mashinostroyeniya*. [Effective technology choice for high-precision profiles for mechanical engineering]. *News of HIGH SCHOOLS. Mechanical engineering.* 1981, no. 5, pp. 155-157.
10. Rubin G.Sh., Gun G.S., Pudov E.A. and others. *Kompleksnaya otsenka kachestva stal'noy kanatnoy provoloki.* [The Complex estimation of steel rope wire quality]. *Steel.* 1983. no. 1, pp. 56-57.
11. Zakirov D.M., Rubin G.Sh., Salnikov V.V. *Apparat matematicheskoy logiki dlya kompleksnoy otsenki effektivnosti tekhnologicheskikh protsessov*. [Mathematical logic device for complex evaluation of processing efficiency]. *Rolling.* 2006, no. 12, pp. 35-58.
12. Chukin V.V., Rubin G.Sh., Vakhitova F.T. et al. *Problema povysheniya kachestva krepezhnykh izdeliy* [The problem of fastener quality improving]. *Vestnik Magnitogorskogo gosudarstvennogo tehnicheskogo universiteta im. G.I. Nosova.* [Vestnik of Nosov Magnitogorsk State Technical University]. 2007, no. 4. pp. 99-102.
13. Rubin G.Sh., Kamalutdinov I.M. *Funktsional'nyy analiz struktury svoystv geofizicheskogo kabelya* [Functional analysis of the structure of cable geophysical properties]. *Vestnik Magnitogorskogo gosudarstvennogo tehnicheskogo universiteta im. G.I. Nosova.* [Vestnik of Nosov Magnitogorsk State Technical University]. 2010, no. 1(29), pp. 70-71.
14. Rubin G. Sh. Funktsionalno - tselevoy analiz kachestva izdeliy [Functional-target analysis of products quality]. *Vestnik Magnitogorskogo gosudarstvennogo tehnicheskogo universiteta im. G.I. Nosova.* [Vestnik of Nosov Magnitogorsk State Technical University]. 2011, no. 2(34), pp. 29-30.
15. Rubin G.Sh., Storozhev S.B., Gun G.S. et al. *Vybor ratsionalnoy tekhnologii pri proizvodstve vysokotochnykh profiley s primeneniem metodov kolichestvennogo izmereniya kachestva.* [Choice of a rational technology during the manufacturing of high-precision profiles with application of methodology of the quantitative quality measurment]. *Pyatiletke kachestva i effektivnosti – trud i poisk molodykh metallurgov. Vsesoyuznaya nauchno-tekhnicheskaya konferentsiya*. [Labour and search of young metallurgists for the five year plan of quality and efficiency. All-union scientific and technical conference]. Tula, 1978, pp. 92-93.
16. Rubin G.Sh., Chukin V.V., Zakirov D.M. et al. *Vybor effektivnoy tekhnologii proizvodstva metizov avtomobilnogo naznacheniya*. [Choice of efficient production technology of metal products for automotive use]. *Trudy VII kongressa prokatchikov*. [Proceedings of the VII Congress of rollermen]. Moscow, 2007, vol. 1, pp. 395-399.
17. Mezin I.Yu., Rubin G.Sh., Zakirov D.M. et al. *Metodologiya kompleksnoy otsenki protsessov kholodnoy obyemnoy shtampovki.* [Methodology of a complex process evaluation of a cold die forging]. *Sovremennye dostizheniya v teorii i tekhnologii plasticheskoy obrabotki metallov : tretya mezhdunarodnaya nauchno-tekhnicheskaya konferentsiya*. [Modern achievements in theory and technology of plastic metal working : third International scientific and technical conference]. Saint Petersburg : Publishing house of Polytechnical University, 2007, pp. 388-391.
18. Rubin G.Sh. Funktsionalnyi analiz kak metodologicheskaya osnova upravleniya kachestvom metizov. [Functional analysis as a methodological basis of metal products quality management]. *Trudy VIII kongressa prokatchikov.* [Proceedings of VIII rollermen congress]. Magnitogorsk, 2010, vol. 1, pp. 397-399.
19. Rubin G.Sh., Korchunov A.G., Lysenin A.V. *Upravlenie rezultativnostyu mnogooperatsionnykh tekhnologicheskikh protsessov*. [Effectiveness management of multioperative technological processes]. *Upravlenie bolshimi sistemami : materialy VIII Vserossiyskoy shkoly-konferentsii molodykh uchenykh.* [Management of the huge systems :materials of VIII All-Russian conference-school of the young scientists]. Moscow, 2011. pp. 327-331.
20. Rubin G.Sh., Chukin M.V., Gun G.S. et al. *Razvitie kvalimetrii metiznogo proizvodstva*. [Quality control development of the metal ware production]. *Innovatsionnye tekhnologii obrabotki metallov davleniem : sbornik dokladov mezhdunarodnoy nauchno-tekhnicheskoy konferentsii.* [Innovation technologies of the metal forming : reports of the International scientific and engineering conference]. Moscow, 2011, pp. 320-325.
21. Chukin M.V., Gun G.S., Korchunov A.G., Polyakova M.A. *Perspektivy proizvodstva vysokoprochnoy stal'noy armatury iz vysokouglerodistykh marok stali*. [The prospects of production high-strength steel bars of high-carbon steel grades]. *Ferrous metals*. December 2012, pp. 8-15.
22. Chukin M.V., Gun G.S., Korchunov A.G., Polyakova M.A. The prospects of high-strength steel bars production for new generation concrete sleepers on the basis of thermal-straining nanostructuring. *Ferrous Metallurgy: Bulletin of Scientific-Technical Information.* Edition 4 (1348), 2012, pp. 100-105.
23. Rubin G.Sh. *Qualimetry of hardware production*. Magnitogorsk : Nosov Magnitogorsk State Technical University, 2012, 167 p.
24. Korchunov A.G., Chukin M.V., Gun G.S., Polyakova M.A. *Product quality management in hardware production technologies*. Moscow: Publishing House «Ore and Metals», 2012, 164 p.

Lutsenko A.N., Rumyantsev M.I., Tulupov O.N., Moller A.B., Novitskiy R.V.

TECHNOLOGICAL RESERVES: REASONABLE IMPLEMENTATION OF SIMPLE SOLUTIONS TO IMPROVE HOT ROLLING TECHNOLOGY

Abstract. This article presents results of solving the multifactorial problem of finding and using process-reserves in flat and long product rolling.

Keywords: hot rolling technology, mechanical properties, quality, technological reserves.

First. To reduce the number of products with non-conforming mechanical properties we improve the technology: realign rolling schedule to minimize the variation of the properties.

Technology improving in order to reduce the amount of low-quality rolling in terms of mechanical properties should be done on account of searching for rolling modes that enable minimum actual variation of product properties. We suggest using properties hereinafter referred to as conformance aspects to estimate process performance in terms of products quality [1]. If the quality is established with maximum tolerable values (top estimate of conformance),

$$q_{PU} = \frac{\Delta_{USL}}{3s}, \quad (1)$$

$$q_{PL} = \frac{\Delta_{LSL}}{3s}. \quad (2)$$

and, if it is established with minimum tolerable value (low estimate of conformance).

If maximum and minimum tolerable values are established (conformance estimate with regard to average position)

$$q_{Pk} = \min\left(q_{PU}; q_{PL}\right). \quad (3)$$

In (1)-(2) $\Delta_{USL} = USL - \bar{x}$ and $\Delta_{LSL} = \bar{x} - LSL$ are tolerable intervals of quality property variation (Fig. 1), and $3s$ is the share of its actual variability, falling within tolerable interval. Standard deviation $s = \sqrt{1/(n-1)\sum_{i=1}^{n}(x_i - \bar{x})^2}$ and sampling mean $\bar{x} = 1/n\sum_{i=1}^{n} x_i$ are used as the property of actual variability and scattering centre appropriate to it, where x_i is single measurement result of quality property for a certain product unit ($i = 1,\ldots,n$).

Conformance aspect q_{pk} is similar to process performance index P_{pk}, known in SPC [2], as they compare tolerable variation of quality property with regard to position of centre of actual variation (numerator) and actual variation (denominator). Though aggregate data presented in sampling made in the course of production of many lots of products of certain types from melts with different chemical compositions for a long period of time are used to calculate P_{pk}. Average value (as actual variation centre) and standard deviation (as actual variation property) for sampling from one lot of products or several lots of the same products, but produced from the same melt are used to calculate q_{pk}. Due to such similarity of conformance aspects to process indexes, «excellent», «good» and «satisfactory» process performance estimates that correspond to the following values of aspects (1)-(3): more than 1.67; 1.33-1.67 and 1.00-1.33 can be used.

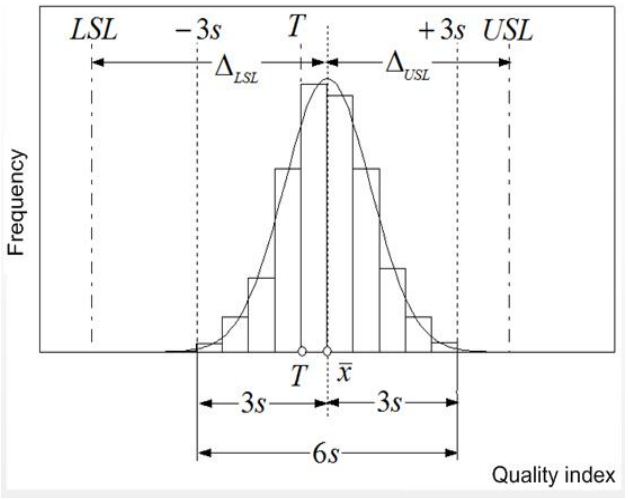

Fig. 1. For calculation of conformance aspect at bilateral restiction of quality property (**T** is tolerance field middle)

As one of the examples of suggested approach application we provide results of estimating quality of hot rolled steel of current production to requirements of GOST 16523 to mechanical properties of cold rolled steel of strength groups K270B and OK300B. Actual variation of aspects analyzed in comparison with tolerable variation is demonstrated with data in Table 1. If we compare sampling means $\bar{x}$ with limits of rated intervals of variation LSL and USL, estimated hot rolled stripes can be deemed good to replace cold rolled steel profile in terms of strength group OK300B, as well as K270B group (in both cases $LSL < \bar{x} < USL$). Though comparison of actual variation of temporary resistance with tolerable variation of group K270B shows that $\bar{x}$ is shifted towards top limit of tolerance, and aspect range ($6s = 6 \cdot 9,9 = 59,4$ MPa) makes 42% of tolerable vari-

ation ($USL - LSL$ =410-270=140 MPa). Thus, at excellent low estimate of conformance (q_{PL} =3.85) top estimate, as well as final differential estimates of temporary resistance are unsatisfactory ($q_{pk} = q_{PU}$ =0.89).

Table 1

Estimate of conformance of mechanical properties of hot rolled stripes of 2 mm in thickness from steel 08ps to requirements of GOST 16523–97 to cold rolled steel [3]

Quality aspects	Tolerable variation		Actual variability		Differential estimates		
	LSL	USL	$\bar{x}$	s	q_{PL}	q_{PU}	q_{pk}
strength group K270B							
$\sigma_в$, MPa	270	410	383.8	9,9	3.85	0.89	0.89
δ , %	25	-	34.38	1.31	2.39	-	-
strength group OK300B							
$\sigma_в$, MPa	300	480	383.8	9.9	2.83	3.25	2.83
δ %	25	-	34.38	1.31	2.39	-	-

If we compare actual variability of properties of hot rolled stripes with requirements for strength group OK300B it can be seen that centre of resistance variation almost coincides with the middle of rated variation range, and scatter does not exceed 33% of rated range value. Therefore, in this case we see excellent differential estimates of mechanical properties, certifying that these lots metal can be used for deliveries instead of cold rolled steel.

Based on the obtained results production method of hot rolled steel to replace cold rolled steel of normal, deep and extremely deep drawing has been developed to include hot rolling of steel bars with set temperatures of end and reeling, and its difference lies in application of steel containing 0.09…0.11% of carbon and 0.25…0.56% of manganese with carbon equivalent $C^* = C + Mn/6 + Si/3$ = = 0.12…0.18, and temperature of rolling end and reeling is set with regard to the following ratios (°C): $t_{кп} = Ar_3 + 300C^* - 40$ and $t_{см} = Ar_1 - (100\ldots110)$ [4]. Whereas temperature values of the beginning (Ar_3) and end (Ar_1) of phase transformation are calculated with regard to actual chemical composition of a certain melt by formulas [5]

$$Ar_3 = 913,7 - 207,13C - 46,6Mn + \\ +110,54Cr + 108,1N; \quad (4)$$

$$Ar_1 = 741,7 - 7,13C - 14,09Mn + \\ +16,26Si + 11,54Cr - 49,69Ni. \quad (5)$$

Dependencies application (4)-(5) enables prompt changing of temperature $t_{кп}$ and $t_{см}$ for real-scale compensation of natural deviations of steel chemical composition, thus ensuring specified properties of hot rolled stripes designed to replace cold rolled steel of general purpose.

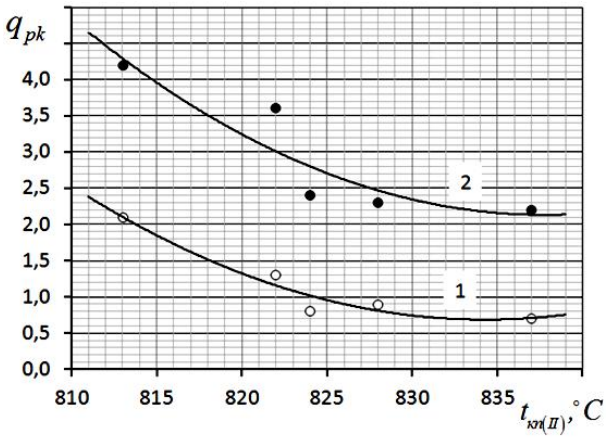

Fig. 2. Influence of rolling end temperature in the field of non-recrystallizing austenite on conformance aspects for yield strength (1) and ultimate strength (2)

The temperature mode improvement of 5,000 heavy-duty sheets production of 16-20 mm in thickness on plate mills for ship-building from steel grade D32 can be used as example of application of conformance aspects to improve the technology. Sheets are produced by controlled rolling (CR) technology followed by accelerated cooling. Where deformation process is divided in two stages – rolling in the field of recrystallizing austenite (stage *I*) and rolling in the field of inhibited recrystallizing (stage *II*). In this relation, the following reference properties of temperature mode can be defined as: $t_{нп(I)}$ and $t_{нп(II)}$ is the temperature of stages *I* and *II* rolling beginning; $t_{кп(I)}$ and $t_{кп(II)}$ is the temperature of stages *I* and *II* rolling end; $t_{нуо}$ and $t_{куо}$ is the temperature of accelerated cooling beginning and end. The application of conformances aspects to ensure required mechanical properties of rolled steel at minimum variation is as follows.

The higher q_{Pk} the better applied technology ensures conformance of actual values of product quality to requirements specified in regulatory documentation (i.e. the closer actual quality values are to the middle of interval of tolerated variation and the smaller their actual variability is). Therefore values of references aspects of technology process that produce maximum values q_{Pk} [1] are preferable. Conformance aspect value dependencies for yield strength and ultimate strength on temperature at the end of rolling in the field of non-recrystallizing austenite are shown as an example in Fig. 2. If conformance aspect is more than 2 for the whole yield strength range $t_{кп(II)}$, q_{Pk} < 1 for ultimate strength at $t_{кп(II)}$ = 825°C and more. It certifies insufficient performance of the process in terms of ultimate strength. To ensure good performance in terms of ultimate strength (q_{Pk} > 1.33), $t_{кп(II)}$ <820°C should be ensured. Similar analysis of performance in terms of other aspects enabled recommendations given in Table 2.

The specific feature of suggested temperature mode is the following. For stage *I* temperature of the rolling beginning should be at least 1050°C, and temperature of the rolling end should be at least 1020°C, that is higher than under the current technology (1020 and 980°C, respectively). At the same time temperature of the rolling end

should be reduced at the second stage (810-820°C instead of 810-850°C under current technology). It has been also suggested to set requirements to temperature of accelerated cooling in the range of 790-800°C (not specified before testing) and reduce the temperature of accelerated cooling end to 610-620°C instead of 600-650°C currently used.

Table 2

Recommendations how to improve temperature mode of heavy-duty steel sheets production for ship building from steel grade D32 at plate mill 5000 [6]

Rating	Temperature, °C					
	$t_{нп(I)}$	$t_{кп(I)}$	$t_{нп(II)}$	$t_{кп(II)}$	$t_{нуо}$	$t_{куо}$
Current	1,020-1,100	980-1,060	790-830	810-850	Not rated	600-650
Recommended	1,050-1,100	1,020-1,060	820-830	810-820	790-800	600-620

Second. Identifying technological reserves in analyzing the effectiveness of various roll pass designs of structural shapes (e.g. channels) through the assessment of valid power parameters.

Matrix approach helps to solve a wide range of technological tasks for various processes of long product rolling [7, 8]. Decision was taken to improve and use it for the mentioned problem.

The demand for rolled steel with improved performance properties is constantly increasing. It is very difficult to get high mechanical properties of channel beams using low-alloy steel, in particular channel beams from 09G2S steel grade according to GOST 19281-89, at continuous high-speed mills.

Differentiated cooling of shaped profiles and modification of heating and metal rolling temperatures can be used as possible resources of improving strength properties. Implementation of the cooling idea is related to equipment and associated technology costs. Thus, modification of temperature mode of rolling is a more flexible and cost-effective tool to achieve required complex of mechanical properties.

Reduced temperature of billet heating at continuous mills results in reduced heat loss of metal in roughing mill stands. That certifies about reasonable reduction of temperature at heating. Whereas increased power consumption for billet deformation at roughing stands is greatly compensated by reduced fuel consumption for billet heating, and total energy saving makes at least 15%. Whereas, metal loss in furnace is reduced, i.e. good metal output is increased.

Reduced temperature of metal in the mill will result in metal yield strength increase and equipment increased loads. To ensure rolling at reduced temperature energy reserve is required to be used at rolling with reduced temperature. Such reserve is established on account of deformation distribution that is mainly caused by pass design scheme at rolling of channel beams. Therefore, search for the ways of purposeful redistribution of metal deformation at rolling of channel beams is a vital task.

The main tasks of estimating performance of channel beam pass design in terms of structural-matrix approach are the following:

– to establish a method to improve roll pass design with reasonable distribution of deformation [9] enabling of rolling at reduced temperature in order to improve operation properties of channel beams;

– to improve roll pass design of channel beam at continuous rolling mill.

Availability of a single centre describing profile of complex shape (Fig. 3) enables applying estimates of deformation efficiency with the use of previous experience of making use of performance indexes and non-uniform deformation of simple profiles [10, 11].

New roll pass design developed within the framework of this study covers finishing milling group. Shapes of the second and third passes opposite to rolling direction have been changed in suggested calibration. For identification purposes suggested calibration is called KZ and is compared with two current roll pass designs: AVD and DAN.

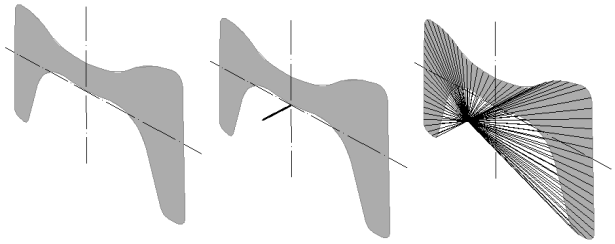

Fig. 3. Suggested way of description with one centre

Developed roll pass design enables reducing rolling force in stands 13, 14 and 15. DAN roll pass design uses more traditional approach and it thickens the wall during rolling. As far as such method stipulates wall thickening for 2-3 mm for every run, it requires a certain “stock” of metal to ensure wall thickness increase, as far as natural thickening of the wall does not give such growth. Thus, upstream rolled width is smaller than that of pass width and the stripe is free at least in one direction to be shifted in the pass. In other words, the pass is unstable holding rolled metal. Rolled metal is centered in the pass due to holding wings. Results of roll pass design of rolling force, drawing index and non-uniform deformation index are given below (Table 3).

The main differences of developed roll pass design versus existing one:

– wall bending radius increased;
– wall draft is increased for 4% in 13 cage;
– wall draft is reduced for 3% in 14 cage;
– changed wall bending radius resulted in reduced angle between wings. Calibration scheme is closer to traditional one, designed to increase wall;
– increased wing height resulted in improved entry of rolled metal to control pass (in cage with critical load No.14).

Having reached optimum deformation distribution we can say, that a «reserve» on rolling effort is established. Thus, we can assume metal temperature reduction, which will result in increased rolling forces, but such forces will not be excessive and hazardous due to application of established «reserve».

Table 3

Comparative analysis of rated values of rolling aspects for various roll pass design options of finishing mill group

Type of pass design	Stand No.					
	9	11	12	13	14	15
	Force, kN					
AVD	1,796.51	1,448.75	1,574.61	1,233.75	881.31	1,020.55
DAN	2,103.27	1,688.30	1,367.27	1,046.25	1,233.30	920.61
KZ	1,796.51	1,448.75	1,574.61	1,030.01	922.31	961.18
	Elongation					
AVD	1.51	1.40	1.45	1.29	1.17	1.02
DAN	1.63	1.51	1.35	1.29	1.20	1.15
KZ	1.51	1.40	1.45	1.23	1.16	1.08
	Non-uniformity index					
AVD	0.221	0.242	0.287	0.195	0.146	0.399
DAN	0.221	0.242	0.287	0.150	0.135	0.171
KZ	0.200	0.218	0.241	0.168	0.143	0.223

Such solution to control channel beam rolling quality was required by lack of possibility to produce rolled channel beams with uniform conformance of requirements for specified strength class of 345 N/mm^2 of finished products (channel beams No. 16 from steel 09G2S) according to GOST 19281-89.

Temperature in the last stand and temperature of the metal rolling beginning can be taken as function of cast sections rolling temperature in heating furnace of the mill.

Observations for rolling of channel beam No. 16 have been provided to estimate influence of rolling temperature in the last cage on strength properties. Temperature at the end of rolling was recorded.

Yield strength was estimated on 57 sample lots with regard to temperature mode in the last cage (Table 4).

If we connect the temperature at the end of trial samples rolling with received values of yield strength in a linear equation, we can use it to calculate the required temperature at the end of rolling to get strength class 345. Equation of connection is as follows:

$$\sigma_T = -1{,}1078t + 1424{,}6.$$

To ensure strength class 345 (yield no less than 345 N/mm^2) the temperature at the end of rolling not more than 970°C is required, thus enabling production of respective strength class and higher operation properties.

Table 4

Experimental data on influence of temperature at the end of yield strength rollingin finished rolled steel

Temperature after finishing stand, °C	945	950	955	960	965	970	975	980	985	990	995	1,000	1,010
Yield strength of trial samples, N/mm^2	375	376	364	363	359	351	341	339	334	325	323	311	311

Third. Identifying technological reserves to improve roughing process: the influence of square billet's rhomboidity on power parameters and wear in roughing stands.

Billet rhomboidity is a serious problem that influences stability of the rolling process and our ability to ensure the required geometry and quality of the product.

To study specific features of rerolling of continuously cast 150x100 mm billet with rhomboidity up to 30 mm, two boundary conditions of billet feed to the first stand have been considered: locations of big and small diagonals of billet and diamond pass coincides (a), i.e. small diagonal of billet is in vertical plane, and big one is in horizontal and do not coincide (b) (Fig. 4).

Drafts of continuously cast bloom of 150 mm with rhomboidity aspect (with increment 0, 1, 2, 3, 4, 5, 6, 7, 8, 9, 10, 15, 20, 25, 30) for the above ways of feeding to the first cage, as well as drafts of the first cage of three passes ("old", modified and with hold-down), applicable/applied at mill 350 of «Severstal» OJSC for rerolling of 150 mm bloom in 100 mm bloom, have been used to calculate deformation uniformity coefficient (DUC), breakdown pass performance coefficient (Krp) and rolling forces. Results of rolling DUC calculation are given in Table 5. Calculations of the rest aspects have been entered to similar tables.

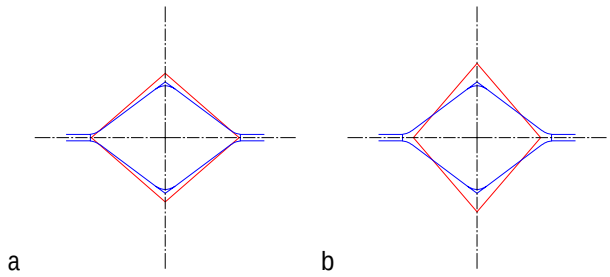

Fig. 4. Locations of big and small diagonals of billet and diamond pass

Calculation of forces was given for St 3 at heating temperature 1200°C.

Based on comparison of two ways of billet feeding into stands and three options of roll pass design has been performed and process options have been estimated with regard to feeding conditions, rolling forces, contact areas between metal and rolls, surface defects and descaling quality. Dependence diagram of force/rhomboidity aspect of the billet for the first way of stripe feeding to cage (alignment of planes) is progressive, whereas it is decreasing for the second way of stripe feeding to cage (misalignment of planes).

Thus, targeted application of new, simple, and effective models and methods enables to find and use various technological reserves in rolling processes.

Table 5

DUC calculation data

Pass design	DUC														
	Rhomboidity, mm														
	0	1	2	3	4	5	6	7	8	9	10	15	20	25	30
Alignment of planes of big and small diagonals of billet and diamond pass															
With hold-down	0.123	0.121	0.120	0.118	0.116	0.114	0.113	0.112	0.110	0.109	0.107	0.099	0.091	0.083	0.075
Old	0.115	0.114	0.113	0.111	0.109	0.107	0.106	0.104	0.103	0.102	0.100	0.092	0.084	0.076	0.069
Modified	0.141	0.139	0.138	0.136	0.134	0.132	0.131	0.129	0.127	0.126	0.124	0.116	0.107	0.099	0.091
Misalignment of planes of big and small diagonals of billet and diamond pass															
With hold-down	0.123	0.124	0.125	0.127	0.129	0.131	0.132	0.134	0.135	0.136	0.138	0.146	0.154	0.162	0.169
Old	0.115	0.117	0.118	0.120	0.122	0.124	0.125	0.126	0.128	0.129	0.131	0.139	0.147	0.155	0.163
Modified	0.141	0.143	0.144	0.146	0.148	0.149	0.151	0.152	0.154	0.156	0.157	0.166	0.174	0.182	0.191

Conclusion

Targeted application of new, simple, and effective models and methods enables to find and use various technological reserves in rolling processes.

References

1. Rumyantsev M.I., Tsepkin A.S., Oplachko T.V. Unifitsirovannyy podkhod k raschetu differentsial'nykh pokazateley pri kvalimetricheskom otsenivanii kachestva prokata. [Unified approach to the calculation of differential indexes in qualimetry evaluating of the rolled metal quality]. *Vestnik Magnitogorskogo gosudarstvennogo tehnicheskogo universiteta im. G.I. Nosova*. [Vestnik of Nosov Magnitogorsk State Technical Univeersity]. 2007, no. 3, pp. 61-64.
2. *Statisticheskoye upravleniye protsessami. SPC*. Perevod s angl. [Statistical Process Control. SPC. Translated from English]. N. Novgorod: SMC Ltd. «Priority», 2004, 181 p.
3. Rumyantsev M.I., Shubin I.G., Zavalishchin A.N. and other. Razrabotka tekhnologii proizvodstva goryachekatanogo tonkolistovogo prokata dlya zameshcheniya kholodnokatanogo analogichnogo naznacheniya. [Technology development of hot-rolled sheets production to replace cold-rolled of the same purpose]. *Proizvodstvo prokata.* [Rolled production]. 2009, no. 2, pp. 22-28.
4. Kotsar' S.L., Belyanskiy A.D., Mukhin YU.A. *Tekhnologiya listoprokatnogo proizvod-stva*. [Technology of plate rolling production]. Moscow: Metallurgy, 1997, 272 p.
5. Rumyantsev M.I., Shubin I.G., Zavalishchin A.N., Tsepkin A.S. and other. *Sposob proizvodstva goryachekatanoy tonkolistovoy stali.* [A method of producing hot-rolled steel sheets]. Pat. RF, no. 2365639, 2009.
6. Rumyantsev M.I., Denisov S.V., Stekanov P.A., Kuz'min A.A. Analiz parametrov i rezul'tativnosti prokatki v usloviyakh OAO «MMK» listov iz stali marki D32 dlya sudostroyeniya. [Analysis of rolling parameters and results of steel sheets of D32for shipbuilding at OJSC «MMK»]. *Sovershenstvovaniye tekhno-logii v OAO «MMK»: sb. nauch. tr. Vyp. 16.* [Technologies Improvement at OJSC «MMK»: Scientific. papers col., Ed.16]. Magnitogorsk, «Printing», 2011, pp. 111-120.
7. Nalivayko A.V., Ruchinskaya N.A. Povysheniye kachestva i sovershenstvovaniye tekhnologii prokatki armatury v usloviyakh metallurgicheskogo mini-zavoda. [Upgrading and technology improvement of reinforcement rolling under a metallurgic mini-works]. *Chernaya metallurgiya.* [Iron and steel]. 2012, no. 1347, pp. 59-62.
8. Levandovskiy S.A., Nazarov D.V., Limarev A.S., Moller A.B., Tulupov O.N. Razra-botka i primeneniye baz dannykh tekhnologicheskikh parametrov s tsel'yu osvoyeniya i sover-shenstvovaniya sovremennykh sortoprokatnykh stanov. [The development and application of data bases of process parameters with the purpose of modern section mills commission and updating]. *Vestnik Magnitogorskogo gosudarstvennogo tehnicheskogo universiteta im. G.I. Nosova*. [Vestnik of Nosov Magnitogorsk State Technical Univeersity]. 2005, no. 4, pp. 36-40.
9. Kinzin D.I., Rychkov S.S. Ispol'zovaniye programmnogo kompleksa deform-3d pri modelirovanii protsessov sortovoy prokatki. [Utilization of deform-3d software in bar rolling processes modeling]. *Vestnik Magnitogorskogo gosudarstvennogo tehnicheskogo universiteta im. G.I. Nosova*. [Vestnik of Nosov Magnitogorsk State Technical Univeersity]. 2011, no. 2, pp. 45-48.
10. Tulupov O.N. *Strukturno-matrichnyye modeli dlya povysheniya effektivnosti protsessov sortov prokatki: Monografiya.* [Structure-matrix models for efficiency improving of rolling grades: Monograph]. Magnitogorsk: Nosov Magnitogorsk State Technical University, 2002, 224 p.
11. Lutsenko A.N., Monid V.A., Tulupov O.N., Limarev A.S., Moller A.B., Trayno A.I., Nazarov D.V. Sovershenstvovaniye tekhnologii prokatki profiley prostoy formy pri ponizhennykh temperaturakh nagreva zagotovki. [Technology upgrading of simple form profiles rolling at low temperatures of billet heating]. *Trudy sed'mogo kongressa prokatchikov (g. Moskva, 15–18 oktyabrya 2007 g.).* [Proceedings of the Seventh Congress of rollermen (Moscow, 15-18 October 2007)]. Moscow, 2007, vol. 1, pp. 208-212.

Drobny O.F., Cherchintsev V.D.

DEVELOPMENT AND IMPLEMENTATION OF MEASURES TO IMPROVE ENVIRONMENTAL SITUATION WITHIN MAGNITOGORSK INDUSTRIAL HUB

Abstract. The article presents the results of implementation of long-term environmental program at OJSC «Magnitogorsk Iron and Steel Works», which includes measures aimed at reducing harmful environment impact of metallurgical production thus improving the production efficiency and ecological characteristics.

Keywords: environmental, environmental protection, pollutants, industrial wastes, ecological characteristics.

The program of technological, technical, organizational and socio-economic activities as the basis of environmental policy at OJSC «MMK» (Magnitogorsk Iron and Steel Works) has been developed and now is being successfully implemented complying with the Russian Federation state policy in the field of environment protection.

The OJSC «MMK» strategy, aimed at negative environmental impact minimizing, consists in using creative technological processes with environmental protection installations based on the best available technologies and removing obsolete facilities.

The implementation of the technical revamping program has radically changed not only the manufacturing structure at OJSC «MMK» but considerably reduced the environment impact. In 2012 the overall discharge of pollutants into the atmosphere was reduced by 3.7 and the emissivity by 3.5 times as compared with 1989.

Today the environmental complex of OJSC «MMK» includes 445 gas purification units of different capacity, 43 local circulating water systems and 32 water purification installations, as well as 6 complexes for metallurgical slag processing. Over the last 10 years practically all environmental facilities were reconstructed or repaired.

Over the last 5 years capital expenditures for the reconstruction of existing and the construction of new environmental facilities accounted for $250 million. The company annually spends more than $500 million to maintain environmental facilities.

The long-term environmental program up to 2015 has been adopted and is being implemented at OJSC «MMK». The program includes measures aimed at reducing harmful environment impact of metallurgic production, improving production efficiency and ecological characteristics. This program provides to spend more than 4 billion dollars for the construction of new and the reconstruction of existing environmental facilities during the period of 2013-2015.

The problems of planning environmental protection activities are becoming principal taking into account that the implementation of environmental protection program requires substantial resources. The program includes a number of factors and faces great difficulties typical for work organization at any operating enterprise. It is necessary to have a methodology which defines the priorities, considering all factors and characteristics of the enterprise to improve environmental protection efficiency.

Since the atmospheric air pollution control is the principle environmental protection activity at OJSC «MMK», the company has developed and used «Methods of specifying prevalent pollutants in the air basin and the development of discharge technique of the dust collection system at metallurgical enterprises with complete production cycle» [1]. For the effective environment planning and management, the air pollution impact of any enterprise with complete production cycle can be defined by comparing the indices of environment threat of the production «J_{etpj}», which are calculated according to the following formula**:**

$$J_{etpj} = \frac{K_{etpj}}{\sum_{j=1}^{n} K_{etpj}}, \quad (1)$$

where K is the indicator of the environmental threat of the j[th] production.

The environment threat index of any production impact can be defined by the following formula:

$$K_{etpj} = \sum_{i=1}^{m} \left(\frac{C_i^{\max}}{ПДК_{мpi}} \right)^{\alpha_i}, \quad (2)$$

where $C_i^{\max}$ is maximum surface concentration (averaging 20 minute interval) of the pollutant «i», being discharged by the production «j» in a set point (located in a residential area in a close vicinity to the production «j»), mg/m^3; TLV mpi is a maximum threshold limit value of the component «i», mg/m^3; αi is a coefficient, depending on the class of danger of the component «i».

To determine the value «C_i» in the formula (2), we'll use OND-86 recommendations [2].

Surface concentration of the pollutant «i» in a set point at a given wind speed and direction, discharged by all production sources is defined by the following formula:

$$C = \sum_{n=1}^{N} C_n, \quad (3)$$

here C_n is the surface concentration of the pollutant discharged from any pollutant emitter «*n*» (a compound of the production «j») in a set point at designed wind speed and direction, mg/m^3; N is the number of pollutant emitters belonging to the production «j», number of items.

All pollutant emitters at OJSC «MMK» are point, excluded aeration lanterns and outdoor raw material storages. Aeration lanterns and outdoor storages at OJSC «MMK» are linear sources.

For the calculation of surface concentrations of linear sources, they are presented as a group of identical equidistant point sources.

Surface concentration of the pollutant from the emitter «n» in a set point at the designed wind speed and direction is calculated by the following formula:

$$C_n = s_1 \cdot s_2 \cdot r \cdot C_м, \quad (4)$$

where s_1 is a nondimensional coefficient, evaluated according to the distance along the pollution plume axis, between the pollutant emitter and a set point; s_2 is a nondimensional coefficient evaluated according to the vertical distance between a set point and the pollution plume axis; r is a nondimensional coefficient evaluated according to the wind speed; C_m is the maximum pollution surface concentration from the pollutant emitter (a compound of the production «j»), mg/m^3.

The calculation of the maximum surface concentration of the pollutant from a point source is calculated by conventional methods.

The outskirt of the village «Bruskovy», located in a residential area, is accepted as the nominal reference point. Calculation results of the primary production impact on the integral value of the environment threat index are given in the Table.

Whenever choosing dust collection systems at metallurgical enterprises exposed to full or partial revamping, the difficulties arise from the lack of free space sufficient for the installation of large-size dust collection equipment of high-efficiency, devices and facilities for collected dust recycling.

Calculation of the basik production of JSC «MMK» in the integral index of environmental hazards

Production Name (Designation)	Maximum nominal concentration, mg/m³						Production Impact Level in the Test Point	
	dust	nitrogen dioxide	carbon oxide	sulfur dioxide	nitrogen oxide	phenol	K эonj	J эonj
Sinter Production	0,31	0,02	1,467	0,9	0,004		2,86	35,6
Coke industry	0,068	0,025	0,838	0,02	0	0,016	2,34	29,2
Blast-Furnace Process	0,464	0,024	0,99	0,068	0,009		1,44	17,9
Electric Steelmaking Plant	0,062	0,019	0,071	0,004	0,005		0,26	–
Oxygen-Converter Plant	0,113	0,005	0,025	0,003	0,002		0,27	–
Total: Steelmaking Industry							0,53	6,6
Thermal Power Station	0,061	0,029	0,003	0,004	0,01		0,30	–
Central Power Station	0	0,043	0,002	0	0,016		0,26	–
Steam-Air Power Station	0	0,015	0,01	0,014	0,006		0,12	–
Total: Power Generation							0,68	8,5
Rolling. (Sheet Rolling Mill-3, Sheet Rolling Mill-4, Sheet Rolling Mill-5)	0	0,013	0,09	0,006	0,005		0,12	–
Rolling. (Finishing Plant, Sheet Rolling Mill-8)	0,001	0,003	0,003	0,002	0,001		0,02	–
Sheet Rolling Mill-10	0,001	0,007	0	0	0,002		0,04	–
Total: Rolling							0,18	2,2
Maximum threshold limit value (TLV)	0,5	0,2	5	0,5	0,4	0,01		

If we take economic efficiency of a dust collection system as an integral test provided that it achieves maximum permissible emission values MPE as its minimum limit for the given pollutant emitter, it's reasonable to use the following estimating characteristics: efficiency of selected systems, the technical efficiency of dust collection, capital and maintenance cost, system capability by the volume of treated gases, specific energy source consumption per unit volume of treated gases, revenue from sales of the collected dust or the cost of its ground disposal and pay decrease for pollutant discharge into the atmosphere.

In this case, the economic efficiency of the dust collection system $Э_ф$ can be calculated by the following formula [3]:

$$Э_ф = \frac{\sum_{i=1}^{n}\left[F_r\left(\beta_{in}-\beta_{ik}\right)\right]-\Phi_r\left(q_k\right)-\Delta P_r\alpha_r}{K}, \quad (5)$$

where F_r $(\beta_{in}-\beta_{ik})$ is revenue from sales of utilized materials and pay decrease for pollutant discharge per year;Φ_r (q_k) is full costs for the system maintenance for a year; ΔP_r is profit reduction in production work per year; α_r is a coefficient of diverse cost averaging; K is capital expenditures (cost of essential and auxiliary dust collection equipment, assembling and start-up costs of a dust collection system); β_{in}-β_{ik} are concentrations of the element «i» per unit of original and treated gas; q_k is consumption of every resource.

At the final stage of evaluation of dust collection alternatives it is reasonable to estimate the efficiency «$Э_к$» of any of them by the following formula:

$$Э_к = \frac{\sum_{i=1}^{n} C_i\gamma_i\left(\beta_{in}-\beta_{ik}\right)}{\sum_{k=1}^{p} Ц_k q_k + \frac{\sum_{j=1}^{m} Ц_j\cdot\Delta r_j}{V}}, \quad (6)$$

where C_i is specific environmental damage owing to the pollutant «i» discharge into atmosphere; y_i is relative atmospheric pollution threat with the substance «i»; $Ц_k$ is every resource price; Δrj, $Ц_j$ are additional expenditures per unit of resources used in the production process and their cost; V is a volume of gas emission per unit of output.

To make a final choice of the dust collection system it is necessary to take into account the possibility of further dust reduction of treated gases due to improvement of design and technological parameters of the system equipment, maintaining its steady operation in changing operational mode and parameters of the main production process as well as the possibilities and sufficiency of the system application for recycling and recovery of treated gases. Special attention should be paid to recovery and recycling of collected dust at steel mills of complete production cycle.

The developed technology makes it possible to evaluate both ecological-and-economic effectiveness of equipment and dust collecting units of gas cleaning systems to make a proper choice and to estimate ecological-and-economic effectiveness of environmental measures including recovery and disposal of collected products.

The environmental measures taken over the last 5 years resulted in gross emission reduction by 10800 tons (by 5%) and totaled 220200 tons in 2012 and specific wastes decreased by 11% (to 18.57 kg per ton of finished product).

In Fig. 1 one can see that since 2009 there is a steady trend to reduction of polluting substances emission into the environment at OJSC «MMK».

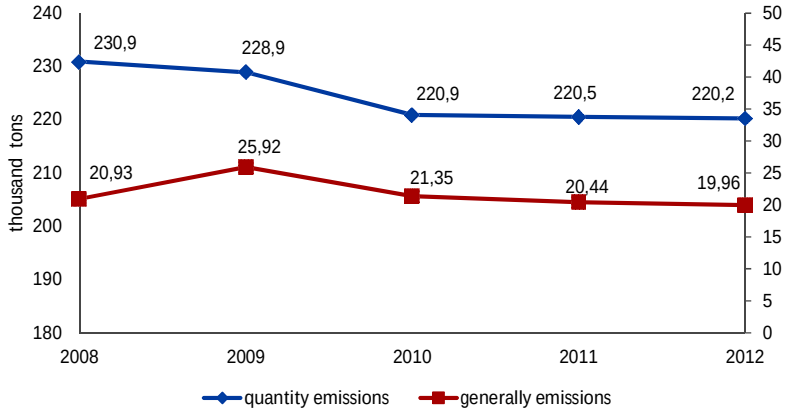

Fig. 1. Emission of polluting substances into the atmosphere from 2008 to 2012

The strategy of water resources protection is aimed at the maximum application of recycled water for process water supply. The share of recycled water supply at OJSC «MMK» has been maintained at the level of 96% for 5 years already.

Water-protective measures within the framework of the Ecological Program made it possible to reduce waste water discharge into water bodies by 42050 tons (27%) to 113800 tons, specific discharges of polluting substances per 1 ton of finished product decreased by 28.6% compared with 2011 and totaled to 10.32 kg/ton (Fig. 2).

OJSC «MMK» pays great attention to industrial waste recycling and control. Some 2.9 million tons of wastes were used as raw material in 2012, which is twice as much as in 2008. The volume of recycled current and dump metallurgical slag doubled over the last 5 years and reached 11.5 million tons a year.

Special attention is paid at OJSC «MMK» to the complex recycling of industrial wastes so that they might be used in the manufacturing processes as well as to the quarry reclamation of the Magnitnaya Mountain which is proved by the data given in Fig. 3.

Actual expenditures on the Ecological Program of the OJSC «MMK» in 2012 reached $38 million (including $34 million invested in capital development).

OJSC «MMK» plans to hold 44 events in 2013 within the framework of the Ecological Program.

Implementation of this program will provide sustainable development of OJSC «MMK» and create favourable economic environment for the South Ural in general.

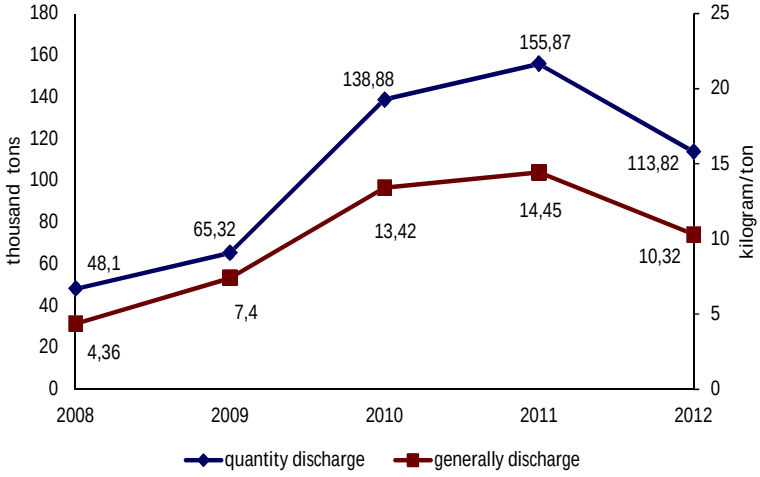

Fig. 2. Change of polluting substances discharge into water bodies

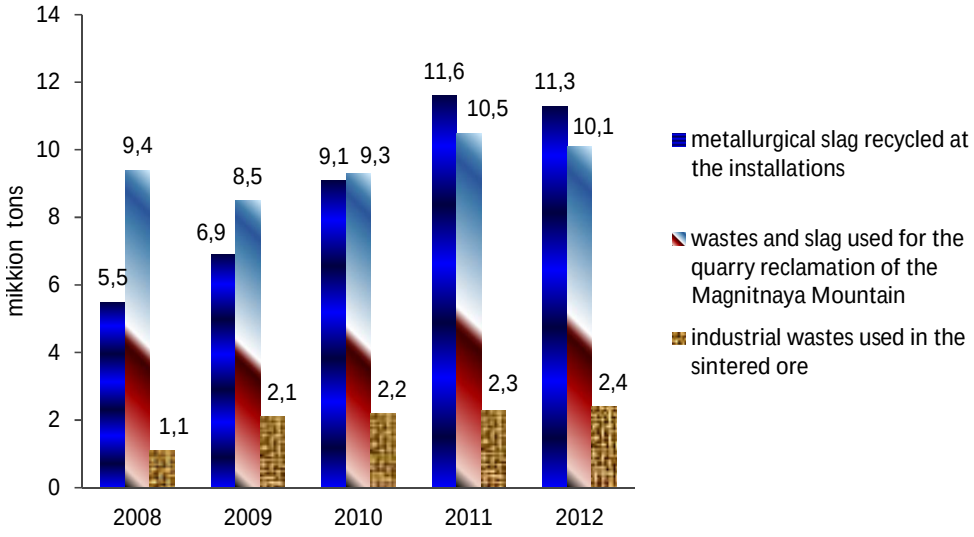

Fig. 3. Change of waste utilization

References

1. Drobny O.F., Cherchintsev V.D. The specification of prevalent pollutants in the air basin at metallurgical enterprises with complete production cycle.*Teoriya i tekhnologiya metallurgicheskogo proizvodstva.* [Theory and technology of metallurgical production. Collected scientific papers]. Magnitogorsk, 2003, vol. 3, pp. 216-223.
2. *Estimation method of hazardous substances content in the atmosphere resulting from industrial wastes emission.* All-Union regulatory document OND-86. Goskongidromet. Leningrad: Gidrometeoizdat, 1987, 92 p.
3. Glukhov V.V., Nekrasova T.P. *Economical fundamentals of ecology.* S-Petersburg: Special literature, 1997, 304 p.

Kolga M., De Smedt V., Van Nerom L.

PLANNING PRINCIPLES IN METALLURGY

Abstract. Metallurgy is known as one of the most challenging areas for planning. Planning systems for metallurgical production are meant to solve a wide range of problems: from day-to-day scheduling at the workshop level to the development of the company strategy for years ahead.

Each level of planning presents specific tasks, degree of abstraction and planning horizon. The modules of the planning system are responsible to find the optimal solution at each level.

A properly selected, installed and operated planning system helps to improve control over production processes and increase the profitability of the company.

Keywords: planning system, production plan, planning horizon, scheduling, material flow, bottlenecks management, strategy plan.

Introduction

In terms of industry, planning serves as the bridge between product design, production capacity and the actual production. Traditionally, planning tasks were performed manually, based on the experience of the specialists. Planning systems were designed to integrate, standardize, streamline and improve company planning, reporting and operational control capabilities.

Although the purposes and principles of the planning are generally the same, these systems vary from industry to industry and from company to company. The more complex the manufacturing, the more sophisticated planning system is required.

Metallurgy is known as one of the most challenging areas for planning. Such complexity of metallurgical production can largely be attributed to the factors as [2]:

- wide range of products (thousands of items)
- variety of routings (alternative routes between lines)
- multiple operating modes of the lines
- complex rules and constraints at the lines
- make-to-stock production and allocation of materials from the stock yard
- the capacity required is difficult to predict (since it depends on the particular mix of products)
- work-in-progress inventory is often large
- throughput times are generally long
- complex and strict quality requirements
- extremely high «cost» of the downtimes
- realtime (or «near-realtime») data exchange with the production level
- etc.

The aim of this article is to give an overview of the basic tasks which planning systems face at different levels of metallurgical production, and to present successful approaches to the problem. The latter is best done by way of example.

PSI Metals GmbH is one of the leading international companies providing IT solutions for the metals industry [1]. Planning system of PSI Metals presents a group of products which are meant to solve planning tasks at different levels.

Levels of Planning

Each level of planning varies in purpose, time span, and degree of abstraction.

At the basic workshop level, the aim of planning is optimal schedules of the production lines. The level of detail is very high; the planning horizon lies in the short-term. Given a big variety of specific rules and constraints, which are never completely independent, the conflicts are inevitable and a compromise is not easy to find.

Optimization models implemented in PSI Metals scheduling tools are based on tried-and-tested algorithms, which use the customer's priorities to range the goals and ensure the most preferable of feasible results.

Depending on the line type, the set of rules can vary greatly. For example, when talking on the continuous casting machine, one has to take into account fixed ladle batch sizes, acceptable steel grade transitions and steel grade nesting, variable geometry of the output products (slabs or billets), tundish wear and molds changes with the related stops, as well as many other factors. In case of the hot strip mill, the focus shifts to the problems like furnace-charge, width / thickness profile, run up, specific rolling rules («coffin rule»), stops for equipment re-adjustments and rolls changes, stockpiling, etc.

Thus, each production case requires individual approach; and this means one more challenge for planning systems – they must be «tailorable». The planning solution of PSI Metals meets this challenge due to the modular structure: a set of line-specific modules delivers the optimal results to the upper level of planning, where they are integrated and can be analyzed in the context.

The context of the higher level implies a full scope of the production lines available. The objective of the planning system is well-balanced load of the equipment with

respect to delivery dates of the orders. Considering alternative routes and the bottlenecks, the system must establish start and finish dates for each operation required to complete the order on time. PSI Metals planning system also takes care of successive lines synchronization to solve tasks such as hot charging, which is critical for the hot rolling. To develop a reliable schedule, the planning algorithm operates with information on routing, required and available capacity, competing jobs, and manufacturing lead times at each line involved.

The problem of materials allocation takes place at the same level. PSI Metals planning solution offers several task-specific products for assignment of orders to material. Actually this procedure deserves a separate article, because of its complexity and obvious economic effect it provides due to minimization of scrap, optimization of cutting plan, maximization of orders fulfillment, etc.

The next level deals with capacity management and material flow. The planning horizon is usually a few months; the level of detail is reduced to product groups or families. The objective is to define the target product mix per period and make the best use of manufacturing resources, while keeping inventory levels down.

The next level of planning deals with capacity management and material flow. The objective is to meet delivery dates, to make the best use of manufacturing resources, while keeping inventory levels down. It involves establishing start and finish dates for each operation required to complete the order on time.

In metallurgical production, it is very difficult to balance the available capacities of the various lines with the demand for their capacity. As a result, some lines are overloaded and some are underloaded. The overloaded lines are called bottlenecks. The bottlenecks are critical to the throughput of the whole system and usually have problems with high work-in-progress inventory level. Bottlenecks management is one of the most important advantages provided by PSI Metals planning system at this level. To develop a reliable schedule, the planning algorithm operates with information on routing, required and available capacity, competing jobs, and manufacturing lead times at each line involved.

The next in the planning hierarchy is sales and demand planning level. The planning horizon for this level is at most a year, and revised every month or quarter. The next level in the planning hierarchy deals with the sales and demand planning. The level of detail is not high; the planning horizon can be up to several months. The aim of the planning system is a plan to satisfy market demand within the resources available to the company, determine from the demand forecast, that is the best way to accept orders in order to maximize the throughput of the factory and EBIT profit of the company, reconcile the commercial demand and technical restriction of the plant. The plan is devised in terms of product groups or families.

The basic approach of PSI Metals planning solution is to find a balance between priority and capacity. It is the privilege of the customer to define the requirements and rank them in order of importance.

The result of this level must, at the same time, agree with implementing the strategic business plan. The strategic business plan is a statement of the major goals and long-term objectives of the company and this is the top level of manufacturing planning.

Strategy planning takes into account the market-, products and pricing strategies of the company, alternatives for the supply chains, and the corresponding procurement strategies.

The plan of this level is the guideline for all further decisions in planning and execution processes, and thus must be considered very carefully.

PSI Metals Planning provides the ability to model «what-if» scenarios to see the impact of various factors before making a decision. This helps a company to more thoroughly assess potential risks, more quickly identify opportunities, and more promptly react on the market changes.

Figure summarizes the preceding description of the planning hierarchy, and establishes a correspondence between the planning levels and existing solutions of PSI Metals.

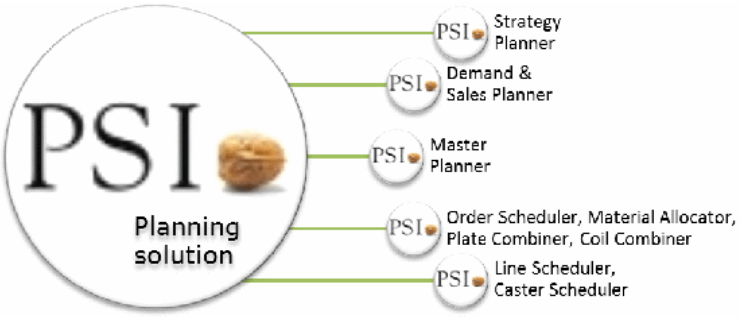

Planning Level
Strategy Planning
Capacity & Master Planning
Material Planning & Order Scheduling
Demand & Sales Planning
Line Scheduling

Planning Levels and PSI Metals Planning Products

Advantages of Planning Systems

Depending on the scope of the planning system, the benefits can be obtained in such operational areas as manufacturing, sales and marketing, management and others [3].

In manufacturing: the planning systems provide faster identification of production process problems and bottlenecks; facilitate more accurate raw materials planning and control; improve inventory control. Besides, more thorough shop floor planning reduces waste and re-work.

In sales and marketing demand planning, the main benefits are: improved due date performance, reduced increased factory throughput and better management of supply and more flexible delivery times; improved accuracy in sales forecasts; increased accuracy in purchase orders, etc.

In management: the planning systems help to improve the quality of decisions; faster identify and assess risks; provide more accurate and timely information. Increased structure and discipline in planning, reporting and forecasting activities improve control over production processes in general.

Conclusion

The automation of planning activities at metallurgical enterprises presents many challenges, since it involves a multitude of conflicting criteria and competing objectives and also requires a great deal of expertise and knowledge, both of which are not easy to model and codify.

A properly selected, installed and operated planning system helps to speed up production, reduce costs and increase the profitability of the company.

References

1. www.psimetals.de.
2. Tony Arnold J.R., Chapman Stephen N., Clive Lloyd M. Introduction to materials management. 7th ed. p. cm.
3. Fawls Tom. A Business Primer for Understanding Integrated Planning, Reporting and Control Systems. www.SpinningDisc.com.

Polikarpova M.G.

FUZZY-LOGIC-BASED RISK MANAGEMENT OF M&A DEALS OUTCOME: A CASY-STUDY A LARGE RUSSIAN METALLURGIC HOLDING

Abstract. The paper researches the application of several fuzzy logic concepts to evaluating risk rating of M&A projects undertaken by a large Russian Metallurgic Holding: maxmin compression, fuzzy relationship of preferences, additive compression. The way of expert answer treatment is presented for the possibility of further fuzzy logic methods application. 20 M&A projects are used as the empirical basis for the research. The methods applied show consistency in final estimates proving the ability of their use in MA deals' risk outcomes evaluation. The proposed method can be used to evaluate risk consequences for M&A deals.

Keywords: fuzzy logic, fuzzy set, membership functions, rule matrix, risk, M&A, metallurgy

Currently M&A is one of the most solicited ways of developing an industrial enterprise. Though M&A deals embed material risks they are efficient to achieve the objectives that are unattainable given other long-term development strategies.

Being highly risky M&A deals often result in losses for the acquirer. As McKinsey found in 2008 70% of M&A resulted in business value destruction. Same time Russian M&A differ in several ways from abroad ones:

- no common regulator and no unique pricing procedure exist;
- market is rather closed, no unified statistics available;
- there legal blank points enabling raider activity etc.;
- legal system drawback in corporate conflicts resolution [2].

Generally the corporate culture to dealing with M&A deal consequences is not well worked out. As the M&A deal associated risks need to be dealt with, the paper has its objective to present the way of evaluating M&A risks based on fuzzy logic concept.

M&A deal realization passes three stages of its livecycle:

1) project integration (negotiation process);

2) company reorganization (sales-and purchase agreement execution);

3) company integration (incl. corporate cultures) [4].

The majority of M&A deals are subject to UK common law, including deals taking place in off-shore jurisdictions.

When working out methodological principles of M&A deal risks evaluation for an industrial enterprise considering metallurgic holding as an example industry-specifics should be accounted for:

- geographic distance of integrated companies and their corporate cultures difference;
- high capital-intensity of metallurgy, demand for huge initial investments, long period of investment pay-back;
- acquisition of current and developing new plants is subject to external groups of interest influence. Dealing with them is of objective necessity;
- all large metallurgy plants in Russia provide employment for whole cities implying high social responsibility of M&A projects;
- technological similarity needs to be accounted for when merging metallurgical companies.

The M&A process complexity is driven by a high number of involved parties. Thus different stakeholders' possible actions were analyzed to account for most of the M&A deal risks.

Figure below presents the worked out process of project gross risk evaluation. The mechanism is self-adaptive and self-regulative. As risks at each of the stages are difficult to qualify fuzzy logic is used to evaluate gross risk. The fuzzy logic permits us to treat heterogeneous factors given lack of sufficient quantitative data [5].

According to the proposed mechanism individual risks were evaluated based on expert judgments for alternative investment projects.

The research is based on expert judgments for 20 M&A deals of one of the largest Russian metallurgy enterprises. 51 risk criteria have been chosen. Nine top-managers were questioned to obtain their expert judgments.

As expert judgment might are subjective and are reasonably different from manager to manager the Delfi-method is used to iteratively process the filled-in questionnaires.

When ranking alternatives experts tend to provide different opinions. Therefore it becomes necessary to estimate consistency on expert judgments (the degree of expert concordance). Arriving at the quantitative measure of expect non-concordance helps to analyze the reasons for differences in opinions.

To measure expert judgments degree of concordance following measures are often used [7]:

- spearman rank correlation coefficient;
- dispersion concordance coefficient (Kendall rank correlation coefficient);
- entropy concordance coefficient.

Non-parametric module of Statistics software was used to estimate experts concordance within identified criteria of M&A deals risks. χ^2-Pearson criteria for Kendall rank correlation coefficient was used. For all risk criteria the following holds: $\chi^2_{набл.} \geq \chi^2_{кр.}(0,05;19)$. Thus the null hypothesis of expert judgments being consistent is not rejected.

Expert competence coefficients were estimated given ex post data on questionnaire output [6]. Rykov iterative algorithm was used to obtain competence coefficients.

Let's take as an example the case of country risk at the third statge of M&A deal estimation. Firstly take a look at the ranks of all M&A deals for each expert.

Secondly, at zero stage prior expert competence coefficients are estimated: $K_i^0 = \frac{1}{m} = \frac{1}{9}$. Then average group estimated are calculated: $x_j^1 = \sum_{i=1}^{m} K_i^0 \cdot x_{ij}$. Then adjusted expert competence coefficients were obtained given the below formula:

$$\Delta K_i^1 = \frac{1}{\varepsilon + \max\limits_{j=\overline{1,n}} \left\{ \left| x_j^1 - x_{ij} \right| \right\}}, \quad (1)$$

$$i = \overline{11,m}, \varepsilon = 0,001.$$

Coefficient add-ons were based on the values of $\left| x_j^1 - x_{ij} \right|$. Additive approach was used to estimate adjusted competence coefficients:

$$K_i^{1^*} = K_i^0 + \Delta K_i^1. \quad (2)$$

As the sum of coefficients needs to equal to unity, the obtained values were normalized using the following formula (3):

$$K_i^1 = \frac{K_i^{1^*}}{\sum_{i=1}^{9} K_i^{1^*}}. \quad (3)$$

Final estimates are presented in Table 1.

When the 1st iteration is accomplished, the following condition was checked:

$$\max_{i=\overline{1,m}} \left\{ \left| K_i^1 - K_i^0 \right| \right\} \leq 0,0001. \quad (4)$$

Table 1

1st iteration results for Rykov algorithm are presented

$\Delta K_1^1 = 0,196$	$K_1^{1^*} = 0,307$	$K_1^1 = 0,139$
$\Delta K_2^1 = 0,117$	$K_2^{1^*} = 0,228$	$K_2^1 = 0,103$
$\Delta K_3^1 = 0,108$	$K_3^{1^*} = 0,219$	$K_3^1 = 0,099$
$\Delta K_4^1 = 0,105$	$K_4^{1^*} = 0,216$	$K_4^1 = 0,098$
$\Delta K_5^1 = 0,120$	$K_5^{1^*} = 0,231$	$K_5^1 = 0,105$
$\Delta K_6^1 = 0,099$	$K_6^{1^*} = 0,211$	$K_6^1 = 0,095$
$\Delta K_7^1 = 0,142$	$K_7^{1^*} = 0,253$	$K_7^1 = 0,114$
$\Delta K_8^1 = 0,153$	$K_8^{1^*} = 0,264$	$K_3^1 = 0,119$
$\Delta K_9^1 = 0,171$	$K_9^{1^*} = 0,283$	$K_9^1 = 0,128$

As condition (4) does not hold, then 1st iteration steps are repeated once more. To accomplish the procedure 11 steps were needed. Final output by iteration is presented in Table 2. Expert competence coefficients on other risks were estimated similarly.

Table 2

Rykov algorithm application for expert competence coefficients estimation for country risk

Iteraion No.	Deviation from previous iteration	Expert competence coefficients								
		K1	K2	K3	K4	K5	K6	K7	K8	K9
1	0,02768	0,139	0,103	0,099	0,098	0,105	0,095	0,114	0,119	0,128
2	0,01208	0,151	0,099	0,093	0,091	0,102	0,087	0,116	0,124	0,137
3	0,01294	0,138	0,103	0,099	0,097	0,107	0,096	0,113	0,120	0,126
4	0,01255	0,150	0,100	0,093	0,091	0,103	0,088	0,115	0,124	0,136
5	0,00534	0,156	0,098	0,089	0,087	0,102	0,084	0,116	0,127	0,141
6	0,00235	0,158	0,097	0,087	0,086	0,102	0,082	0,116	0,128	0,143
7	0,00111	0,159	0,097	0,086	0,085	0,102	0,081	0,116	0,129	0,144
8	0,00056	0,159	0,096	0,086	0,085	0,102	0,080	0,117	0,130	0,145
9	0,00027	0,159	0,096	0,086	0,085	0,102	0,080	0,117	0,130	0,145
10	0,00015	0,159	0,096	0,086	0,085	0,102	0,080	0,117	0,130	0,145
11	0,00009	0,159	0,096	0,086	0,085	0,102	0,080	0,117	0,130	0,145

Generalized rank is obtained accounting for expert competence based on the ranking of risk sums for all objects (competence coefficients are used as the weights):

$$Risk^k(j) = \sum_{i=1}^{9} K_i * Risk_i^k(j), \quad (5)$$

$$k = \overline{1,51}, j = \overline{1,20}.$$

Based on the proposed adaptively regulating mechanism of gross risk evaluation next step would be to estimate the M&A deals gross risk.

Fuzzy logic concept is an approach enabling to process information when purely quantitative data in not available*. To mention it is possible to proceed from conventional models in theory of probability and expert judgments to fuzzy sets descriptions. As an example traditional distribution can be substituted by a distribution with fuzzy parameters. Expert judgments might be interpreted like membership functions that form the fuzzy classificatory [1].

Consequently membership functions for 51 criteria were formulated (expert values of [1;9] were mapped to unit interval [0;1]). As the risk criteria was a monotonically increasing function, the following transformation took place:

$$\tilde{x} = \frac{x - x_{\min}}{x_{\max} - x_{\min}} = \frac{1}{8}(x-1). \quad (6)$$

As a result risk was scaled to [0;1] values where the minimal ones corresponded to minimum risk and vice versa.

Four methods of fuzzy sets orderings were used in the paper based on:

1) maxmin compression;
2) fuzzy relationship of preferences;
3) additive compression.

1. Multivariate choice of alternatives based on maxmin compression

Let trace the algorithm for M&A deals ranking based on fuzzy logic:

1. As the maximum values of membership function should correspond to the best alternative, it was transformed as follows:

$$\mu_{c_j}(a_i) = 1 - \mu_{c_j}^{ucx.}(a_i).^{**} \quad (7)$$

2. Relative importance coefficients ω_j are obtained on the basis of the first eigenvalue of the rule matrix. Rule matrix is produced with respect to the indicator hierarchy. The degree of indicator significance is determined according to the principles presented in Table 3.

$$\omega_j = m\alpha_j^2, \quad (8)$$

where α_j is eigenvalue of the first eigenvector.

3. The alternatives ranking rule given different indicator significance is determined as the fuzzy sets intersection:

$$D = C_1^{\omega_1} \bigcap C_2^{\omega_2} \bigcap ... \bigcap C_m^{\omega_m}. \quad (9)$$

Several approaches can be used to intersect the fuzzy sets. Nevertheless mostly the minimum is taken:

$$\mu_D(a_i) = \min_{j=1,m}(\mu_{c_j}(a_i))^{\omega_j}, i = \overline{1,n}. \quad (10)$$

4. The best alternative a_i^* is characterized by the highest value:

$$\mu_D(a_i^*) = \max_{i=1,n} \mu_D(a_i). \quad (11)$$

5. The values of $\mu_D(a_i^*)$ correspond to non-riskiness level of M&S deals. Considering our objective of risk measurement the inverse values should be taken:

$$\mu_D^{FINAL.}(a_i^*) = 1 - \mu_D(a_i^*) \quad (12)$$

Table 3

Table of indicator significance

Degree of significance	Definition	Description
1	Equal significance	Both indicators equally contribute to the outcome
3	Immaterial significance dominance of parameter	One of the indicators is somewhat more important, though it is immaterial
5	Strong significance	Clear evidence is to choose on of the indicators
7	Very strong significance	Strong evidence exists to prefer one indicator to another
9	Absolute significance	One indicator should be definitely preferred to another
2,4,6,8	Intermediary values	
Inverse to values presented above	When i-th indicator is compared to j-th indicator the above presented values are assigned, when on opposite j-th indicator is compared to i-th the inverse of the above values are assigned	

Then the higher is $\mu_D^{FINAL.}(a_i^*)$ value, the higher is the risk of deal.

When characteristic equation was solved, first eigenvalue for the rule matrix was $\lambda_1 = 63{,}386$. Solving for the equation (8) relative importance coefficients ω_j were also obtained.

Having analyzed the outcome of ω_j expert values third stage risks as the most important. Inter alia country risk, risk of the duties not accomplishment, and risk of company goods price decrease were considered to be the most important with the respective values assigned $\omega_{46} = 7{,}0895$, $\omega_{50} = 7{,}0648$, $\omega_{49} = 6{,}0752$.

Finally all projects were ranked based on $\mu_D^{FINAL.}(a_i^*)$. First place corresponds to the highest risk, last – to the minimal. Based on the ranking Pakistan, Canada, Germany, Turkey were the riskiest M&A deals.

* Fuzzy logic was actively applied after Lotfi Zadeh published his article in 1965 (Zadeh, 1965). The motivation for the paper was to process complex and difficult-to-formalize real-world problems that conventional methods of systemic analysis fail to deal with.

** To mention new membership functions produce the non-riskiness measure.

2. Multivariate choice of alternatives based on fuzzy relationship of preferences

When the alternatives are compared with respect to preference relationship, it is logical to assume non-dominating alternatives to be preferred. Mathematically speaking the problem converges to tracing out no dominating subset of alternatives within the fuzzy set.

Given R three corresponding fuzzy relationship can be formulated [3]:

- fuzzy relationship of indifference:

$$\mu_{R_j}(a_p,a_i)=\max\begin{Bmatrix}\min\{1-\mu_{C_j}(a_p),1-\mu_{C_j}(a_i)\},\\ \min\{\mu_{C_j}(a_p),\mu_{c_j}(a_i)\}\end{Bmatrix}; \quad (13)$$

- fuzzy relationship of quasi-equivalence:

$$\mu_{R_j}(a_p,a_i)=\min\{\mu_{C_j}(a_p),\mu_{C_j}(a_i)\}; \quad (14)$$

- fuzzy relationship of strong preference:

$$\mu_{R_j}(a_p,a_i)=$$
$$=\begin{cases}\mu_{C_j}(a_i)-\mu_{C_j}(a_p), if\ \mu_{C_j}(a_i)\ge\mu_{C_j}(a_p).\\ 0, if\ \mu_{C_j}(a_i)<\mu_{C_j}(a_p).\end{cases} \quad (15)$$

As the obtained alternatives are non-dominated given the available information, they are considered to be the best.

Let there is A set and each alternative has several features $j=\overline{1,m}$. Information on pairwise comparison for all alternatives is presented in R_j relationship. The rational choice needs to be done given m relationships R_j on A set.

Matrixes of fuzzy relationships are formulated for all the fuzzy relationship $R_1, R_2, ..., R_m$ according to formula (15).

1. Fuzzy realtionship Q_1 is constructed that symbolizes the intersection of relationships $Q_1=R_1\cap R_2\cap...\cap R_m$:

$$\mu_{Q_1}(a_p,a_i)=$$
$$=\min\{\mu_{R_1}(a_p,a_i),\mu_{R_2}(a_p,a_i),...,\mu_{R_m}(a_p,a_i)\}. \quad (16)$$

2. Subset of non-dominated alternatives is chosen $\{A,\mu(Q_1)\}$ for all p and i $(i=\overline{1,n};\ p=\overline{1,n})$:

$$\mu^{ND}_{Q_1}(a_p)=$$
$$=1-\sup_{a_p\in A}\{\mu_{Q_1}(a_p,a_i)-\mu_{Q_1}(a_i,a_p)\}\ \forall p,i,\ p\ne i. \quad (17)$$

3. Fuzzy relationship Q_2 is obtained:

$$\mu_{Q_2}(a_p,a_i)=\sum_{j=1}^{m}\omega_j\mu_{R_j}(a_p,a_i). \quad (18)$$

4. Subset of non-dominated alternatives is found for $\{A,\mu(Q_2)\}$ for all p and i $(i=\overline{1,n};\ p=\overline{1,n})$.

5. Final subset of non-dominating alternatives is found as the intersection of subsets $\{A,\mu(Q_1)\}$ and $\{A,\mu(Q_2)\}$:

$$\mu^{ND}(a)=\mu^{ND}_{Q_1}\cap\mu^{ND}_{Q_2}=\min(\mu^{ND}_{Q_1},\mu^{ND}_{Q_2}). \quad (19)$$

6. The most rational alternative to choose is the one having the highest degree of non-dominance:

$$a^{ND}=\left\{a\mid a\in A,\mu^{ND}(a)=\sup_{a'\in A}\mu^{ND}(a')\right\}. \quad (20)$$

To note not only a^{ND} alternatives are the best, sometimes weekly dominated alternatives might be of interest, i.e. the ones belonging to $\mu^{ND}(a)$ given the degree of confidence is no less then preapproved.

For 20 alternatives' membership functions 51 matrixes $R_1,R_2,...,R_{51}$ of fuzzy relationship were constructed. Based on formula (16) Q_1 fuzzy relationship was obtained as the intersection $Q_1=R_1\cap R_2\cap...\cap R_m$. Based on formula (17) subset of non-dominated alternatives was found $\{A,\mu(Q_1)\}$. Referring to principle (20) the final set was obtained.

Similar to maxmin compression four deals were considered as the most risky being assigned respective values of riskiness: Canada ($\mu^{ND}(a_{20})=0,9593$), Germany ($\mu^{ND}(a_{17})=0,9335$), Pakistan ($\mu^{ND}(a_4)=0,8870$), Turkey ($\mu^{ND}(a_1)=0,7915$).

3. Multivariate choice of alternatives based on additive compression

Current method presents expert judgments as fuzzy numbers having membership functions of triangular form.

1. To estimate the importance parameters ω_j linguistic variables are used: «not very important», «important», «very important». Linguistic variables are represented by the fuzzy numbers from the membership functions of triangular form.

Respectively:

1) not very important (HOB): $\mu_{HOB}=\left\{\frac{0}{0};\frac{1}{0,2};\frac{0}{0,4}\right\}$;

2) important (B): $\mu_B=\left\{\frac{0}{0,3};\frac{1}{0,5};\frac{0}{0,7}\right\}$;

3) very important (OB): $\mu_{OB}=\left\{\frac{0}{0,6};\frac{1}{0,8};\frac{0}{1,0}\right\}$.

2. To estimate criteria R_{ij} linguistic variables are also used: «very low risk», «low risk», «medium risk», «high risk», «very high risk».

Respectively:

1) very low risk (OH): $\mu_{OH}=\left\{\frac{1}{0};\frac{0}{0,2}\right\}$;

2) low risk (H): $\mu_H = \left\{\frac{0}{0};\frac{1}{0,2};\frac{0}{0,4}\right\}$;

3) medium risk (C): $\mu_C = \left\{\frac{0}{0,2};\frac{1}{0,4};\frac{0}{0,6}\right\}$;

4) high risk (B): $\mu_B = \left\{\frac{0}{0,4};\frac{1}{0,6};\frac{0}{0,8}\right\}$;

5) very high risk (OB): $\mu_{OB} = \left\{\frac{0}{0,6};\frac{1}{0,8};\frac{0}{1,0}\right\}$.

3. Criteria values for alternatives and their importance parameters are recorded.

4. Weighted estimates R_i are obtained as follows:

$$R_i = \sum_{j=1}^{m} \omega_j * R_{ij}, i = \overline{1,n},\ j = \overline{1,m}.$$

5. When weighted estimates R_i are obtained, objects are compared. For the purpose fuzzy set I is introduced with values following the below rule:

$$\mu_I(a_i) = \sup_{r_p \geq r_i} \min_{i=\overline{1,n}} \mu_{R_i}(r).$$

The best alternative is the one having the highest $\mu_I(a_i)$ value. I function values are interpreted as the alternative level of riskiness.

Similarly to the previous approaches the metallurgy holding experts would treat the following projects as the most risk: Pakistan $(\mu(a_4) = 1)$, Canada $(\mu(a_{20}) = 0,9260)$, Turkey $(\mu(a_1) = 0,9240)$, Germany $(\mu(a_{17}) = 0,9200)$.

The findings suggest fuzzy logic is a useful tool to evaluating gross risk of M&A projects. The gross risk estimate obtained enables to forecast the outcome of M&A deal, adjust the key financials and make the decision on whether to proceed with the deal or not during the first stage of M&A process.

Currently risk-management becomes an invaluable resort of strategic planning of Russian industrial enterprises that impacts the company value and might imply the rise of productivity. The proposed algorithm of M&A deals gross risk evaluation at OJSC Magnitogorsk Metallurgy Plant has proven its applicability and might be advised for further implementation at industrial enterprises in order to:

- Identify and classify risks mostly impacting M&A deal outcome;
- Provide complex and regular work on risk-management when running M&A deal to separate the duties within the Divisions and Levels of Management;
- Improve the KPIs of M&A deals by decreasing the associated risks and optimizing costs to handle risk minimization;
- Increase the efficiency of M&A project management by introducing additional criteria for decision-making and by receiving and analyzing feedback on M&A deals realization;
- Support the growth in market capitalization, increase in credit and investment ratings;
- Achieve the most beneficial state and to protect the current market niche.

References

1. Andreichikov A.V., Andreichikova O.H. *Analysis, synthesis and planning of decision in the economic environment.* Moscow: Finance and Statistics Publishing House, 2002 (rus).
2. Bogatikov A.A. Why raiders and corruption prospers in Russia? *M&A Journal,* 2010, no. 7-8, pp. 91-95 (rus).
3. Borisov A.N., Alekseev A.V., Merkurieva G.V. et al. *Fuzzy information treatment within the decision-support systems.* Moscow: Radio and communication, 1989 (rus).
4. Polikarpova M.G. Current status and trends of integration in the Russian economy. *ECO*, 2010. no. 2, pp. 75-84 (rus).
5. Polikarpova M.G. Economic and mathematical analysis of the integration activities of the economic sectors of the Russian Federation. *Vestnik Magnitogorskogo gosudarstvennogo tehnicheskogo universiteta im. G.I. Nosova*. [Vestnik of Nosov Magnitogorsk State Technical Univeersity]. 2010. no. 3(31), pp. 73-77 (rus).
6. Rykov A.S. *Systemic analysis: models and methos of decision-making and search optimization*. Moscow: MISiS Publishing House, 2009.
7. Shmoilova R.A., Minashkin V.G., Sadovnikova N.A., Shuvalova E.B. Ed. Shmoilova R.A. *Theory of statistics textbook*. Moscow: Finance and Statistics Publ., 2003.

THE INFORMATION ABOUT THE AUTHORS

Akhmetov Timur Uralovich – serviceman engineer of Limited Liability Company Scientific and Production Association «Automatica» (Automatics). Phone: 8(3519)29-85-58. E-mail: pksu035@gmail.com.

Andreev Sergey Mikhailovich – PhD in engineering, Associate Professor, Head of «Industrial cybernetics and control systems» Department, «Nosov Magnitogorsk State Technical University», Russia. Phone: 8(3519)29-85-27. E-mail: pk_su@bk.ru.

Antsupov Alexandr Victorovich – PhD in engineering, Associate Professor of «Mechanical Engineering» Department, «Nosov Magnitogorsk State Technical University», Russia. Phone: 8(3519)29-85-19. E-mail: ants@mgn.ru

Antsupov Alexei Victorovich – PhD in engineering, Associate Professor of «Steel Works Machinery» Department, «Nosov Magnitogorsk State Technical University», Russia. Phone: 8(3519)29-85-07. E-mail: ants@mgn.ru.

Antsupov Victor Petrovich – Doctor of Technical Sciences (D.Sc.), Professor of «Steel Works Machinery» Department, «Nosov Magnitogorsk State Technical University », Russia. Phone: 8(3519)29-85-07. E-mail: ants@mgn.ru.

Bigeev Vahit Abdrashitovich –Doctor of Technical Sciences, Professor, Director of the «Metallurgy, Mechanic Engineering and Materials Processing» Institute, «Nosov Magnitogorsk State Technical University», Russia. Phone: 8(3519)29-85-59. E-mail: v.bigeev11@yandex.ru.

Borovik Pavel Vladimirovich – PhD in engineering, Associate Professor, Donbass State Technical University, Alchevsk, doctoral student of Donbass State Engineering Academy, Kramatorsk, Ukraine. E-mail: borovikpv@mail.ru.

Cherchintsev Veacheslav Dmitrievich – Doctor of Technical Sciences, Professor, Head of «Industrial Ecology and Security» Department, «Nosov Magnitogorsk State Technical University». Phone: 8(3519)29-85-15. E-mail: eco_safe@magtu.ru.

Chukin Michail Vital'evich – Doctor of Technical Sciences, Professor, Vice-rector for Scientific and Innovation Work, Head of «Machine-building and Metallurgical Technologies» Department, «Nosov Magnitogorsk state technical university», Russia. Phone: 8(3519) 29-85-26. E-mail: m.chukin@mail.ru.

Danilyuk Victoria Alexandrovna – postgraduate student of «Automated Metallurgical Machinery and Equipment» Department, Donbass State Engineering Academy, Kramatorsk, Ukraine. E-mail: viktoriya1987@yandex.ru.

De Smedt Vivian – PhD in mathematics, Director Planning at PSI Metals, GmbH, Brussels Area, Belgium. E-mail: vdesmedt@psi.de.

Drobny Oleg Fedorovich – PhD in engineering, chief of the department of the environmental protection at the OJSC «Magnitogorsk Iron and Steel Works», Russia. Phone: 8(3519)24-79-83. E-mail: drobny@mmk.ru.

Dyja Henrik – Professor, Doctor of Technical Sciences, Director of the Institute of Metal Forming and Engineering Security, Czestochowa University of Technology Poland. E-mail: dyja@wip.pcz.pl.

Gorlenko Dmitriy Alexandrovich – assistant of the department of «Materials Science and Thermal Treatment» of «Nosov Magnitogorsk State Technical University», Russia. E-mail: gorldima@yandex.ru.

Gribkov Eduard Petrovich – PhD. in engineering, Associate Professor, «Automated Metallurgical Machinery and Equipment» Department, Donbass State Engineering Academy, Kramatorsk, Ukraine. E-mail: amm@dgma.donetsk.ua.

Gun Gennadiy Semenovich – Doctor of Technical Sciences, Professor, «Machine-building and Metallurgical Technologies» Department, «Nosov Magnitogorsk State Technical University», Russia. Phone: 8(3519) 29-85-26. E-mail: mgtu@magtu.ru.

Gun Igor Gennadyevich – Doctor of Technical Sciences, Full Professor, Head of «Technologies, Certification and Vehicles Service» Department, «Nosov Magnitogorsk State Technical University», Russia. Phone: 8(3519)29-84-31.

Hamedon Zamzuri – Department of Mechanical Engineering, Toyohashi University of Technology, Aichi, Japan.

Ishmetyev Evgeniy Nikolayevich – KonsOM SKS company, Magnitogorsk, Russia.

Kawałek Anna – Dr.Sc., Assistant Professor, Czestochowa University of Technology, Poland. E-mail: kawalek@wip.pcz.pl.

Kinzin Dmitry Ivanovich – PhD in engineering, Associate Professor, «Metal Forming» Department, «Nosov Magnitogorsk State Technical University», Russia. Phone: (3519) 298525. E-mail: kinzin@mail.ru.

Kolga Maria – Research Engineer PSI Metals GmbH, Germany. E-mail: mkolga@psi.de.

Kolokoltsev Valeriy Mikhailovich – Doctor of Technical Sciences, Professor, Rector of «Nosov Magnitogorsk State Technical University», Russia. Phone: 8(3519)29-84-02. E-mail: kwm@magtu.ru.

Koptseva Natalya Vasilyevna – Doctor of Technical Sciences, Professor, «Material Science and Metals and Alloys Heat Treatment» Department, «Nosov Magnitogorsk state technical university», Russia. Phone: 8(3519) 29-85-67. E-mail: koptsev2002@mail.ru.

Korchunov Alexei Georgievich – Doctor of Technical Sciences, Professor, Vice-Rector for International Relations, «Nosov Magnitogorsk State Technical University», Russia. Phone: 8 (3519) 29-84-09. E-mail: international@magtu.ru.

Korenko Marina Georgiyevna – PhD in engineering, Assistant Professor, MT Department, Krivoy Rog Metallurgical Institute of the State institution of higher education, «National University of Krivoy Rog», Ukraine. Phone: 75873245. E-mail: marinak 2010@ bk.ru.

Levandovskiy Sergey Anatolievich – PhD in engineering, Associate Professor, «Metal forming» Department, «Nosov Magnitogorsk State Technical University», Russia. Phone: 8(3519) 29-85-25. E-mail: levandovskiy@mail.ru.

Logunova Oxana Sergeevna – Doctor of Technical Sciences, Associate Professor, Head of Department, «Nosov Magnitogorsk State Technical University», Russia. Phone: 8(3519)22-03-17. E-mail: logunova66@mail.ru

Lutsenko Andrey Nikolaevich – Severstal, Cherepovets, Russia.

Maeno Tomoyoshi – Department of Mechanical Engineering, Toyohashi University of Technology, Aichi, Japan.

Manashev Ildar Raufovich – PhD in engineering, Limited Company STIF «Etalon». Phone: 8(3519) 58-01-57. E-mail: mirney@yandex.ru.

Matsko Igor Igorevich – PhD., engineer, Research and Development Center «Ausferr». E-mail: matskoigor@gmail.com.

Mezin Igor Yurjevitch – Doctor of Technical Sciences, Professor, Head of «Technologies, Certification and Automobile Service » Department, «Nosov Magnitogorsk State Technical University», Russia. Phone: 8(3519)29-84-31. E-mail: meziniy1@mail.ru.

Moller Alexander Borisovich – Doctor of Technical Sciences, Professor «Metal forming» Department, «Nosov Magnitogorsk State Technical University», Russia.Phone: 8(3519)29-85-25. E-mail: moller@hotbox.ru.

Mori Ken-ichiro – Professor, Department of Mechanical Engineering, Toyohashi University of Technology, Aichi, Japan.

Mukhina Elena Yurievna – Assistant Professor, «Industrial Cybernetics and Control Systems» Department, «Nosov Magnitogorsk State Technical University», Russia. Phone: 8(3519)298558. E-mail: pksu035@gmail.com.

Nalivaiko Alexander Vladimirovich – First Deputy General Director of OJSC «AHK VNIIMETMASH», Moscow. Phone: 8(495)7304530. E-mail: mail@vniimetmash.ru.

Nastoshchaya Svetlana Sergeyevna – assistant of «Automated Metallurgical Machinery and Equipment» Department, Donbass State Engineering Academy, Kramatorsk, Ukraine. Phone: (0626) 41-46-81. E-mail: amm@dgma.donetsk.Ua

Novitskiy Ruslan Vitalievich – OJSC «Magnitogorsk Iron and Steel Works», Russia.

Parsunkin Boris Nikolaevich – Doctor of Technical Science (D.Sc.), Professor, «Industrial Cybernetics and Control Systems» Department, «Nosov Magnitogorsk State Technical University», Russia. Phone: 8(3519)29-84-32. E-mail: pksu035@gmail.com.

Perekhodchenko Viktor Aleksandrovich –senior engineer, Novokramatorsk Machine Building Plant Public Joint Stock Company, Kramatorsk, Ukraine. Phone: (0626) 41-46-81. E-mail: amm@ dgma.donetsk.ua.

Pesin Alexander Moiseevich – Doctor of Technical Sciences, Professor, «Metal Forming» Department, «Nosov Magnitogorsk State Technical University», Russia. Phone: 8(3519)29-85-25. E-mail: pesin@bk.ru.

Petrochenko Elena Vasilyevna – Doctor of Technical Sciences, Professor, «Materials Science and Thermal Treatment» Department, «Nosov Magnitogorsk State Technical University», Russia. E-mail: evp3738@mail.ru.

Pietrzyk Maciej – Professor, «Applied Computer Science and Modelling» Departament, AGH Akademia Górniczo-Hutnicza, Kraków, Poland

Polikarpova Maria Gennadievna – PhD in economics, Assistant Professor, «Mathematical Methods in Economics» Department, «Nosov Magnitogorsk State Technical University», Russia. E-mail: marjyshka@rambler.ru.

Polyakova Marina Andreevna – PhD in engineering, Associate Professor, «Machine-building and Metallurgical Technologies» Department, «Nosov Magnitogorsk state technical university», Russia. Phone: 8(3519) 29-84-81. E-mail: m.polyakova-64@mail.ru.

Posokhov Ivan Alexandrovich – graduate student, «Nosov Magnitogorsk State Technical University». Phone: 8(3519)29-85-63. Email: posohoff@bk.ru.

Rubin Gennadiy Shmulyevich – PhD in engineering, Associate Professor, «Technologies, certification and vehicles service» Department, «Nosov Magnitogorsk State Technical University», Russia. Phone: (3519)298563.

Ruchinskaya Natalia Aleksandrovna – PhD in engineering, Associate Professor, «Metal Forming» Department, «Nosov Magnitogorsk State Technical University», Russia. Phone: 8(3519) 29-85-25.

Rumyantsev Mihail Igorevich – PhD in engineering, Professor, «Metal Forming» Department, «Nosov Magnitogorsk State Technical University», Russia. E-mail: mihigrum@rambler.ru.

Rychkov Sergey Sergeyevich – Open Joint-Stock Company «Magnitogorsk Iron and Steel Works», Russia.

Satonin Alexander Vladimirovich – DSc., Professor, Donbas State Machine-Building Academy, Kramatorsk, Ukraine; Phone: (0626) 41-46-81. E-mail: amm@dgma.donetsk.ua.

Shatohin Igor Mihaylovich – general manager of STIF Etalon Ltd. Co. Phone: 8(3519) 58-01-55. E-mail: mail@ntpf-etalon.ru.

Shaymardanov Kamil Ramilevich – postgraduate student, «Ferrous Metals Metallurgy» Department, «Nosov Magnitogorsk State Technical University», Russia. E-mail: kem-lmgn@gmail.com.

Shigorina Anna Yurievna – Master's program student, «Ferrous Metals Metallurgy» Department, «Nosov Magnitogorsk State Technical University», Russia. E-mail: shigorina89@mail.ru.

Sztangret Mateusz – Departament of Applied Computer Science and Modelling, AGH Akademia Górniczo-Hutnicza Kraków, Poland.

Tulupov Oleg Nikolayevich – Doctor of Technical Sciences, Professor, «Metal Forming» Department, «Nosov Magnitogorsk State Technical University», Russia. Phone: 8(495)7304999. E-mail: o.tulupov(@mail.ru.

Van Nerom Luc – Director of Software Architecture, Methods and Quality PSI Metals GmbH, Germany. E-mail: lvannerom@psi.de.

Vdovin Konstantin Nikolaevich – Doctor of Technical Science, Professor, Head of «Electrometallurgy and Foundry» Department, «Nosov Magnitogorsk State Technical University», Russia. Phone: 8(3519)29-84-19. E-mail: Vdovin@magtu.ru.

YamashitaYuya – Department of Mechanical Engineering, Toyohashi University of Technology, Aichi, Japan.

Zavalischin Alexander Nicolaevich – Doctor of Technical Sciences, Professor, «Materials Science and Thermal Treatment» Department, «Nosov Magnitogorsk State Technical University», Russia. Phone: 8(3519)29-85-67. E-mail: zaval1313@mail.ru.